Bernhard Weigand

# Analytical Methods for Heat Transfer and Fluid Flow Problems

*Second Edition*

Springer

# Mathematical Engineering

More information about this series at http://www.springer.com/series/8445

Bernhard Weigand

# Analytical Methods for Heat Transfer and Fluid Flow Problems

Second Edition

🦄 Springer

Bernhard Weigand
Institut für Thermodynamik der Luft- und
    Raumfahrt
Universität Stuttgart
Stuttgart
Germany

Printed on acid-free paper

*For Irmi, my wife*

# Preface to the Second Edition

Roughly 10 years ago the first edition of this book was published. Since then a lot of the material of this book has been used for lectures at the University of Stuttgart, for Bachelor- and Master-Thesis work and for research.

I am happy about all the positive responses to this book during the past years from my students and researchers all over the world. For this edition, the chapters have been updated and extended, where necessary. In addition, Appendix E has been added. Here the reader can find short solutions to the problems given at the end of each chapter.

In the web page www.uni-stuttgart.de/itlr/Analytical-Methods the reader can find additional material for the book. Here, also a solution manual for the problems given in the book is provided. The Login and Password for this web page is

Login: Analytical-Methods
Password: methods1000

I would like to thank Kathrin Eisenschmidt and Dr. Hassan Gomaa for the helpful discussions of the second edition of this book. In addition, I would like to thank Christian Biegger for helping me with some of the figures.

Finally, I would like to express my thanks to Springer Press for the very good cooperation during the preparation of this manuscript.

Filderstadt, January 2015                                    Bernhard Weigand

# Preface to the First Edition

Partial differential equations are the basis for nearly all technical processes in heat transfer and fluid mechanics. In my lectures over the past 7 years I became aware of the fact that a lot of the students studying mechanical or aerospace engineering and also a lot of the engineers in industry today focus more and more on numerical methods for solving these partial differential equations. Analytical methods, taught in undergraduate mathematics, in thermodynamics and fluid mechanics, are quickly discarded, because most people believe that almost all problems, appearing in *real* applications, can easily be solved by numerical methods. In addition, most of the examples shown in basic lectures are *so simple* that the students develop the impression that analytical methods are inappropriate for more complicated *realistic technical* problems.

It was exactly the above described mindset that inspired me several years ago to give lectures on analytical methods for heat and mass transfer problems. The basic idea of these lectures is to show some selected analytical methods and to explain their application to more complicated problems, which are technically relevant. Of course, this means that some of the standard analytical methods might not be discussed in these lectures and are also not present in this book (for example, integral transforms). On the other hand, it can be shown that the analytical methods discussed here are applicable to interesting problems and the student or engineer learns how to solve useful technical problems analytically.

This means that the main intent of this book is to show the usefulness of analytical methods, in a world, which focuses more and more on numerical methods. Of course, there is no doubt that the knowledge of numerical solution methods is very important and there is a big chance in using numerical tools to gain inside into flow physics and heat transfer characteristics. However, numerical methods are always dependent on grid quality and grid size and also on a lot of implementation features. Analytical methods can be used to validate and improve numerical methods. So the engineer might simplify a problem up to the extent that he can obtain an analytical solution. This analytical solution might be used later to check and to improve the numerical solution for the full problem without any simplifications.

This book has been written for graduate students and engineers. The mathematics needed to understand the solution approach is developed mostly during the actual solution of the problem under consideration. This means that the book includes only few proofs. The reader is referred in these situations to other books for these more basic mathematical considerations. This approach has been taken in order to keep the focus of the book on the solution method itself and not to disrupt the analysis of the technical problem.

The book is structured into six chapters. Chapter 1 provides a short introduction to the topic.

Chapter 2 provides an introduction to the solution of linear partial differential equations. After discussing the classification and the character of the solutions of second-order partial differential equations, the method of separation of variables is discussed in detail.

Chapter 3 is concerned with the solution of thermal entrance problems for pipe and channel flows. This means that solutions of the energy equation are considered for a hydrodynamically fully developed velocity profile. These problems lead to the solution of Sturm-Liouville eigenvalue problems, which are discussed for laminar and turbulent flows and for different wall boundary conditions. For the problems considered in Chap. 3, axial heat conduction within the flow can be ignored, because the Peclet number in the flow is sufficiently large. This means that the problems under consideration are parabolic in nature. Because such eigenvalue problems normally cannot be solved analytically, a numerical procedure is discussed on how to solve them. In Appendix C, this numerical solution method is explained in detail and the reader is provided links to an Internet page containing several source codes and executables.

Chapter 4 explains analytical solution methods for Sturm-Liouville eigenvalue problems for large eigenvalues. Here the focus is to explain an asymptotic analysis for a complicated problem, which is technically relevant. This chapter also provides comparisons between numerically and analytically predicted eigenvalues and constants. These comparisons show the usefulness of the analytical solution. Furthermore, it is explained how the method can be used for related problems.

In Chapter 5 the heat transfer in pipe and channel flows for small Peclet numbers is considered. In contrast to the problems discussed in Chaps. 3 and 4, the axial heat conduction in the fluid cannot be ignored. This leads to elliptic problems. A method is presented, which gives rise to solutions that are as simple as the ones presented in Chap. 3. The extension of this method to more complicated problems, for example, for the heat transfer in hydrodynamically fully developed duct flows with a heated zone of finite length, is also explained.

Chapter 6 is devoted finally to the solution of nonlinear partial differential equations. The idea behind this chapter was to provide a short overview of different solution methods for nonlinear partial differential equations. However, the main focus is on the derivation of similarity solutions. Here, different solution methods are explained. These are the method of dimensional analysis, group-theory methods, and the method of the free parameter. The methods are demonstrated for a

simple heat conduction problem as well as for complicated boundary layer problems.

Many people helped me in all phases of the preparation of this book. I am very grateful for many helpful discussions with my colleague Prof. Jens von Wolfersdorf concerning all aspects of the analytical solution methods. I also thank very much Martin Stricker and Marco Schüler who helped me with the figures. Many thanks also go to Dr. Grazia Lamanna for the helpful discussions and her support in finishing this book. Also, I would like to thank Karl Straub very much for reading the manuscript.

I kindly acknowledge the permission from ASME for reprinting Figs. 1.2 and 1.3 and from ELSEVIER for reprinting Figs. 3.7, 3.13–3.15, 5.1, 5.9–5.13, 5.18, 5.19 and 5.25 in this book. I also kindly acknowledge the permission from IMECHE for reprinting Fig. 3.12, from KLUWER for reprinting Figs. 5.3 and 5.4, B2–B7 and from SPRINGER for reprinting Figs. 3.8, 3.9, 3.17–3.19 in this book. The reference of the paper, where the figures have originally been published, is always included in the individual figure legend.

Finally, I am very grateful for the very good cooperation with Springer Press during the preparation of this manuscript.

Filderstadt, April 2004                                                                                      Bernhard Weigand

# Contents

# Symbols

| | |
|---|---|
| $a$ | Heat diffusivity (m$^2$/s) |
| $a_1$, $a_2$ | Functions (–) |
| $A$ | Flow area (m$^2$) |
| $A_j$ | Constants (–) |
| Bi | Biot number (–) |
| $c$ | Velocity of sound (m/s) |
| $c_f$ | Friction factor (–) |
| $c_p$ | Specific heat at constant pressure (J/(kg K)) |
| Ch | Chapman-Rubesin parameter (–) |
| $D$ | Hydraulic diameter (m) |
| $E$ | Dimensionless energy flow (–) |
| $F$ | Flow index (0 for planar channel, 1 for pipe) (–) |
| $F_x$, $F_y$, $F_z$ | Forces (N) |
| $G$ | Function (–) |
| $h$ | Half channel height of a planar channel (m) |
| $h$ | Heat transfer coefficient (W/(m$^2$ K)) |
| $J_i(s)$ | Bessel function of order $i$ (–) |
| $k$ | Thermal conductivity (W/(m K)) |
| $k$ | Transformed eigenvalue (–) |
| $K$ | Sink intensity (W/m$^3$) |
| $L$ | Length scale ($h$ for planar channel, $R$ for pipe) (m) |
| $L_{th}$ | Thermal entrance length (m) |
| $L[\,]$ | Matrix operator (–) |
| $l$ | Mixing length (m) |
| $M[\,]$ | Operator (–) |
| Ma$_\infty$ | Mach number (–) |
| $n$ | Coordinate orthogonal to the flow direction (m) |
| N | Rotation rate (–) |
| Nu$_L$ | Nusselt number based on $L$ (–) |
| Nu$_\infty$ | Nusselt number for the fully developed flow (–) |

| | |
|---|---|
| $p$ | Pressure (Pa) |
| $Pe_L$ | Peclet number based on $L$ (–) |
| $Pe_t$ | Turbulent Peclet number (–) |
| Pr | Prandtl number (–) |
| $Pr_t$ | Turbulent Prandtl number (–) |
| $R$ | Gas constant (J/(kg K)) |
| $R$ | Pipe radius (m) |
| $Re_L$ | Reynolds number based on $L$ (–) |
| $Re_\varphi$ | Rotational Reynolds number (–) |
| Ri | Richardson number (–) |
| $t$ | Time (s) |
| $T$ | Temperature (K) |
| $T'$ | Temperature fluctuation (K) |
| $T_b$ | Bulk-temperature (K) |
| $T_W$ | Wall temperature (K) |
| $u_\tau$ | Shear velocity (m/s) |
| $\bar{u}$ | Mean velocity (m/s) |
| $u, v, w$ | Velocity components (m/s) |
| $u', v', w'$ | Fluctuating velocity components (m/s) |
| $U$ | Wetted perimeter (m) |
| $V$ | Dimensionless velocity gradient at the wall (–) |
| $x, y, z$ | Coordinates (m) |
| $y^+$ | Wall coordinate (–) |
| Z | Modified rotation parameter (–) |

## Greek Letter Symbols

| | |
|---|---|
| $\beta$ | Volumetric coefficient of expansion (1/K) |
| $\beta_1, \beta_2$ | Constants (–) |
| $\Gamma$ | Gamma function (–) |
| $\varepsilon_m$ | Eddy diffusivity for momentum transfer (m$^2$/s) |
| $\varepsilon_{hx}, \varepsilon_{hy}, \varepsilon_{hr}$ | Eddy diffusivity for heat transfer (m$^2$/s) |
| $\xi, \eta$ | Characteristic coordinates (–) |
| $\eta$ | Similarity variable (–) |
| $\vartheta$ | Transformed eigenfunction (–) |
| $\Theta$ | Dimensionless temperature (–) |
| $\Theta_b$ | Dimensionless bulk-temperature (–) |
| $\lambda_j$ | Eigenvalue (–) |
| $\mu$ | Dynamic viscosity (kg/(m s)) |
| $v$ | Kinematic viscosity (m$^2$/s) |
| $\rho$ | Density (kg/m$^3$) |
| $\tau$ | Dimensionless time (–) |

$\phi$              Enthalpy function (–)
$\Phi$              Velocity potential ($m^2$/s)
$\Phi_j$            Eigenfunctions (–)
$\Phi_{Dis}$        Dissipation function ($1/s^2$)
$\Psi$              Stream function ($m^2$/s)
$\omega$            Angular velocity (1/s)

## Subscripts

0              Refers to inlet conditions
C              Centerline of the duct
$\infty$       Free stream conditions
$\sim$, +      Dimensionless quantities

## Definition of Non-dimensional Numbers

$$\mathrm{Bi} = \frac{hD}{k}$$                            Biot number

$$Ch = \frac{\rho\mu}{\rho_\infty \mu_\infty}$$           Chapman-Rubesin parameter

$$\mathrm{Ma}_\infty = \frac{u_\infty}{\sqrt{\kappa p/\rho}}$$   Mach number

$$N = \frac{\mathrm{Re}_\varphi}{\mathrm{Re}_D}$$          Rotation rate

$$\mathrm{Nu}_L = \frac{hL}{k} = \frac{-\frac{\partial T}{\partial n}\big|_W L}{T_W - T_b}$$   Nusselt number

$$\mathrm{Pe}_L = \frac{\bar{u}L}{a} = \mathrm{Re}_L\,\mathrm{Pr}$$   Peclet number

$$\mathrm{Pr} = \frac{\mu c_p}{k} = \frac{v}{a}$$          Prandtl number

$$\mathrm{Re}_L = \frac{\bar{u}L}{v}$$                     Reynolds number

$$\mathrm{Re}_\varphi = \frac{w_W D}{v}$$                  Rotational Reynolds number

$$\mathrm{Re}_\tau = \frac{u_\tau L}{v}$$                  Shear stress Reynolds number

$$\mathrm{Ri} = \frac{2\frac{w}{r^2}\frac{\partial}{\partial r}(wr)}{\left(\frac{\partial u}{\partial r}\right)^2 + \left(r\frac{\partial}{\partial r}\left(\frac{w}{r}\right)\right)^2}$$   Richardson number

$$Z = N\,\frac{\mathrm{Re}_D}{2\,\mathrm{Re}_\tau} = N/\sqrt{\frac{c_f}{8}}$$   Modified rotation parameter

# List of Copyrighted Figures

# Chapter 1
# Introduction

Fluid flow and heat transfer problems are present in all of our daily life. For example, if we walk along a river and look at the water flowing with high speed over the river-bed, we actually observe a fluid mechanics problem. If we put some sugar into our coffee and stir it, we are faced with a complicated heat and mass transfer problem. In particular, convective heat transfer problems are present everywhere in our world. Most of the problems encountered in fluid mechanics or heat transfer are described by partialdifferential equations. One good example of such equations are the Navier-Stokes equations and the energy equation for an incompressible flow with constant fluid properties. If we consider a three-dimensional, steady-state problem, these equations read

$$\rho\left(u\frac{\partial u}{\partial x} + v\frac{\partial u}{\partial y} + w\frac{\partial u}{\partial z}\right) = F_x - \frac{\partial p}{\partial x} + \mu\left(\frac{\partial^2 u}{\partial x^2} + \frac{\partial^2 u}{\partial y^2} + \frac{\partial^2 u}{\partial z^2}\right) \qquad (1.1)$$

$$\rho\left(u\frac{\partial v}{\partial x} + v\frac{\partial v}{\partial y} + w\frac{\partial v}{\partial z}\right) = F_y - \frac{\partial p}{\partial y} + \mu\left(\frac{\partial^2 v}{\partial x^2} + \frac{\partial^2 v}{\partial y^2} + \frac{\partial^2 v}{\partial z^2}\right) \qquad (1.2)$$

$$\rho\left(u\frac{\partial w}{\partial x} + v\frac{\partial w}{\partial y} + w\frac{\partial w}{\partial z}\right) = F_z - \frac{\partial p}{\partial z} + \mu\left(\frac{\partial^2 w}{\partial x^2} + \frac{\partial^2 w}{\partial y^2} + \frac{\partial^2 w}{\partial z^2}\right) \qquad (1.3)$$

$$\rho c\left(u\frac{\partial T}{\partial x} + v\frac{\partial T}{\partial y} + w\frac{\partial T}{\partial z}\right) = \mu\, \Phi_{Dis} + k\left(\frac{\partial^2 T}{\partial x^2} + \frac{\partial^2 T}{\partial y^2} + \frac{\partial^2 T}{\partial z^2}\right) \qquad (1.4)$$

where $\Phi_{Dis}$ denotes the dissipation function in the energy equation. This function is given by

$$\Phi_{Dis} = 2\left[\left(\frac{\partial u}{\partial x}\right)^2 + \left(\frac{\partial v}{\partial y}\right)^2 + \left(\frac{\partial w}{\partial z}\right)^2\right] + \left(\frac{\partial v}{\partial x} + \frac{\partial u}{\partial y}\right)^2$$
$$+ \left(\frac{\partial w}{\partial y} + \frac{\partial v}{\partial z}\right)^2 + \left(\frac{\partial u}{\partial z} + \frac{\partial w}{\partial x}\right)^2 \qquad (1.5)$$

This set of equations is closed by adding the mass continuity equation for an incompressible flow

$$\frac{\partial u}{\partial x} + \frac{\partial v}{\partial y} + \frac{\partial w}{\partial z} = 0 \tag{1.6}$$

In the above equations, $x$, $y$, $z$ denote the cartesian coordinates, $p$ indicates the pressure, $T$ the temperature, $F_x$, $F_y$ and $F_z$ are forces, and $u$, $v$, $w$ are the velocity components in the $x$-, $y$- and $z$-direction, respectively.

From the above equations it can be seen that fluid flow and heat transfer problems are described by a set of partial differential equations. In general, these complicated differential equations can only be solved numerically. However, analytical solutions for fluid mechanics or heat transfer problems can still play an important role in science and in engineering, even in the current age of super-computers. This is because analytical solutions have the big advantage of showing directly which parameters influence the solution. This is illustrated by the following short example (see Fig. 1.1). We are interested in the answer to the question on how a periodic change of the surface temperature of the earth will influence the temperature in the soil. Here, we are primarily interested in the behavior for increasing $x$, i.e. the distance from the surface, and growing values of time. Since we are only interested in the temperature change in the radial direction, we can approximate the earth as a semi-infinite body. In addition, we might use a cartesian coordinate system to describe this problem, because the radius of curvature of the earth is very large compared to all other dimensions.

If we write down the energy equation for this problem and if we consider the physical properties of the body to be constant, the energy equation can be simplified to

$$\rho c \frac{\partial T}{\partial t} = k \left( \frac{\partial^2 T}{\partial x^2} + \frac{\partial^2 T}{\partial y^2} + \frac{\partial^2 T}{\partial z^2} \right) \tag{1.7}$$

Furthermore, the heat conduction in the $y$- and $z$-direction can be neglected compared to the heat conduction in the $x$-direction. If we do so, we obtain

**Fig. 1.1** Semi-infinite body with a periodically changing surface temperature



$$T = T_1 \cos(\omega t - \varepsilon)$$

$x$

semi-infinite body
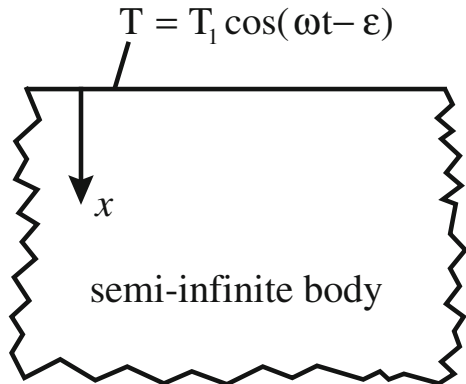
$$\frac{\partial T}{\partial t} = a\frac{\partial^2 T}{\partial x^2}; \quad a = \frac{k}{\rho c} \tag{1.8}$$

The boundary conditions for this problem are given by

$$x = 0 : \quad T = T_1 \cos(\omega t - \varepsilon) \tag{1.9}$$

$$t = 0 : \quad T = T_0; \quad x > 0 \tag{1.10}$$

where $T_0$ is the constant initial temperature of the solid body and $\omega$ and $\varepsilon$ are given constants. The solution of this problem is (see Carslaw and Jaeger 1992)

$$\Theta = e^{-\eta}\cos(\tau - \eta - \varepsilon) + \frac{2}{\sqrt{\pi}}\int_0^{\eta/\sqrt{2\tau}}\cos\left[\tau - \frac{\eta^2}{2\mu^2} - \varepsilon\right]e^{-\mu^2}d\mu \tag{1.11}$$

with the dimensionless quantities

$$\Theta = \frac{T - T_0}{T_1}, \quad \tau = \omega t, \quad \eta = x\sqrt{\frac{\omega}{2a}} \tag{1.12}$$

From the above given analytical solution (1.11), one sees very clearly that the solution consists of two parts. The second part of Eq. (1.11) determines the behavior of the solution for short times

$$\Theta_T = \frac{2}{\sqrt{\pi}}\int_0^{\eta/\sqrt{2\tau}}\cos\left[\tau - \frac{\eta^2}{2\mu^2} - \varepsilon\right]e^{-\mu^2}d\mu \tag{1.13}$$

For a fixed value of $x$ ($\eta$ = const.), this part of the solution tends to zero with increasing time, as it can be seen from the upper boundary of the integral.

The first part of the solution (1.11) is a periodic part, which is multiplied by an exponential-function

$$\Theta_P = e^{-\eta}\cos(\tau - \eta - \varepsilon) \tag{1.14}$$

From this part of the solution, we can see that the amplitude of the oscillation of the surface temperature decreases with increasing values of $\eta$. Additionally, one can notice that the maximum of the oscillation appears at different depths of the material with a time delay. Furthermore, it can be seen that the solution for $\Theta$ only depends on the following dimensionless quantities:

$$\tau = \omega t \tag{1.15}$$

$$\eta = x\sqrt{\frac{\omega}{2a}} \tag{1.16}$$

In this context, it is of special interest to have a closer look on the variable $\eta$. If $\sqrt{\omega/(2a)}$ is large (which means: $\omega$ is large or $a = k/(\rho c)$ is very small, for example because of a low heat conducting material), $\eta$ will be large even for small values of $x$. This means that the temperature wave will be damped out very fast.

The behavior of the solution (1.11) is demonstrated for one example. We consider the case $\varepsilon = 0$. The complete solution is depicted in Fig. 1.2. It can be seen from Fig. 1.2 that the maximum temperature appears at different times for increasing values of $\eta$. In addition, it is clear from Fig. 1.2 that the solution satisfies the initial condition that $\Theta = 0$ for $\tau = 0$ inside the solid body (i.e. $\eta > 0$). Figure 1.3 shows only the first part of the solution $\Theta_P$. As stated before, it can be seen that $\Theta_P$ is a very good approximation of the complete solution of the problem for larger times. For $\tau > 0.1$ the complete solution is nicely approximated.

This also shows that, for some problems, it might suffice to determine the solution $\Theta_P$ but not the full solution of the problem. This sort of solution can be determined very easily also for more complicated variations of the surface temperature (see for example Myers 1987 or Carslaw and Jaeger 1992). One example is depicted in Fig. 1.4, which shows the annual oscillation of the temperature in the soil in Alaska at various depths. The figure shows nicely how the minimum temperature at a certain depth in the soil gets shifted to different times. In addition it can be seen how the amplitude of the temperature oscillation decreases with increasing depth. This leads to the interesting fact, that at certain times in the year the temperature stratification in the soil can get reversed.

The examples discussed above show clearly the power of the analytical methods. The analytical solution shows clearly the dependence of the solution on the dimensional quantities. Furthermore, short time effects or long time behavior are clearly visible. Analytical solutions might therefore be derived for strongly simplified problems, before a numerical solution is carried out. The simplified model can then be used to understand the basic physical phenomena and behavior of the



**Fig. 1.2** Temperature distribution for $\varepsilon = 0$ as a function of $\eta$ and $\tau$ (Burow and Weigand 1990)
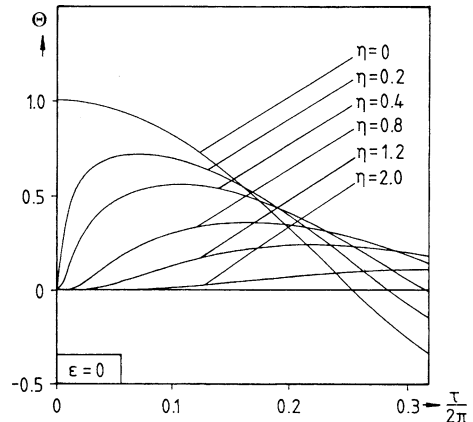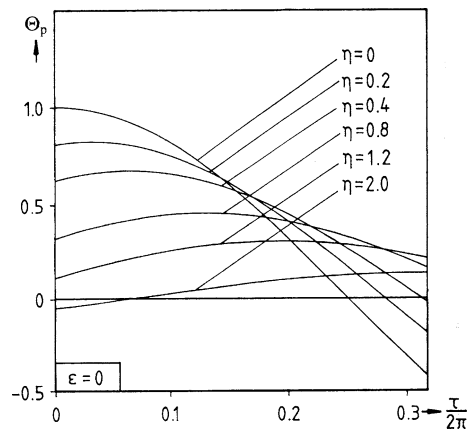
**Fig. 1.3** Temperature distribution $\Theta_P$ for $\varepsilon = 0$ as a function of $\eta$ and $\tau$ (Burow and Weigand 1990)
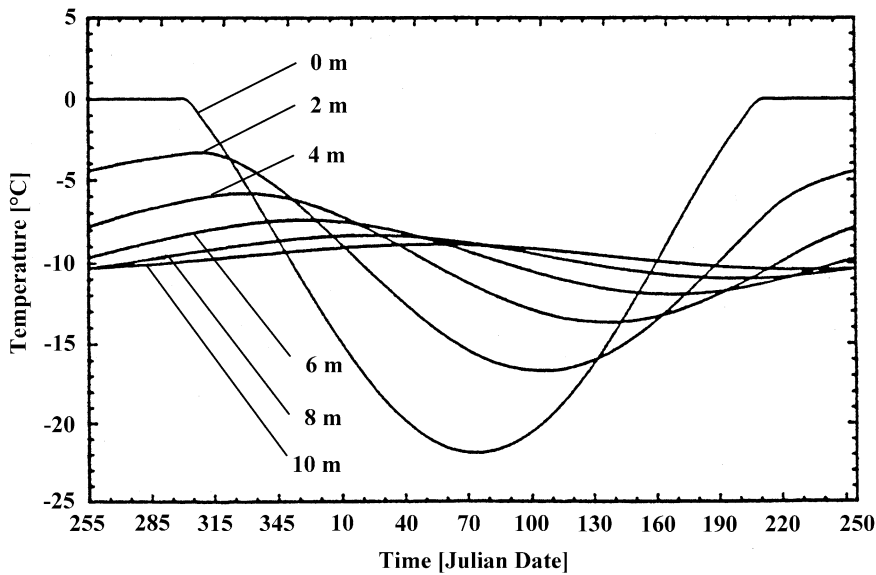


**Fig. 1.4** Annual oscillation of the soil temperature in Alaska at different depths (Zhang et al. 1991)

problem. Additionally, analytical solutions can be used for validating the numerical calculations and proving that all the settings, e.g. grid quality, meshing technique, numerical scheme and so on, are adequate for the considered problem. This is especially important for nonlinear problems, where grid size and grid quality might play a very important role for the final accuracy obtained by the numerical method.

In a next step, we want to address the question on how to classify the partial differential equations (PDE). In general, partial differential equations are classified

by their order and by the fact that they are linear, quasilinear or nonlinear (the classification of second order linear partial differential equations is discussed in detail in Chap. 2).

An example of a linear second-order partial differential equation is the energy equation describing the heat conduction within a solid body, which has constant physical properties

$$\rho c \frac{\partial T}{\partial t} = k \left( \frac{\partial^2 T}{\partial x^2} + \frac{\partial^2 T}{\partial y^2} + \frac{\partial^2 T}{\partial z^2} \right) \tag{1.17}$$

Another example of a linear second-order partial differential equation is the potential flow equation. Here we are considering an incompressible, irrotational flow with velocity components $u$ and $v$. The velocity components are related to the velocity potential $\Phi$ by

$$u = \frac{\partial \Phi}{\partial x}, \quad v = \frac{\partial \Phi}{\partial y} \tag{1.18}$$

From mass continuity, one obtains the following partial differential equation for the function $\Phi$

$$\frac{\partial^2 \Phi}{\partial x^2} + \frac{\partial^2 \Phi}{\partial y^2} = 0 \tag{1.19}$$

In contrast to the above given equations, the partial differential equation, which describes the flow of a compressible inviscid flow, is a nonlinear second-order partial differential equation

$$\left( \left( \frac{\partial \Phi}{\partial x} \right)^2 - c^2 \right) \frac{\partial^2 \Phi}{\partial x^2} + 2 \frac{\partial \Phi}{\partial x} \frac{\partial \Phi}{\partial y} \frac{\partial^2 \Phi}{\partial x \partial y} + \left( \left( \frac{\partial \Phi}{\partial y} \right)^2 - c^2 \right) \frac{\partial^2 \Phi}{\partial y^2} = 0 \tag{1.20}$$

where $c$ denotes the speed of sound. Another example of a nonlinear partial differential equation is the energy equation describing the one-dimensional transient heat conduction within a solid body whose thermal conductivity is a function of temperature. Additionally, an energy source term is incorporated in the material
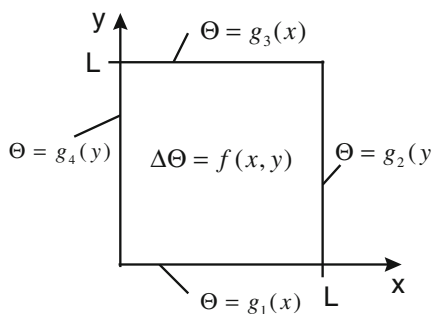
$$\rho c \frac{\partial T}{\partial t} = \frac{\partial}{\partial x} \left( k(T) \frac{\partial T}{\partial x} \right) + \dot{q}_i(x) \tag{1.21}$$

Summarizing, one can say that the order of a partial differential equation is given by the highest-ordered partial derivative appearing in the equation. A partial differential equation is called linear if it is linear in the unknown function and all its derivatives, i.e. the multiplying coefficients depend only on the independent variables. If the equation is linear in the highest-order derivative, it is called quasilinear. The Navier-Stokes

equations are a good example of quasilinear equations. If the nonlinearity appears also in the highest-order derivative, it is called a nonlinear partial differential equation. Finally, it should be noted that the equation is called non-homogeneous, if it contains one term which is only a function of the independent variables, otherwise it is called homogeneous. Equation (1.21) is a non-homogeneous equation, because it contains a heat source which is a function of $x$. On the other hand Eqs. (1.17), (1.19) and (1.20) are homogeneous equations.

The striking advantage in dealing with linear partial differential equations is that the final solution can be constructed by using the superposition method. This means that we can superimpose a number of solutions of much simpler problems to finally obtain the solution of a complicated problem. This is illustrated by the following simple example.
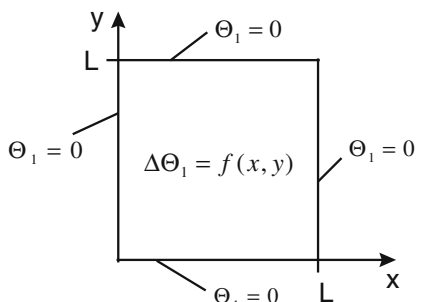
We consider the heat conduction within a quadratic flat plate which has the dimensions $L$ in the $x$- and $y$-direction. The region contains a heat source and the four boundaries are kept at different temperatures. The physical properties of the material are considered constant. The problem is then described by the following sketch and equations:



$$\frac{\partial^2 \Theta}{\partial x^2} + \frac{\partial^2 \Theta}{\partial y^2} = f(x,y)$$

$$\Theta(x,0) = g_1(x)$$
$$\Theta(L,y) = g_2(y)$$
$$\Theta(x,L) = g_3(x)$$
$$\Theta(0,y) = g_4(y)$$

Since the problem under consideration is described by a second-order linear partial differential equation, the solution can be obtained by superimposing the solutions of the following five simpler problems:



$$\Delta\Theta_1 = f(x,y)$$

$$\Theta_1(x,0) = 0$$
$$\Theta_1(L,y) = 0$$
$$\Theta_1(x,L) = 0$$
$$\Theta_1(0,y) = 0$$
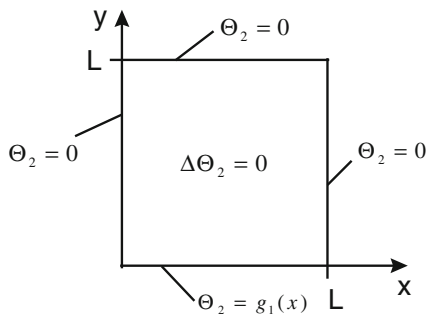
$$\Delta\Theta_2 = 0$$

$$\Theta_2(x,0) = g_1(x)$$
$$\Theta_2(L,y) = 0$$
$$\Theta_2(x,L) = 0$$
$$\Theta_2(0,y) = 0$$

+
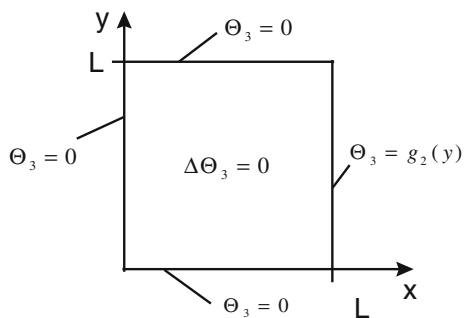


$$\Delta\Theta_3 = 0$$

$$\Theta_3(x,0) = 0$$
$$\Theta_3(L,y) = g_2(y)$$
$$\Theta_3(x,L) = 0$$
$$\Theta_3(0,y) = 0$$

+
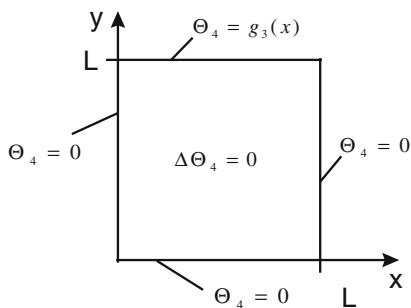


$$\Delta\Theta_4 = 0$$

$$\Theta_4(x,0) = 0$$
$$\Theta_4(L,y) = 0$$
$$\Theta_4(x,L) = g_3(x)$$
$$\Theta_4(0,y) = 0$$
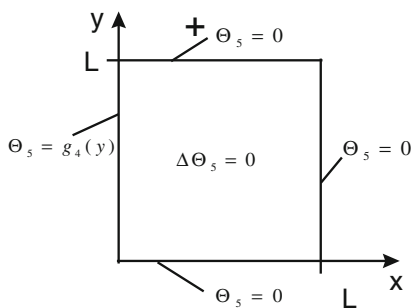


$$\Delta\Theta_5 = 0$$

$$\Theta_5(x,0) = 0$$
$$\Theta_5(L,y) = 0$$
$$\Theta_5(x,L) = 0$$
$$\Theta_5(0,y) = g_4(y)$$

After solving the above given individual problems, we know the solutions $\Theta_1$, $\Theta_2$, $\Theta_3$, $\Theta_4$ and $\Theta_5$. The solution of the original problem can then be obtained by simply adding all the solutions of the five sub-problems

$$\Theta = \sum_{i=1}^{5} \Theta_i \tag{1.22}$$

This can be visualized by looking at the individual equations and the related boundary conditions. Adding up the five individual partial differential equations results in

$$\frac{\partial^2 (\Theta_1 + \Theta_2 + \Theta_3 + \Theta_4 + \Theta_5)}{\partial x^2} + \frac{\partial^2 (\Theta_1 + \Theta_2 + \Theta_3 + \Theta_4 + \Theta_5)}{\partial y^2} = f(x, y)$$
$$\tag{1.23}$$

By adding up the boundary conditions of the individual problems, the boundary conditions of the original problem will be obtained.

This example shows clearly how powerful the superposition method is. Furthermore, the superposition method makes linear partial differential equations so much easier to solve than nonlinear partial differential equations, where the superposition approach fails.

**Problems**

1-1  State for each of the following partial differential equations if it is linear, quasilinear or nonlinear. In addition, state if the equation is homogeneous or non-homogeneous and give its order:

$$\rho c \frac{\partial T}{\partial x} = k \frac{\partial^2 T}{\partial y^2}$$

$$\frac{\partial^2 T}{\partial x^2} + \frac{\partial^2 T}{\partial y^2} = f(x, y)$$

$$\frac{\partial^4 u}{\partial x^4} + \frac{\partial^4 u}{\partial y^4} + 3 \frac{\partial^4 u}{\partial x^2 \partial y^2} + \frac{\partial u}{\partial x} = 5xy$$

$$2 \frac{\partial^2 u}{\partial x^2} + \ln u = 3 \left( x^2 + y^2 \right)$$

$$\frac{\partial^2 u}{\partial x^2} + u \frac{\partial u}{\partial x} = e^y$$

1-2  Consider the steady-state temperature distribution in a quadratic plate. The
     problem is given by

$$\frac{\partial^2 \Theta}{\partial \tilde{x}^2} + \frac{\partial^2 \Theta}{\partial \tilde{y}^2} = 0$$

with the boundary conditions

$$\Theta(0, \tilde{y}) = 0$$
$$\Theta(1, \tilde{y}) = \sin(\pi \tilde{y})$$
$$\Theta(\tilde{x}, 0) = 0$$
$$\Theta(\tilde{x}, 1) = \sin(3\pi \tilde{x})$$

(a) Use the superposition method to solve this problem. Split therefore the
    problem in two different problems (one which includes only the non-
    homogeneous boundary condition $\Theta_1(1, \tilde{y}) = \sin(\pi \tilde{y})$ and one including
    the condition with $\Theta_2(\tilde{x}, 1) = \sin(3\pi \tilde{x})$).
(b) By adding the equations and boundary conditions of the two problems
    $\Theta_1 + \Theta_2$, show that the original problem is obtained.
(c) Show by inserting, that the two problems have the solutions:

$$\Theta_1 = \frac{\sinh(\pi \tilde{x})}{\sinh(\pi)} \sin(\pi \tilde{y})$$

$$\Theta_2 = \frac{\sinh(3\pi \tilde{y})}{\sinh(3\pi)} \sin(3\pi \tilde{x})$$

(d) Show by insertion that $\Theta = \Theta_1 + \Theta_2$ satisfies the original problem.

1-3  An engineer wants to calculate the temperature distribution in a triangular
     plate with the dimensionless side length 1, which is shown in the following
     figure.
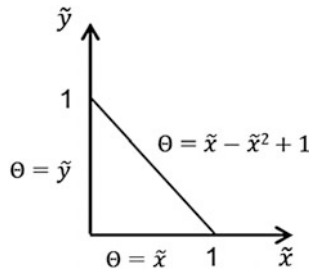
The dimensionless steady-state temperature distribution is given by the energy equation

$$\frac{\partial^2 \Theta}{\partial \tilde{x}^2} + \frac{\partial^2 \Theta}{\partial \tilde{y}^2} = 0$$

The dimensionless temperature takes the following values on the three sides of the triangle

$$
\begin{array}{llll}
\tilde{x} = 0: & \Theta = \tilde{y}, & 0 < \tilde{x} < 1 \\
\tilde{y} = 0: & \Theta = \tilde{x}, & 0 < \tilde{y} < 1 \\
\tilde{y} = 1 - \tilde{x}: & \Theta = \tilde{x} - \tilde{x}^2 + 1 &
\end{array}
$$

Because the engineer can't find a solution to this problem in his standard text books, he has the following idea: He wants to calculate the steady-state temperature in the following rectangular region.
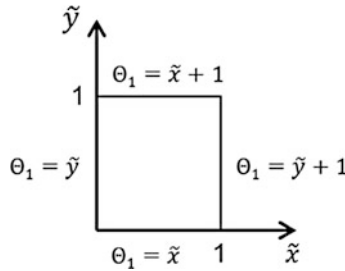


He thinks that when he is just using the temperature distribution in the lower triangular region, he will obtain the temperature distribution he is looking for.

(a) Solve the temperature distribution in the rectangular region by using the expression $\Theta = a_0 + a_1\tilde{x} + a_2\tilde{y} + a_3\tilde{x}\tilde{y}$. Which values do the constants $a_i$ take?

(b) Predict now the dimensionless temperature distribution on the side $\tilde{y} = 1 - \tilde{x}$ of the triangle and show that the engineer was not right with his assumption.

(c) Which additional problem needs the engineer to solve in order to solve the original problem?

(d) Use the above given expression for the dimensionless temperature again to solve the new problem and show that the combined solution fulfills now all boundary conditions.

# Chapter 2
# Linear Partial Differential Equations

Several important heat and fluid flow processes in technical applications and in nature can approximately be described by linear partial differential equations. As stated in the previous chapter, linear partial differential equations are normally much simpler to solve than nonlinear partial differential equations. In addition, a large body of literature exists on how to solve linear PDEs.

The following four chapters focus on the solution of linear partial differential equations. This chapter is concerned with the classification of second order partial differential equations and presents a short introduction into the method of separation of variables. Chapter 3 focuses on convective heat transfer in laminar and turbulent pipe and channel flows. Here parabolic problems are considered and the general eigenvalue problems, associated with these equations, are explained. Chapter 4 discusses some specific methods for the analytical solution of eigenvalue problems, in the case of large eigenvalues. Finally, Chap. 5 deals with convective heat transfer problems in laminar or turbulent pipe and channel flows for low Peclet numbers (liquid metals). For this type of applications, the axial heat conduction within the flow can no longer be ignored and the resulting energy equation remains elliptic in nature. This has strong implications on the solution method for the energy equation.

## 2.1 Classification of Second-Order Partial Differential Equations

In the following, we are concerned with a linear second order partial differential equation which depends on the two independent variables $x$ and $y$. The most general form of the homogeneous equation is given by

$$A(x,y)\frac{\partial^2 u}{\partial x^2} + 2B(x,y)\frac{\partial^2 u}{\partial x\partial y} + C(x,y)\frac{\partial^2 u}{\partial y^2} \tag{2.1}$$
$$+ D(x,y)\frac{\partial u}{\partial x} + E(x,y)\frac{\partial u}{\partial y} + F(x,y)u = 0$$

where $A, \ldots, F$ are constants or functions of $x$ and $y$ and are sufficiently differentiable in the domain of interest.

The form of Eq. (2.1) resembles the quadratic equation of a conic sections in analytical geometry. The equation

$$a x^2 + 2b\,xy + c\,y^2 + d\,x + e\,y + f = 0 \tag{2.2}$$

represents an ellipse, parabola or hyperbola depending on whether $b^2 - ac <, =, > 0$, respectively.

The classification of the second-order partial differential equation is based on the fact that Eq. (2.1) can be transformed into a standard form. This is very similar to the treatment of the quadratic Eq. (2.2) of conic sections in analytical geometry. We distinguish the following different cases (for the point $x_0$, $y_0$ under consideration):

$$1.\ B^2(x_0, y_0) - A(x_0, y_0)\,C(x_0, y_0) > 0 \tag{2.3}$$

is of hyperbolic type. There exist two real characteristic curves.

$$2.\ B^2(x_0, y_0) - A(x_0, y_0)\,C(x_0, y_0) = 0 \tag{2.4}$$

is of parabolic type. There exists one real characteristic curve.

$$3.\ B^2(x_0, y_0) - A(x_0, y_0)\,C(x_0, y_0) < 0 \tag{2.5}$$

is of elliptic type. The two characteristic curves are conjugate complex.

Each of these equations can be transformed into its standard form, if we introduce the following new coordinates into Eq. (2.1)

$$\begin{aligned} \xi &= \xi(x, y) \\ \eta &= \eta(x, y) \end{aligned} \tag{2.6}$$

Is the equation of hyperbolic type, the standard form is given by

$$\frac{\partial^2 u}{\partial \xi \partial \eta} = f_1\left(\xi, \eta,\, u,\, \frac{\partial u}{\partial \xi},\, \frac{\partial u}{\partial \eta}\right) \tag{2.7}$$

If we introduce the new coordinates

$$\begin{aligned} \bar{\bar{\xi}} &= \xi + \eta \\ \bar{\eta} &= \xi - \eta \end{aligned} \tag{2.8}$$

we obtain an alternative standard form of the hyperbolic equation

$$\frac{\partial^2 u}{\partial \bar{\bar{\xi}}^2} - \frac{\partial^2 u}{\partial \bar{\eta}^2} = f_2\left(\bar{\bar{\xi}}, \bar{\eta},\, u,\, \frac{\partial u}{\partial \bar{\bar{\xi}}},\, \frac{\partial u}{\partial \bar{\eta}}\right) \tag{2.9}$$

If the equation is of parabolic type, then the standard form is given by

$$\frac{\partial^2 u}{\partial \xi^2} = f_3\left(\xi, \eta, u, \frac{\partial u}{\partial \xi}, \frac{\partial u}{\partial \eta}\right) \quad \text{or} \quad \frac{\partial^2 u}{\partial \eta^2} = \bar{f}_3\left(\xi, \eta, u, \frac{\partial u}{\partial \xi}, \frac{\partial u}{\partial \eta}\right) \tag{2.10}$$

Finally, if the equation is of elliptic type, the standard form of the equation is given by

$$\frac{\partial^2 u}{\partial \tilde{\xi}^2} + \frac{\partial^2 u}{\partial \tilde{\eta}^2} = f_4\left(\tilde{\xi}, \tilde{\eta}, u, \frac{\partial u}{\partial \tilde{\xi}}, \frac{\partial u}{\partial \tilde{\eta}}\right) \tag{2.11}$$

where the new coordinates $\tilde{\xi}$, $\tilde{\eta}$ are defined by

$$\tilde{\xi} = \frac{1}{2}(\xi + \eta), \quad \tilde{\eta} = \frac{1}{2i}(\xi - \eta) \tag{2.12}$$

In order to obtain one of the above standard or canonical forms of the equation, we need to perform the coordinate transformation given by Eq. (2.6). Since we want the transformed equation to be equivalent to the original equation, we assume that $\xi$ and $\eta$ are twice continuously differentiable and we insist that the Jacobian $J \neq 0$

$$J = \left| \begin{pmatrix} \frac{\partial \xi}{\partial x} & \frac{\partial \xi}{\partial y} \\ \frac{\partial \eta}{\partial x} & \frac{\partial \eta}{\partial y} \end{pmatrix} \right| = \frac{\partial \xi}{\partial x}\frac{\partial \eta}{\partial y} - \frac{\partial \xi}{\partial y}\frac{\partial \eta}{\partial x} \neq 0 \tag{2.13}$$

in the region under consideration. By assuming that Eq. (2.13) holds, we have always a unique transformation between $x$, $y$ and $\xi$, $\eta$.

Use of the chain rule gives:

$$\left(\frac{\partial u}{\partial x}\right)_y = \left(\frac{\partial u}{\partial \xi}\right)_\eta \left(\frac{\partial \xi}{\partial x}\right)_y + \left(\frac{\partial u}{\partial \eta}\right)_\xi \left(\frac{\partial \eta}{\partial x}\right)_y \tag{2.14}$$

$$\left(\frac{\partial u}{\partial y}\right)_x = \left(\frac{\partial u}{\partial \xi}\right)_\eta \left(\frac{\partial \xi}{\partial y}\right)_x + \left(\frac{\partial u}{\partial \eta}\right)_\xi \left(\frac{\partial \eta}{\partial y}\right)_x$$

and also

$$\frac{\partial^2 u}{\partial x^2} = \frac{\partial^2 u}{\partial \xi^2}\left(\frac{\partial \xi}{\partial x}\right)^2 + 2\frac{\partial^2 u}{\partial \xi \partial \eta}\frac{\partial \xi}{\partial x}\frac{\partial \eta}{\partial x} + \frac{\partial^2 u}{\partial \eta^2}\left(\frac{\partial \eta}{\partial x}\right)^2 \tag{2.15}$$
$$+ \frac{\partial u}{\partial \xi}\frac{\partial^2 \xi}{\partial x^2} + \frac{\partial u}{\partial \eta}\frac{\partial^2 \eta}{\partial x^2}$$
$$\frac{\partial^2 u}{\partial x \partial y} = \frac{\partial^2 u}{\partial \xi^2}\frac{\partial \xi}{\partial x}\frac{\partial \xi}{\partial y} + \frac{\partial^2 u}{\partial \xi \partial \eta}\left(\frac{\partial \xi}{\partial x}\frac{\partial \eta}{\partial y} + \frac{\partial \xi}{\partial y}\frac{\partial \eta}{\partial x}\right)$$
$$+ \frac{\partial^2 u}{\partial \eta^2}\frac{\partial \eta}{\partial x}\frac{\partial \eta}{\partial y} + \frac{\partial u}{\partial \xi}\frac{\partial^2 \xi}{\partial x \partial y} + \frac{\partial u}{\partial \eta}\frac{\partial^2 \eta}{\partial x \partial y}$$
$$\frac{\partial^2 u}{\partial y^2} = \frac{\partial^2 u}{\partial \xi^2}\left(\frac{\partial \xi}{\partial y}\right)^2 + 2\frac{\partial^2 u}{\partial \xi \partial \eta}\frac{\partial \xi}{\partial y}\frac{\partial \eta}{\partial y} + \frac{\partial^2 u}{\partial \eta^2}\left(\frac{\partial \eta}{\partial y}\right)^2$$
$$+ \frac{\partial u}{\partial \xi}\frac{\partial^2 \xi}{\partial y^2} + \frac{\partial u}{\partial \eta}\frac{\partial^2 \eta}{\partial y^2}$$

After inserting the above expressions into Eq. (2.1), one obtains

$$\bar{A}(\xi,\eta)\frac{\partial^2 u}{\partial \xi^2} + 2\bar{B}(\xi,\eta)\frac{\partial^2 u}{\partial \xi \partial \eta} + \bar{C}(\xi,\eta)\frac{\partial^2 u}{\partial \eta^2}$$

$$+ \bar{D}(\xi,\eta)\frac{\partial u}{\partial \xi} + \bar{E}(\xi,\eta)\frac{\partial u}{\partial \eta} + Fu = 0 \tag{2.16}$$

with the coefficients

$$\bar{A} = A\left(\frac{\partial \xi}{\partial x}\right)^2 + 2B\frac{\partial \xi}{\partial x}\frac{\partial \xi}{\partial y} + C\left(\frac{\partial \xi}{\partial y}\right)^2 \tag{2.17}$$

$$\bar{B} = A\frac{\partial \xi}{\partial x}\frac{\partial \eta}{\partial x} + B\left(\frac{\partial \xi}{\partial x}\frac{\partial \eta}{\partial y} + \frac{\partial \xi}{\partial y}\frac{\partial \eta}{\partial x}\right) + C\frac{\partial \xi}{\partial y}\frac{\partial \eta}{\partial y}$$

$$\bar{C} = A\left(\frac{\partial \eta}{\partial x}\right)^2 + 2B\frac{\partial \eta}{\partial x}\frac{\partial \eta}{\partial y} + C\left(\frac{\partial \eta}{\partial y}\right)^2$$

$$\bar{D} = A\frac{\partial^2 \xi}{\partial x^2} + 2B\frac{\partial^2 \xi}{\partial x \partial y} + C\frac{\partial^2 \xi}{\partial y^2} + D\frac{\partial \xi}{\partial x} + E\frac{\partial \xi}{\partial y}$$

$$\bar{E} = A\frac{\partial^2 \eta}{\partial x^2} + 2B\frac{\partial^2 \eta}{\partial x \partial y} + C\frac{\partial^2 \eta}{\partial y^2} + D\frac{\partial \eta}{\partial x} + E\frac{\partial \eta}{\partial y}$$

Now we need to specify our change of variables, expressed by Eq. (2.6), in order to obtain one of the previously given standard or canonical forms. For example, if we want to obtain the hyperbolic equation in the form of Eq. (2.7) we have to assume that $\bar{A}$ and $\bar{C}$ are equal to zero. Because these two expressions are identical if we exchange $\xi$ and $\eta$, we can achieve the condition $\bar{A} = \bar{C} = 0$, only if $\xi$ and $\eta$ are both solutions of the following equation

$$A\left(\frac{\partial \Omega}{\partial x}\right)^2 + 2B\left(\frac{\partial \Omega}{\partial x}\right)\left(\frac{\partial \Omega}{\partial y}\right) + C\left(\frac{\partial \Omega}{\partial y}\right)^2 = 0; \quad \Omega = \xi \text{ or } \eta \tag{2.18}$$

Along a curve $\Omega = $ const. one has

$$d\Omega = \frac{\partial \Omega}{\partial x}dx + \frac{\partial \Omega}{\partial y}dy = 0 \quad \Rightarrow \frac{dy}{dx} = -\frac{\partial \Omega}{\partial x}\bigg/\frac{\partial \Omega}{\partial y} \tag{2.19}$$

we obtain from Eqs. (2.18) and (2.19) the following ordinary differential equation

$$A\left(\frac{dy}{dx}\right)^2 - 2B\left(\frac{dy}{dx}\right) + C = 0 \tag{2.20}$$

This differential equation can be solved for $dy/dx$ and one obtains the following two cases:

$$\frac{dy}{dx} = \left(B + \sqrt{B^2 - AC}\right)\Big/A \tag{2.21}$$

$$\frac{dy}{dx} = \left(B - \sqrt{B^2 - AC}\right)\Big/A$$

These two equations are known as the characteristic equations. They prescribe the functional relationship between the families of curves in the $xy$-plane for which $\xi$ = const. and $\eta$ = const. This means that a change of variables according to

$$\xi = f_1(x, y) \tag{2.22}$$

$$\eta = f_2(x, y)$$

will transform Eq. (2.1) into its standard form. From Eq. (2.21) it is apparent that there are three cases to be considered:

**Case 1** Hyperbolic equation $(B^2 - AC) > 0$
The preceding analysis results in a canonical form for the hyperbolic equation. For this case we have two real characteristics, which can be obtained from the ordinary differential Eq. (2.21).

**Case 2** Elliptic equation $(B^2 - AC) < 0$
For this case, one obtains from Eq. (2.21) no real, but two conjugate complex solutions. Therefore, the elliptic equation has two conjugate complex characteristics. The elliptic case needs not to be recalculated again, because it can be deduced from the calculation of the hyperbolic case. This can be shown as follows: let us consider the canonical form

$$\frac{\partial^2 u}{\partial \xi \partial \eta} = f_1\left(\xi, \eta, u, \frac{\partial u}{\partial \xi}, \frac{\partial u}{\partial \eta}\right) \tag{2.7}$$

Now, we have two conjugate complex characteristics. Therefore, we can introduce into the above equation the coordinate transform given by Eq. (2.12)

$$\tilde{\xi} = \frac{1}{2}(\xi + \eta) \tag{2.12}$$

$$\tilde{\eta} = \frac{1}{2i}(\xi - \eta)$$

Use of the chain rule according to Eq. (2.15) gives

$$
\begin{aligned}
\frac{\partial^2 u}{\partial \xi \partial \eta} &= \frac{\partial^2 u}{\partial \tilde{\xi}^2} \frac{\partial \tilde{\xi}}{\partial \xi} \frac{\partial \tilde{\xi}}{\partial \eta} + \frac{\partial^2 u}{\partial \tilde{\xi} \partial \tilde{\eta}} \left( \frac{\partial \tilde{\xi}}{\partial \xi} \frac{\partial \tilde{\eta}}{\partial \eta} + \frac{\partial \tilde{\xi}}{\partial \eta} \frac{\partial \tilde{\eta}}{\partial \xi} \right) \\
&+ \frac{\partial^2 u}{\partial \tilde{\eta}^2} \frac{\partial \tilde{\eta}}{\partial \xi} \frac{\partial \tilde{\eta}}{\partial \eta} + \frac{\partial u}{\partial \tilde{\xi}} \frac{\partial^2 \tilde{\xi}}{\partial \xi \partial \eta} + \frac{\partial u}{\partial \tilde{\eta}} \frac{\partial^2 \tilde{\eta}}{\partial \xi \partial \eta} \\
&= \frac{\partial^2 u}{\partial \tilde{\xi}^2} \frac{1}{4} + \frac{\partial^2 u}{\partial \tilde{\xi} \partial \tilde{\eta}} \left( -\frac{1}{4i} + \frac{1}{4i} \right) + \frac{\partial^2 u}{\partial \tilde{\eta}^2} \frac{1}{4} = \frac{1}{4} \left( \frac{\partial^2 u}{\partial \tilde{\xi}^2} + \frac{\partial^2 u}{\partial \tilde{\eta}^2} \right)
\end{aligned}
$$

and Eq. (2.7) is transformed into the standard form for the elliptic type, given by Eq. (2.11)

$$
\frac{\partial^2 u}{\partial \tilde{\xi}^2} + \frac{\partial^2 u}{\partial \tilde{\eta}^2} = f_4 \left( \tilde{\xi}, \tilde{\eta}, u, \frac{\partial u}{\partial \tilde{\xi}}, \frac{\partial u}{\partial \tilde{\eta}} \right) \tag{2.11}
$$

**Case 3** Parabolic equation $(B^2 - AC) = 0$
For this case, it can be seen from Eq. (2.21) that only one family of real characteristics exists. Because of this fact, we can set in Eq. (2.17) for example $\eta = x$. Note that this is only possible if $\xi$ depends on $y$, so that the Jacobian, defined by Eq. (2.13), is not zero. Then we obtain immediately from Eq. (2.17) that $\bar{C} = A$ while $\bar{B}$ is equal to

$$
\bar{B} = A \frac{\partial \xi}{\partial x} + B \frac{\partial \xi}{\partial y} \tag{2.23}
$$

This expression is identical to zero, as it can be deduced from Eq. (2.18) rewritten as follows—for the case $(B^2 - AC) = 0$:

$$
A \left( \frac{\partial \xi}{\partial x} \right)^2 + 2B \left( \frac{\partial \xi}{\partial x} \right) \left( \frac{\partial \xi}{\partial y} \right) + \frac{B^2}{A} \left( \frac{\partial \xi}{\partial y} \right)^2 = \frac{1}{A} \left( A \frac{\partial \xi}{\partial x} + B \frac{\partial \xi}{\partial y} \right)^2 = 0 \tag{2.24}
$$

Finally, the standard or canonical form of the parabolic equation, given by Eq. (2.10), is obtained if we divide Eq. (2.16) by $A$.

In order to illustrate the above shown classification, we will investigate some simple examples:

**Example 1** The equation

$$
\frac{\partial^2 u}{\partial x^2} + 2 \frac{\partial^2 u}{\partial x \partial y} + \frac{\partial^2 u}{\partial y^2} = 0 \tag{2.25}
$$

is parabolic, because the expression $B^2 - AC = 1 - 1 = 0$. The characteristic Eq. (2.21) reduces to

$$\frac{dy}{dx} = 1 \qquad (2.26)$$

which has the solution

$$y - x = C_1 \qquad (2.27)$$

If we change the coordinates according to

$$\xi = y - x \qquad (2.28)$$
$$\eta = x$$

where $\eta$ has been selected arbitrarily, although always respecting the condition that the Jacobian, defined in Eq. (2.13), is not equal to zero. Introducing the new coordinates into Eq. (2.25), we obtain

$$\frac{\partial^2 u}{\partial \eta^2} = 0 \qquad (2.29)$$

This equation has the general solution

$$u = \eta F(\xi) + H(\xi) = xF(y - x) + H(y - x) \qquad (2.30)$$

**Example 2** Consider the equation

$$y^4 \frac{\partial^2 u}{\partial x^2} - x^4 \frac{\partial^2 u}{\partial y^2} - 2yx^2 \frac{\partial u}{\partial x} = 0 \qquad (2.31)$$

From this equation, we obtain $B^2 - AC = x^4 y^4 > 0$. This shows that Eq. (2.31) is hyperbolic everywhere except along the coordinate axis ($x = 0$ or $y = 0$).

From Eq. (2.21) we obtain the following two ordinary differential equations for the characteristics

$$\frac{dy}{dx} = \left(B + \sqrt{B^2 - AC}\right) \Big/ A = \frac{x^2 y^2}{y^4} = \left(\frac{x}{y}\right)^2 \qquad (2.32)$$

and

$$\frac{dy}{dx} = -\left(\frac{x}{y}\right)^2 \qquad (2.33)$$

From the two Eqs. (2.32) and (2.33) we calculate the characteristic curves to be:

$$\frac{1}{3}\left(y^3 - x^3\right) = C_1; \quad \frac{1}{3}\left(y^3 + x^3\right) = C_2 \tag{2.34}$$

In order to transform Eq. (2.31) into its standard form, we have to perform the following coordinate transformation

$$\xi = \frac{1}{3}\left(y^3 - x^3\right) \tag{2.35}$$

$$\eta = \frac{1}{3}\left(y^3 + x^3\right)$$

Using Eqs. (2.14) and (2.15), one obtains

$$-4x^4 y^4 \frac{\partial^2 u}{\partial \xi \partial \eta} - 2\left(xy^4 + yx^4\right)\frac{\partial u}{\partial \xi} + 2\left(xy^4 - yx^4\right)\frac{\partial u}{\partial \eta} \tag{2.36}$$

$$- 2yx^2\left(-x^2 \frac{\partial u}{\partial \xi} + x^2 \frac{\partial u}{\partial \eta}\right) = 0$$

and after simplifying and replacing *x and y* by $\xi$ and $\eta$ we finally get

$$\frac{\partial^2 u}{\partial \xi \partial \eta} - \frac{1}{3}\frac{1}{\xi - \eta}\frac{\partial u}{\partial \xi} - \frac{1}{3}\frac{3\xi - \eta}{\eta^2 - \xi^2}\frac{\partial u}{\partial \eta} = 0 \tag{2.37}$$

**Example 3** We consider the wave equation

$$\frac{\partial^2 \Phi}{\partial t^2} - c^2 \frac{\partial^2 \Phi}{\partial x^2} = 0 \tag{2.38}$$

This equation describes for example the one-dimensional propagation of sound in a pipe. Because $B^2 - AC > 0$, the equation is hyperbolic in the region of interest.

The characteristic equations are given by

$$\frac{dt}{dx} = \left(B + \sqrt{B^2 - AC}\right)\Big/A = \frac{c}{-c^2} = -\frac{1}{c} \tag{2.39}$$

and

$$\frac{dt}{dx} = \frac{1}{c} \tag{2.40}$$

From these two equations we obtain $ct + x = C_1$ and $-ct + x = C_2$ and we get the following new coordinates:

$$\xi = x + ct \qquad (2.41)$$
$$\eta = x - ct$$

If we introduce this new coordinates into Eq. (2.38), we get the following simple partial differential equation

$$\frac{\partial^2 \Phi}{\partial \xi \, \partial \eta} = 0 \qquad (2.42)$$

which has the general solution

$$\Phi(\xi, \eta) = \Psi_1(\eta) + \Psi_2(\xi) \qquad (2.43)$$

or rewritten in $x$, $t$ coordinates

$$\Phi(x, t) = \Psi_1(x - ct) + \Psi_2(x + ct) \qquad (2.44)$$

This shows that the solution of Eq. (2.38) can be expressed as the superposition of two waves, which travel with constant velocity $c$ into different directions of the solution domain. This shows also nicely how the information in the problem is transported by the two real characteristics. The solution obtained here is known in literature as the d'Alembert solution.

## 2.2 Character of the Solutions for the Partial Differential Equations

In the preceding section we have concentrated on the classification of the different second-order partial differential equations. However, for solving actual physical problems, it is of great importance to discuss also the character of their solutions as well as the associated boundary conditions.

### 2.2.1 Parabolic Second-Order Equations

Let us start our discussion with the parabolic partial differential equation. As stated before, this equation has one real characteristic. As an example, we look at the heat conduction equation for a one-dimensional unsteady conduction problem in a slab (see Fig. 2.1). The slab has the thickness $l$ and the spatial coordinate ranges from $0 < x < l$.
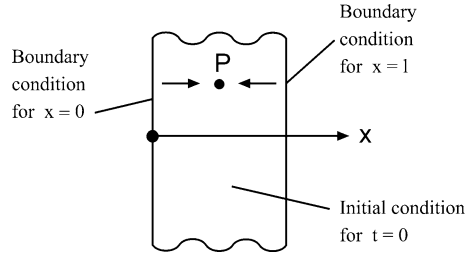
Assuming that the material properties of the slab are constant, the temperature
distribution in the slab can be obtained from the solution of the following equation

$$\rho c \, \frac{\partial T}{\partial t} = k \, \frac{\partial^2 T}{\partial x^2} \tag{2.45}$$

The temperature distribution of the slab at the beginning of the process ($t = 0$) is
given. This is the initial condition of the problem

$$T(0, x) = f_1(x) \tag{2.46}$$

In addition to this initial condition, boundary conditions have to be prescribed at
the surface of the slab for $x = 0$ and $x = l$. Here the following different types of
boundary conditions are possible:

- Boundary conditions of the first kind (Dirichlet wall boundary conditions). Here
  the temperature at the boundary is specified, for example

$$T(t, 0) = f_2(t), \quad T(t, l) = f_3(t) \tag{2.47}$$

- Boundary conditions of the second kind (Neumann conditions). For this type of
  boundary conditions the gradient is specified at the boundaries, for example

$$\left( \frac{\partial T}{\partial x} \right)_{x=0} = f_4(t), \quad \left( \frac{\partial T}{\partial x} \right)_{x=l} = f_5(t) \tag{2.48}$$

- Boundary conditions of the third kind. Here a combination of temperature and
  temperature gradient is prescribed at the surface. Such boundary conditions are
  relatively common in technical systems, since they describe, for example, the
  case of a slab which is heated or cooled by a fluid at temperature $T_1$ or $T_2$
  flowing over the boundaries of the slab. A typical example is

$$k \left( \frac{\partial T}{\partial x} \right)_{x=0} = h_1(T(t, 0) - T_1), \tag{2.49}$$

$$k \left( \frac{\partial T}{\partial x} \right)_{x=l} = h_2(T(t, l) - T_2)$$

where $h_1$ and $h_2$ are heat transfer coefficients.

Of course, all the above mentioned boundary conditions can be present in any possible combination, for example: at $x = 0$, a constant wall temperature is prescribed; whereas, at $x = l$, a boundary condition of the third kind is applied.

Summarising the above discussion, it can be seen that for the parabolic second-order partial differential equation an initial condition together with boundary conditions at the surface need to be specified. This means that the temperature at an arbitrary point P in the domain (see Fig. 2.1) is always influenced by the wall boundary conditions at $x = 0$ and $x = l$. In addition, all disturbances, which are specified for $t = 0$, will propagate into the solution domain for all subsequent times. On the other hand disturbances, which are introduced at a later time $t_1$, can not influence the solution for $t < t_1$. This shows nicely the character of the solution, which depends only on one real characteristic.

### 2.2.2  Elliptic Second-Order Equations

For the elliptic equation, the characteristic curves are families of conjugate complex functions. In order to investigate the character of the solutions and the boundary conditions needed for this type of equations, we select as an example the steady-state heat conduction in a square plate $(0 \leq x \leq a, \ 0 \leq y \leq a)$, as shown in Fig. 2.2.

The steady-state temperature distribution is obtained from the solution of the following equation

$$\frac{\partial^2 T}{\partial x^2} + \frac{\partial^2 T}{\partial y^2} = 0 \tag{2.50}$$

For this type of equation, boundary conditions have to be prescribed along each point of the boundary. We might illustrate this for the here given example. Here the following different types of boundary conditions can be assigned:

**Fig. 2.2**  Steady-state heat conduction in a square plate
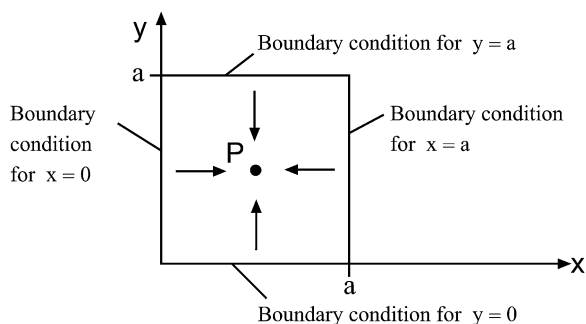
- Boundary conditions of the first kind (Dirichlet conditions). The temperature is specified at each point of the boundary

$$T(x,0) = T_1(x), \quad T(x,a) = T_2(x) \tag{2.51}$$
$$T(0,y) = T_3(y), \quad T(a,y) = T_4(y)$$

- Boundary conditions of the second kind (Neumann conditions). The heat flux normal to the wall is specified along the boundary.

$$\left(\frac{\partial T}{\partial x}\right)_{x=0} = f_1(y), \quad \left(\frac{\partial T}{\partial x}\right)_{x=a} = f_2(y) \tag{2.52}$$
$$\left(\frac{\partial T}{\partial y}\right)_{y=0} = f_3(x), \quad \left(\frac{\partial T}{\partial y}\right)_{y=a} = f_4(x)$$

- Boundary conditions of the third kind. This might be again a combination of the normal gradient at the surface and the temperature. One example is:

$$k\left(\frac{\partial T}{\partial x}\right)_{x=0} = f_1(T(0,y) - T_1), \quad k\left(\frac{\partial T}{\partial x}\right)_{x=a} = f_2(T(a,y) - T_2) \tag{2.53}$$
$$k\left(\frac{\partial T}{\partial y}\right)_{y=0} = f_3(T(x,0) - T_3), \quad k\left(\frac{\partial T}{\partial y}\right)_{y=a} = f_4(T(x,a) - T_4)$$

Again, the boundary conditions can be applied as mixed boundary conditions.

From the above examples, it can be seen that for an elliptic equation we have to deal with a boundary-value problem, whereas for the parabolic equation, we had to solve a combined initial-boundary value problem. This means that for the elliptic problem any disturbance, which is brought into the region of interest (for example by slightly changing one boundary condition), will immediately influence the solution of the problem at a given point in the domain (see point P in Fig. 2.2).

### 2.2.3 Hyperbolic Second-Order Equations

Hyperbolic partial differential equations mainly appear in vibration and wave problems. These equations have two real characteristics. The one-dimensional wave equation for a perfectly flexible string serves here as an example to explain the character of the solution and the associated boundary conditions (see Fig. 2.3).

The differential equation is given by

$$\frac{\partial^2 u}{\partial x^2} - \frac{1}{b^2} \frac{\partial^2 u}{\partial t^2} = 0 \tag{2.54}$$
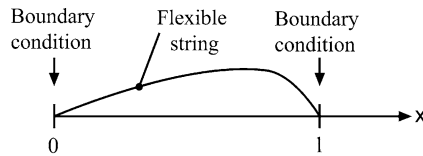
**Fig. 2.3** Flexible string

where $b$ is a constant. As shown in the previous section (see Eq. (2.44)), the general solution of this equation is given by

$$u(x,t) = \Psi_1(x + bt) + \Psi_2(x - bt) \tag{2.55}$$

Therefore, it would be easiest to prescribe boundary conditions for Eq. (2.54) along two parts of the characteristics intersecting at one point. This would be a complete initial value problem. However, for most physical problems, this description of the boundary conditions is not typical. Instead, the following boundary conditions might be normally applied:

- Boundary conditions of the first kind. Here the deflection of the string at the location $x = 0$ and $x = l$ might be prescribed.

$$u(0,t) = f_1(t), \quad u(l,t) = f_2(t) \tag{2.56}$$

  If the string is fixed at the locations $x = 0$ and $x = l$, $f_1$ and $f_2$ will be zero.
- Boundary conditions of the second kind. Here we will prescribe $\partial u/\partial x$ for $x = 0$ and $x = l$.
- For the boundary conditions of the third kind, we will specify a combination of $u$ and $\partial u/\partial x$ for $x = 0$ and $x = l$.

As for all other types of equations, the boundary conditions can also be applied in a mixed form.

In addition to the two boundary conditions at $x = 0$ and $x = l$, initial conditions for $t = 0$ have to be specified for the problem. These initial conditions for the finite string could be that $u(x,0) = f_3(x)$, $\partial u/\partial t(x,0) = f_4(x)$.

## 2.3 Separation of Variables

This section gives an introduction into the method of separation of variables. This method is one of the most commonly used methods for solving linear partial differential equations. The method is explained in the following sections by two basic examples. In the next chapters, more advanced problems are considered.
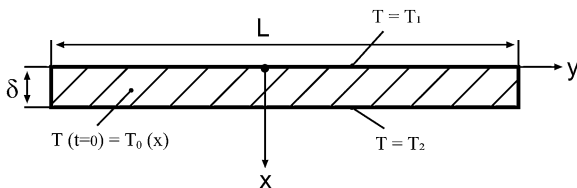
**Fig. 2.4** Transient heat conduction in a slab

## 2.3.1 One-Dimensional Transient Heat Conduction in a Slab

We consider the energy equation for heat conduction in a slab. The problem is depicted in Fig. 2.4. The slab has the thickness $\delta$ and the length $L$. At the two surfaces $x = 0$ and $x = \delta$ the slab is subjected to constant temperatures.

Under the assumption that the material properties of the plate are constant, the energy equation takes the following form

$$\rho c \frac{\partial T}{\partial t} = k \left( \frac{\partial^2 T}{\partial x^2} + \frac{\partial^2 T}{\partial y^2} \right) \tag{2.57}$$

We now assume that the dimension $L$ is much larger than $\delta$, so that the heat conduction in the $y$-direction is negligible compared to the heat conduction in the $x$-direction. Therefore, the problem simplifies to

$$\frac{\partial T}{\partial t} = a \frac{\partial^2 T}{\partial x^2} \tag{2.58}$$

where $a = k/(\rho c)$ is the thermal diffusivity of the material. Equation (2.57) has to be solved together with the following boundary conditions

$$\begin{aligned} x = 0 &: T = T_1 \\ x = \delta &: T = T_2 \end{aligned} \tag{2.59}$$

and the initial condition

$$t = 0 : T = T_0(x) \tag{2.60}$$

This problem is described by a parabolic equation. This means that one real characteristic exists for the solution. Before solving the above given problem, we first introduce the dimensionless quantities

$$\tilde{x} = \frac{x}{\delta}, \quad \tilde{t} = \frac{at}{\delta^2}, \quad \Theta = \frac{T - T_1}{T_2 - T_1} \tag{2.61}$$

This results in the following problem

$$\frac{\partial \Theta}{\partial \tilde{t}} = \frac{\partial^2 \Theta}{\partial \tilde{x}^2} \qquad (2.62)$$

with the boundary conditions

$$\tilde{x} = 0 : \Theta = 0 \qquad (2.63)$$
$$\tilde{x} = 1 : \Theta = 1$$
$$\tilde{t} = 0 : \Theta = (T_0(\tilde{x}) - T_1)/(T_2 - T_1) = \Theta_0(\tilde{x})$$

Before applying the method of separation of variables to the Eqs. (2.62) and (2.63), we want to investigate the solution domain, shown in Fig. 2.5. Here the parabolic nature of the problem is clearly visible. The initial condition for $\tilde{t} = 0$ is propagated into the solution domain for larger times. Any disturbance introduced into the problem at $\tilde{t} = \tilde{t}_1$ will therefore only influence the solution at subsequent times. The solution for $\tilde{t} < \tilde{t}_1$ remains unchanged.

Let us assume that the solution of the problem can be expressed in the form

$$\Theta = H(\tilde{t})G(\tilde{x}) \qquad (2.64)$$

Introducing Eq. (2.64) into the boundary conditions, results in:

$$\tilde{x} = 0 : H(\tilde{t})G(0) = 0 \qquad (2.65)$$
$$\tilde{x} = 1 : H(\tilde{t})G(1) = 1$$

From this equation we notice immediately that using the expression (2.64) can not result in a solution to the present problem, because the boundary condition for $\tilde{x} = 1$ can not be satisfied if $H(\tilde{t})$ is an arbitrary function of $\tilde{t}$. Therefore, we conclude that we first have to make the boundary conditions homogenous, in order to find a solution with the help of Eq. (2.64). This can be done by splitting the solution into two parts

$$\Theta = \Theta_S(\tilde{x}) + \Theta_T(\tilde{x}, \tilde{t}) \qquad (2.66)$$



Fig. 2.5 Solution domain for the transient conduction in the slab

The steady-state solution $\Theta_S$ is simply a linear distribution and is given by

$$\Theta_S(\tilde{x}) = \tilde{x} \tag{2.67}$$

Introducing Eq. (2.66) into the Eqs. (2.62) and (2.63) results in the following problem for $\Theta_T$

$$\frac{\partial \Theta_T}{\partial \tilde{t}} = \frac{\partial^2 \Theta_T}{\partial \tilde{x}^2} \tag{2.68}$$

with the boundary conditions

$$
\begin{aligned}
&\tilde{x} = 0 : \Theta_T = 0 \\
&\tilde{x} = 1 : \Theta_T = 0 \\
&\tilde{t} = 0 : \Theta_T = \Theta_0(\tilde{x}) - \Theta_S(\tilde{t}=0) = \Theta_0(\tilde{x}) - \tilde{x}
\end{aligned}
\tag{2.69}
$$

Introducing now again the product of functions, given by Eq. (2.64), we obtain the boundary conditions

$$
\begin{aligned}
&\tilde{x} = 0 : H(\tilde{t})G(0) = 0 \quad \Rightarrow G(0) = 0 \\
&\tilde{x} = 1 : H(\tilde{t})G(1) = 0 \quad \Rightarrow G(1) = 0
\end{aligned}
\tag{2.70}
$$

This shows that the expression given by Eq. (2.64) is able to satisfy the two boundary conditions of the problem. Therefore, this approach promises to be successful. Introducing Eq. (2.64) into the partial differential Eq. (2.68), one obtains

$$H'(\tilde{t})G(\tilde{x}) = G''(\tilde{x})H(\tilde{t}) \tag{2.71}$$

By separating the variables, this equation can be rewritten as

$$\frac{H'(\tilde{t})}{H(\tilde{t})} = \frac{G''(\tilde{x})}{G(\tilde{x})} \tag{2.72}$$

The left hand side of this equation is only a function of $\tilde{t}$, whereas the right hand side is only a function of $\tilde{x}$. Therefore, both sides of the equation must be constant. This constant is set to $C_1$.

$$\frac{H'(\tilde{t})}{H(\tilde{t})} = \frac{G''(\tilde{x})}{G(\tilde{x})} = C_1 \tag{2.73}$$

Let us first investigate the differential equation for the function $H$. This equation takes the form

$$\frac{H'(\tilde{t})}{H(\tilde{t})} = C_1 \tag{2.74}$$

and can easily been integrated to give

$$H(\tilde{t}) = C_2 \exp(C_1\tilde{t}) \tag{2.75}$$

If we have a closer look at this equation, it can be seen that the function $H(\tilde{t})$ tends to infinity for $\tilde{t} \to \infty$ if $C_1 > 0$. However, this would not lead to a physically meaningful solution for the problem, because the temperature would tend to infinity for large times. For $C_1 = 0$, Eq. (2.75) results in a constant for $H(\tilde{t})$ and the time dependence of the solution would be lost. Therefore, we can conclude that the constant $C_1$ must always be smaller than zero for the problem under consideration. This can be expressed by replacing the constant by $C_1 = -\lambda^2$. Then we obtain for the function $H$

$$H(\tilde{t}) = C_2 \exp(-\lambda^2\tilde{t}) \tag{2.76}$$

For the function $G(\tilde{x})$, one obtains the following ordinary differential equation from Eq. (2.73)

$$\frac{G''(\tilde{x})}{G(\tilde{x})} = -\lambda^2 \quad \Rightarrow G'' + \lambda^2 G = 0 \tag{2.77}$$

This equation has to be solved together with the homogeneous boundary conditions given by Eq. (2.70). It has the trivial solution $G = 0$ and will have further solutions for selected values of $\lambda$. These selected values of $\lambda$ are called the eigenvalues of Eq. (2.77). The problem given by Eq. (2.77) and associated boundary conditions, see Eq. (2.70), is called an eigenvalue problem. This sort of problem is discussed in more detail in Chap. 3. The general solution of Eq. (2.77) is given by

$$G(\tilde{x}) = C_3 \sin(\lambda\tilde{x}) + C_4 \cos(\lambda\tilde{x}) \tag{2.78}$$

where the solution must satisfy the two boundary conditions

$$G(0) = 0, \quad G(1) = 0 \tag{2.79}$$

From the boundary condition $G(0) = 0$, it follows that $C_4$ is zero and one obtains

$$G = C_3 \sin(\lambda\tilde{x}) \tag{2.80}$$

Now, if we apply the second boundary condition $G(1) = 0$, we find

$$0 = C_3 \sin(\lambda \cdot 1) \tag{2.81}$$

Equation (2.81) shows that either $C_3$ has to be zero (which would be the trivial solution of the problem, where $G = 0$) or that $\sin(\lambda)$ has to be zero. The latter is only possible if

$$\lambda = n\pi \quad \text{with} \quad n = 1, 2, 3, \ldots \tag{2.82}$$

These special values of $\lambda$ are the eigenvalues of Eq. (2.77) and are shown in Fig. 2.6.
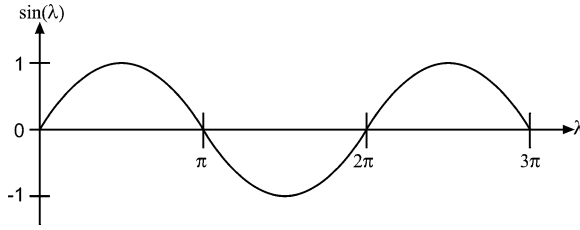
**Fig. 2.6** Eigenvalues of the eigenfunction $\sin(\lambda)$

The solution for $\Theta_T$ is obtained from the Eqs. (2.75) and (2.80) as

$$\Theta_T = C_2 \exp\left(-\lambda^2 \tilde{t}\right) \, C_3 \sin(\lambda \tilde{x}) \tag{2.83}$$

For simplicity, we combine the constants $C_2$ and $C_3$ and have

$$\Theta_T = C \, \sin(\lambda \tilde{x}) \exp\left(-\lambda^2 \tilde{t}\right) \tag{2.84}$$

Now we try to fulfill the initial condition using Eq. (2.84). Inserting Eq. (2.84) into Eq. (2.69) results in

$$\tilde{t} = 0 : \Theta_T = \Theta_0(\tilde{x}) - \tilde{x} = C \sin(\lambda \tilde{x}) \exp\left(-\lambda^2 0\right) \tag{2.85}$$
$$\Rightarrow \Theta_0(\tilde{x}) - \tilde{x} = C \sin(\lambda \tilde{x})$$

From the equation above, one can see that Eq. (2.84) is automatically a solution of the problem if

$$\Theta_0(\tilde{x}) = \tilde{x} + C \sin(n\pi x), \quad n = 1, 2, 3, \ldots \tag{2.86}$$

However, from Eq. (2.82) it is clear that there is an infinite number of eigenvalues. Because the partial differential equation is linear, we use the principle of superposition to construct the final solution of the problem. This means that the solution will be given by

$$\Theta_T = \sum_{n=1}^{\infty} C_n \sin(\lambda_n \tilde{x}) \exp\left(-\lambda_n^2 \tilde{t}\right) \tag{2.87}$$

This solution has to fulfil the initial condition. Inserting Eq. (2.87) into Eq. (2.69) results in

$$\Theta_0(\tilde{x}) - \tilde{x} = \sum_{n=1}^{\infty} C_n \sin(\lambda_n \tilde{x}) \tag{2.88}$$

which means that we have to represent the function $\Theta_0(\tilde{x}) - \tilde{x}$ by a Fourier series (see Stephenson 1986, Myint-U and Debnath 1987, Zauderer 1989, Sommerfeld 1978).

In order to obtain the unknown coefficients $C_n$, from Eq. (2.88), we multiply both sides of the equation by $\sin(\lambda_m \tilde{x})$ and integrate the resulting expressions across the region of interest for $\tilde{x}$ between zero and one. This results in

$$\int_0^1 (\Theta_0(\tilde{x}) - \tilde{x}) \sin(\lambda_m \tilde{x}) d\tilde{x} = \int_0^1 \sum_{n=1}^{\infty} C_n \sin(\lambda_n \tilde{x}) \sin(\lambda_m \tilde{x}) d\tilde{x} \tag{2.89}$$

Exchanging the summation and integration signs on the right hand side of this equation leads to

$$\int_0^1 (\Theta_0(\tilde{x}) - \tilde{x}) \sin(\lambda_m \tilde{x}) d\tilde{x} = \sum_{n=1}^{\infty} C_n \int_0^1 \sin(\lambda_m \tilde{x}) \sin(\lambda_n \tilde{x}) d\tilde{x} \tag{2.90}$$

If we now evaluate the integrals on the right side of Eq. (2.90), we find that

$$\int_0^1 \sin(\lambda_m \tilde{x}) \sin(\lambda_n \tilde{x}) d\tilde{x} = 0 \quad \text{for } n \neq m \tag{2.91}$$

$$= \int_0^1 \sin^2(\lambda_n \tilde{x}) d\tilde{x} = \frac{1}{2} \quad \text{for } n = m$$

Writing Eq. (2.90) in detail gives

$$\int_0^1 (\Theta_0(\tilde{x}) - \tilde{x}) \sin(m\pi\tilde{x}) d\tilde{x} = C_1 \int_0^1 \sin(m\pi\tilde{x}) \sin(\pi\tilde{x}) d\tilde{x} \tag{2.90}$$

$$+ C_2 \int_0^1 \sin(m\pi\tilde{x}) \sin(2\pi\tilde{x}) d\tilde{x}$$

$$+ C_n \int_0^1 \sin^2(n\pi\tilde{x}) d\tilde{x} \quad (\text{for } n = m)$$

$$+ C_\alpha \int_0^1 \sin(m\pi\tilde{x}) \sin(\alpha\pi\tilde{x}) d\tilde{x} + \cdots$$

From Eq. (2.91) one can see that in the sum on the right hand side of this equation only the term containing $C_n$ will be non-zero. Therefore, Eq. (2.90) reduces to

$$\int_0^1 (\Theta_0(\tilde{x}) - \tilde{x}) \sin(n\pi\tilde{x}) d\tilde{x} = C_n \int_0^1 \sin^2(n\pi\tilde{x}) d\tilde{x} \tag{2.92}$$

From Eq. (2.92), the unknown constants $C_n$ can be evaluated to be

$$C_n = \frac{\int_0^1 (\Theta_0(\tilde{x}) - \tilde{x}) \sin(n\pi\tilde{x})d\tilde{x}}{\int_0^1 \sin^2(n\pi\tilde{x})d\tilde{x}} = 2 \int_0^1 (\Theta_0(\tilde{x}) - \tilde{x}) \sin(n\pi\tilde{x})d\tilde{x} \qquad (2.93)$$

Thus the solution of the problem is given by Eq. (2.66) with the steady-state solution according to Eq. (2.67) and the transient solution according to Eq. (2.87). Thus,

$$\Theta = \tilde{x} + \sum_{n=1}^{\infty} C_n \sin(n\pi\tilde{x}) \exp\left(-(n\pi)^2\tilde{t}\right) \qquad (2.94)$$

In order to show the transient evolution of the temperature field, we select $\Theta_0(\tilde{x}) = 1$ for the above example. Using this initial condition, Eq. (2.93) becomes

$$C_n = 2 \int_0^1 (1 - \tilde{x}) \sin(n\pi\tilde{x})d\tilde{x} = \frac{2}{n\pi} \qquad (2.95)$$

and the temperature distribution in the solid is given by

$$\Theta = \tilde{x} + \sum_{n=1}^{\infty} \frac{2}{n\pi} \sin(n\pi\tilde{x}) \exp\left(-(n\pi)^2\tilde{t}\right) \qquad (2.96)$$

This temperature distribution is shown in Fig. 2.7 for different times. One can see nicely that the temperature distribution in the solid changes from the prescribed



Fig. 2.7 Transient temperature distribution in the slab for selected times
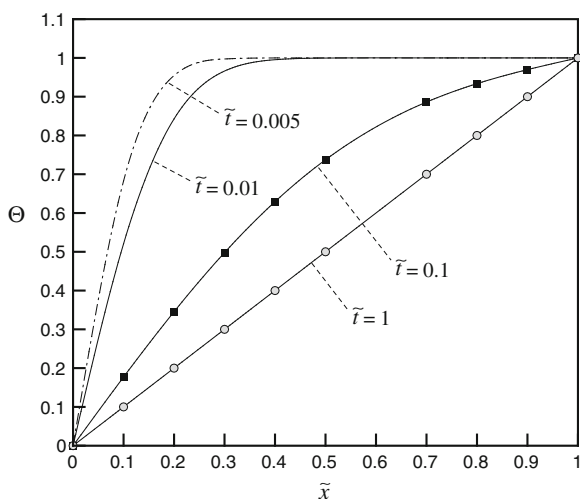
constant initial temperature distribution to the linear temperature shape for the steady-state temperature distribution for $\tilde{t} \to \infty$.

In addition, one can see from Eq. (2.96) that the individual parts of the sum in this equation are decaying rapidly with increasing time (notice that the argument of the exponential function contains $(n\pi)^2$ as a multiplier).

## 2.3.2 Steady-State Heat Conduction in a Rectangular Plate

As a second example to explain the method of separation of variables, we investigate the heat conduction in a rectangular plate, with the height $c$ and width $b$ (see Fig. 2.8).

All four sides of the plate are set to a constant temperature $T_0$. Inside the rectangular area, a sink is located with constant sink intensity $K$. Assuming constant physical properties, the energy equation for this steady-state heat conduction problem is given by

$$0 = k\left(\frac{\partial^2 T}{\partial x^2} + \frac{\partial^2 T}{\partial y^2}\right) + K \tag{2.97}$$

with the boundary conditions

$$T(b/2, y) = T_0, \quad T(-b/2, y) = T_0 \tag{2.98}$$
$$T(x, c/2) = T_0, \quad T(x, -c/2) = T_0$$

As in the first example we first introduce dimensionless quantities, before proceeding with the solution of the problem. Suitable dimensionless quantities are given by

$$\Theta = \frac{T - T_0}{T_0}, \quad \tilde{x} = \frac{x}{c/2}, \quad \tilde{y} = \frac{y}{c/2} \tag{2.99}$$



**Fig. 2.8** Geometrical configuration and boundary conditions for the heat conduction problem in a flat plate
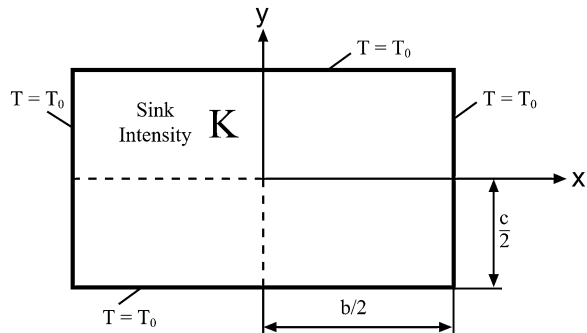
Introducing these quantities into Eqs. (2.97) and (2.98) results in

$$0 = \frac{\partial^2 \Theta}{\partial \tilde{x}^2} + \frac{\partial^2 \Theta}{\partial \tilde{y}^2} + \bar{K} \tag{2.100}$$

$$\Theta(A, \tilde{y}) = 0, \quad \Theta(-A, \tilde{y}) = 0 \tag{2.101}$$
$$\Theta(\tilde{x}, 1) = 0, \quad \Theta(\tilde{x}, -1) = 0$$

where the following abbreviations have been used:

$$\bar{K} = \frac{Kc^2}{4kT_0}, \quad A = \frac{b}{c} \tag{2.102}$$

This problem is described by an elliptic second-order partial differential equation. The boundary conditions, expressed by Eq. (2.101), are homogeneous, but the differential Eq. (2.100) is not.

In order to find a solution of the problem, we make once again use of the method of superposition, since the partial differential equation is linear, and split the solution into two parts

$$\Theta = \Theta_h + \Theta_p \tag{2.103}$$

$\Theta_h$ represents the solution of the homogeneous differential equation (without a sink, $K = 0$) and $\Theta_p$ is one particular solution of the problem. Let us first focus on the particular solution of the problem. In order to find this solution, we assume that $\Theta_p = f(\tilde{y})$. Alternatively, we could also assume $\Theta_p = f(\tilde{x})$ and obtain the same final solution of the problem. The analysis, however, would be altered.

If we substitute $\Theta_p = f(\tilde{y})$, into Eq. (2.100), the following relation for the function $f(\tilde{y})$ is obtained

$$f''(\tilde{y}) = -\bar{K} \quad \Rightarrow f(\tilde{y}) = -\frac{1}{2}\bar{K}\tilde{y}^2 + C_1\tilde{y} + C_2 \tag{2.104}$$

Since we need only one particular solution of the problem, we could set $C_1$ and $C_2$ equal to zero. However, a better choice is to select the constants $C_1$ and $C_2$ in such a way that the two boundary conditions $\Theta_p(\tilde{x}, 1) = 0$, $\Theta_p(\tilde{x}, -1) = 0$ are satisfied. If we do so, we obtain the following solution of the problem

$$\Theta_p = \frac{\bar{K}}{2}\left(1 - \tilde{y}^2\right) \tag{2.105}$$

After having obtained the solution for $\Theta_p$, one has to solve the following problem for $\Theta_h$ which is deduced from the Eqs. (2.100) and (2.101)

$$0 = \frac{\partial^2 \Theta_h}{\partial \tilde{x}^2} + \frac{\partial^2 \Theta_h}{\partial \tilde{y}^2} \tag{2.106}$$

$$\Theta_h(A, \tilde{y}) = -\bar{K}/2\left(1 - \tilde{y}^2\right), \quad \Theta_h(-A, \tilde{y}) = -\bar{K}/2\left(1 - \tilde{y}^2\right) \tag{2.107}$$
$$\Theta_h(\tilde{x}, 1) = 0, \qquad\qquad \Theta_h(\tilde{x}, -1) = 0$$

Note that the differential equation for $\Theta_h$ is now homogeneous, whereas two of the boundary conditions are non-homogeneous. Furthermore, note that the two boundary conditions, corresponding to a constant value of $\tilde{y}$, are still homogeneous. This is of importance for the subsequent analysis of the problem.

We now assume that Eq. (2.106) has a solution, which can be obtained by the method of separation of variables. Thus

$$\Theta_h = F(\tilde{x}) G(\tilde{y}) \tag{2.108}$$

Introducing Eq. (2.108) into the Eqs. (2.106) and (2.107) results in

$$F''(\tilde{x}) G(\tilde{y}) + G''(\tilde{y}) F(\tilde{x}) = 0 \tag{2.109}$$

from which we obtain

$$\frac{F''(\tilde{x})}{F(\tilde{x})} = -\frac{G''(\tilde{y})}{G(\tilde{y})} = \pm \lambda^2 \tag{2.110}$$

From Eq. (2.110), one notices that a physically plausible solution occurs for both $+\lambda^2$ and $-\lambda^2$. In order to investigate this problem further, we analyse in more detail the solutions for the function $G(\tilde{y})$. From Eq. (2.110) we get

$$G_1''(\tilde{y}) + \lambda^2 G_1(\tilde{y}) = 0 \quad \text{for } +\lambda^2 \tag{2.111}$$

$$G_2''(\tilde{y}) - \lambda^2 G_2(\tilde{y}) = 0 \quad \text{for } -\lambda^2 \tag{2.112}$$

which gives rise to the following two possible solutions

$$G_1(\tilde{y}) = C_3 \cos(\lambda \tilde{y}) + C_4 \sin(\lambda \tilde{y}) \tag{2.113}$$

$$G_2(\tilde{y}) = C_3 \cosh(\lambda \tilde{y}) + C_4 \sinh(\lambda \tilde{y}) \tag{2.114}$$

If we now reconsider the problem to be solved (Eqs. (2.106) and (2.107)), one can see that $\Theta_h = F(\tilde{x}) G(\tilde{y})$ has to be zero for $\tilde{y} = \pm 1$. If we satisfy these two boundary conditions by Eq. (2.114), we obtain only the trivial solution, because the functions $\cosh(\lambda \tilde{y})$ and $\sinh(\lambda \tilde{y})$ have only one zero point. Instead, if we satisfy the two boundary conditions by Eq. (2.113), we obtain an equation, which determines the eigenvalues. Therefore, Eq. (2.113) is the desired solution and thus, we have to select $+\lambda^2$ in Eq. (2.110).

For the function $F(\tilde{x})$, one obtains from Eq. (2.110)

$$F''(\tilde{x}) - \lambda^2 F(\tilde{x}) = 0 \tag{2.115}$$

which has the solution

$$F(\tilde{x}) = C_5 \cosh(\lambda \tilde{x}) + C_6 \sinh(\lambda \tilde{x}) \tag{2.116}$$

Combining the solutions for $F$ and $G$ leads to the following expression for $\Theta_h$

$$\Theta_h = (C_3 \cos(\lambda \tilde{y}) + C_4 \sin(\lambda \tilde{y}))(C_5 \cosh(\lambda \tilde{x}) + C_6 \sinh(\lambda \tilde{x})) \tag{2.117}$$

This expression has to satisfy the boundary conditions given by Eq. (2.107)

$$\begin{aligned} \Theta_h(A, \tilde{y}) &= -\bar{K}/2(1 - \tilde{y}^2), \quad \Theta_h(-A, \tilde{y}) = -\bar{K}/2(1 - \tilde{y}^2) \\ \Theta_h(\tilde{x}, 1) &= 0, \qquad\qquad\qquad \Theta_h(\tilde{x}, -1) = 0 \end{aligned} \tag{2.107}$$

Applying the two boundary conditions for fixed values of $\tilde{y}$, the following two equations are obtained

$$\begin{aligned} C_3 \cos(\lambda) + C_4 \sin(\lambda) &= 0 \\ C_3 \cos(\lambda(-1)) + C_4 \sin(\lambda(-1)) &= 0 \end{aligned} \tag{2.118}$$

Because $\cos(\lambda) = \cos(-\lambda)$ and $\sin(\lambda) = -\sin(-\lambda)$, one obtains from the above equations that $C_4 = 0$ and that

$$C_3 \cos(\lambda) = 0 \tag{2.119}$$

From this equation it follows that

$$\lambda = \frac{2n - 1}{2} \pi, \quad n = 1, 2, 3, \dots \tag{2.120}$$

and the following solution for $\Theta_h$ is obtained

$$\Theta_h = C_3 \cos(\lambda \tilde{y})(C_5 \cosh(\lambda \tilde{x}) + C_6 \sinh(\lambda \tilde{x})) \tag{2.121}$$

From the two boundary conditions, corresponding to a fixed value of $\tilde{x}$ in Eq. (2.107), it can be seen that $\Theta_h(A, \tilde{y}) = \Theta_h(-A, \tilde{y})$, which indicates $\Theta_h$ is an even function in $\tilde{x}$. Therefore, it follows that $C_6 = 0$. Thus

$$\Theta_h = C \cos(\lambda \tilde{y}) \cosh(\lambda \tilde{x}), \quad C = C_3 C_5 \tag{2.122}$$

Since an infinite number of eigenvalues has been found from Eq. (2.120), the solution for $\Theta_h$ can be constructed by superimposing all these individual solutions.

This results in

$$\Theta_h = \sum_{n=1}^{\infty} C_n \cos(\lambda_n \tilde{y}) \cosh(\lambda_n \tilde{x}) \tag{2.123}$$

The unknown coefficients $C_n$ can be obtained by matching the boundary condition $\Theta_h(A, \tilde{y}) = -\bar{K}/2\,(1 - \tilde{y}^2)$ by Eq. (2.122). This results in

$$-\frac{\bar{K}}{2}(1 - \tilde{y}^2) = \sum_{n=1}^{\infty} C_n \cos(\lambda_n \tilde{y}) \cosh(\lambda_n A) \tag{2.124}$$

If we multiply both sides of the above equation by $\cos(\lambda_m \tilde{y})$ and integrate the resulting expressions between −1 and 1 we obtain:

$$-\frac{\bar{K}}{2} \int_{-1}^{1} (1 - \tilde{y}^2) \cos(\lambda_m \tilde{y}) d\tilde{y} = \int_{-1}^{1} \left( \sum_{n=1}^{\infty} C_n \cos(\lambda_n \tilde{y}) \cos(\lambda_m \tilde{y}) \cosh(\lambda_n A) \right) d\tilde{y} \tag{2.125}$$

Again, the summation and integration signs on the right hand side of Eq. (2.125) can be interchanged. Then, it is obvious that from the sum only one term will not be equal to zero, because the integral

$$\int_{-1}^{1} \cos(\lambda_n \tilde{y}) \cos(\lambda_m \tilde{y}) d\tilde{y} = 0 \quad \text{for} \quad \lambda_n \neq \lambda_m \tag{2.126}$$

$$= 1 \quad \text{for} \quad \lambda_n = \lambda_m$$

Finally, the following equation is obtained for the determination of the unknown coefficients

$$C_n = \frac{-\frac{\bar{K}}{2} \int_{-1}^{1} (1 - \tilde{y}^2) \cos(\lambda_n \tilde{y}) d\tilde{y}}{\cosh(\lambda_n A)} = \frac{2\bar{K}(-1)^n}{\lambda_n^3 \cosh(\lambda_n A)} \tag{2.127}$$

The solution of the problem, given by Eqs. (2.100) and (2.101), is obtained by combining the two parts of the solution $\Theta_h$ and $\Theta_p$. This gives finally

$$\Theta = \frac{\bar{K}}{2} \left( 1 - \tilde{y}^2 + \sum_{n=1}^{\infty} \frac{4(-1)^n}{\lambda_n^3 \cosh(\lambda_n A)} \cos(\lambda_n \tilde{y}) \cosh(\lambda_n \tilde{x}) \right) \tag{2.128}$$

The solution obtained here shall serve as an example that solutions, which are obtained for heat conduction problems, can be very useful for other applications.
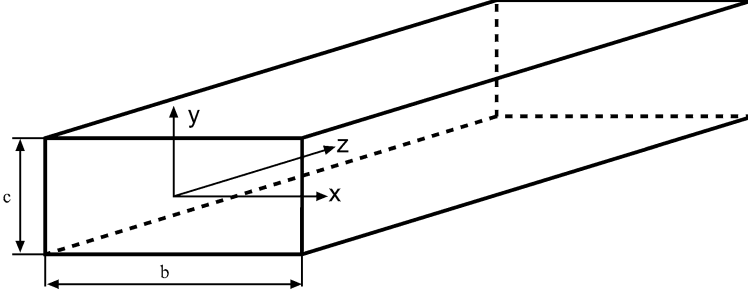
**Fig. 2.9** Geometrical configuration and coordinate system for the flow in a rectangular channel

To that aim, let us investigate the flow in a rectangular channel. The channel has the width $b$ and height $c$. The geometry under consideration is shown in Fig. 2.9.

For this problem, $u$, $v$, $w$ are the flow velocities in the $x$-, $y$- and $z$-direction. Under the assumption of a steady, incompressible, laminar flow with constant fluid properties, the Navier-Stokes equations reduce to

$$\rho\left(u\frac{\partial u}{\partial x} + v\frac{\partial u}{\partial y} + w\frac{\partial u}{\partial z}\right) = F_x - \frac{\partial p}{\partial x} + \mu\left(\frac{\partial^2 u}{\partial x^2} + \frac{\partial^2 u}{\partial y^2} + \frac{\partial^2 u}{\partial z^2}\right) \tag{1.1}$$

$$\rho\left(u\frac{\partial v}{\partial x} + v\frac{\partial v}{\partial y} + w\frac{\partial v}{\partial z}\right) = F_y - \frac{\partial p}{\partial y} + \mu\left(\frac{\partial^2 v}{\partial x^2} + \frac{\partial^2 v}{\partial y^2} + \frac{\partial^2 v}{\partial z^2}\right) \tag{1.2}$$

$$\rho\left(u\frac{\partial w}{\partial x} + v\frac{\partial w}{\partial y} + w\frac{\partial w}{\partial z}\right) = F_z - \frac{\partial p}{\partial z} + \mu\left(\frac{\partial^2 w}{\partial x^2} + \frac{\partial^2 w}{\partial y^2} + \frac{\partial^2 w}{\partial z^2}\right) \tag{1.3}$$

and the mass continuity equation is

$$\frac{\partial u}{\partial x} + \frac{\partial v}{\partial y} + \frac{\partial w}{\partial z} = 0 \tag{1.6}$$

If we now further assume that the flow is hydrodynamically fully developed, i.e. the velocity profile does not change along the axial direction, only the $w$ component of the flow velocity is present. The $u$ and $v$ components are identically zero. Additionally, the $w$ component of the flow can only be a function of the $x$ and $y$ coordinate for the hydrodynamically fully developed flow. Then the problem simplifies to (see for example Spurk 1987)

$$0 = -\frac{\partial p}{\partial z} + \mu\left(\frac{\partial^2 w}{\partial x^2} + \frac{\partial^2 w}{\partial y^2}\right) \tag{2.129}$$

where the pressure gradient in the axial direction is constant for a hydrodynamically fully developed flow. The boundary conditions are the no slip conditions at all boundaries of the channel. Thus

$$w(b/2, y) = 0, \quad w(-b/2, y) = 0 \tag{2.130}$$
$$w(x, c/2) = 0, \quad w(x, -c/2) = 0$$

If we introduce into Eq. (2.129) the abbreviation $\bar{K} = -1/\mu \, \partial p/\partial z$, it can be seen that the problem for determining the fully developed velocity profile is identical to the heat conduction problem in a plate containing a heat sink with constant sink intensity (the derivation of the fully developed velocity field in a rectangular channel is given for example in Spurk (1987)). This shows nicely the similarity of the equations describing problems in Fluid Mechanics and Heat Transfer.

### 2.3.3  Separation of Variables for the General Case of a Linear Second-Order Partial Differential Equation

At the beginning of this chapter, we have been concerned with a linear second order partial differential equation, which depended on the two variables $x$ and $y$. The most general form of this homogeneous equation is given by

$$A(x,y)\frac{\partial^2 u}{\partial x^2} + 2B(x,y)\frac{\partial^2 u}{\partial x \partial y} + C(x,y)\frac{\partial^2 u}{\partial y^2} \tag{2.1}$$
$$+ D(x,y)\frac{\partial u}{\partial x} + E(x,y)\frac{\partial u}{\partial y} + F(x,y)u = 0$$

where $A,\ldots, F$ are constants or functions of $x$ and $y$, which are sufficiently differentiable in the domain of interest.

In the previous two examples, we used the method of separation of variables to derive a solution of the linear partial differential equation as an infinite sum. However, we only addressed very special cases of Eq. (2.1). It is now interesting to evaluate, under which conditions a separation of variables is possible for Eq. (2.1). In order to answer this question, we consider the transformed Eq. (2.16)

$$\bar{A}(\xi,\eta)\frac{\partial^2 u}{\partial \xi^2} + 2\bar{B}(\xi,\eta)\frac{\partial^2 u}{\partial \xi \partial \eta} + \bar{C}(\xi,\eta)\frac{\partial^2 u}{\partial \eta^2} \tag{2.16}$$
$$+ \bar{D}(\xi,\eta)\frac{\partial u}{\partial \xi} + \bar{E}(\xi,\eta)\frac{\partial u}{\partial \eta} + F(\xi,\eta)u = 0$$

where the new coordinates $\xi$ and $\eta$, defined by Eq. (2.6), have been used. Let us substitute

$$u = H(\xi)\,G(\eta) \tag{2.131}$$

into Eq. (2.16). From this we obtain

$$\bar{A}(\xi,\eta)H''(\xi)G(\eta) + 2\bar{B}(\xi,\eta)H'(\xi)G'(\eta) + \bar{C}(\xi,\eta)H(\xi)G''(\eta) \tag{2.132}$$
$$+ \bar{D}(\xi,\eta)H'(\xi)G(\eta) + \bar{E}(\xi,\eta)H(\xi)G'(\eta) + FH(\xi)G(\eta) = 0$$

where the prime indicates the differentiation of the functions $H(\xi)$ and $G(\eta)$ with respect to the independent variable. Dividing Eq. (2.132) by $H(\xi)\,G(\eta)$ results in

$$\bar{A}(\xi,\eta)\frac{H''(\xi)}{H(\xi)} + 2\bar{B}(\xi,\eta)\frac{H'(\xi)}{H(\xi)}\frac{G'(\eta)}{G(\eta)} + \bar{C}(\xi,\eta)\frac{G''(\eta)}{G(\eta)} \tag{2.133}$$
$$+ \bar{D}(\xi,\eta)\frac{H'(\xi)}{H(\xi)} + \bar{E}(\xi,\eta)\frac{G'(\eta)}{G(\eta)} + F(\xi,\eta) = 0$$

From the above equation it can be seen that the variables can only be separated if $\bar{B}(\xi,\eta) = 0$. According to Eq. (2.17), this requires that the new coordinates are chosen in a way to ensure that

$$\bar{B} = A\frac{\partial \xi}{\partial x}\frac{\partial \eta}{\partial x} + B\left(\frac{\partial \xi}{\partial x}\frac{\partial \eta}{\partial y} + \frac{\partial \xi}{\partial y}\frac{\partial \eta}{\partial x}\right) + C\frac{\partial \xi}{\partial y}\frac{\partial \eta}{\partial y} = 0 \tag{2.134}$$

After setting $\bar{B}(\xi,\eta) = 0$, Eq. (2.132) can be rewritten in the following way

$$\frac{\bar{A}(\xi,\eta)}{N(\xi,\eta)}\frac{H''(\xi)}{H(\xi)} + \frac{\bar{D}(\xi,\eta)}{N(\xi,\eta)}\frac{H'(\xi)}{H(\xi)} + \frac{\bar{C}(\xi,\eta)}{N(\xi,\eta)}\frac{G''(\eta)}{G(\eta)} \tag{2.135}$$
$$+ \frac{\bar{E}(\xi,\eta)}{N(\xi,\eta)}\frac{G'(\eta)}{G(\eta)} + \frac{F(\xi,\eta)}{N(\xi,\eta)} = 0$$

where the whole equation has been divided by the function $N(\xi,\eta)$. If we further assume that

$$\frac{F(\xi,\eta)}{N(\xi,\eta)} = f_1(\xi) + f_2(\eta) \tag{2.136}$$

Equation (2.135) can be written as

$$\frac{\bar{A}(\xi,\eta)}{N(\xi,\eta)}\frac{H''(\xi)}{H(\xi)} + \frac{\bar{D}(\xi,\eta)}{N(\xi,\eta)}\frac{H'(\xi)}{H(\xi)} + f_1(\xi) \tag{2.137}$$
$$= -\frac{\bar{C}(\xi,\eta)}{N(\xi,\eta)}\frac{G''(\eta)}{G(\eta)} - \frac{\bar{E}(\xi,\eta)}{N(\xi,\eta)}\frac{G'(\eta)}{G(\eta)} - f_2(\eta) = \text{const.}$$

The left side of this equation should now only be a function of $\xi$ and the right side of the equation should only be a function of $\eta$. This is only possible, if the following restrictions are satisfied:

$$\frac{\bar{A}(\xi,\eta)}{N(\xi,\eta)} = f_3(\xi), \quad \frac{\bar{D}(\xi,\eta)}{N(\xi,\eta)} = f_4(\xi), \qquad (2.138)$$

$$\frac{\bar{C}(\xi,\eta)}{N(\xi,\eta)} = f_5(\eta), \quad \frac{\bar{E}(\xi,\eta)}{N(\xi,\eta)} = f_6(\eta)$$

The present analysis might be very helpful in order to check in advance if the method of separation of variables can be applied to the problem under consideration. It would be incorrect, however, to assume that the method leads to a solution in all cases, where the separation of variables is possible.

## Problems

2-1  Consider the partial differential equation

$$4\frac{\partial^2 u}{\partial x^2} + 5\frac{\partial^2 u}{\partial x \partial y} + \frac{\partial^2 u}{\partial y^2} + \frac{\partial u}{\partial x} + \frac{\partial u}{\partial y} = 2$$

(a) Determine the type of the differential equation.
(b) What are the characteristics of this equation?
(c) Transform the equation into its standard form.
(d) Determine the general solution of the above given differential equation (*hint*: use the substitution: $v = \partial u/\partial \eta$).

2-2  Consider the partial differential equation

$$-x\frac{\partial^2 u}{\partial x^2} + y\frac{\partial^2 u}{\partial y^2} - \frac{1}{2}\frac{\partial u}{\partial x} + A(x,y)\frac{\partial u}{\partial y} = 0$$

Solve this equation using the method of separation of variables.

(a) Insert $u = F(x)G(y)$ into the equation. How should the function $A(x, y)$ look like, so that the method of separation of variables can lead to a solution of the above equation?
(b) Determine the type of the partial differential equation. Show the result in a $x$, $y$-diagram for $-\infty < x < +\infty$ and $-\infty < y < +\infty$.
(c) Calculate for $x > 0, y > 0$ the characteristics of the equation and transform the equation into its standard form (use for this $A(x, y) = -1/2$).

2-3  Consider the partial differential equation

$$\frac{\partial^2 u}{\partial x^2} + 5\frac{\partial^2 u}{\partial x \partial y} + 4\frac{\partial^2 u}{\partial y^2} + 10\frac{\partial u}{\partial y} = \sin x$$

(a)  Determine the type of the differential equation.
(b)  What are the characteristics of this equation?
(c)  Transform the equation into its standard form.

2-4  A thin rectangular plate with side lengths $a$ and $b$ is subjected to a constant temperature $T_1$ at three sides $(T(x,0) = T(x,b) = T(0,y) = T_1)$, whereas the remaining side of this plate is subjected to the temperature distribution

$$T(a,y) = T_1 \left\{ \sin^3\left(\frac{2\pi y}{b}\right) + 1 \right\}$$

We are interested in the steady-state temperature distribution in the plate. All material properties of the plate are constant. The steady-state temperature distribution can be calculated from the energy equation

$$\frac{\partial^2 T}{\partial x^2} + \frac{\partial^2 T}{\partial y^2} = 0$$

with the above given boundary conditions.

(a)  Make the energy equation and the boundary conditions dimensionless.
(b)  Solve the problem using the method of separation of variables.

2-5  Consider a slab, which has extensions in the $y$- and $z$-direction much bigger than in the $x$-direction. The slab has constant initial temperature $T_i$. At $t = 0$, the slab is exposed at both sides $(x = 0, x = \delta)$ to convective cooling. The temperatures of the surrounding fluid are given by $T_C$ and $T_G$. The problem under consideration is described by the following, simplified energy equation

$$\rho c \frac{\partial T}{\partial t} = k\frac{\partial^2 T}{\partial x^2}$$

and the following boundary conditions

$$t = 0 : T = T_i$$

$$x = 0 : h_G(T_G - T(x = 0)) + k\frac{\partial T}{\partial x}\bigg|_{x=0} = 0$$

$$x = \delta : h_G(T_C - T(x = \delta)) - k\frac{\partial T}{\partial x}\bigg|_{x=\delta} = 0$$

(a)   Introduce dimensionless quantities into the above equations. Use

$$\Theta = \frac{T_G - T}{T_G - T_i}, \quad \tilde{t} = \frac{at}{\delta^2}, \quad a = \frac{k}{\rho c}, \quad \tilde{x} = \frac{x}{\delta},$$

$$Bi_G = \frac{h_G \delta}{k}, \quad Bi_C = \frac{h_C \delta}{k}$$

(b)   Split the solution of the problem into the steady-state solution and into the solution of the transient part. Show that for the transient part of the solution, the two boundary conditions for $\tilde{x} = 0$ and $\tilde{x} = 1$ are homogeneous.

(c)   Solve the first problem. What is the steady-state temperature distribution in the slab?

(d)   Solve the transient problem. What is the complete solution of the problem?

2-6   Consider the transient heat conduction in a slab of length $l$. The slab has the initial temperature distribution

$$T(0, x) = \frac{x - l}{l}(T_2 - T_1) + T_2$$

At both sides of the slab, the following constant temperatures are applied

$$T(t, 0) = T_1, \quad T(t, l) = T_2$$

In addition, the slab contains a heat source. The above given problem can be described by the following partial differential equation (where $a$ and $B$ are constants)

$$\frac{\partial T}{\partial t} = a \frac{\partial^2 T}{\partial x^2} + \frac{xBa(T_2 - T_1)}{l^3}$$

(a)   Make the differential equation and the boundary conditions dimensionless by introducing suitable variables.

(b)   Split the problem into different simpler problems.

(c)   Solve the different problems and give the complete solution.

2-7   Consider a sphere with radius $R$. For $t = 0$ the sphere has constant temperature $T_i$. The surface of the sphere is set to the constant temperature $T_0$ for $t > 0$. The sphere contains also a heat source with constant source intensity $\dot{q}_{i0}$. The material properties of the sphere are considered to be constant. The temperature distribution in the sphere can be calculated from the energy equation in spherical coordinates

$$\rho c \frac{\partial T}{\partial t} = \frac{k}{r^2} \frac{\partial}{\partial r}\left(r^2 \frac{\partial T}{\partial r}\right) + \frac{k}{r^2 \sin \Psi} \frac{\partial}{\partial \Psi}\left(\sin \Psi \frac{\partial T}{\partial \Psi}\right)$$

$$+ \frac{k}{r^2 \sin \Psi} \frac{\partial}{\partial \varphi}\left(\frac{\partial T}{\partial \varphi}\right) + \dot{q}_{i0}$$

(a) Simplify the above given energy equation for the case of rotational symmetry. What are the needed boundary conditions?
(b) Transform the problem under consideration by using $T(r,t) = U(r,t)/r$. What is the resulting differential equation and what are the boundary conditions?
(c) Introduce dimensionless quantities, so that the spatial boundary conditions are homogeneous.
(d) Solve the transformed problem by using the method of separation of variables.
(e) Derive from the solution given under (d) the temperature distribution $T(r,t)$.

2-8 An older professor investigates at home a linear second order partial differential equation. The function $u$ is dependent on $x$ and $y$. After a while he obtains the two characteristics of the partial differential equation, given by

$$\xi = y - 2x$$
$$\eta = y + 2x$$

With this, he is able to reduce the original partial differential equation to

$$B^* \frac{\partial^2 u}{\partial \xi \partial \eta} = (\xi + \eta)(\xi - \eta)$$

After achieving this, he goes for lunch. When he returns, he notices that his dog has eating the manuscript. He can't remember how the original equation was looking like. The only thing he knows is that the coefficient in front of the term $\partial^2 u/\partial x^2$ was equal to "1".

(a) Please help the professor and try to reconstruct the original linear second order partial differential equation for $u$.
(b) Determine the coefficient $B^*$ in the above equation.
(c) Determine the general solution of the above given partial differential equation.

2-9 Consider the following partial differential equation

$$\frac{\partial^2 u}{\partial x^2} + m\frac{\partial^2 u}{\partial xy} + m\frac{\partial^2 u}{\partial y^2} = 2xy$$

where $m$ is a rational number.

(a)  Determine the type of the differential equation in dependence of $m$. When will the equation be elliptic, hyperbolic and parabolic? Please set now the parameter $m = 0$. The resulting equation should now be solved together with the boundary conditions

$$u(0, y) = y^2$$
$$\frac{\partial u}{\partial x}\bigg|_{x=0} = y$$

(b)  Determine first the general solution of the problem.
(c)  Use the two above given boundary conditions in order to predict the solution of the problem.

# Chapter 3
# Heat Transfer in Pipe and Channel Flows (Parabolic Problems)

The method of separation of variables has been briefly explained in the last chapter by solving two simple examples. In general, this solution method leads to eigenvalue problems which have to be solved either analytically or numerically. For most technical problems, where analytical solutions based on the method of separation of variables are still obtainable, these eigenvalue problems might become quite difficult.

In order to show how the method can be applied to more complicated problems, the present chapter focuses on the solution of heat transfer problems in pipe and channel flows with hydrodynamically fully developed velocity profiles. In this chapter, we will also explore some of the general properties of the eigenvalue problems under consideration.

## 3.1 Heat Transfer in Pipe and Channel Flows with Constant Wall Temperature

As a first example, we investigate the technical important and scientific very interesting problem of convective heat transfer in a turbulent flow of a liquid, flowing in a pipe or a planar channel. We assume that the flow is hydrodynamically fully developed and that the fluid properties are constant. Due to their technical and scientific relevance, these types of flows have been investigated in great detail in the past. Good reviews can be found in Tietjens (1970), Schlichting (1982) and in Bhatti and Shah (1987).

Heat transfer problems in laminar pipe or channel flows are also of great theoretical and practical interest. Due to the simplicity of the velocity profile for the hydrodynamically fully developed flow, the heat transfer characteristics for the thermal entry length have been investigated relatively early by Graetz (1883, 1885) and independently by Nusselt (1910). This is the reason why this kinds of problems are sometimes referred in literature as Graetz problems. For the heat transfer characteristics in laminar pipe and channel flows, a large number of publications does exist. Good reviews can be found in Shah and London (1978) and in Bhatti

and Shah (1987). In particular, with respect to the thermal development of a
hydrodynamically fully developed laminar flow, several theoretical and numerical
methods have been evaluated and compared. The reader is referred to Shah and
London (1978) for more details. On the other hand, the thermal entrance of a
hydrodynamically fully developed turbulent pipe or channel flow has a much
broader technical relevance and has not yet been investigated in such detail in the
past. Furthermore, this kind of application leads to complicated eigenvalue prob-
lems and can be considered as a challenging case for any analytical method. Of
course, the present analysis holds also for laminar pipe and channel flows, as
stressed in the following sections when relevant. In addition, the program for the
solution of the eigenvalue problems, described in Appendix C, can be used for both
laminar and turbulent flows.

### 3.1.1 Velocity Distribution of Hydrodynamically Fully Developed Pipe and Channel Flows

Figure 3.1 shows the geometry and the coordinate system of the problem under
consideration. We assume a hydrodynamically fully developed flow, which means
that the velocity distribution does not change with increasing values of $x$. This has
the implication that only the velocity component $u$ in the $x$-direction is non-zero.
Furthermore, $u$ is only a function of the coordinate orthogonal to the flow direction.
This coordinate is $y$ in case of a planar channel and $r$ in case of a circular pipe. In
the following the pipe radius is denoted by $R$ and the distance between the two
parallel plates by $2h$.

Furthermore, we assume that the fluid properties are constant. This is a suitable
assumption if the temperature differences in the problem are not to large. Then the
velocity distribution for the pipe and channel flow can be calculated analytically
from the momentum equations. A detailed description is given in Appendix A. For
a laminar flow, very simple expressions are obtained:

**Laminar Pipe Flow**

$$\frac{u}{\bar{u}} = 2\left(1 - \left(\frac{r}{R}\right)^2\right) \tag{3.1}$$
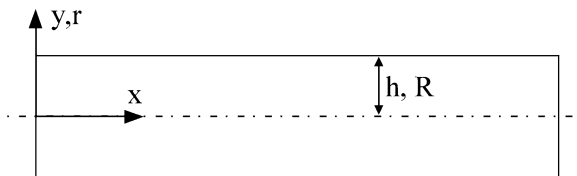


**Fig. 3.1** Geometry and coordinate system

### Laminar Flow in a Planar Channel

$$\frac{u}{\bar{u}} = \frac{3}{2}\left(1 - \left(\frac{y}{h}\right)^2\right) \tag{3.2}$$

where $\bar{u}$ is the mean velocity of the pipe or channel flow. This mean velocity can be calculated from the measured flow rate in the pipe or channel.

For a turbulent hydrodynamically fully developed pipe or channel flow, the turbulent shear stress in the momentum equation in the $x$-direction has to be modelled by using a turbulence model. For pipe and channel flows, this can be done efficiently by using a simple mixing length model (Cebeci and Bradshaw 1984; Cebeci and Chang 1978; Schlichting 1982). After some algebra, one finally obtains a description of the velocity distribution in the pipe or in the channel of the following form (the reader is referred to Appendix A for a detailed derivation of the Eqs. (3.3) and (3.4)).

### Turbulent Pipe Flow

$$\frac{u}{\bar{u}} = f\left(\frac{r}{R}, \, \text{Re}_R\right) \tag{3.3}$$

### Turbulent Flow in a Planar Channel

$$\frac{u}{\bar{u}} = f\left(\frac{y}{h}, \text{Re}_h\right) \tag{3.4}$$

Obviously, in a turbulent flow the velocity distribution depends on the Reynolds number. Increasing values of the Reynolds number lead to an enhanced turbulent mixing within the cross sectional area of the duct and, therefore, to a flatter velocity profile.

Figure 3.2 shows predicted and measured velocity profiles for hydrodynamically fully developed turbulent flows in a pipe and in a planar channel, respectively. In Fig. 3.2, the velocity is scaled by its maximum value in the center. The figure on the left hand side shows a calculation for the flow in a planar channel. It can be seen that the predictions using the simple mixing length model agree quite well with the measurements of Laufer (1950). The hydrodynamically fully developed velocity profile in a pipe is depicted on the right hand side of Fig. 3.2. It can be seen that the velocity profile changes its shape by increasing the Reynolds number from $2.3 \times 10^4$ to $3.2 \times 10^6$. In addition, the good agreement between calculations and measurements of Nikuradse (1932) can be observed (see also Appendix A).
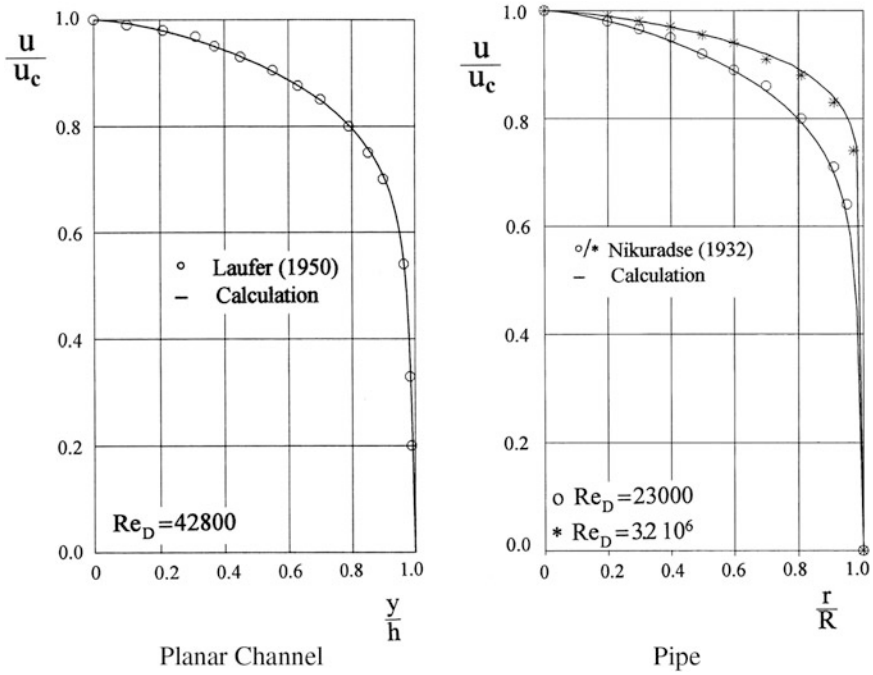
**Fig. 3.2** Hydrodynamically fully developed velocity distribution in a pipe and in a planar channel for different Reynolds numbers

## 3.1.2 Thermal Entrance Solutions for Constant Wall Temperature

Once the velocity profile is known, the energy equation can be analyzed. If we assume an incompressible flow with constant fluid properties and neglect viscous dissipation, the energy equation takes the following form for the hydrodynamically fully developed turbulent flow:

*Pipe*

$$
\rho c_p u(r) \frac{\partial T}{\partial x} = \frac{1}{r} \frac{\partial}{\partial r} \left[ r \left( k \frac{\partial T}{\partial r} - \rho c_p \overline{v'T'} \right) \right] + \frac{\partial}{\partial x} \left[ k \frac{\partial T}{\partial x} - \rho c_p \overline{u'T'} \right]
\tag{3.5}
$$

*Planar Channel*

$$
\rho c_p u(y) \frac{\partial T}{\partial x} = \frac{\partial}{\partial y} \left[ k \frac{\partial T}{\partial y} - \rho c_p \overline{v'T'} \right] + \frac{\partial}{\partial x} \left[ k \frac{\partial T}{\partial x} - \rho c_p \overline{u'T'} \right]
\tag{3.6}
$$
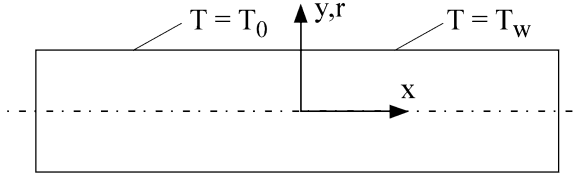
**Fig. 3.3** Geometry and boundary conditions

Figure 3.3 shows the geometry and the boundary conditions. It can be seen that at $x = 0$ the wall temperature is suddenly increased from $T_0$ to $T_W$. The fluid temperature has a uniform value $T_0$ for $x \rightarrow -\infty$. Far away from the entrance ($x \rightarrow \infty$), the fluid temperature will attain asymptotically the uniform wall temperature $T_W$.

For laminar flow ($\overline{u'T'} = 0$, $\overline{v'T'} = 0$), the Eq. (3.5) or (3.6) are elliptic in nature. This is caused by the second term on the right hand side of these equations, representing the axial heat conduction effect within the flow. For turbulent flow, the nature of the equation depends also on the turbulent heat fluxes. The turbulent heat fluxes $-\rho c_p \overline{v'T'}$ and $-\rho c_p \overline{u'T'}$ have to be modelled. This can be done for example by using a simple eddy viscosity model:

$$-\overline{v'T'} = \varepsilon_{hy} \frac{\partial T}{\partial y} \text{(planar channel)}, \quad -\overline{v'T'} = \varepsilon_{hr} \frac{\partial T}{\partial r} \text{(pipe)} \tag{3.7}$$

$$-\overline{u'T'} = \varepsilon_{hx} \frac{\partial T}{\partial x} \text{(planar channel and pipe)} \tag{3.8}$$

where $\varepsilon_{hy}$, $\varepsilon_{hr}$ and $\varepsilon_{hx}$ are only functions of the coordinate orthogonal to the flow direction. Inserting Eqs. (3.7) and (3.8) into Eqs. (3.5) and (3.6) results in

**Pipe**

$$\rho c_p u(r) \frac{\partial T}{\partial x} = \frac{1}{r} \frac{\partial}{\partial r} \left[ r \left( k + \rho c_p \varepsilon_{hr} \right) \frac{\partial T}{\partial r} \right] + \frac{\partial}{\partial x} \left[ \left( k + \rho c_p \varepsilon_{hx} \right) \frac{\partial T}{\partial x} \right] \tag{3.9}$$

**Planar Channel**

$$\rho c_p u(y) \frac{\partial T}{\partial x} = \frac{\partial}{\partial y} \left[ \left( k + \rho c_p \varepsilon_{hy} \right) \frac{\partial T}{\partial y} \right] + \frac{\partial}{\partial x} \left[ \left( k + \rho c_p \varepsilon_{hx} \right) \frac{\partial T}{\partial x} \right] \tag{3.10}$$

Introducing the following dimensionless quantities into the above equations,

$$\Theta = \frac{T - T_W}{T_0 - T_W}, \quad \tilde{x} = \frac{x}{L} \frac{1}{\text{Re}_L \text{Pr}}, \quad \tilde{y} = \frac{y}{L}, \quad \tilde{r} = \frac{r}{L}, \quad \text{Re}_L = \frac{\bar{u}L}{v}, \tag{3.11}$$

$$\tilde{\varepsilon}_{hx} = \frac{\varepsilon_{hx}}{v}, \quad \tilde{\varepsilon}_{hr} = \frac{\varepsilon_{hr}}{v}, \quad \tilde{\varepsilon}_{hy} = \frac{\varepsilon_{hy}}{v}, \quad \tilde{u} = \frac{u}{\bar{u}}, \quad \text{Pe}_L = \text{Re}_L \text{Pr}, \quad \text{Pr} = \frac{v}{a}$$

where the length scale $L = R$ for pipe flow and $L = h$ for the flow in a planar channel has been used. We obtain

**Pipe**

$$\tilde{u}(\tilde{r})\frac{\partial\Theta}{\partial\tilde{x}} = \frac{1}{\tilde{r}}\frac{\partial}{\partial\tilde{r}}\left[\tilde{r}(1 + \text{Pr}\,\tilde{\varepsilon}_{hr})\frac{\partial\Theta}{\partial\tilde{r}}\right] + \frac{1}{\text{Pe}_L^2}\frac{\partial}{\partial\tilde{x}}\left[(1 + \text{Pr}\,\tilde{\varepsilon}_{hx})\frac{\partial\Theta}{\partial\tilde{x}}\right] \qquad (3.12)$$

**Planar Channel**

$$\tilde{u}(\tilde{y})\frac{\partial\Theta}{\partial\tilde{x}} = \frac{\partial}{\partial\tilde{y}}\left[(1 + \text{Pr}\,\tilde{\varepsilon}_{hy})\frac{\partial\Theta}{\partial\tilde{y}}\right] + \frac{1}{\text{Pe}_L^2}\frac{\partial}{\partial\tilde{x}}\left[(1 + \text{Pr}\,\tilde{\varepsilon}_{hx})\frac{\partial\Theta}{\partial\tilde{x}}\right] \qquad (3.13)$$

For Peclet numbers $\text{Pe}_L > 100$ and a semi-infinite heating length, axial heat conduction in the fluid can be neglected with good accuracy. This means that the second term on the right hand side of the Eqs. (3.12) and (3.13) can be ignored. This leads to

**Pipe**

$$\tilde{u}(\tilde{r})\frac{\partial\Theta}{\partial\tilde{x}} = \frac{1}{\tilde{r}}\frac{\partial}{\partial\tilde{r}}\left[\tilde{r}(1 + \text{Pr}\,\tilde{\varepsilon}_{hr})\frac{\partial\Theta}{\partial\tilde{r}}\right] \qquad (3.14)$$

**Planar Channel**

$$\tilde{u}(\tilde{y})\frac{\partial\Theta}{\partial\tilde{x}} = \frac{\partial}{\partial\tilde{y}}\left[(1 + \text{Pr}\,\tilde{\varepsilon}_{hy})\frac{\partial\Theta}{\partial\tilde{y}}\right] \qquad (3.15)$$

These two equations can be combined into one relation, if we introduce a vertical coordinate $n$, which is equal to $y$ for a planar channel and equal to $r$ for pipe flows. This results in

$$\tilde{u}(\tilde{n})\frac{\partial\Theta}{\partial\tilde{x}} = \frac{1}{\tilde{r}^F}\frac{\partial}{\partial\tilde{n}}\left[\tilde{r}^F(1 + \text{Pr}\,\tilde{\varepsilon}_{hn})\frac{\partial\Theta}{\partial\tilde{n}}\right] \qquad (3.16)$$

where the superscript $F$ specifies the geometry and has to be set to 0 for a planar channel and 1 for pipe flows. If we examine the nature of Eq. (3.16), we see that the equation is parabolic. The boundary conditions for Eq. (3.16) are therefore given by

$$\tilde{x} = 0 : \Theta(0, \tilde{n}) = 1$$
$$\tilde{n} = 0 : \left.\frac{\partial\Theta}{\partial\tilde{n}}\right|_{\tilde{n}=0} = 0 \qquad (3.17)$$
$$\tilde{n} = 1 : \Theta(\tilde{x}, 1) = 0$$

From Eq. (3.17) it can be seen that the boundary condition $T = T_0$ for $x \rightarrow -\infty$ has been moved to $x = 0$. This means that the process of heating the wall has no influence on the temperature field for $x < 0$. This shows nicely the parabolic nature of the equation.

In Eq. (3.16) the dimensionless eddy diffusivity for heat $\tilde{\varepsilon}_{hn}$ appears as an additional unknown. This quantity is related to the eddy viscosity $\tilde{\varepsilon}_m$ through the similarity between heat and momentum transfer. This is normally indicated by introducing a turbulent Prandtl number defined by

$$\Pr_t = \frac{\varepsilon_m}{\varepsilon_{hn}} = \frac{\tilde{\varepsilon}_m}{\tilde{\varepsilon}_{hn}} \tag{3.18}$$

The turbulent Prandtl number would be equal to one, if there would be full similarity between momentum and heat transfer. However, this is not the case. Therefore, the turbulent Prandtl number will, in general, be a function of the Reynolds and molecular Prandtl number as well as of the distance from the wall. In literature, there are many different models for the turbulent Prandtl number. Good reviews on this subject can be found in Reynolds (1975), Jischa (1982), Kays et al. (2004) and Kays (1994). For the moment, it is sufficient to know that, for the problems under consideration, $\Pr_t$ is only a function of $\tilde{n}$. In the following sections, a few models for the turbulent Prandtl number $\Pr_t$ are provided, which can be used for the calculations of the heat transfer in pipe and channel flows.

Introducing the turbulent Prandtl number into Eq. (3.16) leads to

$$\tilde{u}(\tilde{n})\frac{\partial\Theta}{\partial\tilde{x}} = \frac{1}{\tilde{r}^F}\frac{\partial}{\partial\tilde{n}}\left[\tilde{r}^F a_2(\tilde{n})\frac{\partial\Theta}{\partial\tilde{n}}\right], \quad a_2(\tilde{n}) = 1 + \frac{\Pr}{\Pr_t}\tilde{\varepsilon}_m \tag{3.19}$$

The energy Eq. (3.19) has to be solved together with the associated boundary conditions given by Eq. (3.17). This can be done by using the method of separation of variables. Therefore, we assume that the temperature can be described by

$$\Theta_j = \Phi_j(\tilde{n})G_j(\tilde{x}) \tag{3.20}$$

Introducing Eq. (3.20) into Eq. (3.19) results in

$$\frac{\left(\tilde{r}^F a_2(\tilde{n})\Phi_j'(\tilde{n})\right)'}{\tilde{r}^F\tilde{u}(\tilde{n})\Phi_j(\tilde{n})} = \frac{G_j'(\tilde{x})}{G_j(\tilde{x})} = C_j \tag{3.21}$$

From this equation, we first solve the ordinary differential equation for the function $G_j(\tilde{x})$

$$\frac{G_j'(\tilde{x})}{G_j(\tilde{x})} = C_j \tag{3.22}$$

This equation has the general solution

$$G_j(\tilde{x}) = D_j \exp(C_j\tilde{x}) \tag{3.23}$$

From Eq. (3.23) it is obvious that the unknown constant $C_j$ must be smaller than zero, since, for $C_j = 0$, the dependence of the solution on $\tilde{x}$ would be lost and, for $C_j > 0$, the temperature would tend to infinity for $\tilde{x} \to \infty$. If we introduce $C_j = -\lambda_j^2$ into Eq. (3.23), we obtain

$$G_j(\tilde{x}) = D_j \exp\left(-\lambda_j^2\tilde{x}\right) \tag{3.24}$$

For the function $\Phi_j$ the following ordinary differential equation has to be solved

$$\tilde{r}^F \tilde{u}(\tilde{n})\lambda_j^2\Phi_j(\tilde{n}) + \left[\tilde{r}^F a_2(\tilde{n})\Phi_j'(\tilde{n})\right]' = 0 \tag{3.25}$$

Inserting Eq. (3.20) into the boundary conditions Eq. (3.17) results in

$$
\begin{aligned}
&\tilde{n} = 0 : \left.\frac{\partial\Theta}{\partial\tilde{n}}\right|_{\tilde{n}=0} = 0 &&\Rightarrow G(\tilde{x})\Phi'(0) = 0 &&\Rightarrow \Phi'(0) = 0 \\
&\tilde{n} = 1 : \Theta(\tilde{x},1) = 0 &&\Rightarrow G(\tilde{x})\Phi(1) = 0 &&\Rightarrow \Phi(1) = 0
\end{aligned} \tag{3.26}
$$

The differential Eq. (3.25) has to be solved together with the homogeneous boundary conditions (3.26). As we have seen in Chap. 2 for the elementary examples, non-trivial solutions for this problem exist only for selected values of $\lambda_j^2$, which are the eigenvalues of Eq. (3.25). Thus, the problem of solving the differential Eq. (3.25) with boundary conditions (3.26) has been reduced to an eigenvalue problem and is known in literature as a Sturm-Liouville problem (see for example Reid (1980), Kamke (1983), Collatz (1981), Courant and Hilbert (1991), Sauer and Szabo (1969)). This sort of self-adjoint eigenvalue problem is very common in a lot of physical applications and has been investigated in great detail by several researchers in the past. In the following sections, a short summary of some of the most important properties of this system is given.

**Properties of the Sturm-Liouville System**

In order to show the basic properties of the Sturm-Liouville system, we consider the problem given by the Eqs. (3.25) and (3.26) in the following general form

$$L[\Phi_j] = \bar{\lambda}_j M[\Phi_j] \tag{3.27}$$

with the boundary conditions for the function $\Phi_j$ given by Eq. (3.26). For the eigenvalue problem under consideration, the operators $L$ and $M$ take the following form

$$L[\Phi_j] = -\frac{d}{d\tilde{n}}\left[\tilde{r}^F a_2 \frac{d\Phi_j}{d\tilde{n}}\right] \tag{3.28}$$

$$M[\Phi_j] = \tilde{r}^F \tilde{u}(\tilde{n})\Phi_j \tag{3.29}$$

The most important properties of the Sturm-Liouville system are:

1. **The Problem is Self-Adjoint and Positive Definite**
   In order to show that the eigenvalue problem under consideration (Eqs. (3.25) and (3.26)) is self-adjoint and positive definite, let us define the following two inner products

$$\langle v, w \rangle = \int_0^1 v L[w] d\tilde{n} \tag{3.30}$$

and

$$(v, w) = \int_0^1 v M[w] d\tilde{n} \tag{3.31}$$

where $v$ and $w$ are two "compare-functions". These functions are assumed to be continuously differentiable functions of $\tilde{n}$ in the interval [0, 1]. They satisfy the boundary conditions of the problem given by Eq. (3.26) without vanishing in the whole interval. The eigenvalue problem is now called self-adjoint, if

$$\langle v, w \rangle = \langle w, v \rangle, \quad (v, w) = (w, v) \tag{3.32}$$

are satisfied. This means that the inner products, defined by Eqs. (3.30) and (3.31) are symmetric. Additionally, the eigenvalue problem is called positive definite, if

$$\langle v, v \rangle > 0, \quad (v, v) > 0 \tag{3.33}$$

Let us first consider the case that the problem is self-adjoint, then

$$\langle v, w \rangle = -\int_0^1 v\left[\tilde{r}^F a_2(\tilde{n})w'\right]' d\tilde{n} = -\int_0^1 w\left[\tilde{r}^F a_2(\tilde{n})v'\right]' d\tilde{n} = \langle w, v \rangle \tag{3.34}$$

must be satisfied. Rearranging Eq. (3.34) gives

$$\int_0^1 \left\{v\left[\tilde{r}^F a_2(\tilde{n})w'\right]' - w\left[\tilde{r}^F a_2(\tilde{n})v'\right]'\right\} d\tilde{n} = 0 \tag{3.35}$$

The expression in the integral in Eq. (3.35) can be rewritten according to

$$v\big[\tilde{r}^F a_2(\tilde{n})w'\big]' - w\big[\tilde{r}^F a_2(\tilde{n})v'\big]' = \big[v\big(\tilde{r}^F a_2 w'\big) - w\big(\tilde{r}^F a_2 v'\big)\big]' \qquad (3.36)$$

Inserting Eq. (3.36) into Eq. (3.35) and evaluating the integral results in

$$0 = v\big(\tilde{r}^F a_2 w'\big)\big|_0^1 - w\big(\tilde{r}^F a_2 v'\big)\big|_0^1 = vw'\big|^1 - vw'\big|_0 - wv'\big|^1 + wv'\big|_0 \qquad (3.37)$$

From the given boundary conditions, Eq. (3.26), we obtain

$$\begin{aligned}\tilde{n} = 0 : \Phi_j' = 0 &\quad \Rightarrow \quad v'(0) = 0, w'(0) = 0 \\ \tilde{n} = 1 : \Phi_j = 0 &\quad \Rightarrow \quad v(1) = 0, w(1) = 0\end{aligned} \qquad (3.38)$$

From Eq. (3.38), we see that Eq. (3.37) is identically zero, thus showing that $\langle v, w\rangle = \langle w, v\rangle$ is satisfied.

The second requirement is that $(v, w) = (w, v)$. This is also satisfied as

$$(v, w) = \int_0^1 v\big(\tilde{r}^F \tilde{u}w\big)d\tilde{n} = \int_0^1 w\big(\tilde{r}^F \tilde{u}v\big)d\tilde{n} = (w, v) \qquad (3.39)$$

From the preceding analysis, it has been shown that the eigenvalue problem under consideration is self-adjoint. We want now to show that the problem is also positive definite. Therefore, we have to prove that

$$(v, v) = \int_0^1 v\big(\tilde{r}^F \tilde{u}v\big)d\tilde{n} = \int_0^1 v^2\big(\tilde{r}^F \tilde{u}\big)d\tilde{n} > 0 \qquad (3.40)$$

This is easy to show, since the expression $(\tilde{r}^F \tilde{u})$ is a function $\geq 0$ in the interval under consideration. For the second inner product, we have to show that

$$\langle v, v\rangle = -\int_0^1 v\big[\tilde{r}^F a_2 v'\big]' d\tilde{n} > 0 \qquad (3.41)$$

This can be shown by partial integration of Eq. (3.41). From

$$-\int_0^1 \underbrace{v}_{a}\underbrace{\big[\tilde{r}^F a_2 v'\big]'}_{b'} d\tilde{n} - \int_0^1 \underbrace{v'}_{a'}\underbrace{\big[\tilde{r}^F a_2 v'\big]}_{b} d\tilde{n} = -v\big[\tilde{r}^F a_2 v'\big]\big|_0^1 \qquad (3.42)$$

one obtains

$$\langle v, v \rangle = \int_0^1 \tilde{r}^F a_2(v')^2 d\tilde{n} > 0 \tag{3.43}$$

From Eq. (3.43) it is obvious that the expression is larger than zero because $\tilde{r}^F a_2(\tilde{n})$ is always $\geq 0$. Therefore, it has been shown that the eigenvalue problem under consideration is self-adjoint and positive definite. For other wall boundary conditions (constant wall heat flux or boundary conditions of the third kind), the proof that the eigenvalue problem is self-adjoint and positive definite is analogous.

2. ***Eigenvalues and Eigenfunctions***
   Having shown that the eigenvalue problem under consideration is self-adjoint, it is relatively simple to prove that the resulting eigenfunctions are orthogonal with respect to a weighting function. In order to show this, the eigenvalue problem (3.27) for two different eigenfunctions $\Phi_i$ and $\Phi_j$ is considered

$$\begin{aligned} L[\Phi_j] &= \bar{\lambda}_j M[\Phi_j] \\ L[\Phi_i] &= \bar{\lambda}_i M[\Phi_i] \end{aligned} \tag{3.44}$$

Multiplying the first equation by $\Phi_i$ and the second by $\Phi_j$ gives, after subtraction

$$\Phi_i L[\Phi_j] - \Phi_j L[\Phi_i] = \bar{\lambda}_j \Phi_i M[\Phi_j] - \bar{\lambda}_i \Phi_j M[\Phi_i] \tag{3.45}$$

Integrating both sides of Eq. (3.45) between zero and one gives

$$\langle \Phi_j, \Phi_i \rangle - \langle \Phi_i, \Phi_j \rangle = (\bar{\lambda}_i - \bar{\lambda}_j) \int_0^1 \Phi_i M[\Phi_j] d\tilde{n} \tag{3.46}$$

Because the problem under consideration is self-adjoint, the left hand side of Eq. (3.46) is identical to zero. Thus

$$(\bar{\lambda}_i - \bar{\lambda}_j) \int_0^1 \Phi_i M[\Phi_j] d\tilde{n} = 0 \tag{3.47}$$

From this equation, it is obvious that for $i = j$, the left hand side of Eq. (3.47) is identical to zero, because the eigenvalues are the same. For $i \neq j$, the integral $\int_0^1 \Phi_i M[\Phi_j] d\tilde{n}$ has to be zero in order to fulfill Eq. (3.47). Inserting the definition of the operator $M$ into Eq. (3.47) results in

$$\int_0^1 \tilde{r}^F \tilde{u}(\tilde{n}) \Phi_i \Phi_j d\tilde{n} = 0 \quad \text{for } i \neq j \tag{3.48}$$

This means that the eigenfunctions are a set of orthogonal functions in the interval [0, 1] with respect to the weighting function $g(\tilde{n})$ defined by

$$g(\tilde{n}) = \tilde{r}^F \tilde{u}(\tilde{n}) \tag{3.49}$$

Equation (3.48) is an important result for the solution of the partial differential equation, as it can be used later to expand an arbitrary function in terms of eigenfunctions.

3. **The Eigenvalues of the Sturm-Liouville System**

   Normally, the eigenvalues of Eq. (3.27) can only be obtained numerically. Therefore, it is important to find out if we can restrict in advance the search interval for these values. Let us assume that one eigenvalue is complex $\bar{\lambda}_j = \alpha + i\beta$ with the eigenfunction $\Phi_j = a + ib$. Then its complex conjugate $\bar{\lambda}_i = \alpha - i\beta$ is also an eigenvalue with the eigenfunction $\Phi_i = a - ib$. If we introduce these values into Eq. (3.47), one obtains

$$2i\beta \int_0^1 \tilde{r}^F \tilde{u} \left( a^2 + b^2 \right) d\tilde{n} = 0 \tag{3.50}$$

   Since the weighting function $g(\tilde{n}) = \tilde{r}^F \tilde{u}(\tilde{n})$ is larger or equal to zero in the investigated interval, the integral in Eq. (3.50) must be bigger than zero. Therefore, in order to satisfy relation (3.50), $\beta$ must be equal to zero. This shows that the eigenvalue problem has only real eigenvalues. Since the eigenvalue problem is also positive definite, it can be shown (see Collatz 1981) that all eigenvalues are larger or equal to zero. This shows the correctness of our previous assumption $C_j = -\lambda_j^2$, which was based only on physical reasoning.

4. **Eigenfunction Expansions for an Arbitrary Function**

   We have already shown that the eigenfunctions form an orthogonal set of functions. Now we want to prove that an arbitrary "well behaved" function $f(\tilde{n})$ can be represented by an infinite number of eigenfunctions. We assume, therefore, that

$$f(\tilde{n}) = \sum_{j=0}^{\infty} A_j \Phi_j(\tilde{n}) \tag{3.51}$$

   is an uniformly convergent series. Multiplying both sides of Eq. (3.51) by $g(\tilde{n})\Phi_i(\tilde{n})$ and integrating over $\tilde{n}$ between zero and one leads to

$$\int_0^1 f(\tilde{n})g(\tilde{n})\Phi_i(\tilde{n})d\tilde{n} = \int_0^1 \sum_{j=0}^{\infty} A_j g(\tilde{n})\Phi_i\Phi_j d\tilde{n} \tag{3.52}$$

Interchanging summation and integration on the right hand side of the equation results in

$$\int_0^1 f(\tilde{n})g(\tilde{n})\Phi_i(\tilde{n})d\tilde{n} = \sum_{j=0}^{\infty} A_j \int_0^1 g(\tilde{n})\Phi_i\Phi_j d\tilde{n} \qquad (3.53)$$

From Eqs. (3.53) and (3.48) it can be seen that the integral on the right hand side is equal to zero if $i \neq j$. Therefore, the constants $A_j$ are given by

$$A_j = \frac{\int_0^1 g(\tilde{n})f(\tilde{n})\Phi_j(\tilde{n})d\tilde{n}}{\int_0^1 g(\tilde{n})\Phi_j^2(\tilde{n})d\tilde{n}} \qquad (3.54)$$

The present investigation is intended only to show some of the important properties of the Sturm-Liouville system. The reader is referred to Coddington and Levinson (1955), Sagan (1989), Reid (1980), Kamke (1977) and Myint-U and Debnath (1987) for a more detailed and rigorous mathematical treatment of the Sturm-Liouville eigenvalue problems.

From the previous analysis, it is clear that the solution of the partial differential equation (3.19) can be constructed by linear superposition of solutions given by Eq. (3.20). This results in the following expression for the temperature distribution in the fluid

$$\Theta = \sum_{j=0}^{\infty} A_j \Phi_j(\tilde{n}) \exp\left(-\lambda_j^2 \tilde{x}\right) \qquad (3.55)$$

The constants $A_j$ in Eq. (3.55) can be obtained by satisfying the boundary condition for $\tilde{x} = 0$. Here we have

$$1 = \sum_{j=0}^{\infty} A_j \Phi_j(\tilde{n}) \qquad (3.56)$$

From Eq. (3.54) it is obvious that the constants $A_j$ in Eq. (3.56) are given by

$$A_j = \frac{\int_0^1 \tilde{r}^F \tilde{u} \Phi_j d\tilde{n}}{\int_0^1 \tilde{r}^F \tilde{u} \Phi_j^2 d\tilde{n}} \qquad (3.57)$$

The numerator of Eq. (3.57) can be further simplified, by using the differential equation for the eigenvalue system given by Eq. (3.25). Replacing the expression in the integral by Eq. (3.25) leads to

$$\int\limits_0^1 \tilde{r}^F \tilde{u} \Phi_j d\tilde{n} = \int\limits_0^1 -\frac{1}{\lambda_j^2} \left[ \tilde{r}^F a_2(\tilde{n}) \Phi_j'(\tilde{n}) \right]' d\tilde{n}$$

$$= -\frac{1}{\lambda_j^2} \left[ \tilde{r}^F a_2 \Phi_j' \right] \Big|_0^1 = -\frac{1}{\lambda_j^2} \Phi_j'(1) \qquad (3.58)$$

where $a_2(1) = 1$ has been used. Thus, the constants $A_j$ are finally given by

$$A_j = \frac{-\Phi'_j(1)}{\lambda_j^2 \int_0^1 \tilde{r}^F \tilde{u} \Phi_j^2 d\tilde{n}} \qquad (3.59)$$

Combining Eqs. (3.55) and (3.59), the temperature distribution in the fluid is completely known.

In Chap. 2, we have seen how the eigenvalues and eigenfunctions can be predicted analytically. However, for most technical relevant cases, the eigenvalues and eigenfunctions can only be predicted numerically. In Appendix C a FORTRAN program is described which can be used for this purpose. However, it should be noted, that larger eigenvalues ($j > 10$) might be predictable by asymptotic formulas. This is explained in detail in Chap. 4.

After the temperature distribution in the fluid is known, the Nusselt number can be calculated. The Nusselt number is defined as

$$\mathrm{Nu}_D = \frac{hD}{k} \qquad (3.60)$$

In Eq. (3.60), the Nusselt number depends on the heat transfer coefficient $h$ and the hydraulic diameter $D$. The hydraulic diameter $D$ is defined as

$$D = \frac{4A}{U} \qquad (3.61)$$

where $A$ is the cross-sectional flow area of the duct and $U$ is the wetted perimeter. For a circular pipe, one obtains $D = 2R$. For a rectangular channel, the geometrical parameters are shown in Fig. 3.4.

The channel has width $W$ and height $2h$. Following Eq. (3.61), the hydraulic diameter is equal to

$$D = \frac{4W(2h)}{4h + 2W} = \frac{4h}{\frac{2h}{W} + 1} \qquad (3.62)$$

**Fig. 3.4** Geometry of a rectangular channel
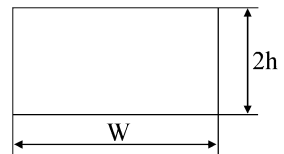
For the here considered case of a two-dimensional channel ($h/W \rightarrow 0$), Eq. (3.62) leads to $D = 4h$.

The heat transfer coefficient $h$, which appears in Eq. (3.60), can be obtained from an energy balance at the surface where the heat transfer process occurs. Here we have

$$h(T_W - T_b) = -k\frac{\partial T}{\partial n}\Big|_{n=L} \tag{3.63}$$

Replacing the heat transfer coefficient $h$ in Eq. (3.60) with Eq. (3.63), we obtain the following definition for the Nusselt number

$$\mathrm{Nu}_D = \frac{D\frac{\partial T}{\partial n}\Big|_{n=L}}{T_W - T_b} \tag{3.64}$$

From this definition, it is obvious that the Nusselt number is a dimensionless temperature gradient at the wall. In Eq. (3.64), $T_W$ denotes the wall temperature, while $T_b$ is the "bulk-temperature" defined by

$$T_b = \frac{\int_0^L uTr^F dn}{\int_0^L ur^F dn} \tag{3.65}$$

The bulk-temperature is a mass averaged fluid temperature. Introducing the dimensionless quantities defined by Eq. (3.11), we obtain the Nusselt number and the bulk-temperature in dimensionless form

$$\mathrm{Nu}_D = \frac{-4\frac{\partial \Theta}{\partial \tilde{n}}\Big|_{\tilde{n}=1}}{2^F \Theta_b} \tag{3.66}$$

$$\Theta_b = 2^F \int_0^1 \tilde{u}\tilde{r}^F \Theta \, d\tilde{n} \tag{3.67}$$

Introducing now the known temperature distribution in the fluid (Eq. (3.55)) results in the following expression for the bulk-temperature

$$\Theta_b = -2^F \sum_{j=0}^{\infty} A_j \frac{\Phi'_j(1)}{\lambda_j^2} \exp\left(-\lambda_j^2 \tilde{x}\right) \tag{3.68}$$

and for the Nusselt number

$$\mathrm{Nu}_D = \frac{4 \sum_{j=0}^{\infty} A_j \Phi'_j(1) \exp\left(-\lambda_j^2 \tilde{x}\right)}{4^F \sum_{j=0}^{\infty} A_j \frac{\Phi'_j(1)}{\lambda_j^2} \exp\left(-\lambda_j^2 \tilde{x}\right)} \tag{3.69}$$

where $F = 0$ denotes the heat transfer in a planar channel whereas $F = 1$ denotes the heat transfer in a circular pipe. If we are only interested in the Nusselt number for the hydrodynamically and thermaly fully developed flow, we can obtain the Nusselt number for the fully developed flow from Eq. (3.69) by investigating the case of $\tilde{x} \to \infty$. For this limit only the first term of the sums has to be retained because of the very fast growing eigenvalues with increasing $j$. One obtains therefore the very simple expression

$$\lim_{\tilde{x} \to \infty} \mathrm{Nu}_D = \mathrm{Nu}_\infty = \frac{4}{4^F} \lambda_0^2 \tag{3.70}$$

We have obtained the result that, in case of a fully developed flow, the Nusselt number (for the constant wall temperature boundary condition) depends solely on the first eigenvalue. This result is important for turbulent flows where the thermal entrance length is normally quite short due to the rapid mixing in the flow.

### Laminar Flows

As stated earlier, the heat transfer process in hydrodynamically fully developed laminar flow in a planar channel and in a pipe has been extensively studied in literature (see e.g. Shah and London (1978)). Therefore, only some results are reported here which help to understand the general behaviour of the heat transfer process in laminar duct flows. One of the most important results for this type of problems is that the temperature distribution as well as the distribution of the Nusselt number depend only on the dimensionless axial coordinate

$$\tilde{x} = \frac{x}{L} \frac{1}{\mathrm{Re}_L \, \mathrm{Pr}} \tag{3.71}$$

and not explicitly on the Reynolds- or Prandtl number (for a pipe flow $L = R$ and for a flow in a planar channel $L = h$). This can easily be understood, if we examine Eq. (3.19). For laminar flows, the velocity distribution is only a function of $\tilde{n}$ and not a function of the Reynolds number (see Eqs. (3.1) and (3.2)). Additionally, the function $a_2(\tilde{n}) = 1$. Therefore, the problem given by Eqs. (3.19) and (3.17) does not depend on the Reynolds- and the Prandtl number. This fact leads to great simplifications for these type of problems, because the eigenvalues and eigenfunctions have only to be calculated once. The qualitative distribution of the bulk-temperature is displayed in Fig. 3.5, whereas the qualitative distribution of the Nusselt number is shown in Fig. 3.6. From Fig. 3.5, it can be seen that the bulk-temperature at the inlet of the duct is equal to the uniform inlet temperature $T_0$. This is obvious from the definition of $T_b$, given by Eq. (3.65). With increasing values of $\tilde{x}$, the bulk-temperature attains asymptotically the uniform wall temperature $T_W$. The distribution of the Nusselt number is shown in Fig. 3.6. Here it can be seen that the value of the Nusselt number is extremely high for very small values of the $\tilde{x}$-coordinate. This is caused by the temperature jump in the wall temperature at the inlet of the duct, which leads to the development of the temperature boundary layer at $\tilde{x} = 0$.

**Fig. 3.5** Distribution of the bulk-temperature for a laminar, hydrodynamically fully developed pipe flow with constant wall temperature
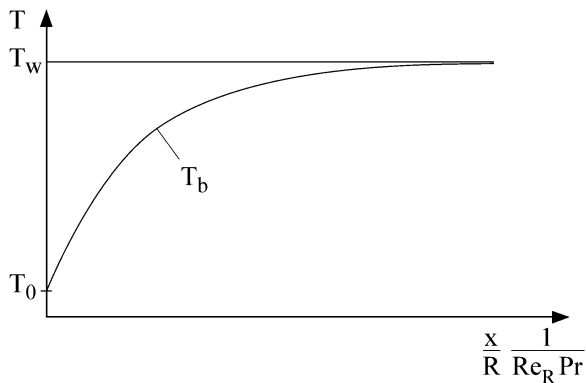


**Fig. 3.6** Distribution of the Nusselt number for a laminar, hydrodynamically fully developed pipe flow with constant wall temperature
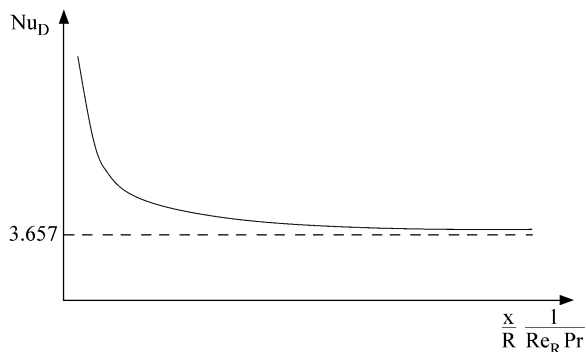


With increasing values of the axial coordinate, the Nusselt number decreases and reaches asymptotically a constant value.

The value of this constant however, depends on the geometry and applied wall boundary conditions. For the present case of a constant wall temperature, the value for the fully developed Nusselt number is

$$
\begin{aligned}
\mathrm{Nu}_\infty &= 3.657 \quad \text{for the pipe} \\
\mathrm{Nu}_\infty &= 7.5407 \quad \text{for the planar channel}
\end{aligned}
\tag{3.72}
$$

Having shown that, for hydrodynamically fully developed flows, both the temperature field and the distribution of the Nusselt number depend only on the axial coordinate $\tilde{x}$, simple correlations can be obtained quite easily for calculating the Nusselt number and, thus, the heat transfer in ducts for laminar flow. For example, the distribution of the Nusselt number in a pipe for the thermal entrance region can be approximated by (see Shah and London (1978))

$$
\mathrm{Nu}_D =
\begin{cases}
\dfrac{1.077}{(x^*)^{1/3}} - 0.7, & x^* \leq 0.01 \\[2ex]
3.657 + \dfrac{6.874}{(10^3 x^*)^{0.488}} \exp(-57.2\, x^*), & x^* > 0.01
\end{cases}
\tag{3.73}
$$

where a slightly modified axial coordinate has been used

$$x^* = \frac{x}{D}\frac{1}{\mathrm{Re}_D \,\mathrm{Pr}} \tag{3.74}$$

$D$ is the hydraulic diameter ($D = 2R$ for the pipe and $D = 4h$ for the planar channel). For the heat transfer in a planar duct similar expressions can be obtained (see Shah and London (1978))

$$\mathrm{Nu}_D = \begin{cases} \dfrac{1.233}{(x^*)^{1/3}} - 0.4, & x^* \le 0.001 \\[2ex] 7.541 + \dfrac{6.874}{(10^3 x^*)^{0.488}} \exp(-245 x^*), & x^* > 0.001 \end{cases} \tag{3.75}$$

It is interesting to note that the dependence on the axial coordinate is quite similar for both solutions (Eqs. (3.73) and (3.75)). Only the matching constants differ in order to approximate the heat transfer in a pipe or in a planar channel.

### Turbulent Flows

Heat transfer in turbulent duct flows is of greater technical relevance than in laminar flows. In turbulent flows, the mixing process is much more effective than in laminar flows. This produces a shorter hydrodynamic entrance length compared to laminar duct flows, while the velocity profiles are much flatter. Thanks to the shorter hydrodynamic entrance length, the flow can be described for a lot of applications either as hydrodynamically fully developed or as hydrodynamically and thermally fully developed. Exceptions are represented by turbulent flows of liquid metals. Due to the very low Prandtl number for these types of applications, the heat transfer behaviour of such flows might be more similar to laminar flows.

Before discussing some heat transfer results, the turbulent Prandtl number ($\mathrm{Pr}_t = \varepsilon_m/\varepsilon_h$) has to be specified. As it can be seen in Eq. (3.19), the turbulent Prandtl number will significantly influence the term $a_2(\tilde{n})$. If we assume that the transfer of momentum and heat is similar, we can set $Pr_t = 1$. Unfortunately, this simple approximation is not realistic for many applications. In literature, a lot of different approaches are described to model the turbulent Prandtl number. The reader is referred to Reynolds (1975), Jischa (1982), Kays et al. (2004) and Kays (1994) for good reviews and comparisons between different models. In general it can be noted that

$$\begin{aligned} \mathrm{Pr}_t &\to \infty & \text{for } \mathrm{Re}_D \ne 0 & \quad \text{and } \mathrm{Pr} \to 0 \\ \mathrm{Pr}_t &\to \text{const.} & \text{for } \mathrm{Re}_D \to \infty & \quad \text{and } \mathrm{Pr} \ge 0 \end{aligned} \tag{3.76}$$

This can be explained in the following way: for $Pr \ll 1$ an eddy has a very high molecular heat conduction. Therefore, such an eddy exchanges much more rapidly heat than momentum. This means, that the turbulent Prandtl number increases with decreasing molecular Prandtl number. However, this result is also dependent on the Reynolds number. For increasing Reynolds numbers, the turbulent mixing increases

and the influence of molecular heat conduction decreases. This means that, for increasing Reynolds numbers and Prandtl numbers larger than one, the turbulent Prandtl number approaches a constant value. On the other hand, experimental and DNS (Direct Numerical Simulation) results show that the turbulent Prandtl number reaches values larger than one close to the wall. For small Prandtl numbers, the value of $\Pr_t$ can be much larger than one, which has been shown by DNS and LES calculations e.g. by Bricteux et al. (2012). These results show nicely that the heat and momentum transfer differ in proximity of a solid wall.

There are only few reliable measurement data of the turbulent Prandtl number reported in literature (see Jischa 1982, Kays 1994). The scatter of these measurements is moderate for large molecular Prandtl numbers ($\Pr > 0.2$) and relatively large for lower molecular Prandtl numbers (liquid metal flows). Note that the models presented here for the turbulent Prandtl number can also be applied for liquid metal flows.

Many of the models for the turbulent Prandtl number are based on the Prandtl mixing length concept. Cebeci and Bradshaw (1984), for example, developed a model for the turbulent Prandtl number given by:

$$\Pr_t = \frac{\kappa}{\kappa_h} \frac{1 - \exp(-y^+/A^+)}{1 - \exp(-y^+/B^+)}, \quad y^+ = \frac{y_W u_\tau}{v} \tag{3.77}$$

with the quantities

$$\kappa = 0.4, \quad \kappa_h = 0.44, \quad A^+ = 26$$

$$B^+ = \frac{1}{\sqrt{\Pr}} \left( \begin{array}{c} 34.96 + 28.79 \log_{10} \Pr + 33.95 (\log_{10} \Pr)^2 \\ +6.33 (\log_{10} \Pr)^3 - 1.186 (\log_{10} \Pr)^4 \end{array} \right) \tag{3.78}$$

Kays and Crawford (1993) proposed a model for the turbulent Prandtl number, given by

$$\Pr_t = \left( \frac{1}{2 \Pr_{t\infty}} + C \Pe_t \sqrt{\frac{1}{\Pr_{t\infty}}} - (C \Pe_t)^2 \left[ 1 - \exp\left( -\frac{1}{C \Pe_t \sqrt{\Pr_{t\infty}}} \right) \right] \right)^{-1} \tag{3.79}$$

where $\Pe_t = \tilde{\varepsilon}_m \Pr$, $C = 0.3$ and $\Pr_{t\infty} = 0.85$.

Jischa and Rieke (1979) derived a model from modeled transport equations. As a result of their analysis, they obtained the following simple formulation for the turbulent Prandtl number

$$\Pr_t = 0.9 + \frac{182.4}{\Pr \Re_D^{0.888}} \tag{3.80}$$

The dependence of the turbulent Prandtl number on the wall coordinate has not been incorporated by Jischa and Rieke (1979).

One weakness of the model by Kays and Crawford (1993) is that the value for $\mathrm{Pr}_{t\infty}$ is a constant for all molecular Prandtl numbers. Using the functional dependence of the turbulent Prandtl number, given in Eq. (3.80), the value of $\mathrm{Pr}_{t\infty}$ in Eq. (3.79) can be improved. Following the work of Weigand et al. (1997a), the model given by Eq. (3.79) can be modified by using the following description for $\mathrm{Pr}_{t\infty}$

$$\mathrm{Pr}_{t\infty} = 0.85 + \frac{100}{\mathrm{Pr}\,\mathrm{Re}_D^{0.888}} \tag{3.81}$$

By using the above given values for $\mathrm{Pr}_{t\infty}$ in Eq. (3.79), the model for the turbulent Prandtl number is able to predict quite reliably the heat transfer for a lot of different applications and a broad range of molecular Prandtl numbers (see Weigand et al. (1997a, b), Kays et al. (2004)).

Another quite popular model is the one by Azer and Chao (1960). The original expressions for the turbulent Prandtl number given by Azer and Chao (1960) are very complicated. However, the authors reported in their paper the following approximation for $\mathrm{Pr} \ll 1$:

$$\mathrm{Pr}_t = \frac{1 + 380/\mathrm{Pe}_D^{0.58}\exp\left(-(1-\tilde{n})^{0.25}\right)}{1 + 135/\mathrm{Re}_D^{0.45}\exp\left(-(1-\tilde{n})^{0.25}\right)} \tag{3.82}$$

and for $0.6 \leq \mathrm{Pr} \leq 15$

$$\mathrm{Pr}_t = \frac{1 + 57\,\mathrm{Re}_D^{0.46}\,\mathrm{Pr}^{0.58}\exp\left(-(1-\tilde{n})^{0.25}\right)}{1 + 135/\mathrm{Re}_D^{0.45}\exp\left(-(1-\tilde{n})^{0.25}\right)} \tag{3.83}$$

Additionally, there are a lot of models for the turbulent Prandtl number reported in literature, which are mainly empirical or simply based on measurements. For example, for air flow the measurements of Ludwieg (1956) can be approximated by (see Reich and Beer 1989)

$$\mathrm{Pr}_t = \left(1.53 - 2.82\,\tilde{n}^2 + 3.85\,\tilde{n}^3 - 1.48\,\tilde{n}^4\right)^{-1} \tag{3.84}$$

After this short review of models for the turbulent Prandtl number we now want to proceed with the discussion of the turbulent heat transfer in a pipe.

### Heat Transfer in Turbulent Pipe Flow

If we set the flow index $F = 1$ in the above equations, the equations describing the heat transfer in a hydrodynamically fully developed pipe flow are obtained. This problem has been investigated first by Latzko (1921), who simplified the analysis by putting $Pr_t = 1$ in the energy Eq. (3.19). After neglecting the molecular heat conduction in Eq. (3.19), Latzko was able to predict the first three eigenvalues for

this problem. Later, Sleicher and Tribus (1957) were concerned with the turbulent Graetz problem. They calculated the first three eigenvalues for various Prandtl and Reynolds numbers. Notter and Sleicher (1972) investigated the problem in great detail. They used a universal turbulent velocity profile for their calculations. For the turbulent Prandtl number, an empirical model was used. For Pr < 1, they applied

$$\frac{1}{\mathrm{Pr}_t} = \frac{(\mathrm{Pr}\,\tilde{\varepsilon}_m)^{0.39}}{1 + (\mathrm{Pr}\,\tilde{\varepsilon}_m)^{0.39}} \left( 1 + \frac{5.64\,\sqrt{\mathrm{Pr}}}{1.39\,+\,\sqrt{\tilde{\varepsilon}_m}} \right) \tag{3.85}$$

For larger molecular Prandtl numbers, the turbulent Prandtl number was specified by

$$\frac{1}{\mathrm{Pr}_t} = \frac{1}{\tilde{\varepsilon}_m} \frac{0.0009(y^+)^3}{\left( 1 + (0.0818y^+)^2 \right)^{1/2}}, \quad 0 \le y^+ < 45 \tag{3.86}$$

For $y^+ > 45$, Eq. (3.85) was used again.

As stated before, the Nusselt number for fully developed flow depends only on the first eigenvalue, which can be predicted easily from the previously discussed eigenvalue problem. The Nusselt number for fully developed flow depends on the Reynolds number as well as on the Prandtl number. With increasing Reynolds number, the turbulent mixing increases and therefore the Nusselt number increases for a fixed Prandtl number. For a given value of the Reynolds number, an increasing value of the Prandtl number leads also to an increasing Nusselt number. For the fully developed Nusselt number a lot of correlations are reported in literature. One example is (see Cebeci and Bradshaw 1984)

$$\mathrm{Nu}_\infty = \frac{\mathrm{Re}_D\,\mathrm{Pr}\,\sqrt{c_f/8}}{0.833\left[ 5\,\mathrm{Pr} + 5\ln(5\,\mathrm{Pr} + 1) + 2.5\ln\left( \mathrm{Re}_D\sqrt{c_f/8}\Big/60 \right) \right]} \tag{3.87}$$

with the friction factor $c_f$ given by

$$c_f = \frac{0.3164}{\mathrm{Re}_D^{0.25}} \tag{3.88}$$

The above equation is valid only for Pr ≥ 0.2. For smaller molecular Prandtl numbers, the correlation

$$\mathrm{Nu}_\infty = 4.8 + 0.0156\mathrm{Re}_D^{0.85}\,\mathrm{Pr}^{0.93} \tag{3.89}$$

can be used (Sleicher and Rouse 1975). Figure 3.7 shows a comparison between predicted and measured Nusselt numbers for a fully developed liquid metal flow. The measured data are from Sleicher et al. (1973) and Gilliland et al. (1951). For the

**Fig. 3.7**  Nusselt number for fully developed pipe flow as a function of the Peclet number (Weigand et al. 1997a)
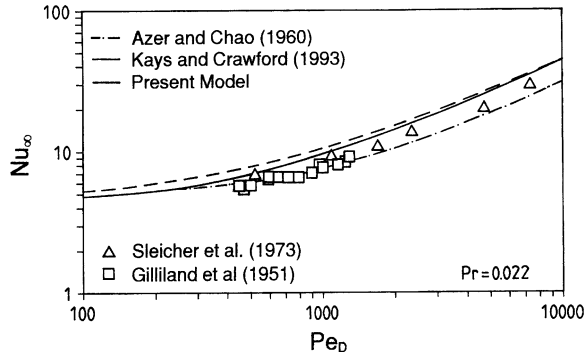


calculations, the turbulent Prandtl number model by Azer and Chao (1960) and Kays and Crawford (1993) have been used. It can be seen that both models lead to good agreement between measured and calculated values for a broad range of Peclet numbers. The distribution of the Nusselt number in the thermal entrance region for air flow is shown in Fig. 3.8. Here, experimental data by Abbrecht and Churchill (1960) have been compared with calculations of the Nusselt number, using the velocity distribution given in Appendix A and the turbulent Prandtl number model of Sleicher, Eq. (3.85). Very similar results can be obtained using the turbulent Prandtl number concept of Kays and Crawford (1993).

As it can be seen, the agreement between calculations and measurements is satisfactory. Figure 3.9 shows also some results for the thermal entrance region of a liquid metal flow (Pr = 0.022) for two different Reynolds numbers. For these calculations, the modified turbulent Prandtl number model of Weigand et al. (1997a) has been used (see Kays et al. 2004). As it can be seen, the agreement between calculations and measurement is good. This shows nicely the quality of the used turbulent Prandtl number model, which reproduces the correct behavior in the whole thermal entrance region.

**Fig. 3.8**  Variation of the Nusselt number in the thermal entrance region of a pipe for Pr = 0.72 (Weigand and Beer 1989)
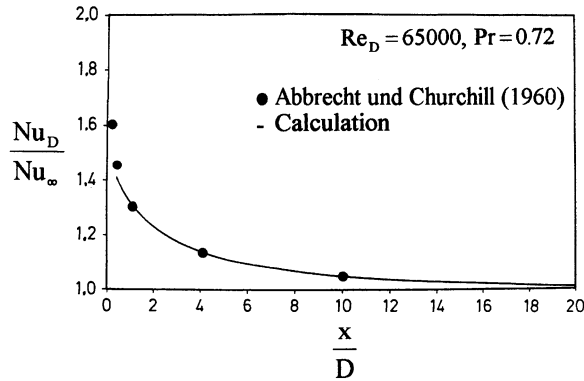
**Fig. 3.9** Variation of the
Nusselt number in the thermal
entrance region of a pipe for
$Pr = 0.022$ (Weigand et al.
1997a)

Fig. 3.9 Variation of the
Nusselt number in the thermal
entrance region of a pipe for
$Pr = 0.022$ (Weigand et al.
1997a)
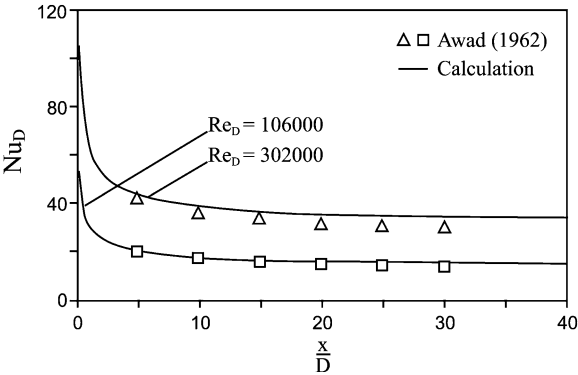


### Turbulent Heat Transfer in a Planar Channel

If we set the flow index $F = 0$ in the above equations, then the equations describing the heat transfer in a hydrodynamically fully developed channel flow are obtained. This problem has been investigated by Sakakibara and Endoh (1977), Shibani and Özisik (1977b) and Özisik et al. (1989). Özisik et al. (1989) pointed out that the eigenvalues in Shibani and Özisik (1977b) have been calculated with a wrong distribution of the wall coordinate $y^+$ in the turbulence model (a factor of 2 was missing in the definition of $y^+$). The Nusselt numbers calculated by Özisik et al. (1989) are based on a three layer approximation for the hydrodynamic fully developed velocity distribution (see for details Appendix A, Kays et al. 2004, and Reichhardt 1951). The turbulent eddy viscosity has been calculated according to Spalding (1961) for $y^+ < 40$ and according to Reichhardt for $y^+ \geq 40$. Figure 3.10 shows the distribution of the Nusselt number in the thermal entrance region of a planar channel for three different Reynolds numbers and for air ($Pr = 0.72$). The Nusselt number distribution according to Özisik et al. (1989), which is in good agreement to existing correlations, agrees very well with own predictions using the velocity distribution given in Appendix A.

**Fig. 3.10** Variation of the
Nusselt number in the thermal
entrance region of a planar
channel for $Pr = 0.72$
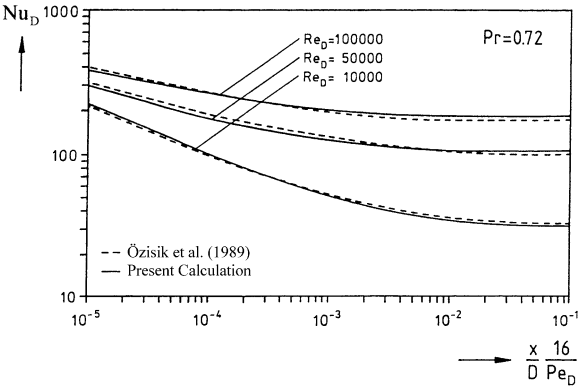
## 3.2 Thermal Entrance Solutions for an Arbitrary Wall Temperature Distribution

Having obtained the solution for the uniform wall temperature case, the present section deals with the general case of an arbitrary wall temperature distribution. We assume that the wall temperature changes continuously with $\tilde{x}$ (for $\tilde{x} > 0$). Note that if there is a jump in the wall temperature distribution, the solution for this case is given by Eq. (3.55) and has only to be added to the solution obtained here. The problem under consideration is shown in Fig. 3.11.

If we introduce a new dimensionless temperature $\Theta_1$, defined by

$$\Theta_1 = \frac{T - T_W(\tilde{x})}{T_0 - T_W(0)} \tag{3.90}$$

the energy equation becomes

$$\tilde{u}(\tilde{n}) \frac{\partial \Theta_1}{\partial \tilde{x}} = \frac{1}{\tilde{r}^F} \frac{\partial}{\partial \tilde{n}} \left[ \tilde{r}^F (1 + Pr\tilde{\varepsilon}_{hn}) \frac{\partial \Theta_1}{\partial \tilde{n}} \right] + \tilde{u}(\tilde{n}) \frac{d\Theta_W}{d\tilde{x}} \tag{3.91}$$

with the boundary conditions

$$
\begin{aligned}
&\tilde{x} = 0 : \Theta_1(0, \tilde{n}) = 1, \quad \text{temperature jump at } \tilde{x} = 0 \\
&\tilde{n} = 0 : \left. \frac{\partial \Theta_1}{\partial \tilde{n}} \right|_{\tilde{n}=0} = 0 \\
&\tilde{n} = 1 : \Theta_1(\tilde{x}, 1) = 0
\end{aligned}
\tag{3.92}
$$

and the abbreviation $\Theta_W = (T_0 - T_W(\tilde{x}))/(T_0 - T_W(0))$.

As it can be seen from the boundary conditions, Eq. (3.92), and also from Fig. 3.11, the wall temperature distribution has a jump at $\tilde{x} = 0$. Introducing the newly defined temperature $\Theta_1$ into the energy equation results in a new term on the right hand side of Eq. (3.91). On the other hand, the boundary conditions for $\tilde{n} = 0$ and $\tilde{n} = 1$ are homogenous for $\Theta_1$. This means that the solution for the case of an arbitrary wall temperature requires the solution of the non-homogenous equation.
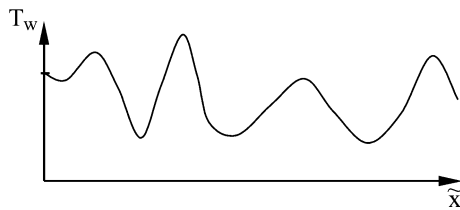


**Fig. 3.11** Duct with arbitrary wall temperature

In the previous section we have seen that an arbitrary function could be represented by an infinite number of eigenfunctions. Thus, the following expression for the temperature distribution is assumed

$$\Theta_1 = \sum_{m=0}^{\infty} B_m(\tilde{x})\, \Phi_m(\tilde{n}) \tag{3.93}$$

The eigenfunctions in Eq. (3.93) are already known from the solution of the eigenvalue problem (see Eqs. (3.25) and (3.26)). In the following analysis, we try to find a solution of the above non-homogeneous problem by using the orthogonality properties of the eigenfunctions. Multiplying both sides of Eq. (3.93) by $\tilde{u}\,\tilde{r}^F \Phi_n(\tilde{n})$ and integrating the resulting expressions between 0 and 1 gives the following equation for the functions $B_m$

$$B_m = \frac{\int_0^1 \tilde{u}\,\tilde{r}^F \Phi_m \Theta_1 \, d\tilde{n}}{\int_0^1 \tilde{u}\,\tilde{r}^F \Phi_m^2 \, d\tilde{n}} = \frac{1}{K_m} \int_0^1 \tilde{u}\,\tilde{r}^F \Phi_m \Theta_1 \, d\tilde{n} \tag{3.94}$$

Because of the boundary condition for $\Theta_1$ at $\tilde{x} = 0$, the functions $B_m$ have to satisfy

$$B_m(0) = \frac{1}{K_m} \int_0^1 \tilde{u}\,\tilde{r}^F \Phi_m \Theta_1 \, d\tilde{n} = \frac{-1}{K_m} \int_0^1 1 \cdot \left[\tilde{r}^F a_2 \Phi_m'\right]' d\tilde{n} = \frac{-\Phi_m'(1)}{\lambda_m^2 K_m} \tag{3.95}$$

The two other boundary conditions for $\tilde{n} = 0$ and $\tilde{n} = 1$ are automatically satisfied by Eq. (3.93) because of the employed eigenfunctions.

If we differentiate Eq. (3.94) with respect to $\tilde{x}$, we obtain an ordinary differential equation for the unknown functions $B_m$

$$\frac{dB_m}{d\tilde{x}} = \frac{1}{K_m} \int_0^1 \tilde{u}\tilde{r}^F \Phi_m \frac{\partial \Theta_1}{\partial \tilde{x}} d\tilde{n} \tag{3.96}$$

The expression $\tilde{u}\,\partial\Theta_1/\partial\tilde{x}$ in the above equation can be replaced by using the energy Eq. (3.91). This results in

$$\frac{dB_m}{d\tilde{x}} = \frac{1}{K_m} \int_0^1 \frac{\partial}{\partial \tilde{n}} \left[\tilde{r}^F a_2(\tilde{n}) \frac{\partial \Theta_1}{\partial \tilde{x}}\right] \Phi_m d\tilde{n} + \frac{1}{K_m} \int_0^1 \tilde{u}\tilde{r}^F \Phi_m \frac{d\Theta_W}{d\tilde{x}} d\tilde{n} \tag{3.97}$$

The first integral on the right hand side of Eq. (3.97) can be solved by partial integration and by taking into account the boundary conditions for $\Theta_1$ and $\Phi_m$. The second integral can be solved directly by using the differential equation for the eigenfunctions, Eq. (3.25). This results in

$$\frac{dB_m}{d\tilde{x}} = -\lambda_m^2 B_m - \frac{\Phi_m'(1)}{\lambda_m^2 K_m} \frac{d\Theta_W}{d\tilde{x}} \qquad (3.98)$$

The ordinary differential Equation (3.98) has the general solution

$$B_m = C_m \exp\left(-\lambda_m^2 \tilde{x}\right) - \frac{\Phi_m'(1)}{\lambda_m^2 K_m} \int\limits_0^{\tilde{x}} \frac{d\Theta_W}{d\tilde{x}} \exp\left(-\lambda_m^2(\xi - \tilde{x})\right) d\xi \qquad (3.99)$$

The constants $C_m$ can be determined by comparing Eq. (3.99) with Eq. (3.95) for $\tilde{x} = 0$. This results in

$$B_m = -\frac{\Phi_m'(1)}{\lambda_m^2 K_m} \left\{ \exp\left(-\lambda_m^2 \tilde{x}\right) + \int\limits_0^{\tilde{x}} \frac{d\Theta_W}{d\tilde{x}} \exp\left(-\lambda_m^2(\xi - \tilde{x})\right) d\xi \right\} \qquad (3.100)$$

Introducing Eq. (3.100) into Eq. (3.93) results in the following equation for the temperature distribution

$$\Theta_1 = \Theta(\tilde{x}, \tilde{n}) + \int\limits_0^{\tilde{x}} \Theta((\tilde{x} - \xi), \tilde{n}) \frac{d\Theta_W}{d\tilde{x}} d\xi \qquad (3.101)$$

In this equation, $\Theta(\tilde{x}, \tilde{n})$ denotes the temperature distribution for the constant wall temperature solution. For $\Theta_W = \text{const.}$ Eq. (3.101) states that $\Theta_1 = \Theta$. From Eq. (3.101) it is obvious, that the temperature distribution for the case of an arbitrary wall temperature can be constructed if the temperature distribution for the uniform wall temperature case is known. This shows very nicely the power of the superposition approach.

It should be noted here, that the solution according to Eq. (3.101) can also be obtained by other methods, for example, by using Duhamel's theorem. The reader is referred to Kays et al. (2004) for a different method to derive the above solution for the temperature field for an axial varying wall temperature. The present solution has the advantage that the solution method can also be used in the same way for an arbitrary source term in the energy equation.

## 3.3  Flow and Heat Transfer in Axially Rotating Pipes with Constant Wall Heat Flux

Fluid flow and heat transfer in rotating systems are not only of considerable theoretical interest, but also of great practical importance. Therefore, transport phenomena in rotating systems have challenged engineers and scientists for a long time. For example, Lord Rayleigh (1917) investigated the dynamics and stability of revolving fluids. Also some of the classical solutions of the Navier-Stokes equations were obtained for rotating systems (see Schlichting (1982)). Von Kármán (1921) investigated the flow induced by a rotating disk and the associated convective heat transfer. The stability of a circular flow in an annulus, formed between two concentric rotating cylinders, was studied by Taylor (1923).

   The turbulent flow and heat transfer in an axially rotating pipe is a rather elementary configuration and is therefore suitable as a test case for new turbulence models. Furthermore, many technical applications in rotating machinery are using this simple type of geometry. One of these technical applications is the cooling of gas turbine shafts by means of air flowing through a longitudinal hole in the shaft itself. When a fluid enters a pipe revolving around its axis, tangential forces acting between the rotating pipe and the fluid cause the fluid to rotate with the pipe, resulting in a flow pattern rather different from the one observed in a non-rotating pipe. Rotation was found to have a remarkable influence on the suppression of the turbulent motion because of radially growing centrifugal forces. The effect of pipe rotation on the hydraulic loss has been investigated experimentally by Levy (1929), White (1964) and Shchukin (1967). If the flow is turbulent, the flow is stabilized with increasing rotation rate and the turbulence is suppressed by the centrifugal forces. This can be seen in Fig. 3.12, where flow visualization results from White (1964) are shown. For turbulent flow in a rotating pipe, Borisenko et al. (1973) studied the effect of rotation on the turbulent velocity fluctuations using hot-wire probes and showed that they were suppressed.

**Fig. 3.12**  Flow visualization experiments for the flow in an axially rotating pipe (White 1964)
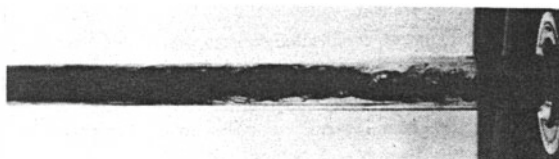


$Re_D = 3520$, $Re_\varphi = 0$: Turbulent Flow
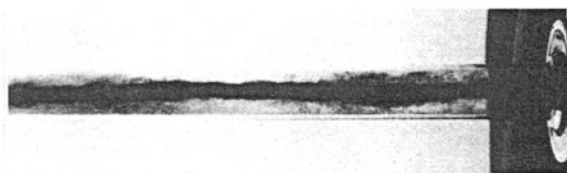


$Re_D = 3520$, $Re_\varphi = 4800$: Laminarized Flow

Murakami and Kikuyama (1980) measured the time-mean velocity components and hydraulic losses in an axially rotating pipe when a fully developed turbulent flow was introduced into the pipe. The results were obtained in dependence of the Reynolds number $\mathrm{Re}_D = \bar{u}D/v$, the rotation rate $\mathrm{N} = w_W/\bar{u}$ and the length of the rotating pipe. The rotation was found to suppress the turbulence in the flow, and also to reduce the hydraulic loss. With increasing rotational speed, the axial velocity distribution finally approaches the Hagen-Poiseuille flow. Kikuyama et al. (1983) calculated, for the case of a hydrodynamically fully developed flow, the distribution of the axial velocity component by using a simple mixing length approach according to Bradshaw (1969). The distribution of the tangential velocity component was approximated by

$$\frac{w}{w_W} = \left(\frac{r}{R}\right)^2 \tag{3.102}$$

which is in good agreement with experimental data from Murakami and Kikuyama (1980), Kikuyama et al. (1983) and Reich and Beer (1989). Reich and Beer (1989) extended the mixing length approach of Kikuyama et al. (1983) and calculated, for the case of a hydrodynamically and thermally fully developed flow, the axial velocity component and the temperature distribution in the fluid. They showed that in agreement with their measurements, the heat transfer decreased with increasing rotation rate. Hirai and Takagi (1987) and Hirai et al. (1988) calculated the velocity distribution and the heat transfer for the fully developed flow in the axial rotating pipe. In their calculations, it has not been necessary to prescribe the tangential velocity distribution (like Eq. (3.102)) at the beginning of the calculation procedure as it has been done by Kikuyama et al. (1983) and Reich and Beer (1989). However, they obtained the universal distribution of the tangential velocity as a result of their calculations. For the hydrodynamically fully developed flow Weigand and Beer (1989a) solved analytically the energy equation and calculated the local distribution of the Nusselt number for the thermal entrance region. The calculated Nusselt numbers compared very well with the experimentally obtained results of Reich (1988). For the case of a convectively cooled pipe, Weigand and Beer (1992b) obtained an analytical solution for the Nusselt number distribution in the thermal entrance region. It could be shown, that the thermal wall boundary condition influenced the values of the Nusselt number. This is because of the laminarization effect within the pipe. For the case of a hydrodynamically and thermally developed flow, Weigand and Beer (1992a) calculated numerically the distribution of the axial velocity and the local Nusselt number as a function of the axial coordinate. Because of the simple geometry involved, the fully developed flow in an axial rotating pipe has been investigated both by using LES (large eddy simulation) and DNS (Direct Numerical Simulation). Eggels and Nieuwstadt (1993) calculated the axial and tangential velocity distribution in the axial rotating pipe by using LES. Their calculations showed the parabolic distribution of the tangential velocity component and agreed well with measurements of Reich (1988) and Nishibori et al. (1987). Orlandi and Fatica (1997) and Olandi and Ebstein (2000)

investigated the flow by DNS for low Reynolds numbers. Satake and Kunugi (2002) performed a DNS for a Reynolds number of 5283 and various rotation rates. Ould-Rouiss et al. (2010) studied the turbulent heat transfer in a rotating pipe by using LES and DNS. They found that the streamwise turbulent heat flux is reduced and the azimuthal one is increased with increasing rotation rates. They also showed a reduction in Nusselt number and friction factor. Malin and Younis (1997) employed the closures for the transport equations of Gibson and Younis (1986) and Speziale et al. (1991) to predict the flow and heat transfer in an axially rotating pipe. The results were compared to experimental data and LES results and good agreement was found for both models. Rinck and Beer (1999) used a modified Reynolds stress model to predict the fully developed flow in an axially rotating pipe. They found good agreement between their predictions and experimental data of Reich (1988). Speziale et al. (2000) presented a comprehensive analysis of the modeling of turbulent flows in rotating pipes. They discussed also the main physical characteristics of the flow and surveyed the capabilities of different classes of closure models to reproduce them.

### 3.3.1 Velocity Distribution for the Hydrodynamically Fully Developed Flow in an Axial Rotating Pipe

The hydrodynamically fully developed velocity distribution in an axially rotating pipe can be calculated by using a simple mixing length approach. This procedure is only briefly outlined here, since our main focus is on analytical methods relevant for solving heat transfer problem. A more detailed explanation of the method as well as a review on other methods for calculating the velocity distribution in an axial rotating pipe is given in Appendix B.

Figure 3.13 shows the geometry and the cylindrical coordinate system with the $x$, $r$, $\varphi$ axis and the related velocity components $u$, $v$, $w$.



**Fig. 3.13** Physical model and coordinate system (Reich and Beer 1989)
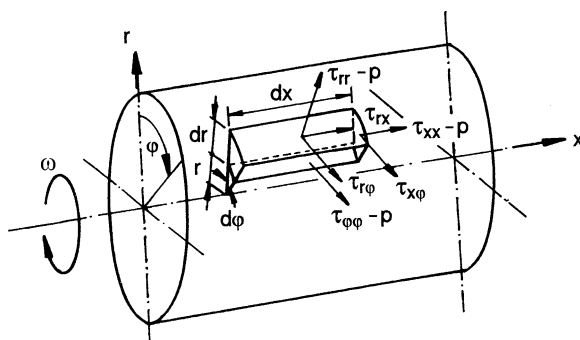
If we assume a hydrodynamically fully developed turbulent flow with constant
fluid properties, the Navier-Stokes equations for the rotational symmetric case are
given by (see for example Reich 1988):

$$-\rho \frac{w^2}{r} = -\frac{\partial p}{\partial r} - \frac{\rho}{r}\frac{\partial}{\partial r}\left(r\overline{v'v'}\right) + \rho \frac{\overline{w'w'}}{r} \tag{3.103}$$

$$0 = \frac{1}{r^2}\frac{\partial}{\partial r}\left(\mu r^3 \frac{\partial}{\partial r}\left(\frac{w}{r}\right) - \rho r^2 \overline{v'w'}\right) \tag{3.104}$$

$$0 = \frac{\partial p}{\partial x} + \frac{1}{r}\frac{\partial}{\partial r}\left(\mu r \frac{\partial u}{\partial r} - \rho r\overline{u'v'}\right) \tag{3.105}$$

with the boundary conditions

$$\begin{aligned}
r = 0 &: w = 0, \ \ v = 0, \ \frac{\partial u}{\partial r} = 0 \\
r = R &: w = w_W, \ \ u = 0, \ v = 0
\end{aligned} \tag{3.106}$$

Since we assume a hydrodynamically fully developed flow, the radial velocity
component $v$ is zero everywhere and the continuity equation results in the fact that the
axial velocity component $u$ is only a function of $r$. As mentioned before, experimental
data indicate that the tangential velocity distribution is universal and can be
approximated by Eq. (3.102). Figure 3.14 shows the tangential velocity distribution
for different rotation rates N as well as for different Reynolds numbers. From Fig. 3.14
it is obvious that Eq. (3.102) is a very good approximation for the tangential velocity
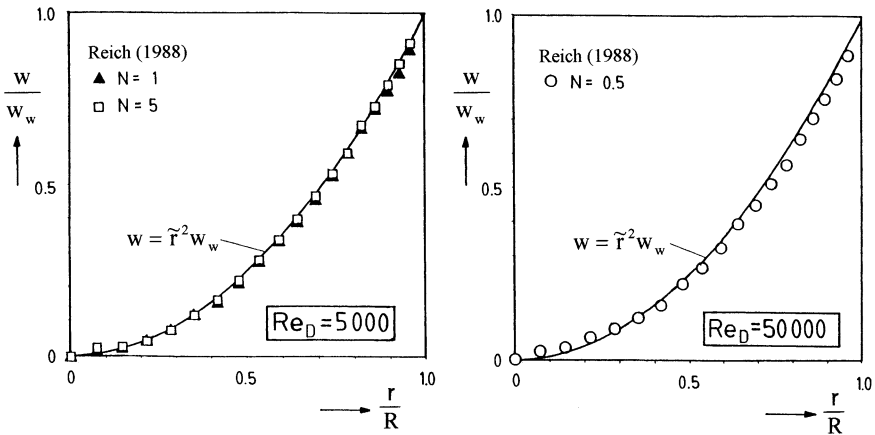


**Fig. 3.14** Tangential velocity distribution (Reich and Beer 1989)

distribution. Introducing Eq. (3.102) into Eq. (3.104) shows that $\overline{v'w'} \sim C\,r$. This relation is of course only correct far away from the wall. However, it is interesting to note that the above given linear relation has been confirmed by DNS.

The axial velocity distribution $u(r)$ can be calculated from Eq. (3.105). In order to do this, the turbulent shear stress in this equation has to be related to the mean velocity gradients. This can be done by using a mixing length model according to Koosinlin et al. (1975). This results in the following expression for the turbulent shear stress

$$\overline{\rho u'v'} = \rho\, l^2 \left[ \left( \frac{\partial u}{\partial r} \right)^2 + \left( r \frac{\partial}{\partial r} \left( \frac{w}{r} \right) \right)^2 \right]^{1/2} \frac{\partial u}{\partial r} = \varepsilon_m \rho \frac{\partial u}{\partial r} \tag{3.107}$$

where the mixing length distribution $l$ is given by Reich and Beer (1989)

$$\frac{l}{l_0} = \left( 1 - \frac{1}{6} \mathrm{Ri} \right)^2 \tag{3.108}$$

The mixing length distribution $l_0$ is the one for a non-rotating pipe (see Appendix A, Eq. (A.20)). The Richardson number in Eq. (3.108) describes the effect of pipe rotation on the turbulent motion and is defined by

$$\mathrm{Ri} = \frac{2 \dfrac{w}{r^2} \dfrac{\partial}{\partial r} (wr)}{\left( \dfrac{\partial u}{\partial r} \right)^2 + \left( r \dfrac{\partial}{\partial r} \left( \dfrac{w}{r} \right) \right)^2} \tag{3.109}$$

Without rotation, $\mathrm{Ri} = 0$ and there exists a fully developed turbulent pipe flow. If $\mathrm{Ri} > 0$, i.e. for an axially rotating pipe with a radially growing tangential velocity, the centrifugal forces suppress the turbulent fluctuations and the mixing length decreases.

For large rotation rates N the axial velocity profile $u$ will tend to a laminar pipe flow, given by Eq. (3.1). Inserting Eqs. (3.1) and (3.102) into Eq. (3.109) results for the limiting case that $N \to \infty$ in $\mathrm{Ri} = 6$ for the Richardson number.

Inserting Eqs. (3.107) and (3.109) into Eq. (3.105) results in a strongly non-linear ordinary differential equation for the axial velocity component $u$. This is shown in detail in Appendix B. Figure 3.15 shows a comparison between calculated and measured axial velocity distributions according to Reich and Beer (1989). It can be seen that the numerical calculations agree well with the measurements.

In Appendix B, an analytical approximation for the velocity distribution in the axial rotating pipe is given (Weigand and Beer 1994).
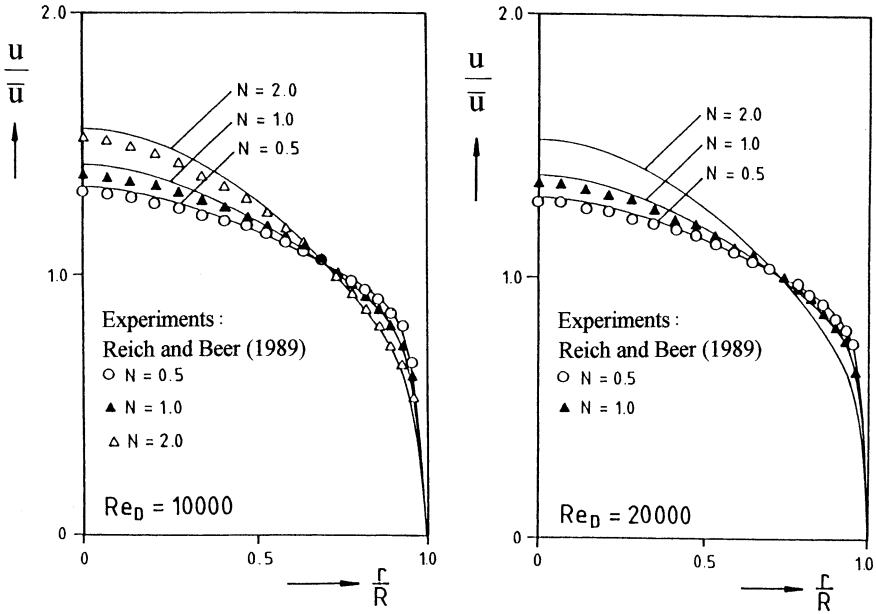
**Fig. 3.15** Axial velocity distribution as a function of the rotation rate N (Reich and Beer 1989)

## 3.3.2 Thermal Entrance Solution for Constant Wall Heat Flux

The thermal entrance solution for the case of a constant heat flux at the wall can also be obtained by the method of separation of variables. However, because of the different wall boundary condition, the approach for solving this problem is different to the case of a constant wall temperature.

If we assume that the flow is incompressible and that the fluid properties are constant, the energy equation for the hydrodynamically fully developed flow, with negligible axial heat conduction effects, takes the form

$$\rho c_p u(r)\frac{\partial T}{\partial x} = \frac{1}{r}\frac{\partial}{\partial r}\left[r\left(k\frac{\partial T}{\partial r} - \rho\overline{v'T'}\right)\right] \tag{3.110}$$

If we replace the turbulent heat flux in Eq. (3.110) by the eddy viscosity and the turbulent Prandtl number, we obtain

$$\rho c_p u(r)\frac{\partial T}{\partial x} = \frac{1}{r}\frac{\partial}{\partial r}\left[\left\{k + \rho c_p \frac{l^2}{\text{Pr}_t}\left[\left(\frac{\partial u}{\partial r}\right)^2 + \left(r\frac{\partial}{\partial r}\left(\frac{w}{r}\right)\right)^2\right]^{1/2}\right\}r\frac{\partial T}{\partial r}\right] \tag{3.111}$$

with the turbulent Prandtl number for air flow given by (see Reich and Beer 1989)

$$\frac{1}{Pr_t} = 1.53 - 2.82 \left(\frac{r}{R}\right)^2 + 3.85 \left(\frac{r}{R}\right)^3 - 1.48 \left(\frac{r}{R}\right)^4 \tag{3.84}$$

Equation (3.111) has to be solved with the following boundary conditions

$$x = 0 : T = T_0$$
$$r = 0 : \frac{\partial T}{\partial r} = 0, \quad r = R : -k\frac{\partial T}{\partial r} = \dot{q}_W = \text{const.} \tag{3.112}$$

For the constant wall temperature case, the driving temperature potential $T_W - T_0$ can be used to scale the temperature. This is not the case for a constant wall heat flux. Therefore, the following quantities are used to make the equations dimensionless:

$$\Theta = \frac{T - T_0}{(\dot{q}_W R/k)}, \quad \tilde{r} = \frac{r}{R}, \quad \tilde{x} = \frac{x}{R}\frac{2}{Re_D\, Pr}, \quad \tilde{u} = \frac{u}{\bar{u}}, \quad Re_D = \frac{\bar{u}\,D}{\nu} \tag{3.113}$$

As it can be seen from Eq. (3.113), the temperature is made dimensionless with the heat flux density at the wall, while the axial and radial coordinates are made dimensionless in the usual way. Introducing the dimensionless quantities into the Eqs. (3.111) and (3.112) results in:

$$\tilde{u}\tilde{r}\frac{\partial\Theta}{\partial\tilde{x}} = \frac{\partial}{\partial\tilde{r}}\left[\tilde{r}a_2(\tilde{r})\frac{\partial\Theta}{\partial\tilde{r}}\right] \tag{3.114}$$

with the boundary conditions

$$\tilde{x} = 0 : \Theta = 0$$
$$\tilde{r} = 0 : \frac{\partial\Theta}{\partial\tilde{r}} = 0, \quad \tilde{r} = 1 : \frac{\partial\Theta}{\partial\tilde{r}} = -1 \tag{3.115}$$

and the function $a_2(\tilde{r})$

$$a_2(\tilde{r}) = 1 + \frac{Pr}{Pr_t}Re_D l^2\left[\left(\frac{\partial\tilde{u}}{\partial\tilde{r}}\right)^2 + \left(\frac{1}{2}\tilde{r}\,N\right)^2\right]^{1/2} \tag{3.116}$$

Because the wall boundary condition for $\tilde{r} = 1$ is non-homogeneous, the solution for the problem given by Eqs. (3.114) and (3.115) has to be split into two problems. In the first problem only a particular solution for the energy equation is searched.

The second problem can then be solved afterwards by using the method of separation of variables. This can be done, because the energy equation, as well as the wall boundary conditions, are linear.

Introducing the function

$$\Theta = \Theta_1 + \Theta_2 \tag{3.117}$$

into the above equations results in the two problems

$$\tilde{u}\tilde{r}\frac{\partial\Theta_1}{\partial\tilde{x}} = \frac{\partial}{\partial\tilde{r}}\left[\tilde{r}a_2(\tilde{r})\frac{\partial\Theta_1}{\partial\tilde{r}}\right] \tag{3.118}$$

with the boundary conditions

$$\tilde{r} = 0 : \frac{\partial\Theta_1}{\partial\tilde{r}} = 0, \quad \tilde{r} = 1 : \frac{\partial\Theta_1}{\partial\tilde{r}} = -1 \tag{3.119}$$

and

$$\tilde{u}\tilde{r}\frac{\partial\Theta_2}{\partial\tilde{x}} = \frac{\partial}{\partial\tilde{r}}\left[\tilde{r}a_2(\tilde{r})\frac{\partial\Theta_2}{\partial\tilde{r}}\right] \tag{3.120}$$

with the boundary conditions

$$\tilde{x} = 0 : \Theta_2 = -\Theta_1$$
$$\tilde{r} = 0 : \frac{\partial\Theta_2}{\partial\tilde{r}} = 0, \quad \tilde{r} = 1 : \frac{\partial\Theta_2}{\partial\tilde{r}} = 0 \tag{3.121}$$

Because only one particular solution of the energy equation has to be found by solving the problem for $\Theta_1$, the boundary condition for $\tilde{x} = 0$ can be ignored. This implies that, for the second problem, the boundary condition for $\tilde{x} = 0$ has to be modified. Physically, the solution $\Theta_1$ represents the temperature distribution for the fully developed flow, i.e. far away from the pipe entrance, where the fluid temperature monotonously increases due to the heat addition through the wall.

**Temperature Distribution for the Fully Developed Flow $(\Theta_1)$**

For the fully developed flow, the temperature distribution in the pipe increases linearly with growing values of the axial coordinate. This can be shown by looking at an energy balance for the pipe section shown in Fig. 3.16.

The energy balance leads to

$$2\pi Rx\dot{q}_W = \int_0^{2\pi}\int_0^R \rho c_p(T - T_0)urdrd\varphi \tag{3.122}$$

**Fig. 3.16** Energy balance for the pipe with an uniform heat flux at the wall
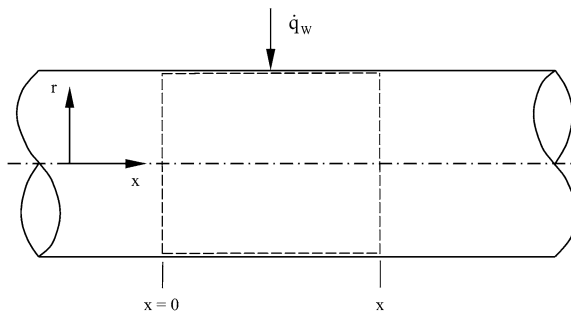
Introducing the dimensionless quantities from Eq. (3.113) into Eq. (3.122) gives

$$\tilde{x} = \int_0^1 \Theta_1 \tilde{u} \tilde{r} d\tilde{r} \qquad (3.123)$$

From Eq. (3.123), it is obvious that the temperature in the fluid increases linearly with growing axial distances for the fully developed flow. This motivates the introduction of the following expression for $\Theta_1$

$$\Theta_1 = C_1 \tilde{x} + \psi(\tilde{r}) \qquad (3.124)$$

Introducing Eq. (3.124) into Eqs. (3.118) and (3.119) and into Eq. (3.123) results in

$$\tilde{u} \tilde{r} C_1 = \frac{d}{d\tilde{r}} \left( a_2(\tilde{r}) \tilde{r} \frac{d\psi}{d\tilde{r}} \right) \qquad (3.125)$$

$$\tilde{r} = 0 : \frac{d\psi}{d\tilde{r}} = 0, \quad \tilde{r} = 1 : \frac{d\psi}{d\tilde{r}} = -1 \qquad (3.126)$$

$$\tilde{x} = \int_0^1 \tilde{x} C_1 \tilde{u} \tilde{r} d\tilde{r} + \int_0^1 \psi(\tilde{r}) \tilde{u} \tilde{r} d\tilde{r} \qquad (3.127)$$

From Eq. (3.127), it can be seen that the unknown constant $C_1$ is determined by the integral energy balance. Solving the above set of ordinary differential equations results in the following temperature distribution for the fully developed flow

$$\Theta_1(\tilde{r}, \tilde{x}) = -2\tilde{x} + \bar{\psi}(\tilde{r}) + C_2 \qquad (3.128)$$

with the abbreviations

$$\bar{\psi}(\tilde{r}) = \int_0^{\tilde{r}} \left( \frac{-2}{\eta a_2(\eta)} \int_0^{\eta} \tilde{u}(\xi) \xi d\xi \right) d\eta, \quad C_2 = - \int_0^1 2\bar{\psi}(\tilde{r}) \tilde{r} \tilde{u} d\tilde{r} \qquad (3.129)$$

### The Temperature Distribution $\Theta_2$

Introducing the obtained temperature distribution for the fully developed flow into Eq. (3.121) results in the following problem for $\Theta_2$

$$\tilde{u}\tilde{r}\frac{\partial\Theta_2}{\partial\tilde{x}} = \frac{\partial}{\partial\tilde{r}}\left[\tilde{r}a_2(\tilde{r})\frac{\partial\Theta_2}{\partial\tilde{r}}\right] \tag{3.120}$$

$$\tilde{x} = 0 : \Theta_2 = \bar{\psi}(\tilde{r}) + C_2$$
$$\tilde{r} = 0 : \frac{\partial\Theta_2}{\partial\tilde{r}} = 0, \quad \tilde{r} = 1 : \frac{\partial\Theta_2}{\partial\tilde{r}} = 0 \tag{3.130}$$

The latter can be solved using the method of separation of variables. Introducing

$$\Theta_{2j} = F_j(\tilde{x})\,\Phi_j(\tilde{r}) \tag{3.131}$$

into Eqs. (3.120), (3.130) results in the following eigenvalue problem

$$\left(a_2(\tilde{r})\tilde{r}\Phi_j'\right)' + \lambda_j^2\tilde{r}\tilde{u}\,\Phi_j' = 0 \tag{3.132}$$

with the boundary conditions

$$\tilde{r} = 0 : \Phi_j' = 0, \tag{3.133}$$

and an arbitrary normalization condition

$$\tilde{r} = 0 : \Phi_j = 1 \tag{3.134}$$

The functions $F_j(\tilde{x})$ are given by

$$F_j(\tilde{x}) = D_j \exp(-\lambda_j^2\tilde{x}) \tag{3.135}$$

The eigenfunctions can be predicted with a program similar to the one given in Appendix C. The temperature distribution $\Theta_2$ is then given by

$$\Theta_2 = \sum_{j=0}^{\infty} A_j\Phi_j(\tilde{r}) \exp\left(-\lambda_j^2\,\tilde{x}\right) \tag{3.136}$$

The constants $A_j$ can be calculated with a procedure similar to the one employed in Sect. 3.1 for the constant wall temperature case. Using the orthogonality of the eigenfunctions leads for the present case to

$$A_j = \frac{\int_0^1 \psi(\tilde{r})\tilde{u}(\tilde{r})\tilde{r}\Phi_j(\tilde{r})d\tilde{r}}{\int_0^1 \tilde{u}\tilde{r}\Phi_j^2(\tilde{r})d\tilde{r}} \tag{3.137}$$

**Table 3.1** Eigenvalues and constants for different rotation rates and different Reynolds numbers (Pr = 0.71)

| **Re$_D$ = 5000** | | | | | |
|---|---|---|---|---|---|
| N | $\lambda_0^2$ | $\lambda_1^2$ | $\lambda_2^2$ | $A_0\Phi_0(1)$ | $A_1\Phi_1(1)$ | $A_2\Phi_2(1)$ |
| 0 | 0 | 152.95 | 436.18 | 0 | 0.0287 | 0.0156 |
| 1 | 0 | 80.76 | 250.74 | 0 | 0.0409 | 0.0183 |
| 2 | 0 | 46.13 | 146.25 | 0 | 0.0654 | 0.0259 |
| 3 | 0 | 30.56 | 97.52 | 0 | 0.0946 | 0.0358 |
| 5 | 0 | 18.62 | 59.73 | 0 | 0.1467 | 0.0537 |
| **Re$_D$ = 20,000** | | | | | |
| N | $\lambda_0^2$ | $\lambda_1^2$ | $\lambda_2^2$ | $A_0\Phi_0(1)$ | $A_1\Phi_1(1)$ | $A_2\Phi_2(1)$ |
| 0 | 0 | 505.25 | 1476.01 | 0 | 0.0077 | 0.0044 |
| 1 | 0 | 216.04 | 687.15 | 0 | 0.0140 | 0.0058 |
| 2 | 0 | 108.93 | 350.64 | 0 | 0.0266 | 0.0010 |
| 3 | 0 | 63.24 | 203.82 | 0 | 0.0450 | 0.0165 |
| 5 | 0 | 28.57 | 92.04 | 0 | 0.0960 | 0.0349 |
| **Re$_D$ = 50,000** | | | | | |
| N | $\lambda_0^2$ | $\lambda_1^2$ | $\lambda_2^2$ | $A_0\Phi_0(1)$ | $A_1\Phi_1(1)$ | $A_2\Phi_2(1)$ |
| 0 | 0 | 1115.14 | 3281.90 | 0 | 0.0034 | 0.0018 |
| 1 | 0 | 436.34 | 1396.90 | 0 | 0.0068 | 0.0027 |
| 2 | 0 | 210.11 | 676.36 | 0 | 0.0136 | 0.0048 |
| 3 | 0 | 115.92 | 375.17 | 0 | 0.0246 | 0.0088 |
| 5 | 0 | 44.17 | 142.76 | 0 | 0.0630 | 0.0225 |

Both the eigenvalues and eigenfunctions can be calculated numerically. Table 3.1 reports some eigenvalues and constants $A_j\Phi_j(1)$ calculated for different Reynolds numbers and rotation rates N. Note that the eigenvalues increase with increasing Reynolds numbers and decrease with increasing rotation rates. This means that increasing Reynolds numbers result in a better mixing in the flow and lead to a shorter thermal entrance length, whereas increasing rotation rates lead to laminarization and therefore to a longer thermal entrance length.

From Table 3.1, an interesting fact can be noticed. For the considered wall boundary conditions, $\lambda_0 = 0$ is a possible eigenvalue. This eigenvalue results in the possible eigenfunction $\Phi_0 = 1$. If we introduce this eigenvalue and the eigenfunction into Eq. (3.137), we obtain $A_0 = 0$ (because the numerator of Eq. (3.137) is zero according to Eq. (3.127)). Therefore, $\lambda_0 = 0$ can be excluded from the considerations and Eq. (3.137) can further be simplified. One finally obtains

$$A_j = \frac{-\Phi_j'(1)/\lambda_j^2}{\int_0^1 \tilde{u}\tilde{r}\Phi_j'(\tilde{r})d\tilde{r}}, \quad j = 1, 2, 3 \ldots \tag{3.138}$$

After having predicted $\Theta_1$ and $\Theta_2$, the temperature distribution in the fluid is completely known

$$\Theta(\tilde{r}, \tilde{x}) = -2\tilde{x} + \psi(\tilde{r}) + \sum_{j=1}^{\infty} A_j \Phi_j(\tilde{r}) \exp\left(-\lambda_j^2 \tilde{x}\right) \qquad (3.139)$$

With the help of Eq. (3.139), the distribution of the Nusselt number can be obtained

$$\mathrm{Nu}_D = \frac{D\frac{\partial T}{\partial r}\big|_{r=R}}{T_W - T_b} = \frac{2}{\bar{\psi}(1) + C_2 + \sum_{j=1}^{\infty} A_j \Phi_j(1) \exp\left(-\lambda_j^2 \tilde{x}\right)} \qquad (3.140)$$

For the hydrodynamically and thermally fully developed flow, the equation for the Nusselt number reduces to

$$\mathrm{Nu}_\infty = \frac{2}{\bar{\psi}(1) + C_2} \qquad (3.141)$$

Figure 3.17 shows the Nusselt number for the fully developed flow, for Pr = 0.71, as a function of the rotation rate N and the Reynolds number (Reich 1988; Reich and Beer 1989). It can be seen that the Nusselt number strongly decreases with increasing rotation rate N, which is caused by flow laminarization. For N → ∞, the Nusselt number approaches the limit $\mathrm{Nu}_\infty = 4.36$ for laminar pipe flow.

Figure 3.18 shows the distribution of $\mathrm{Nu}/\mathrm{Nu}_\infty$ in the thermal entrance region for air flow. It can be seen that the length of the thermal entrance region is increased with increasing rotation rates. This is caused by the laminarization of the flow.



Fig. 3.17 Nusselt number for fully developed flow in an axially rotating pipe (adapted from Reich and Beer (1989), Weigand and Beer (1989a))
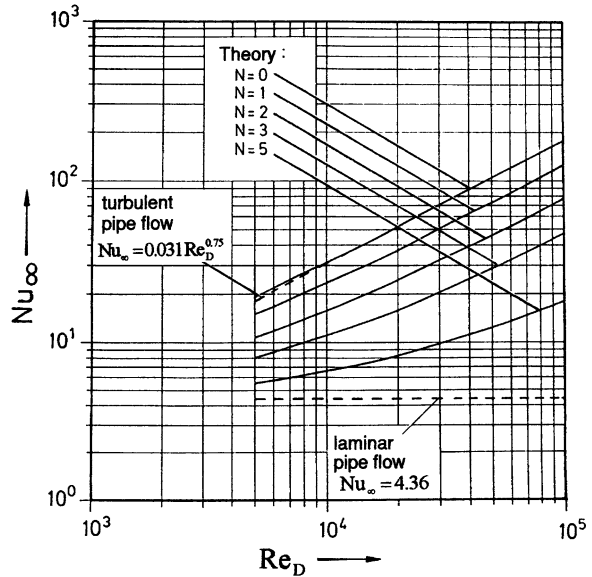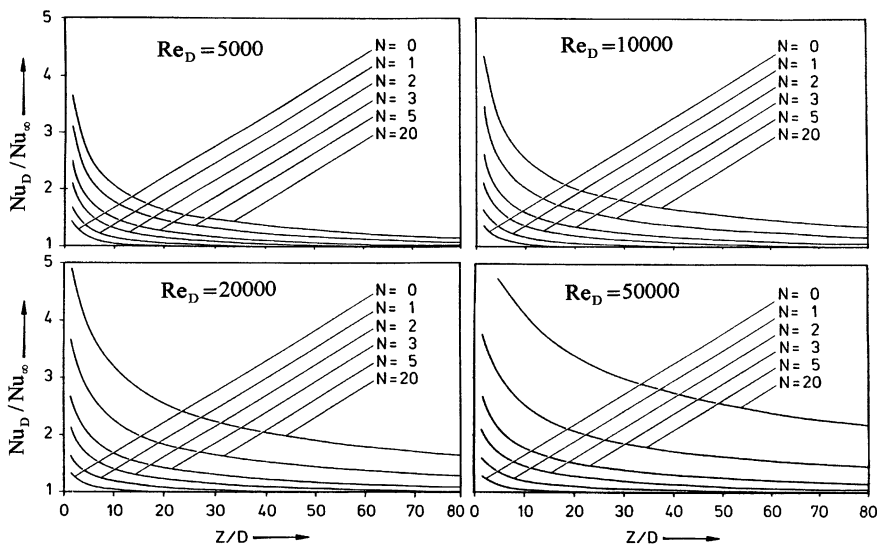
**Fig. 3.18** Nusselt number distribution in the thermal entry length for different rotation rates N and Pr = 0.71 (Weigand and Beer 1989a)

For N → ∞, the thermal entrance length approaches the one for laminar pipe flow which is given by

$$\frac{L_{th}}{D} = 0.05 \ \text{Re}_D \ \text{Pr} \tag{3.142}$$

This effect has interesting implications, especially for larger Reynolds numbers. For example for a Reynolds number of about 50,000, the flow is not even thermally fully developed after 80 pipe diameters for N = 1. This shows clearly that care has to be taken in predicting the heat transfer for such types of flows.

Reich (1988) obtained experimentally the Nusselt numbers in an axially rotating pipe with constant heat flux at the wall. The rotating test section was 40 diameter in length. He compared his experimental results with calculations for a fully developed flow and found that the difference between experimental data and calculated values increased with growing values of the rotation rate.

However, if one calculates the Nusselt numbers from the above solution for the thermal entrance region and compares them to the measured values, very good agreement is obtained. This is shown in Fig. 3.19 (Weigand and Beer 1989a).

The results presented here can easily be extended to other wall boundary conditions like constant wall temperature or uniform external heating or cooling. The reader is referred to Weigand and Beer (1992b) for such cases.

The examples of the present chapter have shown that even complicated technical problems can be solved using analytical methods. It is important to note that in the analytical solution the physical significance of individual effects (wall boundary

**Fig. 3.19** Nusselt numbers at
$x/D = 40$ for various values of
the rotation rate and Pr = 0.71
(Weigand and Beer 1989a)
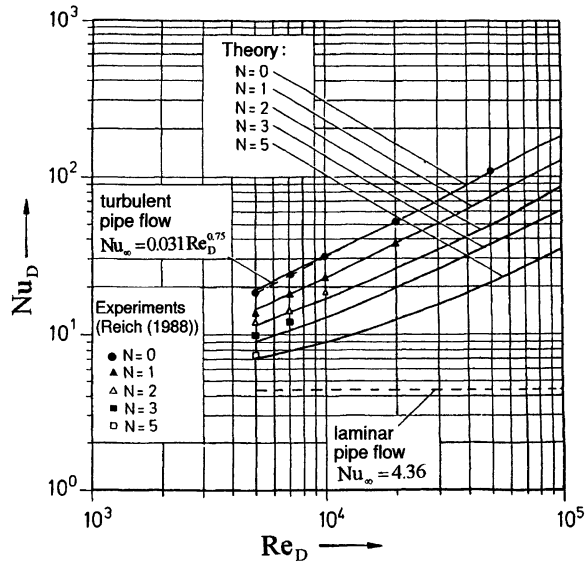


conditions, type of fluid, rotation,…) can be more easily identified than in a
numerical solution of the problem.

### Problems

3-1   Consider the following eigenvalue problem

$$Y_n'' + \lambda_n^2 Y_n = 0$$

with the boundary conditions

$$Y_n'(0) = Y_n(1) = 0$$

(a)   Prove that the eigenvalue problem is self-adjoint and positive definite.
(b)   Show that the eigenfunctions form an orthogonal set of functions in the
interval [0, 1].
(c)   Calculate the eigenfunctions and the eigenvalues. Use a normalizing
condition that $Y(0) = 1$.

3-2   Show that the following three eigenvalue problems are self-adjoint and
positive definite:

$$\left(1 + \tilde{y}^2\right)\lambda_n \Phi_n + \Phi_n'' = 0$$
$$\Phi_n(0) = \Phi_n(1) = 0$$

$$\tilde{r}R_n'' + R_n'' + \lambda_n^2 \tilde{r}R_n = 0$$
$$R'(0) = R(1) = 0$$

$$\left(1 - \tilde{x}^2\right)Y_n'' - 2\tilde{x}Y_n' + \lambda_n(\lambda_n + 1)Y_n = 0$$
$$Y_n(0) = Y_n(1) = 0$$

3-3 Consider the flow and heat transfer is a planar channel with height $2h$. The plates have a constant wall temperature $T_0$ for $x < 0$ and $T_W$ for $x \geq 0$. The velocity profile of the laminar flow in the planar duct can be simplified to be a slug flow profile with $u = \bar{u} = \text{const}$. The velocity component in the $y$-direction $v = 0$. All fluid properties can be considered to be constant. The temperature distribution in the fluid can be calculated from the energy equation

$$u\frac{\partial T}{\partial x} = a\frac{\partial^2 T}{\partial y^2}$$

with the boundary conditions

$$x = 0 : T = T_0$$
$$y = 0 : \frac{\partial T}{\partial y} = 0, \quad y = h : T = T_W$$

(a) Introduce the following dimensionless quantities

$$\tilde{x} = \frac{x}{h}\frac{a}{\bar{u}h}, \quad \tilde{y} = \frac{y}{h}, \quad \Theta = \frac{T - T_W}{T_0 - T_W}$$

What are the resulting equation and the boundary condition in dimensionless form?

(b) Use the method of separation of variables to solve the given problem ($\Theta = f(\tilde{x})g(\tilde{y})$). What equations are obtained for the functions $f$ and $g$?

(c) Calculate the eigenfunctions and display the first and the third eigenfunction as a function of $\tilde{y}$ in the interval $[0, 1]$.

(d) Predict the complete solution for the temperature field.

3-4 A planar channel with the height $2h$ is subjected to a hydrodynamically fully developed laminar flow. The fluid enters the channel with the constant temperature $T_0$. The walls of the channel are adiabatic for $x < 0$, whereas for $x \geq 0$ the walls are heated by a constant heat flux $\dot{q}_W$. Assume that all fluid properties are constant. The velocity distribution is given by

$$\frac{u}{\bar{u}} = \frac{3}{2}\left(1 - \left(\frac{y}{h}\right)^2\right)$$

and the Peclet number is large enough, so that axial heat conduction can be ignored in the fluid.

(a) Calculate the temperature distribution in the fluid for large axial values. Display the form of the radial temperature distribution for a given value of the axial coordinate.
(b) Predict the value of the Nusselt number for the fully developed flow.
(c) Predict the complete solution of the problem (*Hint*: Split the problem in two separate problems).

3-5 Consider the production process of a thin foil. The foil is moved with constant velocity $u_\infty$ through a thin slit and cools down in the surrounding air. The process is schematically shown in the following figure:
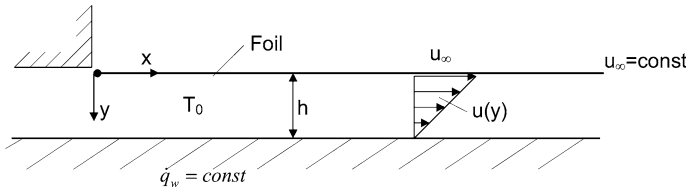


The distance between the foil and the wall is $h$. The wall is cooled for $x > 0$ and takes out heat from the surrounding air with the constant heat flux $\dot{q}_W$. For large axial values, a hydrodynamically fully developed velocity profile according to

$$\frac{u}{\bar{u}} = 1 - \frac{y}{h}$$

is established. The temperature distribution in the air gap should be predicted for large axial values. The upper wall (foil) can be assumed to be adiabatic and all fluid properties are constant.

(a) Simplify the energy equation for the given problem. Derive the boundary conditions for $y = 0$ and $y = h$ and make the energy equation dimensionless.
(b) Derive an integral energy balance for the thermal fully developed flow. What functional form the temperature distribution must have for the fully developed flow?
(c) Introduce the above derived expression for the temperature distribution into the energy equation and solve the equation with the given boundary conditions.
(d) Calculate the Nusselt number at the lower wall. Use $T(x, y = 0) - T(x, y = h)$ as the driving temperature difference for the Nusselt number.

3-6 The velocity profile of a slow river flow is given by

$$u = u_0 \left[ 1 - \left( \frac{y - t_F}{t_F} \right)^2 \right]$$

In this equation $t_F$ denotes the depth of the river and $u_0$ is the flow velocity at the river surface. The coordinate $y$ has its origin on the bottom of the river. The river can be considered in the following as a planar channel. Fully developed laminar flow can be assumed. Axial heat conduction within the fluid and all influences through the surrounding air flow over the river can be neglected. The river has at its start location a temperature $T_0$. From the position $x = 0$ on the sun heats up the river, so that the river surface is heated approximately by the constant heat flux per area $\dot{q}_S$ in $\left[ W/m^2 \right]$. The river bottom can be assumed to be adiabatic.

(a) Sketch the problem (including the coordinate system) and write down the energy equation for the problem. Determine also all needed boundary conditions for the heat transfer problem under investigation.

(b) Make the energy equation and the boundary conditions dimensionless by introducing the following quantities

$$\Theta = \frac{T - T_0}{\dot{q}_S t_F / k}, \quad \tilde{x} = \frac{x}{t_F} \frac{1}{\text{Re Pr}}, \quad \text{Re} = \frac{u_0 t_F}{\nu}, \quad \text{Pr} = \frac{\nu}{a}, \quad a = \frac{k}{\rho c_p}$$

(c) Calculate the temperature distribution over the river height for large axial distances (fully developed flow and heat transfer).

(d) Determine the Nusselt number on the river surface for large axial distances.

(e) Determine now the complete temperature distribution in the river, which is valid from $x = 0$ on. Obtain first the required partial differential equation (energy equation) and the corresponding boundary conditions. Show then the solution method and derive all equations needed to obtain the required constants. Please note, that it is not required to actually predict the constants. Thus, the obtained integrals have not to be solved!

3-7 Consider the following eigenvalue problem

$$\frac{d}{dr} \left[ r^2 \frac{d\Phi_n}{dr} \right] + \lambda_n^2 r^2 \Phi_n = 0$$

with the boundary conditions

$$r \to 0 : r^2 \frac{d\Phi_n}{dr} = 0$$
$$r = 1 : \Phi_n = 0$$

(a) Prove that the eigenvalue problem is self-adjoint and positive definite.
(b) Show that the eigenfunctions form an orthogonal set of functions in the interval [0, 1].
(c) Develop the function $f(r) = 1$ in a series of these eigenfunctions.
(d) Substitute $\Phi_n = h_n/r$ into the differential equation for the eigenfunctions. Which differential equation do you obtain for the functions $h_n$? What are the resulting boundary conditions?
(e) Obtain the general solution of the eigenvalues problem. Which equation do you obtain for the eigenvalues?
(f) Determine with the eigenfunctions from (e) the integrals, which appeared in section (c), and give the series for $f(r) = 1$.

# Chapter 4
# Analytical Solutions for Sturm-Liouville Systems with Large Eigenvalues

The numerical method for obtaining the eigenvalues and eigenfunctions of Eq. (3.25) is explained in Chap. 3 and Appendix C. This numerical procedure gets cumbersome and difficult if the eigenvalues become large, because of the increasing number of zero points of the eigenfunction. This is elucidated in Fig. 4.1, which shows several eigenfunctions for a turbulent pipe flow with constant wall temperature. As it can be seen from Fig. 4.1, the higher eigenfunctions strongly oscillate. It can be shown, that the eigenfunction of number $j$ has also $j$ zero-points. This means that, for larger $j$, it is difficult to capture exactly the shape of the eigenfunctions by means of a numerical method. An increasingly larger number of grid points is needed to resolve the higher eigenfunctions. Because of this reason, there has been a lot of interest in obtaining analytical approximations of eigenfunctions for larger eigenvalues. Good reviews about this subject can be found in Erdelyi (1956) and in Kamke (1983). For laminar flows, the hydrodynamically fully developed velocity profile is a simple quadratic function of the spatial coordinate. In addition, the function $a_2(\tilde{n})$ in Eq. (3.25) is equal to one. These two simplifications allow that asymptotic approximations can be obtained relatively easily for laminar flow problems. A good review on this topic is given in Shah and London (1978). In the following, only some of this work will be presented. Sellars et al. (1956) investigated the Sturm-Liouville eigenvalue problem for large eigenvalues for pipe and channel flows with constant wall temperature. They used the WKB(J)[1] method for obtaining the eigenvalues for $\lambda \to \infty$. As a result, they found that the large eigenvalues can be predicted by

$$\lambda_j = \frac{4}{\sqrt{2}}\left(j+\frac{2}{3}\right); \quad j = 0, 1, 2, \ldots \tag{4.1}$$

---

[1]The acronym WKB(J) stands for Wentzel, Kramer, Brillonin and Jeffreys, who developed the method in the 1920s. However, the method was applied much earlier by Liouville (1837). For an introduction into the method, the reader is referred to Simmonds and Mann (1986) and Plaschko and Brod (1989). For a more detailed description of the method, the reader is referred to Froman and Froman (1965) and to Kumar (1972).
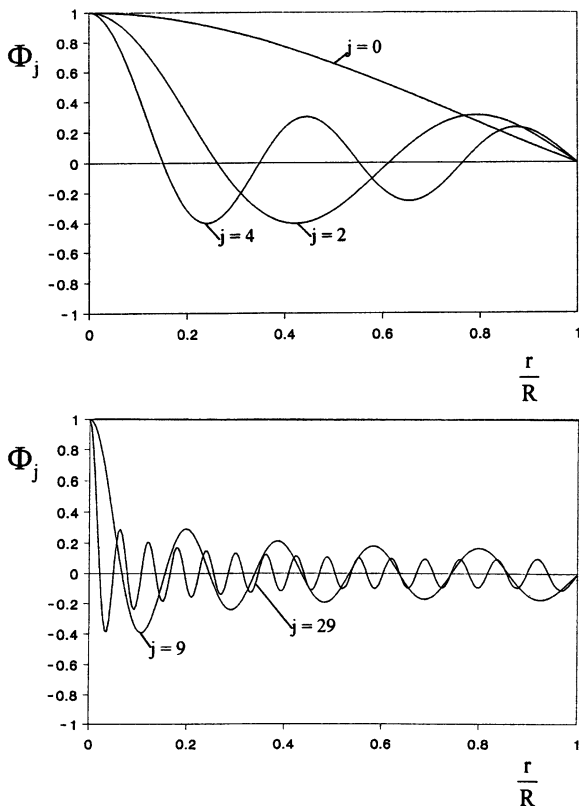
The eigenvalues given by Eq. (4.1) are in good agreement with numerically predicted values for larger j (for $j > 5$ they are nearly identical). Lauwerier (1950) showed, that the solution of the laminar Graetz problem can be expressed by Whittaker functions (see Kamke 1983), where the eigenvalue appears in the argument as well as in the subscript of the function. From the asymptotic behavior of these functions, Lauwerier was able to derive an asymptotic form for the eigenfunctions for large eigenvalues. The value of the eigenfunction at the wall was determined to be

$$
\Phi(1, \lambda) = \frac{\sqrt{3}}{3\pi} \left( \frac{6}{\sqrt{2}\lambda} \right)^{1/3} \Gamma(1/3) \cos\left[ \left( \frac{\sqrt{2}\lambda}{4} - \frac{1}{6} \right) \pi \right] \sum_{p=0} \alpha_p \left( \frac{2}{\sqrt{2}\lambda} \right)^{2p}
$$

$$
+ \frac{\sqrt{3}}{3\pi} \left( \frac{6}{\sqrt{2}\lambda} \right)^{1/3} 3^{1/3} \Gamma(2/3) \cos\left[ \left( \frac{\sqrt{2}\lambda}{4} + \frac{1}{6} \right) \pi \right] \sum_{p=0} \beta_p \left( \frac{2}{\sqrt{2}\lambda} \right)^{2p+4/3}
$$

(4.2)

$$\alpha_0 = 1, \qquad\qquad \beta_0 = -0.0785714857$$
$$\alpha_1 = -0.01444444444, \quad \beta_1 = 0.02887167277$$
$$\alpha_2 = 0.009882467268, \quad \beta_2 = -0.0440553529$$
$$\alpha_3 = -0.02131664753,$$

From Eq. (4.2), the eigenvalues can be calculated for the constant wall temperature case by setting Eq. (4.2) equal to zero. Newman (1969) extended the analysis by Lauwerier and obtained the following expressions

$$\lambda_j = \lambda_0 + s_1 \lambda_0^{-4/3} + s_2 \lambda_0^{-8/3} + s_3 \lambda_0^{-10/3} + s_4 \lambda_0^{-11/3} + O\left(\lambda_0^{-14/3}\right) \tag{4.3}$$

$$A_j \Phi_j'(1) = C \lambda_j^{-1/3} \left[ \begin{array}{c} 1 + L_1 \lambda_0^{-4/3} + L_2 \lambda_0^{-6/3} + L_3 \lambda_0^{-7/3} \\ + L_4 \lambda_0^{-10/3} + L_5 \lambda_0^{-11/3} + O\left(\lambda_0^{-4}\right) \end{array} \right] \tag{4.4}$$

with the quantities

$$\lambda_0 = \frac{4}{\sqrt{2}}\left(j + \frac{2}{3}\right); \quad j = 0, 1, 2, \dots \tag{4.5}$$

$$s_1 = 0.159152288, \qquad L_1 = 0.144335160 \tag{4.6}$$
$$s_2 = 0.0114856354, \qquad L_2 = 0.115555556$$
$$s_3 = -0.224731440, \qquad L_3 = -0.21220305$$
$$s_4 = -0.033772601, \qquad L_4 = -0.187130142$$
$$C = -2.025574576, \qquad L_5 = -0.0918850832$$

For the case of a wall boundary condition of the third kind, Hsu (1971a) derived asymptotic expressions for the eigenvalues and related constants. He showed that his expressions are identical to those of Sellars et al. (1956) for the case of a uniform wall temperature. For the case of an insulated wall, the expressions of Hsu (1971a) are identical to those provided by Hsu (1965) for the case of a constant wall heat flux.

For a turbulent internal flow, the mathematical problem of obtaining asymptotic expressions for the eigenvalues and eigenfunctions is much more complicated than for laminar internal flow. This is due to the complicated description of the velocity profile and the appearance of the eddy diffusivity in Eq. (3.25), which causes the function $a_2(\tilde{n})$ to be a complicated function of the coordinate.

$$\tilde{r}^F \tilde{u}(\tilde{n}) \lambda_j^2 \Phi_j(\tilde{n}) + \left[\tilde{r}^F a_2(\tilde{n}) \Phi_j'(\tilde{n})\right]' = 0 \tag{3.25}$$

$$\tilde{n} = 0 : \Phi'(0) = 0 \tag{3.26}$$
$$\tilde{n} = 1 : \Phi(1) = 0$$

Sternling and Sleicher (1962) derived asymptotic expressions for the eigenvalues and eigenfunctions for heat transfer in a turbulent pipe flow with constant wall temperature. However, it turned out that the accuracy of their results for $A_j$, Eq. (3.59), as well as for $A_j\Phi_j(1)$, Eq. (3.69), was somewhat disappointing. Eight years later, Sleicher et al. (1970) were able to derive more accurate expressions using a matched asymptotic expansion. In the following sections, the method of Sleicher et al. (1970) is described in more detail for the case of a constant wall temperature, because their method is very useful for a lot of similar problems. The method has been successfully used with some modifications by Shibani and Özisik (1977a, b), Sadeghipour et al. (1984) for different wall boundary conditions and different geometries. At the time— the method has been established by Sleicher et al. (1970)—the computational power of the computers did not permit a detailed comparison between their derived asymptotic expressions and numerical solutions of the eigenvalue problem for larger eigenvalues. Therefore, a short section has been added at the end of this chapter which shows a detailed evaluation of the asymptotic expressions compared to numerical calculations. In addition, it is shown that the method of Sleicher et al. (1970) can be adapted quite easily to other related problems. This is demonstrated for the heat transfer process in an axially rotating pipe.

We start our considerations with the Sturm-Liouville problem given by the Eqs. (3.25) and (3.26) and consider a turbulent pipe flow. For this type of application, the equations read ($F = 1$, $\tilde{n} = \tilde{r}$)

$$\frac{d}{d\tilde{r}}\left[\tilde{r}a_2(\tilde{r})\frac{d\Phi_j}{d\tilde{r}}\right] + \tilde{r}\tilde{u}(\tilde{r})\lambda_j^2\Phi_j(\tilde{r}) = 0 \qquad (4.7)$$

with the boundary conditions

$$\begin{aligned} \tilde{r} = 0 &: \Phi'(0) = 0 \\ \tilde{r} = 1 &: \Phi(1) = 0 \end{aligned} \qquad (4.8)$$

In order to obtain an asymptotic expression for large eigenvalues, it is common to transform the Sturm-Liouville system into its standard form. This can be done by introducing the following new quantities (see Kamke 1983)

$$G = \frac{1}{\pi}\int_0^1 \sqrt{\frac{\tilde{u}}{2a_2}}d\tilde{r}, \quad k = \sqrt{2}\lambda_j G, \quad \xi = \frac{1}{G}\int_0^{\tilde{r}} \sqrt{\frac{\tilde{u}}{2a_2}}d\bar{r} \qquad (4.9)$$

$$\vartheta = \left(\frac{\tilde{r}^2 a_2\tilde{u}}{2}\right)^{1/4}\Phi_j, \quad w(\xi) = \left(\frac{\tilde{r}^2 a_2\tilde{u}}{2}\right)^{-1/4}\frac{d^2}{d\xi^2}\left(\frac{\tilde{r}^2 a_2\tilde{u}}{2}\right)^{1/4} \qquad (4.10)$$

One obtains

$$\frac{d^2\vartheta}{d\xi^2} + \left[k^2 - w(\xi)\right]\vartheta = 0 \tag{4.11}$$

with the boundary conditions

$$\xi = 0 : \vartheta(0) = 0, \quad \xi = \pi : \vartheta(\pi) = 0 \tag{4.12}$$

After introducing the new coordinate $\xi$, the interval for the coordinate has changed from [0, 1] to [0, $\pi$]. Before trying to find a solution for the eigenfunction $\vartheta$ for larger eigenvalues, one has to analyze the function $w(\xi)$ in greater detail: the function $w(\xi)$ has singularities at both boundaries ($\xi = 0$, $\xi = \pi$). However, the function can be approximated near both boundaries with sufficient accuracy. Sternling and Sleicher (1962) subdivided the interval into two regions (core region and near wall region). For both regions, they determined solutions for Eq. (4.11) and patched them together. This procedure resulted, however, in a disappointing accuracy for the constants $A_j$. Therefore, Sleicher et al. (1970) chose a different approach. The interval for $\xi$ [0, $\pi$] is split up in three separate regions (core region, near wall region and middle region). The solutions for the separate regions have to be connected later to each other by expansions of the variables.[2]

In order to find a solution for Eqs. (4.11) and (4.12) for large eigenvalues, one can use the following expansion which is based on a perturbation method approach (see van Dyke (1962) or Kevorkian and Cole (1981))

$$\vartheta \sim \sum_{i=0}^{N} \delta_i(k)\vartheta_i(\xi) \tag{4.13}$$

The functions $\delta_i(k)$ are not known a priori and have to be determined during the analysis. In order to show more clearly the solution procedure of Sleicher et al. (1970), these functions are introduced here from the very beginning. Later, during the calculation procedure, we clarify why exactly this sequence of functions is chosen for the present example

$$\begin{array}{llll} \delta_0 = k^{-1/2}, & \delta_1 = k^{-3/2}\ln k, & \delta_2 = k^{-3/2}, & \delta_3 = k^{-5/2}\ln k \\ \delta_4 = k^{-5/2}, & \delta_5 = k^{-5/2}(\ln k)^2 \end{array} \tag{4.14}$$

Introducing Eq. (4.14) into Eq. (4.13) one obtains the following expression for the eigenfunctions

$$\vartheta \sim k^{-1/2}\vartheta_0 + k^{-3/2}\ln k\vartheta_1 + k^{-3/2}\vartheta_2 \tag{4.15}$$
$$+ k^{-5/2}\ln k\vartheta_3 + k^{-5/2}\vartheta_4 + k^{-5/2}(\ln k)^2\vartheta_5$$

---

[2]The analysis presented here follows the excellent work of Sleicher et al. (1970). It should serve as an example on how to solve such a difficult eigenvalue problem.

After describing the asymptotic expansion coefficients for $\vartheta$, approximations for the function $w(\xi)$ have to be derived. Because of the singularities of the function near the boundaries, the behavior of $w(\xi)$ has to be examined separately for all three regions.

### Pipe Center Region

Near the center of the pipe, the axial velocity component can also be approximated with good accuracy by a constant value $U$. The distribution for $a_2$ can be approximated for this area by a constant $A$. If one introduces this assumptions into Eqs. (4.9) and (4.10) one obtains:

$$\xi = \pi\tilde{r} \tag{4.16}$$

$$w(\xi) = \xi^{-1/2}\frac{d^2}{d\xi^2}(\xi)^{1/2} = -\frac{1}{4}\xi^{-2} \tag{4.17}$$

### Middle Region

In this area, the function $w(\xi)$ has no singularities. Since we are interested in solutions for large eigenvalues, the function $w$ can be neglected compared to $k^2$ in Eq. (4.11).

### Near Wall Region

At the boundary ($\xi = \pi$), the function $w(\xi)$ has a second singularity. Very close to the wall, the velocity can be approximated by $\tilde{u} \sim \tilde{y}_W = (1 - \tilde{r})$. The function $a_2$ tends to one in this region. If we introduce the above assumptions into Eq. (4.10), we obtain for $w(\xi)$ after neglecting quadratic terms

$$w(\xi) \approx -\frac{\beta_1}{(\pi - \xi)^2}, \quad \beta_1 = \frac{5}{36} \tag{4.18}$$

The above expression for $w(\xi)$ was first derived by Sternling and Sleicher (1962).[3] Clearly, the region, where Eq. (4.18) is fully valid, is very small. Therefore,

---

[3]The constant $\beta_1$ is determined by the velocity distribution near the wall. The value of the constant is obtained under the assumption of a linear velocity distribution of the form

$$\tilde{u} = 2V\tilde{y}_W, \quad V = \frac{1}{2}\left(\frac{d\tilde{u}}{d\tilde{y}_W}\right)_{\tilde{y}_W=0} = \frac{\mathrm{Re}_D c_f}{32}$$

where $c_f$ is a friction factor (Sleicher et al. 1970). If one uses a velocity distribution according to

$$\tilde{u} = 2c(1 - \tilde{r})^{1/m}, \quad c = \frac{1}{4}\left(\frac{3m+1}{m^2} + 2\right)$$

one obtains for the constant $\beta_1$

$$\beta_1 = \frac{1}{4}\frac{1 + 4m}{(1 + 2m)^2}$$

The reader is referred to Shibani and Özisik (1977a) for this approach.

Sleicher et al. (1970) used the following expression for approximating the function $w(\xi)$ in the near wall region

$$w(\xi) \approx -\frac{\beta_1}{(\pi - \xi)^2} + \frac{\beta_2}{\pi - \xi} \tag{4.19}$$

Equation (4.19) assumes that the function $w(\xi)$ can be expanded into a Laurent series around $\xi = \pi$. Equation (4.19) contains the not yet determined constant $\beta_2$. This constant is determined during the solution process.

After having investigated the functional form of $w(\xi)$ for the different regions, the determination of the eigenfunctions from Eq. (4.11) for the three different regions can be started.

### Pipe Center Region

In the pipe center, the function $w(\xi)$ is given by Eq. (4.17). Inserting this expression into Eq. (4.11) results in

$$\frac{d^2\vartheta_C}{ds^2} + \left[1 + \frac{1}{4s^2}\right]\vartheta_C = 0 \tag{4.20}$$

where the stretched coordinate

$$s = k\xi \tag{4.21}$$

is used. The new coordinate $s$ has the advantage that the eigenvalue does not appear explicitly in the differential equation. Figure 4.2 shows the different coordinates and the geometry under consideration.

Introducing the expansion defined in Eq. (4.15) into Eq. (4.20) results after collecting terms of the same order in $k$ in the following set of equations

$$\frac{d^2\vartheta_{iC}}{ds^2} + \left[1 + \frac{1}{4s^2}\right]\vartheta_{iC} = 0, \quad i = 0, 1, \ldots, 5 \tag{4.22}$$
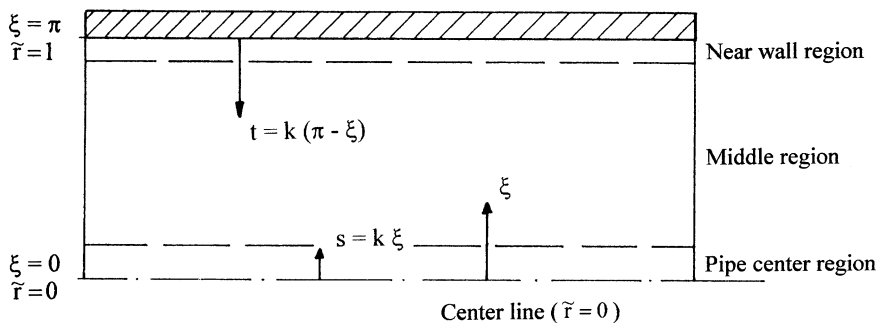


Fig. 4.2 Geometry and different coordinate systems used

Equation (4.22) can be transformed into a Bessel equation after introducing the new function

$$\vartheta_{iC} = \sqrt{s}\tilde{\vartheta}_{iC} \tag{4.23}$$

The solution of this Bessel equation, which is finite for $s = 0$, is given by

$$\vartheta_{iC} = B_i\sqrt{s}\, J_0(s), \quad i = 0, 1, \ldots, 5 \tag{4.24}$$

The complete solution for the pipe center region is therefore given by

$$\vartheta_C = \sqrt{s} J_0(s) \left\{ \begin{array}{l} B_0 k^{-1/2} + B_1 k^{-3/2}\ln k + B_2 k^{-3/2} \\ + B_3 k^{-5/2}\ln k + B_4 k^{-5/2} + B_5 k^{-5/2}(\ln k)^2 \end{array} \right\} \tag{4.25}$$

From the definition of the function $\vartheta$ in Eq. (4.10) it follows that in the pipe center $(\tilde{r} \to 0,\ a_2 = A,\ \tilde{u} = U,\ \Phi_j(0) = 1)$, the function $\vartheta$ will behave like

$$\xi \to 0 : \vartheta_C = \left(\frac{\tilde{r}^2 a_2 \tilde{u}}{2}\right)^{1/4} \Phi_j(0) = \sqrt{GA\xi} \tag{4.26}$$

where the normalizing condition for the eigenfunction $\Phi_j(0) = 1$ has been used. If one introduces now the stretched coordinate $s$ into Eq. (4.26), one obtains in the center of the pipe

$$\xi \to 0 : \vartheta_C(0) = \sqrt{GA\xi} \Rightarrow, \quad s \to 0 : k^{-1/2}\sqrt{GA}\sqrt{s} \tag{4.27}$$

This expression can be compared to Eq. (4.25) for $s \to 0$ ($J_0(0) = 1$). This results in

$$B_0 + B_1 k^{-1}\ln k + B_2 k^{-1} + B_3 k^{-2}\ln k + B_4 k^{-2} + B_5 k^{-2}(\ln k)^2 = \sqrt{GA} \tag{4.28}$$

Because Eq. (4.28) has to be valid for all $k$, it follows

$$B_0 = \sqrt{GA} \tag{4.29}$$
$$B_i = 0, \quad i = 1, \ldots, 5$$

and the solution for the center region of the pipe is

$$\vartheta_C = k^{-1/2}\sqrt{GA}\sqrt{s}\, J_0(s) \tag{4.30}$$

## Middle Region

In the middle region, the function $w(\xi)$ is a continuous function without singularities. Because of this, $w(\xi)$ can be neglected in Eq. (4.11) compared to the large eigenvalues. After introducing again the stretched coordinate $s$, one obtains from Eq. (4.11)

$$\frac{d^2\vartheta_M}{ds^2} + \vartheta_M = 0 \tag{4.31}$$

Introducing the expansion according to Eq. (4.15) into Eq. (4.31) results, after collecting terms of the same order in $k$, in the following set of equations

$$\frac{d^2\vartheta_{iM}}{ds^2} + \vartheta_{iM} = 0, \qquad i = 0, 1, \ldots, 5 \tag{4.32}$$

The solution of Eq. (4.32) can be calculated easily and is given by

$$\vartheta_M = k^{-1/2}(K_0 \sin s + L_0 \cos s) + k^{-3/2} \ln k(K_1 \sin s + L_1 \cos s) \tag{4.33}$$
$$+ k^{-3/2}(K_2 \sin s + L_2 \cos s) + k^{-5/2} \ln k(K_3 \sin s + L_3 \cos s)$$
$$+ k^{-5/2}(K_4 \sin s + L_4 \cos s) + k^{-5/2}(\ln k)^2(K_5 \sin s + L_5 \cos s)$$

The constants $K_i$ and $L_i$, which appear in Eq. (4.33), are yet not known. In contrast to the constants in the solution for the pipe center, they have to be determined during the following solution process.

## Near Wall Region

For the near wall region, the function $w(\xi)$ is given by Eq. (4.19). Inserting this expression into Eq. (4.11) results in

$$\frac{d^2\vartheta_W}{dt^2} + \left[1 + \frac{\beta_1}{t^2} - \frac{\beta_2}{kt}\right]\vartheta_W = 0 \tag{4.34}$$

where the new stretched coordinate

$$t = k(\pi - \xi) = k\pi - s \tag{4.35}$$

is introduced. Inserting the expansion according to Eq. (4.15) into Eq. (4.35) results, after collecting terms of the same order in $k$, in the following set of equations

$$\frac{d^2\vartheta_{iW}}{dt^2} + \left[1 + \frac{\beta_1}{t^2}\right]\vartheta_{iW} = 0, \quad i = 0, 1 \tag{4.36}$$

$$\frac{d^2\vartheta_{2W}}{dt^2} + \left[1 + \frac{\beta_1}{t^2}\right]\vartheta_{2W} = \frac{\beta_2}{t}\vartheta_{0W} \tag{4.37}$$

$$\frac{d^2\vartheta_{3W}}{dt^2} + \left[1 + \frac{\beta_1}{t^2}\right]\vartheta_{3W} = \frac{\beta_2}{t}\vartheta_{1W} \tag{4.38}$$

$$\frac{d^2\vartheta_{4W}}{dt^2} + \left[1 + \frac{\beta_1}{t^2}\right]\vartheta_{4W} = \frac{\beta_2}{t}\vartheta_{2W} \tag{4.39}$$

$$\frac{d^2\vartheta_{5W}}{dt^2} + \left[1 + \frac{\beta_1}{t^2}\right]\vartheta_{5W} = 0 \tag{4.40}$$

The solution of the homogenous differential Eqs. (4.36) and (4.40) can be obtained in the same way as for Eq. (4.22). Introducing again the new function

$$\vartheta_{iW} = \sqrt{t}\,\tilde{\vartheta}_{iW} \tag{4.41}$$

into Eqs. (4.36) and (4.40) results in

$$t^2\vartheta_{iW}'' + t\vartheta_{iW}' + \left(t^2 + (\beta_1 - 1/4)\right)\vartheta_{iW} = 0 \tag{4.42}$$

As it can be seen, Eq. (4.42) is a Bessel equation (see Bowman 1958). For $\beta_1 = 5/36$[4] (this is the value used by Sternling and Sleicher (1962) for the linear velocity distribution near the wall) one obtains

$$t^2\vartheta_{iW}'' + t\vartheta_{iW}' + \left(t^2 + 1/9\right)\vartheta_{iW} = 0 \tag{4.43}$$

This equation has the general solution

$$\vartheta_{iW} = \sqrt{t}\left\{D_i J_{1/3}(t) + E_i J_{-1/3}(t)\right\}, \qquad i = 0, 1, 5 \tag{4.44}$$

Equation (4.44) is also the solution of the homogenous Eqs. (4.37)–(4.39). A particular solution for these equations can be constructed by using the method of variation of constants (see Bronstein and Semendjajew 1981). This leads finally to the complete solution for the near wall region, given by

---

[4]For other values of $\beta_1$, the reader can find some solutions in Shibani and Özisik (1977a).

$$\vartheta_W = k^{-1/2}\sqrt{t}\{D_0 J_{1/3}(t) + E_0 J_{-1/3}(t)\} \tag{4.45}$$

$$+ k^{-3/2}\ln k\sqrt{t}\{D_1 J_{1/3}(t) + E_1 J_{-1/3}(t)\}$$

$$+ k^{-3/2}\sqrt{t}J_{1/3}\left\{\pi\sqrt{3}\beta_2 \int \begin{pmatrix} D_0 J_{1/3}J_{-1/3} \\ + E_0 J_{-1/3}J_{-1/3} \end{pmatrix} d\tilde{t} + D_2\right\}$$

$$- k^{-3/2}\sqrt{t}J_{-1/3}\left\{\pi\sqrt{3}\beta_2 \int \begin{pmatrix} D_0 J_{1/3}J_{1/3} \\ + E_0 J_{1/3}J_{-1/3} \end{pmatrix} d\tilde{t} + E_2\right\}$$

$$+ k^{-5/2}\ln k\sqrt{t}J_{1/3}\left\{\pi\sqrt{3}\beta_2 \int \begin{pmatrix} D_1 J_{1/3}J_{-1/3} \\ + E_1 J_{-1/3}J_{-1/3} \end{pmatrix} d\tilde{t} + D_3\right\}$$

$$- k^{-5/2}\ln k\sqrt{t}J_{-1/3}\left\{\pi\sqrt{3}\beta_2 \int \begin{pmatrix} D_1 J_{1/3}J_{1/3} \\ + E_1 J_{-1/3}J_{1/3} \end{pmatrix} d\tilde{t} + E_3\right\}$$

$$+ k^{-5/2}\pi\beta_2\sqrt{t}\sqrt{3}J_{1/3}$$

$$\times \left[ \begin{array}{l} \int J_{1/3}J_{-1/3}\left\{\pi\sqrt{3}\int\beta_2\begin{pmatrix} D_0 J_{1/3}J_{-1/3} \\ + E_0 J_{-1/3}J_{-1/3} \end{pmatrix}d\tilde{t} + D_2\right\}d\bar{t} \\[2mm] - \int J_{-1/3}J_{-1/3}\left\{\pi\sqrt{3}\int\beta_2\begin{pmatrix} D_0 J_{1/3}J_{1/3} \\ + E_0 J_{-1/3}J_{1/3} \end{pmatrix}d\tilde{t} + E_2\right\}d\bar{t} + D_4 \end{array} \right]$$

$$- k^{-5/2}\pi\beta_2\sqrt{t}\sqrt{3}J_{-1/3}$$

$$\times \left[ \begin{array}{l} \int J_{1/3}J_{1/3}\left\{\pi\sqrt{3}\int\beta_2\begin{pmatrix} D_0 J_{1/3}J_{-1/3} \\ + E_0 J_{-1/3}J_{-1/3} \end{pmatrix}d\tilde{t} + D_2\right\}d\bar{t} \\[2mm] - \int J_{-1/3}J_{1/3}\left\{\pi\sqrt{3}\int\beta_2\begin{pmatrix} D_0 J_{1/3}J_{1/3} \\ + E_0 J_{-1/3}J_{1/3} \end{pmatrix}d\tilde{t} + E_2\right\}d\bar{\bar{t}} + E_4 \end{array} \right]$$

$$+ k^{-5/2}(\ln k)^2\sqrt{t}\{D_5 J_{1/3}(t) + E_5 J_{-1/3}(t)\}$$

The constants $D_i$ and $E_i$, appearing in Eq. (4.45) have to be determined during the following matching procedure for the individual solutions in the different regions.

The matching of the individual solutions is done for overlapping regions, where both solutions are still valid. Here, one increases the eigenvalue for a fixed value of the coordinate. The matching of the solution is demonstrated for simplicity only for the first three terms of the expansion

$$\vartheta \sim k^{-1/2}\vartheta_0 + k^{-3/2}\ln k\vartheta_1 + k^{-3/2}\vartheta_2 \tag{4.46}$$

This has the advantage that the basic ideas behind the matching procedure of the solutions can be shown clearly. The algebra involved by using the expression given by Eq. (4.15) is much more complicated and does not contribute to a better understanding of the method (see also Sleicher et al. 1970).

From the previously obtained solution for $\vartheta_M$, Eq. (4.33), it is clear that trigonometric functions have to be matched within the solution process. Because of this fact, it is important to investigate the approximation of these functions in greater detail. As it is already known, trigonometric functions have an amplitude, a frequency and a phase shift. The question now is whether, in approximating these functions, a small error in amplitude or phase shift (for a given frequency) is allowed. Figure 4.3 shows a function $g$ and two different approximations for this function ($g_1$ and $g_2$). For $g_1$, a small deviation in amplitude is allowed compared to $g$, whereas for $g_2$, a small phase shift is allowed compared to $g$.

It can be seen clearly that the function $g_1$ represents a good approximation of $g$, even though the amplitude of $g_1$ is slightly wrong. On the other side, the function $g_2$ does not approximate $g$ very well, because the difference in the phase shift leads to large errors. This shows clearly that for the matching procedure the phase shift has to be matched always exactly. Small deviations in the amplitude can be allowed, because they lead to satisfactory approximations of the functions. Because we found already a complete solution for $\vartheta_C$, it is consequent to start the process with the two functions $\vartheta_C$ and $\vartheta_M$.

If we investigate Eq. (4.30) for very large values of the eigenvalue, the following asymptotic expansion for the Bessel function can be used (Gradshteyn and Ryzhik 1994)

$$
J_{\pm i}(s) = \sqrt{\frac{2}{\pi s}} \left\{
\begin{array}{l}
\cos\left(s \mp \dfrac{\pi}{2} i - \dfrac{\pi}{4}\right) \left[ \displaystyle\sum_{n=0}^{M-1} \frac{(-1)^n}{(2s)^{2n}} \frac{\Gamma(i + 2n + 1/2)}{(2n)!\,\Gamma(i - 2n + 1/2)} + R_1 \right] \\[4mm]
- \sin\left(s \mp \dfrac{\pi}{2} i - \dfrac{\pi}{4}\right) \left[ \displaystyle\sum_{n=0}^{M-1} \frac{(-1)^n}{(2s)^{n+1}} \frac{\Gamma(i + 2n + 3/2)}{(2n+1)!\,\Gamma(i - 2n - 1/2)} + R_2 \right]
\end{array}
\right\}
$$

$$(4.47)$$
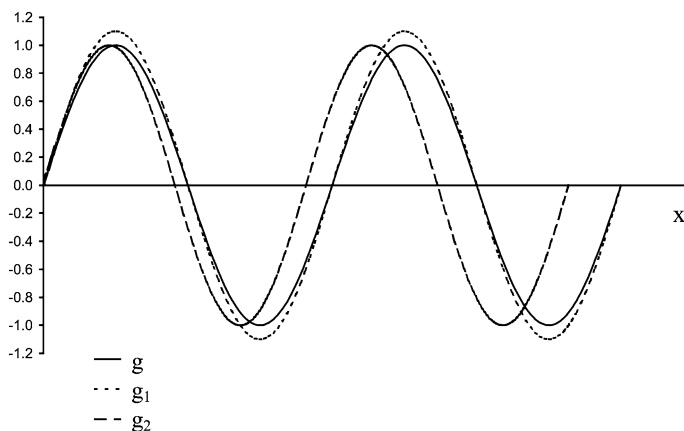


**Fig. 4.3** Influence of a phase shift and a changed amplitude for a trigonometric function

where the two quantities $R_1$ and $R_2$ denote the truncation errors of the sums in Eq. (4.47). These errors are of the order of $M$. Using Eq. (4.47), the distribution in the center region of the pipe, given by Eq. (4.30), can be approximated for large eigenvalues by

$$\vartheta_C = k^{-1/2}\sqrt{\frac{2GA}{\pi}}\left\{\cos(s - \pi/4) + \frac{1}{8s}\sin(s - \pi/4)\right\} \tag{4.48}$$

If one now equates Eqs. (4.48) and (4.33) (which are the solutions for the center region and the middle region), one obtains an equation for determining the unknown constants $K_i$ and $L_i$

$$\sqrt{\frac{2GA}{\pi}}\left\{\cos(s - \pi/4) + \underline{\frac{1}{8s}\sin(s - \pi/4)}\right\} = K_0\sin s + L_0\cos s \tag{4.49}$$
$$+ \frac{\ln k}{k}\{K_1\sin s + L_1\cos s\} + \frac{1}{k}\{K_2\sin s + L_2\cos s\}$$

As stated before, only terms up to the order $O(k^{-3/2})$ are considered here for simplicity. As it can be seen from Eq. (4.49), the coordinate $s$ appears only for the underlined term in the amplitude. The stretched coordinate $s$, rewritten as a function of the second stretched coordinate $t$, according to Eq. (4.35), is $s = k\pi - t$. Matching of the two solutions $\vartheta_C$ and $\vartheta_M$ has now to be done for a fixed value of $t$. This means that $s$ tends to $k\pi$ for large values of $k$. This means also that the amplitude $1/(8s)$ in Eq. (4.49) can be approximated by $1/(8k\pi)$. Applying the addition theorem for trigonometric functions, one obtains from Eq. (4.49)

$$\sqrt{\frac{GA}{\pi}}\left\{\cos s + \sin s + \frac{1}{k}\frac{1}{8\pi}[\sin s - \cos s]\right\} = K_0\sin s \tag{4.50}$$
$$+ L_0\cos s + \frac{\ln k}{k}\{K_1\sin s + L_1\cos s\} + \frac{1}{k}\{K_2\sin s + L_2\cos s\}$$

Comparing the terms in Eq. (4.50) which are of order 1 results in

$$K_0 = L_0 = \sqrt{\frac{GA}{\pi}} \tag{4.51}$$

Comparing terms in Eq. (4.50), which are of the order $1/k\ln k$ and $1/k$ leads to

$$K_1 = L_1 = 0 \tag{4.52}$$

$$K_2 = -L_2 = \frac{1}{8\pi}\sqrt{\frac{GA}{\pi}} \tag{4.53}$$

After the constants $K_i$ and $L_i$ have been determined, the solution for the middle region can be matched to the solution for the near wall region. This gives us the unknown coefficients $D_i$ and $E_i$. In order to do this, the Bessel functions, appearing in Eq. (4.45), have to be approximated for large eigenvalues by the series expansion, Eq. (4.47). This leads, after equating the solutions for the near wall region and the middle region, to the following expression

$$
D_0 \left\{ \cos(t - 5\pi/12) + \frac{5}{72t} \sin(t - 5\pi/12) \right\} \tag{4.54}
$$

$$
+ E_0 \left\{ \cos(t - \pi/12) + \frac{5}{72t} \sin(t - \pi/12) \right\}
$$

$$
\times \frac{\ln k}{k} \{ D_1 \cos(t - 5\pi/12) + E_1 \sin(t - 5\pi/12) \}
$$

$$
+ \frac{1}{k} \left\{ \cos(t - 5\pi/12) \left[ D_2 - \left( \frac{\beta_2 D_0}{\sqrt{3}} + \frac{\beta_2 E_0}{\sqrt{3}} \right) \ln t \right] \right\}
$$

$$
- \frac{1}{k} \left\{ \cos(t - \pi/12) \left[ E_2 - \left( \frac{\beta_2 D_0}{\sqrt{3}} + \frac{\beta_2 E_0}{\sqrt{3}} \right) \ln t \right] \right\}
$$

$$
= \sqrt{\frac{\pi}{2}} \left[ K_0 \sin s + L_0 \cos s + \frac{1}{k} (K_2 \sin s + L_2 \cos s) \right]
$$

From Eq. (4.54), it is immediately clear why the expansion given in Eq. (4.15) contained also logarithmic terms. These terms are needed, because in the asymptotic expansion of the solution for the near wall region, $\vartheta_W$, such terms are present if $w(\xi)$ is approximated by Eq. (4.19). Now the matching procedure works exactly as explained before for Eq. (4.49). The relation between the two stretched coordinates $s$ and $t$ is given by Eq. (4.35). The two solutions $\vartheta_W$ and $\vartheta_M$ have to be matched for a fixed value of $s$ and for $k \to \infty$. This means that in the amplitude $t$ can be replaced by $k\pi$ and $\ln(t)$ by $\ln(k)$. However, as pointed out before, these simplifications are only possible for the amplitude of the function. It must not be done for the phase shift. After selecting terms of order $k^0$ in Eq. (4.54), we obtain

$$
D_0 \cos(t - 5\pi/12) + E_0 \cos(t - 5\pi/12) \tag{4.55}
$$

$$
= \frac{\sqrt{2}}{\pi} [K_0 \sin(k\pi - t) + L_0 \cos(k\pi - t)]
$$

Using the addition theorem for the trigonometric functions, one obtains the two unknown constants $D_0$ and $E_0$ as

$$
D_0 = \left( \frac{4GA}{3} \right)^{1/2} \sin(k\pi - \pi/3), \tag{4.56}
$$

$$
E_0 = -\left( \frac{4GA}{3} \right)^{1/2} \sin(k\pi - 2\pi/3)
$$

Selecting terms of the order $k^{-1} \ln k$ in Eq. (4.54) leads to

$$D_1 = \beta_2 \left( \frac{GA}{3} \right)^{1/2} \cos(k\pi - \pi/3), \tag{4.57}$$

$$E_1 = \beta_2 \left( \frac{GA}{3} \right)^{1/2} \cos(k\pi - 2\pi/3)$$

Finally, equating terms of the order $k^{-1}$ in Eq. (4.54) results in

$$D_2 = - \left( \frac{GA}{3} \right)^{1/2} \cos(k\pi - \pi/3) \left( \frac{7}{18\pi} + \beta_2 \ln \pi \right), \tag{4.58}$$

$$E_2 = - \left( \frac{GA}{3} \right)^{1/2} \cos(k\pi - 2\pi/3) \left( \frac{7}{18\pi} + \beta_2 \ln \pi \right)$$

After this, all the unknown constants have been determined. If the six term expansion is used instead of the three term expansion, the remaining constants $K_i$, $L_i$, $D_i$, $E_i$, $i = 3, 4, 5$ can be determined in the same way. For this constants one obtains (see Sleicher et al. (1970))

$$K_3 = L_3 = 0, \qquad K_4 = L_4 = \frac{1}{\pi^2} \sqrt{\frac{GA}{\pi}}, \qquad K_5 = L_5 = 0 \tag{4.59}$$

$$D_3 = -\frac{\beta_2}{2} \left( \frac{GA}{3} \right)^{1/2} \sin(k\pi - \pi/3) \left( \frac{7}{18\pi} + \beta_2 \ln \pi \right), \tag{4.60}$$

$$E_3 = -\frac{\beta_2}{2} \left( \frac{GA}{3} \right)^{1/2} \sin(k\pi - 2\pi/3) \left( \frac{7}{18\pi} + \beta_2 \ln \pi \right)$$

$$D_4 = - \left( \frac{GA}{3} \right)^{1/2} \sin(k\pi - \pi/3) \left( \frac{\beta_2}{2\pi} + \frac{121}{1296\pi^2} + \frac{7\beta_2 \ln \pi}{36\pi} + \frac{(\beta_2 \ln \pi)^2}{4} \right), \tag{4.61}$$

$$E_4 = - \left( \frac{GA}{3} \right)^{1/2} \sin(k\pi - 2\pi/3) \left( \frac{\beta_2}{2\pi} + \frac{121}{1296\pi^2} + \frac{7\beta_2 \ln \pi}{36\pi} + \frac{(\beta_2 \ln \pi)^2}{4} \right)$$

$$D_5 = \frac{\beta_2^2}{4} \left( \frac{GA}{3} \right)^{1/2} \sin(k\pi - \pi/3), \tag{4.62}$$

$$E_5 = \frac{\beta_2^2}{4} \left( \frac{GA}{3} \right)^{1/2} \sin(k\pi - 2\pi/3)$$

After the eigenfunctions are completely known, the eigenvalues can be calculated by setting the eigenfunction, Eq. (4.45), at the pipe wall equal to zero. One obtains

$$E_0 + \frac{\ln k}{k} E_1 - \frac{1}{k} E_2 = 0 \tag{4.63}$$

For evaluating the eigenvalues, only three terms of the series have been considered here, because this guarantees a satisfactory accuracy (Sleicher et al. 1970). If one introduces the expressions for the constants $E_i$, one finally obtains the following equations for determining the eigenvalues

$$2 \tan\left(k\pi - \frac{2\pi}{3}\right) - \frac{\ln k}{k}\beta_2 + \frac{1}{k}\left(\frac{7}{18\pi} + \beta_2 \ln \pi\right) = 0 \qquad (4.64)$$

Equation (4.64) is an implicit equation for determining the eigenvalues. Sleicher et al. (1970) used several approximations to derive an explicit equation. As a final result they obtained

$$k_j = j + \frac{2}{3} + \frac{\beta_2 \ln(j\pi + 2\pi/3) + 7/(18\pi)}{2\pi(j + 2/3)} \qquad (4.65)$$

The constants $A_j$, which appear in the temperature distribution, Eq. (3.55), can be evaluated from the integrals of the eigenfunctions given by Eq. (3.57). Alternatively, one can derive from the orthogonality of the eigenfunctions the following equation for the constants $A_j$

$$A_j = \frac{-2}{\lambda_j} \bigg/ \frac{d\Phi_j}{d\lambda}\bigg|_{\lambda_j} \qquad (4.66)$$

If Eq. (4.66) is applied to the solution for the near wall region, Eq. (4.45), one obtains

$$A_j = \frac{(-1)^j \Gamma(2/3)3^{2/3}V^{1/6}}{G^{1/3}\pi\sqrt{2GA}k_j^{2/3}2^{1/6}} \bigg/ \left[1 + \frac{1}{k_j^2}\left(\frac{\beta_2}{2\pi}\left(\ln k_j\pi - 3/2\right) + \frac{1}{6\pi^2}\right)\right] \qquad (4.67)$$

For the determination of the constants $A_j$, the complete six term expansion has been used. For technical applications, the engineer may be interested only in the distribution of the Nusselt number. As it can be seen from Eq. (3.69), only the product $A_j\Phi_j'(1) = M_j$ appears in this equation. The quantity $M_j$ can be predicted using the six term expansion

$$M_j = \frac{-\Gamma(2/3)V^{1/3}}{G^{2/3}\pi k_j^{1/3}3^{1/6}\Gamma(4/3)}\left[1 - \frac{1}{k_j^2}\left(\frac{\beta_2}{2\pi}\left(\ln k_j\pi - 1\right) + \frac{7}{36\pi^2}\right)\right] \qquad (4.68)$$

As it can be seen from the Eqs. (4.67) and (4.68), the unknown constant $\beta_2$ is still part of the solution. Sleicher et al. (1970) proposed that the constant $\beta_2$ should be evaluated in such a way that the numerically predicted eigenvalues for $j = 3$ are identical to the asymptotic expressions given above (see Notter and Sleicher (1972) for tabulated values of $\beta_2$ for different Reynolds and Prandtl numbers). This procedure has the advantage that one receives a continuous spectrum of eigenvalues and constants. However, there is the disadvantage, that the asymptotic behavior is

enforced even though it may not be correct at such low values of $j$. On the other hand, Eqs. (4.67) and (4.68) show that the term containing the constant $\beta_2$ decays at least like $k^{-2} \ln k\pi$. This means that the expressions for the constants are always correct for very large values of $j$, independently from the used value of $\beta_2$.

In the following section, the asymptotic values are compared to numerical calculated values for the Sturm-Liouville system. This is done first for the case of a circular pipe with constant wall temperature and hydrodynamically fully developed turbulent internal flow. The second case shows an application of the method to another problem (heat transfer in an axially rotating pipe).

## 4.1 Heat Transfer in Turbulent Pipe Flow with Constant Wall Temperature

As stated before, the here considered case of a hydrodynamically fully developed turbulent pipe flow subjected to a constant wall temperature is exactly the one for which Sleicher et al. (1970) developed their asymptotic method. Before comparing the values from the asymptotic expansion to our numerical calculations, it is important to understand first for which combinations of $Re_D$ and $Pr$ a large number of eigenvalues is needed for correctly predicting the distribution of the Nusselt number correctly. Figure 4.4 shows the influence of the Prandtl number on the length of the thermal entrance region for a turbulent flow in a duct and for a given value of the Reynolds number. It can be seen that with increasing values of the Prandtl number the length of the thermal entrance region decreases dramatically.

This shows nicely that for high Prandtl numbers, the value of the fully developed Nusselt number $Nu_\infty$ is sufficient to describe the heat transfer problem. On the other
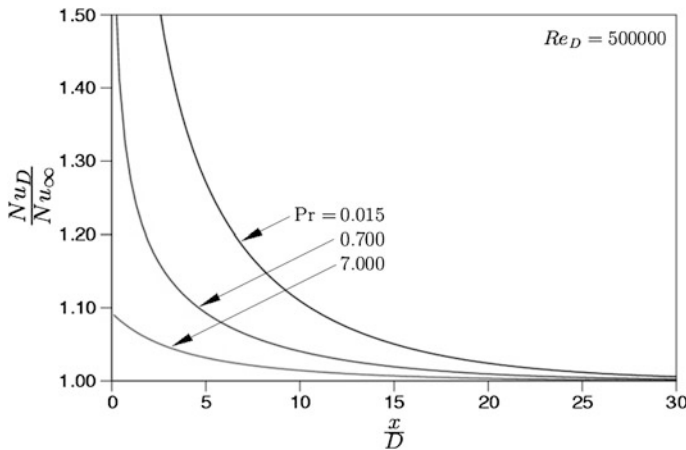


**Fig. 4.4** Influence of the Prandtl number on the distribution of the Nusselt number in the thermal entrance region of a turbulent flow in a duct

hand, it can be seen that for fluids with relatively low Prandtl numbers (for example for liquid metals (Pr < 0.1)) a lot of eigenvalues are necessary for correctly describing the distribution of the Nusselt number in the thermal entrance region. Because of this fact, the focal point of the following study is set on flows with low Prandtl numbers. Sleicher et al. (1970) did not show, for the case of a constant wall temperature, how the asymptotic expressions for $\lambda_j$, $A_j$, and $M_j$ compare to numerical predictions of the problem. However, such a comparison is very useful in order to gain confidence in the method shown before. For the first calculations, the value of $\beta_2$ is set to zero in Eqs. (4.65), (4.67) and (4.68). For the calculation of the eigenvalues only the simple expression $k_j = j + 2/3$ has been used. The case $\beta_2 = 0$ presents the maximum deviation between numerical results and the analytical solution and is, therefore, very important. In order to minimize the error in the numerical calculations, all calculations have been performed with very fine grids (1000–1500 grid points in the radial direction, see Appendix C for a description of the numerical method). In addition, the constants $A_j$ have been calculated separately from Eq. (3.57) and from (4.65). Tables 4.1 and 4.2 show comparisons of the eigenvalues $\lambda_5, \lambda_{10}, \lambda_{20}$ and the constants $M_5, M_{10}, M_{20}$ for different Prandtl numbers. It can be seen that the eigenvalues can be predicted quite accurately for all Prandtl numbers by using the simple approximation $k_j = j + 2/3$. The maximum deviation between numerically calculated eigenvalues and this simple expression is about 3 %. For the constants $M_j$, which are used in calculating the Nusselt number, the behavior is different. Here, the analytical value for $M_5$ is only for the smallest Reynolds number under investigation in fairly good agreement with the numerical calculation. This is not very suprising, because Eq. (4.68) should be correct for large eigenvalues only (This can be proven by calculating for example $M_{40}$ numerically and by the asymptotic expression. For these values only a deviation between the numerically predicted values and the asymptotic approximation of about 0.5 % is found). The analytically predicted values for $M_{10}$ are found to be in fair agreement with the numerical predictions. Instead, for Pr = 0.7, larger deviations can be noticed. However, this is not such a problem, because the length of the thermal entrance region is decreasing with increasing Prandtl numbers and therefore, the impact of the higher eigenvalues and constants on the distribution of the Nusselt number in the thermal entrance region are not so important as for lower Prandtl numbers.

After showing the maximum deviations between the numerical calculations and the asymptotic expressions derived by Sleicher et al. (1970), it is now interesting to see how much the asymptotic analysis can be improved, if the value of $\beta_2$ is adapted for $j = 5$.[5]

---

[5]Sleicher et al. (1970) used $j = 3$ for adapting their asymptotic results to numerically predicted values for the constants. However, a numerical study showed that matching the asymptotic results for $j = 3$ leads to less accurate results compared to the choice $j = 5$. The reason for this is that one is using the asymptotic formulas in a region ($j = 3$) where they are not valid.

**Table 4.1** Comparison between numerically predicted eigenvalues and the asymptotic approximation for $\beta_2 = 0$

| | $\lambda_5$ | $\lambda_{10}$ | $\lambda_{20}$ |
|---|---|---|---|
| Pr = 0.004: | | $Re_D = 20,000$ | |
| Numerical | 17.4214 | 32.6512 | 63.1556 |
| Analytical | 17.3215 | 32.5907 | 63.1363 |
| | | $Re_D = 50,000$ | |
| Numerical | 17.8378 | 33.3973 | 64.5417 |
| Analytical | 17.6861 | 33.2766 | 64.4650 |
| | | $Re_D = 100,000$ | |
| Numerical | 18.5022 | 34.6224 | 66.8782 |
| Analytical | 18.3134 | 34.4568 | 66.7514 |
| Pr = 0.02: | | $Re_D = 20,000$ | |
| Numerical | 17.8526 | 33.4928 | 64.8291 |
| Analytical | 17.7860 | 33.4646 | 64.8294 |
| | | $Re_D = 50,000$ | |
| Numerical | 21.5694 | 40.3435 | 77.9191 |
| Analytical | 21.3428 | 40.1568 | 77.7938 |
| | | $Re_D = 100,000$ | |
| Numerical | 25.7941 | 48.1753 | 92.9565 |
| Analytical | 25.4343 | 47.8550 | 92.7071 |
| Pr = 0.2: | | $Re_D = 20,000$ | |
| Numerical | 30.3566 | 56.7416 | 109.5787 |
| Analytical | 29.9993 | 56.4441 | 109.3464 |
| | | $Re_D = 50,000$ | |
| Numerical | 59.0931 | 110.2750 | 212.3409 |
| Analytical | 57.9515 | 109.0365 | 211.2310 |
| | | $Re_D = 100,000$ | |
| Numerical | 80.9672 | 151.2447 | 291.1758 |
| Analytical | 79.3562 | 149.3097 | 289.2503 |
| Pr = 0.7: | | $Re_D = 20,000$ | |
| Numerical | 58.2822 | 108.1118 | 207.8779 |
| Analytical | 56.6920 | 106.6666 | 206.6399 |
| | | $Re_D = 50,000$ | |
| Numerical | 122.3031 | 227.8361 | 437.2618 |
| Analytical | 118.8246 | 223.5699 | 433.1108 |
| | | $Re_D = 100,000$ | |
| Numerical | 166.9422 | 312.3776 | 600.0760 |
| Analytical | 162.7946 | 306.2999 | 593.3795 |

| | $-M_5$ | $-M_{10}$ | $-M_{20}$ |
|---|---|---|---|
| **Table 4.2** Comparison between numerically predicted constants $M_j$ and the asymptotic approximation for $\beta_2 = 0$ | | | |
| Pr = 0.004: | | Re$_D$ = 20,000 | |
| Numerical | 1.4742 | 1.2873 | 1.0589 |
| Analytical | 1.5135 | 1.2265 | 0.9841 |
| | | Re$_D$ = 50,000 | |
| Numerical | 1.6047 | 1.4745 | 1.2972 |
| Analytical | 1.9278 | 1.5623 | 1.2534 |
| | | Re$_D$ = 100,000 | |
| Numerical | 1.7010 | 1.5969 | 1.4591 |
| Analytical | 2.3599 | 1.9124 | 1.5344 |
| Pr = 0.02: | | Re$_D$ = 20,000 | |
| Numerical | 1.3670 | 1.1360 | 0.8951 |
| Analytical | 1.3088 | 1.0607 | 0.8510 |
| | | Re$_D$ = 50,000 | |
| Numerical | 1.9253 | 1.7012 | 1.4829 |
| Analytical | 2.3303 | 1.7708 | 1.4207 |
| | | Re$_D$ = 100,000 | |
| Numerical | 2.2782 | 2.0945 | 1.8812 |
| Analytical | 2.9376 | 2.3807 | 1.9010 |
| Pr = 0.2: | | Re$_D$ = 20,000 | |
| Numerical | 1.8241 | 1.5246 | 1.2175 |
| Analytical | 1.8546 | 1.5029 | 1.2058 |
| | | Re$_D$ = 50,000 | |
| Numerical | 3.6070 | 3.2018 | 2.7545 |
| Analytical | 4.2530 | 3.4466 | 2.7652 |
| | | Re$_D$ = 100,000 | |
| Numerical | 5.1689 | 4.3931 | 3.9156 |
| Analytical | 6.2727 | 5.0834 | 4.0784 |
| Pr = 0.7: | | Re$_D$ = 20,000 | |
| Numerical | 2.4726 | 2.2432 | 1.8339 |
| Analytical | 2.8348 | 2.2973 | 1.8431 |
| | | Re$_D$ = 50,000 | |
| Numerical | 4.3090 | 4.5051 | 4.3173 |
| Analytical | 6.8644 | 5.5629 | 4.4631 |
| | | Re$_D$ = 100,000 | |
| Numerical | 5.9864 | 5.6555 | 5.9483 |
| Analytical | 10.1275 | 8.2073 | 6.5848 |

Table 4.3 shows a comparison between numerically predicted values for $M_{10}$, $M_{15}$ and $M_{20}$ for the two Reynolds numbers Re$_D$ = 50,000 and Re$_D$ = 100,000. The values for Re$_D$ = 10,000 are not shown, because the agreement for these low Reynolds numbers was already good, even so $\beta_2$ was set to zero. As it can be seen from Table 4.3, the agreement between the numerically predicted constants and the

ones from the asymptotic approximation is generally quite good. It can also be seen that matching the values for $j = 5$ results in a great improvement in the accuracy. The only values where the agreement is still not fully satisfactory, are the ones for $Pr = 0.7$ and $Re_D = 100{,}000$. However, for this value of the Prandtl number, the distribution of $Nu/Nu_\infty$ is not much influenced by the Reynolds number (see for example Kays et al. (2004)). Therefore, the distribution for $Nu/Nu_\infty$ could be approximated by the one for $Re_D = 50{,}000$, where $Nu_\infty$ has to be taken for the correct Reynolds number.

Because of the limited computer power available in the 1970s, the comparison shown here between numerical calculations and the asymptotic expansions has hardly been possible at the time when the asymptotic method has been developed (Sleicher et al. 1970). However, the comparison elucidates very nicely that only the first five eigenvalues need to be calculated numerically. The higher eigenvalues and related constants can than be obtained quite accurately from the asymptotic approximations. The here shown comparisons also give high confidence into the asymptotic approximations developed by Sleicher et al. (1970) by using a perturbation method.

**Table 4.3** Comparison between numerically predicted constants $M_j$ and the asymptotic approximation for a value of $\beta_2$ so that $M_5$ is equal

|  | $-M_{10}$ | $-M_{15}$ | $-M_{20}$ |
|---|---|---|---|
| Pr = 0.004: |  | $Re_D = 50{,}000$ |  |
| Numerical | 1.4745 | 1.3769 | 1.2972 |
| Analytical | 1.4711 | 1.3332 | 1.2301 |
|  |  | $Re_D = 100{,}000$ |  |
| Numerical | 1.5969 | 1.5214 | 1.4869 |
| Analytical | 1.7264 | 1.5982 | 1.4869 |
| Pr = 0.02: |  | $Re_D = 50{,}000$ |  |
| Numerical | 1.7012 | 1.5804 | 1.4829 |
| Analytical | 1.6832 | 1.5183 | 1.3984 |
|  |  | $Re_D = 100{,}000$ |  |
| Numerical | 2.0945 | 1.9751 | 1.8812 |
| Analytical | 2.0945 | 2.0101 | 1.8625 |
| Pr = 0.2: |  | $Re_D = 50{,}000$ |  |
| Numerical | 3.2018 | 2.9606 | 2.7545 |
| Analytical | 3.2643 | 2.9497 | 2.7187 |
|  |  | $Re_D = 100{,}000$ |  |
| Numerical | 4.3931 | 4.1307 | 3.9156 |
| Analytical | 4.7718 | 4.3312 | 3.9989 |
| Pr = 0.7: |  | $Re_D = 50{,}000$ |  |
| Numerical | 4.5051 | 4.5116 | 4.3173 |
| Analytical | 4.8415 | 4.5670 | 4.2790 |
|  |  | $Re_D = 100{,}000$ |  |
| Numerical | 5.6555 | 5.9204 | 5.9483 |
| Analytical | 7.0383 | 6.6904 | 6.2864 |

## 4.2  Heat Transfer in an Axially Rotating Pipe with Constant Wall Temperature

The shown analytical method for calculating larger eigenvalues and constants is now applied to the case of heat transfer in an axially rotating pipe with a hydro-dynamically fully developed, turbulent velocity profile. In order to do this, one has to notice that the correct velocity gradient at the wall is $2V$ for the case of the axially rotating pipe. Sleicher et al. (1970) expressed the velocity gradient at the wall as a function of the friction coefficient for a fully developed turbulent pipe flow without rotation. Using this assumption in the present case would lead to wrong answers for the asymptotic eigenvalues and constants. This is due to the fact, that in the case of the axial rotating pipe the friction coefficient is influenced by the system rotation and the laminarization of the flow field. However, if we apply the definition of $V$ and use the results from Chap. 3 and Appendix B for the hydrodynamically fully developed pipe flow in an axially rotating pipe, the correct asymptotic constants and eigenvalues can be predicted. It should also be mentioned here that the constant $\beta_1$ attains the value 5/36 as long as the velocity gradient at the wall is assumed to be linear. This is, of course, also a suitable choice for the flow in an axially rotating pipe.

In Chap. 3.3, the heat transfer in an axially rotating pipe has been discussed extensively. However, it is noteworthy mentioning that the laminarization of the flow in the pipe increases with increasing values of the rotation rate $N = w_W / \bar{u} = \mathrm{Re}_\varphi / \mathrm{Re}_D$. This leads to decreasing values of the Nusselt number for increasing values of N.

In a first attempt, the value of $\beta_2$ in the asymptotic expressions for the eigenvalues and the constants is set to zero in order to estimate the maximum deviation between numerically predicted values and the ones from the analytical theory. Again, the eigenvalues are predicted by the simple expression $k_j = j + 2/3$ from Eq. (4.65). The results obtained are reported in Table 4.4, where comparisons are shown for Pr = 0.71 and different values of $\mathrm{Re}_D$ and N. It can be seen that the numerically predicted eigenvalues are in very good agreement with the analytical predictions, even for larger values of the rotation rate. This result is at a first glance somewhat surprising, because for larger N, the flow laminarizes and finally for $N \to \infty$ it approaches the behavior of a laminar pipe flow. This means that for $N \to \infty$ $a_2 \to 1$ and $\tilde{u} \to 2(1 - \tilde{r}^2)$. If we investigate the analytic expression for the larger eigenvalues according to Eq. (4.65), it can be seen that one obtains for $\lambda_j$

$$\lambda_j = \frac{1}{\sqrt{2}G} \left( j + \frac{2}{3} \right) \tag{4.69}$$

The quantity $G$, which appears in Eq. (4.69), is defined by Eq. (4.9). Replacing the quantity $a_2$ by one in the definition of the function $G$ and the velocity

**Table 4.4** Comparison between numerically predicted eigenvalues and the asymptotic approximation for $\beta_2 = 0$ for an axially rotating pipe (Pr = 0.71)

| | $\lambda_5$ | $\lambda_{10}$ | $\lambda_{20}$ |
|---|---|---|---|
| $Re_D = 5000$: | | N = 1 | |
| Numerical | 37.4548 | 70.1148 | 135.2362 |
| Analytical | 36.9167 | 69.4903 | 134.6374 |
| | | N = 3 | |
| Numerical | 23.9176 | 44.9527 | 86.9393 |
| Analytical | 23.7882 | 44.7778 | 86.7571 |
| | | N = 5 | |
| Numerical | 18.9059 | 35.5338 | 68.7749 |
| Analytical | 18.8431 | 35.4693 | 68.7218 |
| $Re_D = 10,000$: | | N = 1 | |
| Numerical | 47.6343 | 89.3193 | 172.2480 |
| Analytical | 46.9711 | 88.4161 | 171.3063 |
| | | N = 3 | |
| Numerical | 28.1981 | 53.0729 | 102.6860 |
| Analytical | 28.0821 | 52.8605 | 102.4171 |
| | | N = 5 | |
| Numerical | 20.6890 | 38.9011 | 75.2881 |
| Analytical | 20.6180 | 38.8104 | 75.1951 |
| $Re_D = 20,000$: | | N = 1 | |
| Numerical | 61.4338 | 115.5300 | 222.8338 |
| Analytical | 60.7089 | 114.2756 | 221.4090 |
| | | N = 3 | |
| Numerical | 34.3362 | 64.7308 | 125.3610 |
| Analytical | 34.2711 | 64.5103 | 124.9887 |
| | | N = 5 | |
| Numerical | 23.3372 | 43.9092 | 85.0086 |
| Analytical | 23.2725 | 43.8070 | 84.8761 |
| $Re_D = 50,000$: | | N = 1 | |
| Numerical | 87.4261 | 165.2109 | 319.0354 |
| Analytical | 86.8290 | 163.4429 | 316.6706 |
| | | N = 3 | |
| Numerical | 46.4773 | 87.7990 | 170.3082 |
| Analytical | 46.5653 | 87.6524 | 169.8265 |
| | | N = 5 | |
| Numerical | 29.0058 | 54.6220 | 105.8197 |
| Analytical | 28.9729 | 54.5373 | 105.6660 |

distribution by the one for a hydrodynamically fully developed laminar pipe flow, we obtain

$$G = \frac{1}{\pi} \int\limits_0^1 \sqrt{1 - \tilde{r}^2} d\tilde{r} = \frac{1}{2\pi} \arcsin(1) = \frac{1}{4} \qquad (4.70)$$

**Table 4.5** Comparison between numerically predicted constants $M_j$ and the asymptotic approximation for $\beta_2 = 0$ for an axially rotating pipe (Pr = 0.71)

|  | $-M_5$ | $-M_{10}$ | $-M_{20}$ |
|---|---|---|---|
| Re$_D$ = 5000: |  | N = 1 |  |
| Numerical | 1.5102 | 1.3339 | 1.1157 |
| Analytical | 1.7269 | 1.3986 | 1.1219 |
|  |  | N = 3 |  |
| Numerical | 1.0368 | 0.8485 | 0.7024 |
| Analytical | 1.0918 | 0.8843 | 0.7093 |
|  |  | N = 5 |  |
| Numerical | 0.8287 | 0.6778 | 0.5488 |
| Analytical | 0.8451 | 0.8451 | 0.6844 |
| Re$_D$ = 10,000: |  | N = 1 |  |
| Numerical | 1.8785 | 1.6993 | 1.4754 |
| Analytical | 2.3237 | 1.8820 | 1.5097 |
|  |  | N = 3 |  |
| Numerical | 1.2784 | 1.0065 | 0.8370 |
| Analytical | 1.3429 | 1.0877 | 0.8725 |
|  |  | N = 5 |  |
| Numerical | 0.9212 | 0.7422 | 0.6048 |
| Analytical | 0.9416 | 0.7626 | 0.6118 |
| Re$_D$ = 20,000: |  | N = 1 |  |
| Numerical | 2.4120 | 2.1686 | 1.9620 |
| Analytical | 3.2109 | 2.6006 | 2.0861 |
|  |  | N = 3 |  |
| Numerical | 1.7083 | 1.2660 | 1.0244 |
| Analytical | 1.7340 | 1.4044 | 1.1266 |
|  |  | N = 5 |  |
| Numerical | 1.0992 | 0.8583 | 0.6877 |
| Analytical | 1.0972 | 0.8887 | 0.7129 |
| Re$_D$ = 50,000: |  | N = 1 |  |
| Numerical | 3.6757 | 2.9977 | 2.8559 |
| Analytical | 5.0721 | 4.1080 | 3.2953 |
|  |  | N = 3 |  |
| Numerical | 2.8233 | 1.8908 | 1.4061 |
| Analytical | 2.5829 | 2.0920 | 1.6781 |
|  |  | N = 5 |  |
| Numerical | 1.5958 | 1.1845 | 0.8982 |
| Analytical | 1.4593 | 1.1819 | 0.9481 |

If we insert this value of $G$ into Eq. (4.69), we obtain from Eq. (4.69) exactly the asymptotic expression of the eigenvalues for laminar pipe flow, Eq. (4.1), which has been predicted by Sellars et al. (1956) (the same behavior can be shown also for the constants $M_j$).

As it can be seen from Table 4.5, the numerically predicted values for $M_j$ ($j$ = 5, 10, 20) for N = 3 and N = 5 are in good agreement with the analytical predictions. However, for N = 1, larger deviations between the numerically predicted values for $M_j$ and the analytical approximation can be noticed. For a Reynolds number of 50,000, the largest deviation occurs for N = 1. Here the analytically predicted value for $M_5$ is about 38 % different to the numerically predicted value. For this case, the analytically predicted value of $M_{20}$ is still out by about 15 %.

Following the approach of the last paragraph, we can determine again the value of the constant $\beta_2$ by enforcing the analytical values of $M_5$ to be the same as the numerically calculated values. By doing so, it can be noticed from Table 4.6, that the agreement between the numerically predicted constants and the analytical

**Table 4.6** Comparison between numerically predicted constants $M_j$ and the asymptotic approximation for a value of $\beta_2$ so that $M_5$ is equal (axial rotating pipe, Pr = 0.71)

|  | $-M_{10}$ | $-M_{15}$ | $-M_{20}$ |
|---|---|---|---|
| $Re_D$ = 5000: |  | N = 1 |  |
| Numerical | 1.3339 | 1.2104 | 1.1157 |
| Analytical | 1.3376 | 1.2027 | 1.1063 |
|  |  | N = 3 |  |
| Numerical | 0.8485 | 0.7613 | 0.7024 |
| Analytical | 0.8688 | 0.7709 | 0.7054 |
| $Re_D$ = 10,000: |  | N = 1 |  |
| Numerical | 1.6993 | 1.5777 | 1.4754 |
| Analytical | 1.7565 | 1.5987 | 1.4776 |
|  |  | N = 3 |  |
| Numerical | 1.0965 | 0.8999 | 0.8370 |
| Analytical | 1.0695 | 0.9486 | 0.8679 |
| $Re_D$ = 20,000: |  | N = 1 |  |
| Numerical | 2.1686 | 2.0661 | 1.9620 |
| Analytical | 2.3754 | 2.1856 | 2.0286 |
|  |  | N = 3 |  |
| Numerical | 1.2660 | 1.1057 | 1.0243 |
| Analytical | 1.3972 | 1.2323 | 1.1247 |
| $Re_D$ = 50,000: |  | N = 1 |  |
| Numerical | 2.9977 | 2.9370 | 2.8559 |
| Analytical | 3.7143 | 3.4353 | 3.1948 |
|  |  | N = 3 |  |
| Numerical | 1.8908 | 1.5604 | 1.4061 |
| Analytical | 2.1599 | 1.8712 | 1.6954 |

approximations is strongly improved. Exceptions occur for N = 1 and $Re_D = 50{,}000$, where still larger deviations can be noticed. However, even for this case, the deviations reduce from former 38 % for $M_{10}$ to about 24 % and for the value of $M_{20}$ from 15 % to about 11 %.

This shows very nicely that the method of Sleicher et al. (1970) can be used quite easily for other related problems. It should also be kept in mind that, for the case of an axially rotating pipe, usually much more eigenvalues and constants are needed than in the case of a fully turbulent flow without rotation. This is due to the effect of flow laminarization, which tends to increase dramatically the thermal entrance region (see also Chap. 3). Therefore, the usage of asymptotic values for the eigenvalues and the constants $M_j$ is very beneficial and results in a great simplification for this case.

## 4.3 Asymptotic Expressions for Other Thermal Boundary Conditions

Several authors have used the method of Sleicher et al. (1970) in order to obtain asymptotic expressions for related problems involving turbulent internal flow with other boundary conditions than a constant wall temperature. Since the mathematical approach is similar to the one presented in detail in this chapter, only the resulting expressions for the eigenvalues and the constants are reported here. For the case of a constant heat flux at the pipe wall, Notter and Sleicher (1971) obtained the following expressions for the eigenvalues and the constants

$$k_j = j + \frac{1}{3} - \frac{3^{7/6} G^{2/3} \Gamma(4/3)}{4\pi V^{1/3} \Gamma(2/3)(j + 1/3)^{2/3}} \tag{4.71}$$

$$A_j = \frac{(-1)^{j+1} 3^{4/3} G^{1/3} \Gamma(4/3)}{\sqrt{2A} \pi V^{1/6} k_j^{4/3}} \bigg/ \left\{ 1 - \frac{3^{2/3} G^{2/3} \Gamma(4/3)}{4 V^{1/3} \Gamma(2/3) k_j^{2/3}} \right\} \tag{4.72}$$

$$A_j \Phi_j(1) = \frac{3^{7/6} 2 \, \Gamma(4/3)}{\pi V^{1/3} G^{-2/3} \Gamma(2/3) (k_j)^{5/3}} \bigg/ \left\{ 1 - \frac{3^{2/3} \Gamma(1/3)}{4 G^{-2/3} V^{1/3} \Gamma(2/3) (k_j)^{2/3}} \right\}$$
$$\times \left\{ 1 + \frac{3^{2/3} \Gamma(4/3)}{4 V^{1/3} G^{-2/3} \Gamma(2/3) (k_j)^{2/3}} + \frac{1}{k_j} \frac{1}{2\sqrt{3}} \left( \beta_2 \ln(k_j \pi) + \frac{7}{18\pi} \right) \right\} \tag{4.73}$$

Notter and Sleicher (1971b) compared their analytical results for the eigenvalues and the constants according to Eqs. (4.71) and (4.73) with numerical calculations for $j = 4$ and found good agreement for Pr $\leq 0.06$.

The case of a convective cooled wall is a more general case than the two above considered cases of constant wall temperature and constant wall heat flux. For this case, the eigenvalue problem is given by

$$\frac{d}{d\tilde{r}}\left[\tilde{r}a_2(\tilde{r})\frac{d\Phi_j}{d\tilde{r}}\right] + \tilde{r}\tilde{u}(\tilde{r})\lambda_j^2\Phi_j(\tilde{r}) = 0 \tag{4.7}$$

with the boundary conditions

$$\tilde{r} = 0 : \Phi'(0) = 0 \tag{4.74}$$
$$\tilde{r} = 1 : \Phi'(1) + \text{Bi}\Phi(1) = 0$$

and with the Biot number defined by $\text{Bi} = hR/k$. For $\text{Bi} \to 0$ one obtains from Eq. (4.74) the constant wall heat flux case, while for $\text{Bi} \to \infty$ one obtains the case of a constant temperature at the pipe wall. For the case of a convective cooled pipe, Sadeghipour et al. (1984) derived asymptotic expressions for the eigenvalues and constants. For their analysis, they assumed a turbulent velocity profile according to

$$\tilde{u} = 2c(1 - \tilde{r})^{1/m}, \quad c = \frac{1}{4}\left(\frac{3m+1}{m^2} + 2\right) \tag{4.75}$$

This means that the following expressions cannot be used for the heat transfer in an axially rotating pipe. However, Eqs. (4.71) and (4.73) (for the case of a constant wall heat flux) can be used also for the case of an axially rotating pipe, because in these equations the velocity gradient at the wall, $2V$, has been used. This value needs only to be adopted, as it was discussed in the previous section.

The asymptotic expressions by Sadeghipour et al. (1984) are

$$k_j = \frac{(-1)^j}{2k_j\pi}\left(\frac{\omega\cos\varepsilon_1 + \omega\cos\varepsilon_2}{\omega+1}\right)\left(\beta_2\ln(k_j\pi) + \frac{1-2\gamma^2}{2\pi}\right) \tag{4.76}$$
$$+ j + \frac{1}{2}\left(1 + \gamma\frac{\omega-1}{\omega+1}\right)$$

where the following abbreviations are used

$$\gamma = \frac{m}{2m+1}, \quad \psi_1 = \frac{\pi}{2}(1+\gamma), \quad \psi_2 = \frac{\pi}{2}(1-\gamma), \tag{4.77}$$
$$\varepsilon_1 = k_j\pi - \psi_1, \quad \varepsilon_2 = k_j\pi - \psi_2$$

$$\omega = \frac{1+\gamma}{1-\gamma}\frac{(\text{Bi}-1/2)}{\left(\sqrt{c}\gamma k_j/G\right)^{2\gamma}} \tag{4.78}$$

$$A_j \Phi_j(1) = \frac{4\mathrm{Bi}}{\pi k_j} \left(2\sqrt{\left(\frac{2m+1}{m+1}\frac{G}{k_j}\right)}\right)^{2\gamma} \frac{\Gamma(1+\gamma)}{\Gamma(1-\gamma)} \tag{4.79}$$

$$\frac{-\sin\varepsilon_1 + \frac{1}{2k_j}\left(\frac{1-2\gamma^2}{2\pi} + \beta_2 \ln(k_j\pi)\right)\cos\varepsilon_1}{\cos\varepsilon_2 + \omega\cos\varepsilon_1 + \frac{a_{11}}{2k_j} + \frac{a_{12}}{2\pi k_j^2}}$$

$$a_{11} = \left(-\frac{1+2v^2}{2\pi} + \beta_2 \ln(k_j\pi)\right)(\sin\varepsilon_2 + \omega\sin\varepsilon_1) + \frac{4v}{\pi}\sin\varepsilon_2 \tag{4.80}$$

$$a_{12} = \left[-\beta_2 + \frac{3}{2}\left(\frac{1-2v^2}{2\pi} + \beta_2 \ln(k_j\pi)\right)\right](\cos\varepsilon_2 + \omega\cos\varepsilon_1) \tag{4.81}$$
$$- 2v\left(\frac{1-2v^2}{\pi} + \beta_2 \ln(k_j\pi)\right)\cos\varepsilon_2$$

Based on the approach by Sleicher et al. (1970) and Notter and Sleicher (1971) Weigand and Bogenfeld (2014) predicted asymptotic expressions for the eigenvalues and constants for an axially rotating pipe with a convective boundary condition as given by Eq. (4.74). Because the axial velocity profile was not prescribed by an approximation, the obtained analytical expressions are valid for different axial velocity profiles. Detailed comparisons are shown in Weigand and Bogenfeld (2014) with a numerical solution of the eigenvalue problem. Similar to Sect. 4.2 detailed comparisons between analytically and numerically predicted eigenvalues and constants are presented for various Biot numbers and various rotation rates of the pipe. Also the case of a non-rotating pipe is included. The comparisons between analytically and numerically predicted values, which have been made for small Prandtl numbers, show very good agreement. For the asymptotic eigenvalues the following equation was obtained

$$k_j = j + \frac{1}{3} + \frac{1}{\pi}\arctan\left[\frac{\sqrt{3} + k_j^{-1}(1/2 + C_1)\left(\frac{7}{18\pi} + \beta_2 \ln(k_j\pi)\right)}{1 + 2C_1 - k_j^{-1}\sqrt{3}/2\left(\frac{7}{18\pi} + \beta_2 \ln(k_j\pi)\right)}\right] \tag{4.82}$$

with the quantity $C_1$ given by

$$C_1 = \frac{k_j^{2/3}V^{1/3}\Gamma(2/3)}{(3G)^{2/3}\Gamma(4/3)(\mathrm{Bi} - 1/2)} \tag{4.83}$$

This implicit equation for the asymptotic eigenvalues $k_j$ could be approximated by the very simple following equation

$$k_j = j + \frac{1}{3} + \frac{\mathrm{Bi} - \frac{1}{2}}{(3 + j^{4/5}\mathrm{Bi})\mathrm{Bi}} \tag{4.84}$$

It was shown that the simple approximation equation, given by Eq. (4.84), agrees very well with the exact Eq. (4.82) for various Biot numbers and different Reynolds numbers and rotation rates. Asymptotic expressions for the constants $A_j \Phi_j(1)$ have also been derived. The reader is referred to the paper of Weigand and Bogenfeld (2014) for more details on this.

## Problems

4-1   Consider the heat transfer for laminar pipe flow. The eigenvalue problem for the heat transfer in the thermal entrance region is given by

$$\frac{1}{\tilde{r}} \frac{d}{d\tilde{r}} \left[ \tilde{r} \frac{d\Phi_j}{d\tilde{r}} \right] + 2\left(1 - \tilde{r}^2\right)\Phi_j = 0$$

with the boundary conditions

$$\tilde{r} = 0 : \frac{d\Phi}{d\tilde{r}} = 0$$
$$\tilde{r} = 1 : \Phi = 0$$

Show by introducing the quantities defined by Eqs. (4.9) and (4.10) that the problem can be reduced to the form given by Eqs. (4.11) and (4.12).

4-2   Consider the heat transfer in a parallel plate channel with distance $2\,h$ between the two plates. The flow is laminar and hydrodynamically fully developed. The velocity profile is given by

$$\tilde{u} = \frac{3}{2} \left( 1 - \left(\frac{y}{h}\right)^2 \right)$$

The problem can be described by the following partial differential equation

$$\tilde{u} \frac{\partial \Theta}{\partial \tilde{x}} = \frac{\partial^2 \Theta}{\partial y^2}$$

and the boundary conditions

$$\tilde{x} = 0 : \Theta = 1$$
$$\tilde{y} = 0 : \frac{\partial \Theta}{\partial y} = 0$$
$$\tilde{y} = 1 : \Theta = 0$$

Use the FORTRAN program reported in Appendix C to calculate the eigenvalues for this problem. Plot the first 100 eigenvalues $\lambda_j^2$ as a function of $j$. Provide an equation for large eigenvalues from the plotted results.

# Chapter 5
# Heat Transfer in Duct Flows for Small Peclet Numbers (Elliptic Problems)

In Chaps. 3 and 4, we have been concerned with heat transfer in hydrodynamically fully developed flows in pipes or planar channels. There we made the assumption that the axial heat conduction within the fluid can be ignored. This assumption implies that the Peclet number ($Pe_D = Re_D Pr$) for the problem under consideration is large enough. If one neglects the axial heat conduction term in the energy equation, the partial differential equation (3.5) changes its type from elliptic to parabolic. This means that the original energy equation (3.5) is elliptic, whereas the simplified equation (e.g. Eq. (3.14)) is parabolic. This has the consequence that a boundary condition for the parabolic problem has to be prescribed at the entrance into the heated section at $x = 0$ (see Fig. 3.1). This shows clearly, that for parabolic problems no information can be transferred upstream of the heated zone into the unheated zone ($x < 0$). As stated above, this is a good approximation, if the Peclet number is large ($Pe_D > 100$) and thus axial heat conduction effects in the fluid can be neglected. However, for several technical applications the Peclet number is small, so that the axial heat conduction within the fluid has to be taken into account. A typical situation for this case is a compact heat exchanger using liquid metals as working fluid. For liquid metals, the Prandtl number is very low ($0.001 < Pr < 0.1$) and therefore the Peclet number may attain very small values. In addition to the above mentioned example, there exist other types of applications, where one has to include the effect of axial heat conduction within the fluid, even for larger Peclet numbers. These are applications where the heating section is restricted in length as, for example, in cooling systems for electronic components or in chemical process lines.

The present chapter concentrates on the analytical treatment of such problems. Because of their similarity to the Graetz problems considered in the previous chapters, the problems under consideration are often denoted as "extended Graetz problems". However, the mathematical treatment of these problems is much more complicated than the one for the parabolic problems as discussed later in more detail. In the following section, a short literature overview is given in order to show the work which has been done in the past on this subject. Many investigations have been carried out which deal with the solution of the extended Graetz problem for thermally developing laminar flow in a pipe or in a parallel plate channel. Good literature reviews on this subject are given by Shah and London (1978) and by Reed (1987).

Many of the solutions for the extended Graetz problem, provided in the above review articles, are based on the fundamental assumption that the solution of the problem has the same functional form as in the Graetz problem without axial heat conduction. This approach results in a non self-adjoint eigenvalue problem with eigenvalues that could, at least in principle, be complex and eigenvectors that could be incomplete. Several strategies have been developed in the past to overcome this problem. Hsu (1971b) constructed the solution of the problem from two independent series solutions for $x < 0$ and $x > 0$. Both, the temperature distribution and the temperature gradient were then matched at $x = 0$ by constructing a pair of orthonormal functions from the non orthogonal eigenfunctions by using the Gram-Schmidt orthonormalization procedure (see e.g. Broman 1970 for an explanation of the method). Hence this method is clearly plagued with the uncertainties arising from an expansion in terms of eigenfunctions belonging to a non self-adjoint operator (in order to obtain a solution by the Gram-Schmidt orthonormalization procedure a coupled system of equations has to be solved). Despite these disadvantages, the technique of deriving the solution from two independent solutions for the different regions ($x < 0$, $x > 0$) and matching the resulting expressions for $x = 0$ has been used by several authors in the past. The reader is referred to the work of Hsu (1970), Bayazitoglu and Özisik (1980), Vick et al. (1980) and Vick and Özisik (1981). Jones (1971) used a Laplace transform technique for the elliptic energy equation for laminar pipe flow. A completely different approach was presented by Papoutsakis et al. (1980a, b). They showed that it is possible to derive an entirely analytical solution to the extended Graetz problem for constant wall temperature and constant wall heat flux boundary conditions for laminar pipe flow. Their solution is based on a self-adjoint formalism resulting from a decomposition of the convective diffusion equation into a pair of first order partial differential equations. The method is based on the work of Ramkrishna and Amundson (1979a, b).

Later, an alternative approach for obtaining an analytical solution of the extended Graetz problem was presented by Ebadian and Zhang (1989). They used a Fourier transform of the temperature field and expanded the coefficients of the transformed temperature in terms of the Peclet number. This approach resulted in a set of ordinary differential equations, which have to be solved successively.

In addition, several investigations have been carried out in the past concerning the extended Graetz problem in a parallel plate channel. Deavours (1974) presented an analytical solution for the extended Graetz problem by decomposing the eigenvalue problem for the parallel plate channel into a system of ordinary differential equations for which he proved the orthogonality of the eigenfunctions. Weigand et al. (1993) investigated liquid solidification in a parallel plate channel subjected to laminar internal flow. They applied a regular perturbation expansion to the energy equation. The zero order problem was formally identical to the extended Graetz problem in a parallel plate channel. For the solution of the zero order problem they followed the method of Papoutsakis et al. (1980a) and obtained an analytical solution.

Because of the difficulties involved in solving analytically the extended Graetz problem, researchers focused very early on the usage of numerical solution methods. Hennecke (1968) calculated numerically, by using a finite difference method, the distribution of the temperature and the Nusselt number for laminar pipe flow. Results are obtained for the two different wall boundary conditions: a constant wall temperature and a constant wall heat flux. Hennecke showed that the axial heat conduction effect is more pronounced for the constant wall temperature situation. In addition, he was able to show that the influence of axial heat conduction on the temperature field and the distribution of the Nusselt number can be ignored for $Pe_D > 100$. These results are in good agreement with the investigation of Acrivos (1980), who showed analytically that the region of influence for axial heat conduction, scaled by the pipe radius, is of the order of $Pe_D^{-1}$. Nguyen (1992) and Bilir (1992) investigated numerically the heat transfer for thermally developing flow in a circular pipe and in a planar channel. Nguyen (1992) derived from his computational results accurate engineering correlations for the Peclet number effect on the local Nusselt number in the thermal entry region.

Although axial heat conduction can be ignored for turbulent convection in ordinary fluids and gases, with liquid metals this may not always be justified. In fact, due to the very low Prandtl numbers for liquid metals, the Peclet number can be smaller than five in turbulent duct flows. Reviews on the convective heat transfer in liquid metals can be found in Reed (1987), Stein (1966) and Kays et al. (2004). Lee (1982) studied the extended Graetz problem in turbulent pipe flow. He found that for Peclet numbers smaller than 100 axial heat conduction in the fluid becomes important in the thermal entrance region. He investigated a pipe which was insulated for $x \leq 0$ and had a uniform wall temperature for $x > 0$. Lee (1982) used the method of Hsu (1971b) to obtain a series solution for the problem. In this work, the variation of the Nusselt number for fully-developed flow was shown for several Peclet and Prandtl numbers. In addition, the error in Nusselt number resulting from neglecting the axial heat conduction effect was presented. This error was found to be as high as 40 % for a Peclet number of 5.

For the case of turbulent flow inside a parallel plate channel, the effect of axial heat conduction within the fluid was studied by Faggiani and Gori (1980). They solved numerically the energy equation for a constant heat flux boundary condition. Weigand (1996) extended the method of Papoutsakis et al. (1980a) to solve the extended Graetz problem for turbulent flow in a pipe and in a planar channel. Like the solution given by Papoutsakis et al. (1980a) for laminar internal flow, the solution by Weigand (1996) has not been plagued by the uncertainties arising from expansion in terms of eigenfunctions, which belong to a non self-adjoint eigenvalue system. Later, Weigand et al. (1997) adopted this approach to the Graetz problem in a concentric annulus and obtained analytical solutions for laminar and turbulent flow for constant wall temperature boundary conditions. Weigand and Wrona (2003) extended the method for heat transfer in concentric annuli with piecewise constant wall heat flux, whereas in Weigand and Eisenschmidt (2012) the method

was used for the prediction of the heat transfer for laminar and turbulent flows through a concentric annulus with piecewise constant wall temperatures.

Nearly all studies mentioned here considered only a heating section semi-infinite in size. Hennecke (1968) was one of the few who calculated numerically the temperature distribution at the end of the heating section for laminar internal flow. However, he investigated this problem only for a very large heating section. The problem was solved later analytically by Papoutsakis et al. (1980b) for laminar pipe flow and a heating zone of finite length. They derived expressions for the Nusselt number and the bulk-temperature, but did not show, however, any distributions for these quantities. Only temperature profiles in the fluid were shown. Weigand et al. (2001) calculated the effect of a changing length of the heating zone for laminar and turbulent internal flow and for different Peclet numbers. One of the main results of their study was that, for finite heated sections, the axial heat conduction effect depends also on the length of the heated zone. Axial heat conduction may, therefore, be important also for Peclet numbers larger than 100 if this zone is short. This observation was supported by the works of Weigand and Lauffer (2004) and Weigand and Eisenschmidt (2012) for the case of piecewise constant wall temperatures in a pipe, parallel channel and in a concentric annulus.

The effect of wall conduction for the extended Graetz problem for laminar and turbulent channel flow has been investigated by Weigand and Gassner (2007). The effect of axial heat conduction was found to be important for this conjugated problem for small values of the Peclet number, thin walls and short heating sections.

The present chapter shows an analytical solution method for the extended Graetz problem. The method is based on the approach by Papoutsakis (1980a, b) and can be used for a lot of related problems. First, the method is explained for a duct with a semi-infinite heating section (with constant wall temperature or constant wall heat flux) to highlight the basic ideas behind the solution approach. Later applications of the method to piecewise heated ducts are explained. The goal of this chapter is to show that the derived final solutions for the extended Graetz problem are as simple as the ones for the parabolic problems discussed in Chap. 3.

## 5.1  Heat Transfer for Constant Wall Temperatures for x ≤ 0 and x > 0

We start our considerations for a hydrodynamically fully developed flow with a low Peclet number and constant wall temperature. As for the analysis in Chap. 3, it is assumed that the velocity profile is hydrodynamically fully developed. This means that the vertical velocity component $v$ is zero and the axial velocity component is only a function of the coordinate orthogonal to the main flow direction. The geometry under consideration and the used coordinate system are shown in Fig. 5.1.
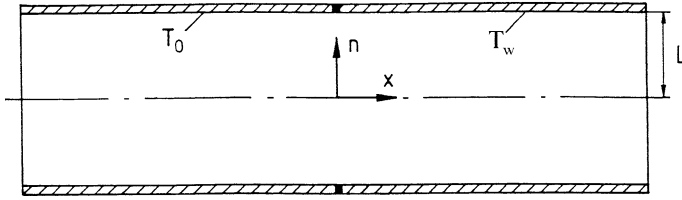
**Fig. 5.1** Geometry and coordinate system (Weigand 1996)

If we assume constant fluid properties, the energy equation is given by Eqs. (3.5) and (3.6)

***Pipe***

$$\rho c_p u(r) \frac{\partial T}{\partial x} = \frac{1}{r} \frac{\partial}{\partial r} \left[ r \left( k \frac{\partial T}{\partial r} - \rho c_p \overline{v'T'} \right) \right] + \frac{\partial}{\partial x} \left[ k \frac{\partial T}{\partial x} - \rho c_p \overline{u'T'} \right] \qquad (3.5)$$

***Planar Channel***

$$\rho c_p u(y) \frac{\partial T}{\partial x} = \frac{\partial}{\partial y} \left[ k \frac{\partial T}{\partial y} - \rho c_p \overline{v'T'} \right] + \frac{\partial}{\partial x} \left[ k \frac{\partial T}{\partial x} - \rho c_p \overline{u'T'} \right] \qquad (3.6)$$

If one analyses Eq. (3.5) or Eq. (3.6) for laminar flow ($\overline{u'T'} = 0$, $\overline{v'T'} = 0$), one finds immediately that the equations are elliptic in nature. This is due to the axial heat conduction effect within the flow, which is represented by the second term on the right hand side of the equations. For turbulent flow, the nature of the equation will also depend on the turbulent heat fluxes. The turbulent heat fluxes $-\rho c_p \overline{v'T'}$ and $-\rho c_p \overline{u'T'}$ have to be modelled. This can be done for example by using a simple eddy viscosity model[1]:

$$-\overline{v'T'} = \varepsilon_{hy} \frac{\partial T}{\partial y} \text{ (planar channel)}, \quad -\overline{v'T'} = \varepsilon_{hr} \frac{\partial T}{\partial r} \text{ (pipe)} \qquad (3.7)$$

$$-\overline{u'T'} = \varepsilon_{hx} \frac{\partial T}{\partial x} \text{ (planar channel and pipe)} \qquad (3.8)$$

---

[1]More advanced models can also be used, which assume the stream-wise component of the turbulent heat flux to be also a function of the cross-stream temperature gradient and vice versa (see Batchelor 1949, So and Sommer 1996 and Younis et al. 2005). Weigand et al. (2002) conducted a numerical analysis of the energy Eq. (3.6) and found the above mentioned simple model to be in perfect agreement with more complicated models for the range of parameters considered here.

where $\varepsilon_{hy}$, $\varepsilon_{hr}$ and $\varepsilon_{hx}$ are only functions of the coordinate orthogonal to the flow direction because we assume a hydrodynamically fully developed flow. Inserting Eqs. (3.7) and (3.8) into Eqs. (3.5) and (3.6) results in

**Pipe**

$$\rho c_p u(r) \frac{\partial T}{\partial x} = \frac{1}{r} \frac{\partial}{\partial r} \left[ r \left( k + \rho c_p \varepsilon_{hr} \right) \frac{\partial T}{\partial r} \right] + \frac{\partial}{\partial x} \left[ \left( k + \rho c_p \varepsilon_{hx} \right) \frac{\partial T}{\partial x} \right] \qquad (3.9)$$

**Planar Channel**

$$\rho c_p \, u(y) \ \frac{\partial T}{\partial x} = \frac{\partial}{\partial y} \left[ \left( k + \rho c_p \varepsilon_{hy} \right) \frac{\partial T}{\partial y} \right] + \frac{\partial}{\partial x} \left[ \left( k + \rho c_p \varepsilon_{hx} \right) \frac{\partial T}{\partial x} \right] \qquad (3.10)$$

If one replaces in Eqs. (3.9) and (3.10) the heat diffusivities $\varepsilon_{hy}$, $\varepsilon_{hr}$ and $\varepsilon_{hx}$ by a turbulent Prandtl number according to Eq. (3.18), one obtains

**Pipe**

$$\rho c_p u(r) \frac{\partial T}{\partial x} = \frac{1}{r} \frac{\partial}{\partial r} \left[ r \left( k + \rho c_p \frac{\varepsilon_m}{Pr_t} \right) \frac{\partial T}{\partial r} \right] + \frac{\partial}{\partial x} \left[ \left( k + \rho c_p \frac{\varepsilon_m}{Pr_t} \frac{\varepsilon_{hx}}{\varepsilon_{hr}} \right) \frac{\partial T}{\partial x} \right] \qquad (5.1)$$

**Planar Channel**

$$\rho c_p u(y) \frac{\partial T}{\partial x} = \frac{\partial}{\partial y} \left[ \left( k + \rho c_p \frac{\varepsilon_m}{Pr_t} \right) \frac{\partial T}{\partial y} \right] + \frac{\partial}{\partial x} \left[ \left( k + \rho c_p \frac{\varepsilon_m}{Pr_t} \frac{\varepsilon_{hx}}{\varepsilon_{hy}} \right) \frac{\partial T}{\partial x} \right] \qquad (5.2)$$

Equations (5.1) and (5.2) can be combined to one equation if we introduce, like in Chap. 3, a vertical coordinate $n$ which is equal to $y$ for a planar channel and equal to $r$ for pipe flows. This results in

$$\rho c_p u(n) \frac{\partial T}{\partial x} = \frac{1}{r^F} \frac{\partial}{\partial n} \left[ r^F \left( k + \rho c_p \frac{\varepsilon_m}{Pr_t} \right) \frac{\partial T}{\partial n} \right] + \frac{\partial}{\partial x} \left[ \left( k + \rho c_p \frac{\varepsilon_m}{Pr_t} \frac{\varepsilon_{hx}}{\varepsilon_{hn}} \right) \frac{\partial T}{\partial x} \right] \quad (5.3)$$

where the superscript $F$ specifies the geometry and has to be set to zero for a planar channel and equal to one for pipe flow. The boundary conditions for Eq. (5.3) are

$$n = L : T = T_0, x \leq 0 \qquad (5.4)$$
$$T = T_W, x > 0$$
$$n = 0 : \partial T / \partial n = 0$$
$$\lim_{x \to -\infty} T = T_0, \qquad \lim_{x \to +\infty} T = T_W$$

Introducing the following dimensionless quantities into the above equations

$$\Theta = \frac{T - T_W}{T_0 - T_W}, \tilde{r} = \frac{r}{R}, \tilde{x} = \frac{x}{L} \frac{1}{Re_L Pr}, \tilde{n} = \frac{n}{L}, Pr = \frac{\mu c_p}{k}, Re_L = \frac{\bar{u} L}{\nu},$$

$$\tilde{\varepsilon}_m = \frac{\varepsilon_m}{\nu}, \tilde{u} = \frac{u}{\bar{u}}, Pe_L = Re_L Pr \tag{5.5}$$

where the length scale $L = R$ for a pipe flow and $L = h$ for the flow in a planar channel, one obtains

$$\tilde{u}(\tilde{n}) \frac{\partial \Theta}{\partial \tilde{x}} = \frac{1}{Pe_L^2} \frac{\partial}{\partial \tilde{x}} \left[ a_1(\tilde{n}) \frac{\partial \Theta}{\partial \tilde{x}} \right] + \frac{1}{\tilde{r}^F} \frac{\partial}{\partial \tilde{n}} \left[ \tilde{r}^F a_2(\tilde{n}) \frac{\partial \Theta}{\partial \tilde{n}} \right] \tag{5.6}$$

with the boundary conditions

$$\begin{array}{ll} \tilde{n} = 1: & \Theta = 1 \text{ for } \tilde{x} \leq 0, \\ & \Theta = 0 \text{ for } \tilde{x} > 0, \\ \tilde{n} = 0: & \partial \Theta / \partial \tilde{n} = 0, \\ \lim_{\tilde{x} \to -\infty} \Theta = 1, & \lim_{\tilde{x} \to +\infty} \Theta = 0 \end{array} \tag{5.7}$$

The functions $a_1(\tilde{n})$ and $a_2(\tilde{n})$ are given by

$$a_1(\tilde{n}) = 1 + \frac{Pr}{Pr_t} \left( \frac{\varepsilon_{hx}}{\varepsilon_{hn}} \right) \tilde{\varepsilon}_m, \quad a_2(\tilde{n}) = 1 + \frac{Pr}{Pr_t} \tilde{\varepsilon}_m \tag{5.8}$$

Papoutsakis et al. (1980a) showed that it is possible to solve Eq. (5.6) for laminar pipe flow ($a_1 = a_2 = 1$, $F = 1$) by decomposing the elliptic partial differential equation into a pair of first order partial differential equations. The ensuing procedure for solving the extended turbulent Graetz problem, given by Eqs. (5.6) and (5.7), follows the method of Papoutsakis et al. (1980a) for deriving the solution of the more general problem where $a_1$ and $a_2$ are functions of $\tilde{n}$.

In order to obtain a solution for the turbulent Graetz problem, given by Eqs. (5.6) and (5.7), one can proceed in the following way: First, we define a function $E(\tilde{x}, \tilde{n})$ which may be called the axial energy flow through a cross-sectional area of height $\tilde{n}$. This function is given by

$$E = \int_0^{\tilde{n}} \left[ \tilde{u} \Theta - \frac{1}{Pe_L^2} a_1(\bar{n}) \frac{\partial \Theta}{\partial \tilde{x}} \right] \tilde{r}^F d\bar{n} \tag{5.9}$$

If one introduces the axial energy flow according to Eq. (5.9) into the energy equation (5.6), one obtains the following system of first order partial differential equations

$$\frac{\partial}{\partial \tilde{x}} \vec{S}(\tilde{x}, \tilde{n}) = \underset{\sim}{L} \vec{S}(\tilde{x}, \tilde{n}) \tag{5.10}$$

where the solution vector $\vec{S}$ and the matrix operator $\underset{\sim}{L}$ are defined by

$$\vec{S} = \begin{bmatrix} \Theta(\tilde{x}, \tilde{n}) \\ E(\tilde{x}, \tilde{n}) \end{bmatrix}, \quad \underset{\sim}{L} = \begin{bmatrix} \dfrac{Pe_L^2 \tilde{u}(\tilde{n})}{a_1(\tilde{n})} & -\dfrac{Pe_L^2}{\tilde{r}^F a_1(\tilde{n})} \dfrac{\partial}{\partial \tilde{n}} \\ \tilde{r}^F a_2(\tilde{n}) \dfrac{\partial}{\partial \tilde{n}} & 0 \end{bmatrix} \tag{5.11}$$

The boundary conditions for the function $E$ can be obtained directly from its definition, Eq. (5.9), by using Eq. (5.7). This results in

$$\lim_{\tilde{x} \to -\infty} E = \int_0^{\tilde{n}} \tilde{u} \tilde{r}^F d\bar{n}, \quad \lim_{\tilde{x} \to +\infty} E = 0 \quad \tilde{n} = 0 : E = 0 \tag{5.12}$$

Before solving Eq. (5.10), some interesting features of the operator $\underset{\sim}{L}$ and the corresponding eigenvalue problem for this equation should be presented. The most remarkable aspect of $\underset{\sim}{L}$ is that it gives rise to a self-adjoint problem even though the original convective diffusion operator is non self-adjoint. This fact is of course dependent on the sort of inner product between two vectors, which will be used. This means that we have to find an inner product which is symmetric. Papoutsakis et al. (1980a) obtained such an inner product for a laminar pipe flow. It is now possible to extend this work for laminar and turbulent duct flows. Let us define the following inner product for two vectors

$$\vec{\Phi} = \begin{bmatrix} \Phi_1(\tilde{n}) \\ \Phi_2(\tilde{n}) \end{bmatrix}, \quad \vec{\Upsilon} = \begin{bmatrix} \Upsilon_1(\tilde{n}) \\ \Upsilon_2(\tilde{n}) \end{bmatrix} \tag{5.13}$$

by

$$\left\langle \vec{\Phi}, \vec{\Upsilon} \right\rangle = \int_0^1 \left[ \frac{a_1(\tilde{n}) \tilde{r}^F}{Pe_L^2} \Phi_1(\tilde{n}) \Upsilon_1(\tilde{n}) + \frac{1}{a_2(\tilde{n}) \tilde{r}^F} \Phi_2(\tilde{n}) \Upsilon_2(\tilde{n}) \right] d\tilde{n} \tag{5.14}$$

The inner product of the two vectors $\vec{\Phi}$, $\vec{\Upsilon}$ incorporates the two functions $a_1$, $a_2$ which contain the heat diffusivity for a turbulent flow. In case of a laminar pipe flow, the two functions will be equal to one. $\underset{\sim}{L}$ belongs to the following domain

$$D(\underset{\sim}{L}) = \left\{ \vec{\Phi} \in H : \underset{\sim}{L}\vec{\Phi} \text{ (exists and)} \in H, \Phi_1(1) = \Phi_2(0) = 0 \right\} \qquad (5.15)$$

Then it can be shown that the matrix operator $\underset{\sim}{L}$ is a symmetric operator in the Hilbert space $H$. This means that

$$\left\langle \vec{\Phi}, \underset{\sim}{L}\vec{\Upsilon} \right\rangle = \left\langle \underset{\sim}{L}\vec{\Phi}, \vec{\Upsilon} \right\rangle \qquad (5.16)$$

Equation (5.16) can be proven by inserting the expressions $\underset{\sim}{L}\vec{\Phi}$ and $\underset{\sim}{L}\vec{\Upsilon}$ into the definition of the inner product according to Eq. (5.14). This results in

$$\left\langle \vec{\Phi}, \underset{\sim}{L}\vec{\Upsilon} \right\rangle = \int\limits_0^1 \left[ \tilde{u}\tilde{r}^F \Phi_1(\tilde{n}) \Upsilon_1(\tilde{n}) - \Phi_1(\tilde{n}) \Upsilon_2'(\tilde{n}) + \Phi_2(\tilde{n}) \Upsilon_1'(\tilde{n}) \right] d\tilde{n} \qquad (5.17)$$

$$\left\langle \underset{\sim}{L}\vec{\Phi}, \vec{\Upsilon} \right\rangle = \int\limits_0^1 \left[ \tilde{u}\tilde{r}^F \Phi_1(\tilde{n}) \Upsilon_1(\tilde{n}) - \Phi_2'(\tilde{n}) \Upsilon_1(\tilde{n}) + \Phi_1'(\tilde{n}) \Upsilon_2(\tilde{n}) \right] d\tilde{n} \qquad (5.18)$$

Subtracting Eq. (5.18) from Eq. (5.17) results after integration in

$$\left\langle \vec{\Phi}, \underset{\sim}{L}\vec{\Upsilon} \right\rangle - \left\langle \underset{\sim}{L}\vec{\Phi}, \vec{\Upsilon} \right\rangle = \Phi_2(1)\Upsilon_1(1) - \Phi_2(0)\Upsilon_1(0) \qquad (5.19)$$
$$- \Phi_1(1)\Upsilon_2(1) + \Phi_1(0)\Upsilon_2(0)$$

The resulting expression on the right hand side of Eq. (5.19) is zero, if the vectors $\vec{\Phi}$ and $\vec{\Upsilon}$ satisfy the conditions given in Eq. (5.15).

The associated eigenvalue problem to Eq. (5.10) is given by

$$\underset{\sim}{L}\vec{\Phi}_j = \lambda_j \vec{\Phi}_j \qquad (5.20)$$

In this equation $\vec{\Phi}_j$ denotes the eigenfunction corresponding to the eigenvalue $\lambda_j$. If we introduce the definition of the matrix operator $\underset{\sim}{L}$ into this equation, the following eigenvalue problem is obtained

$$\text{Pe}_L^2 \left[ \frac{\tilde{u}}{a_1(\tilde{n})} \Phi_{j1} - \frac{1}{\tilde{r}^F a_1(\tilde{n})} \Phi_{j2}' \right] = \lambda_j \Phi_{j1} \qquad (5.21)$$

$$\tilde{r}^F a_2(\tilde{n}) \, \Phi'_{j1} = \lambda_j \, \Phi_{j2} \tag{5.22}$$

From the above system of ordinary differential equations, one differential equation for the first component of the eigenvector $\Phi_{j1}$ can be easily obtained by eliminating $\Phi_{j2}$. This results in

$$\left[\tilde{r}^F a_2(\tilde{n})\Phi'_{j1}\right]' + \tilde{r}^F \left[\frac{\lambda_j a_1(\tilde{n})}{\mathrm{Pe}_L^2} - \tilde{u}\right] \lambda_j \, \Phi_{j1} = 0 \tag{5.23}$$

Equation (5.23) has to be solved together with the homogenous boundary conditions

$$\Phi'_{j1}(0) = 0, \quad \Phi_{j1}(1) = 0 \tag{5.24}$$

Usually Eq. (5.23) can easily be solved numerically with the procedure described in Appendix C. The method used here is a "shooting method", where the differential Eq. (5.23) is integrated from the centreline of the duct ($\tilde{n} = 0$) to the wall and then the boundary condition at the wall $\Phi_{j1}(1) = 0$ is checked for an assumed value of $\lambda_j$. Therefore, an additional condition for $\tilde{n} = 0$ is required. A possible condition is that

$$\Phi_{j1}(0) = 1 \tag{5.25}$$

This condition is a normalizing condition for the eigenfunctions $\Phi_{j1}$. Equation (5.23) shows clearly that the eigenvalues appear as $\lambda_j$ and $\lambda_j^2$ in the equation. This is different to the normal Graetz problem (see Eq. (3.25)). For the eigenvalue problem according to Eq. (5.20) it is possible to show that it is self-adjoint and semi-definite (see e.g. Sauer and Szabo 1969). Therefore, all eigenvalues of Eq. (5.23) have to be real. The real eigenvalues and the associated eigenfunctions of Eq. (5.23) define a complete set of orthogonal functions (see Appendix D). With the help of these eigenfunctions any function can be reconstructed. Because the matrix operator $\underset{\sim}{L}$ is neither positive nor negative definite, one will find both positive and negative eigenvalues $\left(\lambda_j^+, \lambda_j^-\right)$. The eigenfunctions belonging to these eigenvalues, $\left(\Phi_j^+, \Phi_j^-\right)$, form an orthogonal basis in the Hilbert space $H$. It is interesting to note that Eq. (5.23) reduces to the eigenvalue problem for the parabolic case, Eq. (3.25), if the Peclet number tends to infinity. Because the two sets of eigenvectors, normalized according to equation (5.25), constitute an orthogonal basis in $H$, an arbitrary vector $\vec{f}$ can be expanded in terms of eigenfunctions in the following way

$$\vec{f} = \sum_{j=0}^{\infty} D_j \vec{\Phi}_j(\tilde{n}) \tag{5.26}$$

The constants $D_j$ in this equation can be calculated if we apply to both sides of Eq. (5.26) the inner product according to Eq. (5.14). This results in

$$\left\langle \vec{f}, \vec{\Phi}_i \right\rangle = \sum_{j=0}^{\infty} D_j \left\langle \vec{\Phi}_j, \vec{\Phi}_i \right\rangle \tag{5.27}$$

Because the expression $\left\langle \vec{\Phi}_j, \vec{\Phi}_i \right\rangle$ is equal to zero for $i \neq j$ (see Appendix D), Eq. (5.27) can be resolved for the constants $D_j$ and one obtains

$$D_j = \frac{\left\langle \vec{f}, \vec{\Phi}_j \right\rangle}{\left\langle \vec{\Phi}_j, \vec{\Phi}_j \right\rangle} = \frac{\left\langle \vec{f}, \vec{\Phi}_j \right\rangle}{\left\| \vec{\Phi}_j \right\|^2} \tag{5.28}$$

where the vector norm $\left\| \vec{\Phi}_j \right\|^2$ has been introduced into Eq. (5.28). Inserting Eq. (5.28) into Eq. (5.27) results in the following expression for the expansion of an arbitrary vector $\vec{f}$ in terms of eigenfunctions

$$\vec{f} = \sum_{j=0}^{\infty} \frac{\left\langle \vec{f}, \vec{\Phi}_j \right\rangle}{\left\| \vec{\Phi}_j \right\|^2} \vec{\Phi}_j(\tilde{n}) \tag{5.29}$$

If we explicitly distinguish in Eq. (5.29) between positive and negative eigenvectors, the equation takes the following form

$$\vec{f} = \sum_{j=0}^{\infty} \frac{\left\langle \vec{f}, \vec{\Phi}_j^+ \right\rangle}{\left\| \vec{\Phi}_j^+ \right\|^2} \vec{\Phi}_j^+(\tilde{n}) + \sum_{j=0}^{\infty} \frac{\left\langle \vec{f}, \vec{\Phi}_j^- \right\rangle}{\left\| \vec{\Phi}_j^- \right\|^2} \vec{\Phi}_j^-(\tilde{n}) \tag{5.30}$$

After the expansion of an arbitrary vector in terms of eigenfunctions has been developed, we can return to the solution of the system of partial differential equations given by Eq. (5.10). Because of the non-homogeneous boundary condition for the temperature, the vector $\vec{S}$ does not belong to the domain $D\left(\underset{\sim}{L}\right)$ given by Eq. (5.15). However, it can be shown that

$$\left\langle \underset{\sim}{L} \vec{S}, \vec{\Phi}_j \right\rangle = \left\langle \vec{S}, \underset{\sim}{L} \vec{\Phi}_j \right\rangle + \Phi_{j2}(1)g(\tilde{x}) \tag{5.31}$$

holds (see Appendix D). The function $g(\tilde{x})$ is for the case of a semi-infinite heating zone given by

$$g(\tilde{x}) = \begin{cases} 1, & \tilde{x} \leq 0 \\ 0, & \tilde{x} > 0 \end{cases} \tag{5.32}$$

If we apply the inner product, given by Eq. (5.14), to the system of partial differential equations, Eq. (5.10), one obtains

$$\frac{\partial}{\partial \tilde{x}}\left\langle \vec{S}, \vec{\Phi}_j\right\rangle = \left\langle \underset{\sim}{L}\vec{S}, \vec{\Phi}_j\right\rangle \tag{5.33}$$

Inserting Eq. (5.31) into Eq. (5.33) (and taking Eq. (5.20) into account) results in

$$\frac{\partial}{\partial \tilde{x}}\left\langle \vec{S}, \vec{\Phi}_j\right\rangle = \lambda_j\left\langle \vec{S}, \vec{\Phi}_j\right\rangle + g(\tilde{x})\, \Phi_{j2}(1) \tag{5.34}$$

Equation (5.34) represents an ordinary differential equation for the expression $\left\langle \vec{S}, \vec{\Phi}_j\right\rangle$. For the homogenous equation one obtains the solution

$$\left\langle \vec{S}, \vec{\Phi}_j\right\rangle = C_{0j}\exp(\lambda_j \tilde{x}) \tag{5.35}$$

A particular solution of Eq. (5.34) can been found by using the method of the variation of constants (see e.g. Bronstein and Semendjajew 1983). One obtains after splitting the solution into positive and negative eigenvalues

$$\left\langle \vec{S}, \vec{\Phi}_j^-\right\rangle = C_{0j}^-\exp(\lambda_j^- \tilde{x}) + \int_{-\infty}^{\tilde{x}} (g(\bar{x})\Phi_{j2}^-(1))\exp(\lambda_j^-(\tilde{x}-\bar{x}))d\bar{x} \tag{5.36}$$

$$\left\langle \vec{S}, \vec{\Phi}_j^+\right\rangle = C_{0j}^+\exp(\lambda_j^+ \tilde{x}) - \int_{\tilde{x}}^{\infty} (g(\bar{x})\Phi_{j2}^+(1))\exp(\lambda_j^+(\tilde{x}-\bar{x}))d\bar{x} \tag{5.37}$$

Because the solution must be bounded for $\tilde{x} \to +\infty$ and for $\tilde{x} \to -\infty$, the two constants $C_{0j}^-$ and $C_{0j}^+$, appearing in Eqs. (5.36) and (5.37), have to be zero. The integrals in Eqs. (5.36) and (5.37) can be evaluated by inserting the function $g(\tilde{x})$ into these equations. One obtains

$$\tilde{x} \le 0 : \left\langle \vec{S}, \vec{\Phi}_j\right\rangle = \frac{\Phi_{j2}^+(1)}{\lambda_j^+}\exp\left(\lambda_j^+ \tilde{x}\right) - \frac{\Phi_{j2}^+(1)}{\lambda_j^+} - \frac{\Phi_{j2}^-(1)}{\lambda_j^-} \tag{5.38}$$

$$\tilde{x} > 0 : \left\langle \vec{S}, \vec{\Phi}_j\right\rangle = \frac{\Phi_{j2}^-(1)}{\lambda_j^-}\exp\left(\lambda_j^- \tilde{x}\right) \tag{5.39}$$

Introducing these expressions into the expansion for the function $\vec{S}$, Eq. (5.29), and taking the first vector component of $\vec{S}$, the following result is obtained for the temperature distribution in the fluid

$$\tilde{x} \le 0 : \Theta(\tilde{x}, \tilde{n}) = -\sum_{j=0}^{\infty} \frac{\Phi_{j2}^-(1)\Phi_{j1}^-(\tilde{n})}{\lambda_j^- \left\| \vec{\Phi}_j^- \right\|^2} - \sum_{j=0}^{\infty} \frac{\Phi_{j2}^+(1)\Phi_{j1}^+(\tilde{n})}{\lambda_j^+ \left\| \vec{\Phi}_j^+ \right\|^2} \tag{5.40}$$

$$+ \sum_{j=0}^{\infty} \frac{\Phi_{j2}^+(1)\Phi_{j1}^+(\tilde{n})}{\lambda_j^+ \left\| \vec{\Phi}_j^+ \right\|^2} \exp(\lambda_j^+ \tilde{x})$$

$$\tilde{x} > 0 : \Theta(\tilde{x}, \tilde{n}) = -\sum_{j=0}^{\infty} \frac{\Phi_{j2}^-(1)\Phi_{j1}^-(\tilde{n})}{\lambda_j^- \left\| \vec{\Phi}_j^- \right\|^2} \exp(\lambda_j^- \tilde{x}) \tag{5.41}$$

From Eqs. (5.40) and (5.41) it can be seen that the solution for $\tilde{x} \le 0$ contains both, negative and positive eigenfunctions, whereas for $\tilde{x} > 0$ only negative eigenfunctions are needed for the solution of the problem. For Eq. (5.40), it is possible to show that

$$-\sum_{j=0}^{\infty} \frac{\Phi_{j2}^-(1)\Phi_{j1}^-(\tilde{n})}{\lambda_j^- \left\| \vec{\Phi}_j^- \right\|^2} - \sum_{j=0}^{\infty} \frac{\Phi_{j2}^+(1)\Phi_{j1}^+(\tilde{n})}{\lambda_j^+ \left\| \vec{\Phi}_j^+ \right\|^2} = 1 \tag{5.42}$$

This can be shown by expanding the vector $(1,0)^{\mathrm{T}}$ into a series according to Eq. (5.29) (see Appendix D for a derivation of this result). Introducing this result into Eq. (5.40) leads to

$$\tilde{x} \le 0 : \Theta(\tilde{x}, \tilde{n}) = 1 + \sum_{j=0}^{\infty} \frac{\Phi_{j2}^+(1)\,\Phi_{j1}^+(\tilde{n})}{\lambda_j^+ \left\| \vec{\Phi}_j^+ \right\|^2} \exp(\lambda_j^+ \tilde{x}) \tag{5.43}$$

From Eqs. (5.41) and (5.43) one can see that they result in a continuous temperature distribution for $x = 0$. In addition, one notices from Eqs. (5.41) and (5.43) that these equations satisfy all boundary conditions given by Eq. (5.7).

If the Peclet number increases, the eigenvalues $\lambda_j^+$ tend to infinity and Eq. (5.43) (the temperature distribution for $\tilde{x} \le 0$) results in

$$\Theta(\tilde{x}, \tilde{n}) = 1, \quad \text{for Pe}_L \to \infty \tag{5.44}$$

which represents the solution for the parabolic case. Equation (5.44) also elucidates, that it is only correct to prescribe a temperature boundary condition for $\tilde{x} = 0$ for the limiting case of $\text{Pe}_L \to \infty$.

The vector norm $\left\| \vec{\Phi}_j \right\|^2$, which has been used in the above given solution for the temperature field, can be rewritten by using the Eqs. (5.21) and (5.22). One obtains (see Appendix D)

$$\left\| \vec{\Phi}_j \right\|^2 = -\frac{1}{\lambda_j} \int_0^1 \tilde{r}^F \tilde{u} \Phi_{j1}^2 d\tilde{n} + \frac{2}{\text{Pe}_L^2} \int_0^1 \tilde{r}^F a_1(\tilde{n}) \Phi_{j1}^2 d\tilde{n} \tag{5.45}$$

Equation (5.45) shows an interesting result: the second term in this equation depends on the Peclet number and tends to zero for increasing values of $Pe_L$. This means that, for large Peclet numbers, the second term in Eq. (5.45) can be neglected and therefore, the temperature distribution, given by Eq. (5.41), is formally identical to the distribution for the parabolic problem. In addition, it can be shown from the eigenvalue problem, Eq. (5.23), that this equation reduces to the one for the parabolic problem for $Pe_L \to \infty$. This shows nicely that the results presented here approach those given in Chap. 3 for large Peclet numbers. Furthermore, it can be shown that

$$\left\|\vec{\Phi}_j\right\|^2 = \Phi_{j2}(1)\frac{d\Phi_{j1}(1)}{d\lambda}\bigg|_{\lambda_j} \tag{5.46}$$

(see Appendix D). If one introduces the abbreviation

$$A_j = \left(\lambda_j \frac{d\Phi_{j1}(1)}{d\lambda}\bigg|_{\lambda=\lambda_j}\right)^{-1} \tag{5.47}$$

into the equations above, one finally obtains for the temperature field in the flow

$$\tilde{x} \le 0 : \Theta(\tilde{x},\tilde{n}) = 1 + \sum_{j=0}^{\infty} A_j^+ \Phi_{j1}^+(\tilde{n}) \exp(\lambda_j^+ \tilde{x}) \tag{5.48}$$

$$\tilde{x} > 0 : \Theta(\tilde{x},\tilde{n}) = \sum_{j=0}^{\infty} A_j^- \Phi_{j1}^-(\tilde{n}) \exp(\lambda_j^- \tilde{x}) \tag{5.49}$$

After the temperature field in the fluid is known, the bulk-temperature and the Nusselt number can be calculated. Introducing Eqs. (5.48) and (5.49) into the definition of the bulk-temperature, Eq. (3.67), and the Nusselt number, Eq. (3.66), results in

$$\tilde{x} \le 0 : \Theta_b = 1 + 2^F \sum_{j=0}^{\infty} A_j^+ \left\{ \frac{\Phi_{j1}^{\prime +}(1)}{\lambda_j^+} + \frac{\lambda_j^+}{Pe_L^2} \int_0^1 a_1(\tilde{n})\Phi_{j1}^+(\tilde{n})\tilde{r}^F d\tilde{n} \right\} \exp(\lambda_j^+ \tilde{x}) \tag{5.50}$$

$$\tilde{x} > 0 : \Theta_b = 1 + 2^F \sum_{j=0}^{\infty} A_j^- \left\{ \frac{\Phi_{j1}^{\prime -}(1)}{\lambda_j^-} + \frac{\lambda_j^-}{Pe_L^2} \int_0^1 a_1(\tilde{n})\Phi_{j1}^-(\tilde{n})\tilde{r}^F d\tilde{n} \right\} \exp(\lambda_j^- \tilde{x}) \tag{5.51}$$

$$\tilde{x} \leq 0 : \text{Nu}_D = \frac{-4 \sum_{j=0}^{\infty} A_j^+ \Phi_{j1}'^+(1) \exp(\lambda_j^+ \tilde{x})}{4^F \sum_{j=0}^{\infty} A_j^+ \left\{ \frac{\Phi_{j1}'^+(1)}{\lambda_j^+} + \frac{\lambda_j^+}{\text{Pe}_L^2} \int_0^1 a_1(\tilde{n}) \Phi_{j1}^+(\tilde{n}) \tilde{r}^F d\tilde{n} \right\} \exp(\lambda_j^+ \tilde{x})} \tag{5.52}$$

$$\tilde{x} > 0 : \text{Nu}_D = \frac{-4 \sum_{j=1}^{\infty} A_j^- \Phi_{j1}'^-(1) \exp(\lambda_j^- \tilde{x})}{4^F \sum_{j=1}^{\infty} A_j^+ \left\{ \frac{\Phi_{j1}'^-(1)}{\lambda_j^-} + \frac{\lambda_j^-}{\text{Pe}_L^2} \int_0^1 a_1(\tilde{n}) \Phi_{j1}^-(\tilde{n}) \tilde{r}^F d\tilde{n} \right\} \exp(\lambda_j^- \tilde{x})} \tag{5.53}$$

where $F = 0$ denotes the heat transfer in a parallel plate channel, whereas $F = 1$ denotes the heat transfer in a pipe. From Eqs. (5.52) and (5.53) the Nusselt number for the fully developed flow can be obtained. Investigating the limiting case $\tilde{x} \to \infty$ in Eq. (5.53), only the first term of the sum needs to be retained and one obtains

$$\text{Nu}_\infty^- = \frac{4}{4^F} |\lambda_0^-| / \left\{ 1 + \frac{\lambda_0^{-2}}{\Phi_{01}'^-(1) Pe_L^2} \int_0^1 a_1(\tilde{n}) \Phi_{01}^-(\tilde{n}) \tilde{r}^F d\tilde{n} \right\} \tag{5.54}$$

This equation shows again, that for $\text{Pe}_L \to \infty$ the Nusselt number for the fully developed flow is given by an expression similar to Eq. (3.70). For finite values of the Peclet number, this value is changed by the second term in the denominator of Eq. (5.54).

### 5.1.1 Heat Transfer in Laminar Pipe and Channel Flows for Small Peclet Numbers

For laminar flow the functions $a_1$ and $a_2$ are equal to one. In addition, the velocity distribution is given by a simple parabolic expression, according to Eqs. (3.1) and (3.2). As it has been stated before, the eigenvalues and eigenfunctions of Eq. (5.23) have to be calculated numerically. This can be done with the method described in Appendix C.

#### Laminar Pipe Flow

In order to investigate this case, the flow index $F$ in all equations has to be set to 1. This case has been investigated with the method of Papoutsakis et al. (1980a). Table 5.1 shows the first fifteen eigenvalues and constants for two different Peclet numbers. It can be seen that the positive eigenvalues strongly increase with growing values of the Peclet number. For example, the first positive eigenvalue ($\lambda_0^+$) increases by about a factor of three by increasing the Peclet number from 5 to 10. Since larger eigenvalues result, according to Eq. (5.48), in a faster decrease of the influence of axial heat conduction, this elucidates how this effect diminishes with

**Table 5.1**  Eigenvalues and constants for laminar pipe flow for $Pe_D = 5$ and $Pe_D = 10$

| $j$ | $Pe_D = 5$ | | $Pe_D = 10$ | |
|---|---|---|---|---|
|  | $\lambda_j^+$ | $A_j^+$ | $\lambda_j^+$ | $A_j^+$ |
| 0 | 12.289076 | −0.342609 | 37.383579 | −0.107926 |
| 1 | 18.929129 | 0.412438 | 51.950323 | 0.232838 |
| 2 | 26.360733 | −0.374175 | 64.468355 | −0.303513 |
| 3 | 34.041020 | 0.334422 | 78.791847 | 0.296627 |
| 4 | 41.799450 | −0.303680 | 93.763713 | −0.279034 |
| 5 | 49.593035 | 0.279668 | 109.009770 | 0.262030 |
| 6 | 57.405409 | −0.260405 | 124.400395 | −0.247011 |
| 7 | 65.229022 | 0.244561 | 139.876976 | 0.233958 |
| 8 | 73.059822 | −0.231254 | 155.408680 | −0.222598 |
| 9 | 80.895593 | 0.219881 | 170.978041 | 0.212646 |
| 10 | 88.734839 | −0.210023 | 186.574029 | −0.203861 |
| 11 | 96.576707 | 0.201373 | 202.189809 | 0.196042 |
| 12 | 104.420491 | −0.193702 | 217.820419 | −0.189034 |
| 13 | 112.265848 | 0.186843 | 233.462654 | 0.182711 |
| 14 | 120.112354 | −0.180663 | 249.114013 | −0.176971 |
| $j$ | $-\lambda_j^-$ | $A_j^-$ | $-\lambda_j^-$ | $A_j^-$ |
| 0 | 2.844835 | 1.233275 | 3.372024 | 1.379949 |
| 1 | 10.174296 | −0.617349 | 15.383971 | −0.680027 |
| 2 | 17.859425 | 0.464093 | 29.751723 | 0.493104 |
| 3 | 25.617868 | −0.388494 | 44.738343 | −0.406545 |
| 4 | 33.410361 | 0.340928 | 59.986307 | 0.354040 |
| 5 | 41.221752 | −0.307382 | 75.375199 | −0.317634 |
| 6 | 49.044572 | 0.282080 | 90.849326 | 0.290432 |
| 7 | 56.874853 | −0.262122 | 106.378881 | −0.269111 |
| 8 | 64.710161 | 0.245860 | 121.946337 | 0.251826 |
| 9 | 72.549123 | −0.232280 | 137.540929 | −0.237452 |
| 10 | 80.390694 | 0.220720 | 153.155416 | 0.225259 |
| 11 | 88.234332 | −0.210726 | 168.785154 | −0.214752 |
| 12 | 96.079491 | 0.201973 | 184.426542 | 0.205575 |
| 13 | 103.925919 | −0.194223 | 200.077324 | −0.197472 |
| 14 | 111.773292 | 0.187302 | 215.735491 | 0.190250 |

Adapted from Papoutsakis et al. (1980a) and own calculations

increasing values of the Peclet number. The increase of the positive eigenvalues with growing Peclet numbers can been seen clearly in Fig. 5.2, where the first 100 positive eigenvalues are plotted for four different Peclet numbers.

Figure 5.3 shows the temperature distribution along the pipe centerline for different Peclet numbers. It can be seen how the axial heat conduction effect in the fluid decreases rapidly with increasing values of the Peclet number. In addition, it

**Fig. 5.2** Distribution of the
positive eigenvalues for
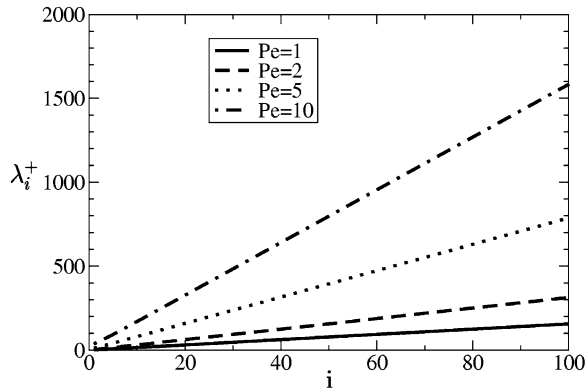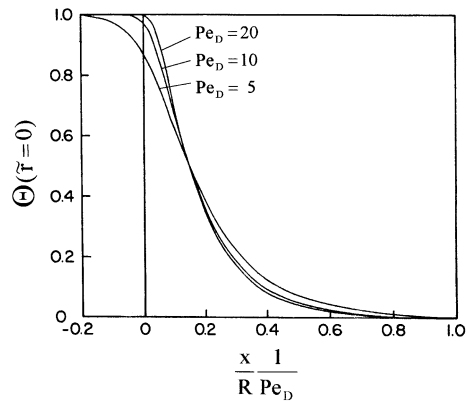different Peclet numbers



**Fig. 5.3** Temperature
distribution at the pipe
centerline for different Peclet
numbers (Papoutsakis et al.
1980a)



can be seen from this figure that, for a Peclet number of 5, the region of influence of the axial heat conduction is about one radius in the negative direction.

Figure 5.4 shows the development of the temperature profile for different axial positions in the pipe (Papoutsakis et al. 1980a). Note that, for growing values of the axial coordinate, the temperature tends to $T_W$ and thus $\Theta$ tends to zero. For $\tilde{x} \leq 0$ the temperature of the fluid rapidly decreases to $T_0$, resulting in values of $\Theta$ close to one for increasing distances from $\tilde{x} = 0$. By comparing the two plots in Fig. 5.4, one can notice how the influence of the axial heat conduction in the flow gets weaker with increasing values of the Peclet number. For $Pe_D = 20$, the temperature distribution at the entrance of the heating section ($\tilde{x} = 0$) becomes rather non-uniform. This shows clearly that, whenever axial heat conduction is not negligible, it is incorrect to prescribe a constant entrance temperature at $\tilde{x} = 0$. In this case, the temperature distribution at $\tilde{x} = 0$ is always a result of the solution.

Papoutsakis et al. (1980a) calculated the value of the Nusselt number for fully developed flow $Nu_\infty^-$, according to Eq. (5.54), and showed graphically the distribution as a function of the Peclet number.
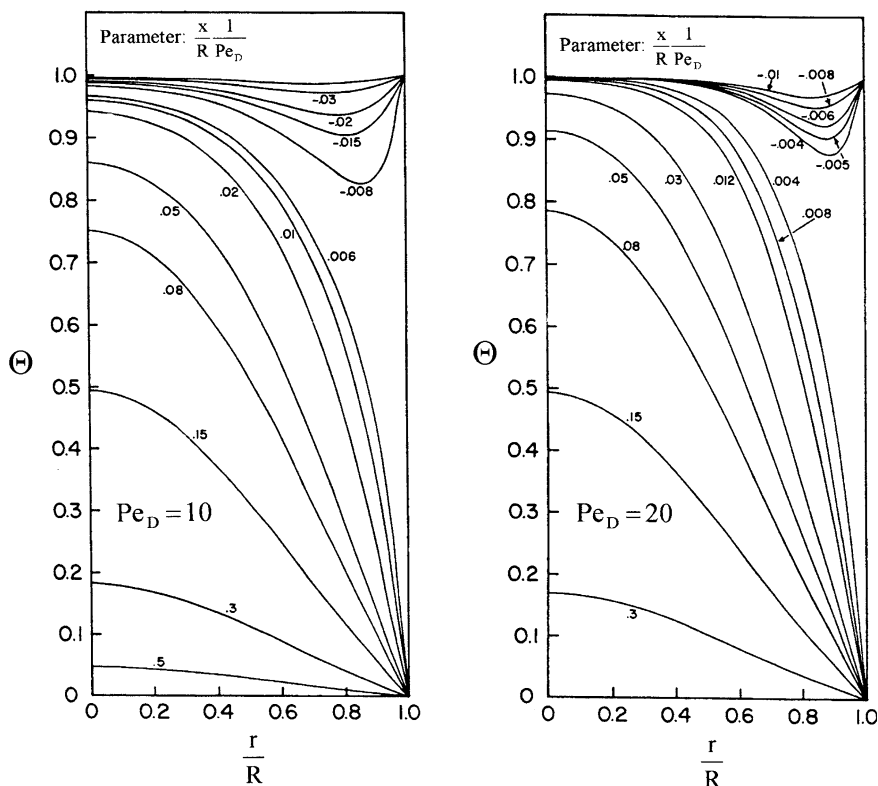
**Fig. 5.4** Temperature distribution for several axial positions $x/(R\,Pe_D)$ and two Peclet numbers (Papoutsakis et al. 1980a)

In general, it can be seen that $Nu_\infty^-$ increases with decreasing values of the Peclet number. Hennecke (1968) predicted numerically the values of $Nu_\infty^-$ for several Peclet number. These values have been tabulated by Shah and London (1978). Table 5.2 shows a comparison between analytically and numerically predicted values of $Nu_\infty^-$. From Table 5.2, a very good agreement between numerically and analytically predicted values can be noted.

In Figs. 5.5 and 5.6, the distribution of the local Nusselt number is shown for laminar pipe flow for $\tilde{x} > 0$. These values have been calculated using the numerical approach described in detail in Appendix C. In order to resolve the distribution of the Nusselt number for very small values of $\tilde{x}$ correctly, a large number of eigenvalues is needed. For the present calculations 200 eigenvalues have been used. If less eigenvalues are used, the Nusselt number for $\tilde{x} \to 0$ will tend to smaller values. This can be seen clearly, if the Nusselt number is plotted on a logarithmic scale. In addition to the large number of eigenvalues, a very fine grid was used in order to resolve the shape of the higher eigenfunctions (see Appendix C). Normally 1500–2000 grid points in the radial direction are sufficient. As it can be seen from

**Table 5.2** Comparison between numerically Hennecke (1968), values taken from Shah and London (1978) and analytically (values in the Table have been predicted by the author using the equations given by Papoutsakis et al. (1980a)) predicted values for $Nu_\infty^-$

| $Pe_D$ | $Nu_\infty^-$ (Papoutsakis et al. 1980a) | $Nu_\infty^-$ (Hennecke 1968) |
|--------|------------------------------------------|-------------------------------|
| 1      | 4.027                                    | 4.03                          |
| 2      | 3.922                                    | 3.92                          |
| 5      | 3.767                                    | 3.77                          |
| 10     | 3.695                                    | 3.70                          |
| 20     | 3.668                                    | 3.67                          |
| 50     | 3.659                                    | 3.66                          |

Figs. 5.5 and 5.6, the analytical method is in excellent agreement with the numerical calculations by Hennecke (1968) for the two shown Peclet numbers.

For $Pe_D = 50$, the analytical solution has also been compared with the investigations of Bayazitoglu and Özisik (1980) and of Singh (1958) and a very good agreement was found.

Weigand and Abdelmoula (2014) developed correlations for the distribution of the local Nusselt numbers for flows in a circular pipe and in a planar channel. The correlations have been based on the asymptotic method of Churchill and Usagi (1972), which has often been used for correlating the local distribution of the Nusselt number (see e.g. Shah and London (1978), Awad (2010) or Haji-Sheikh et al. (2008)). The general form of the correlation for the local Nusselt number is given by

$$\frac{Nu_D}{Nu_\infty^-} = \left[\left(a\tilde{x}^{-b} + c\right)^n + 1\right]^{1/n} \tag{5.55}$$
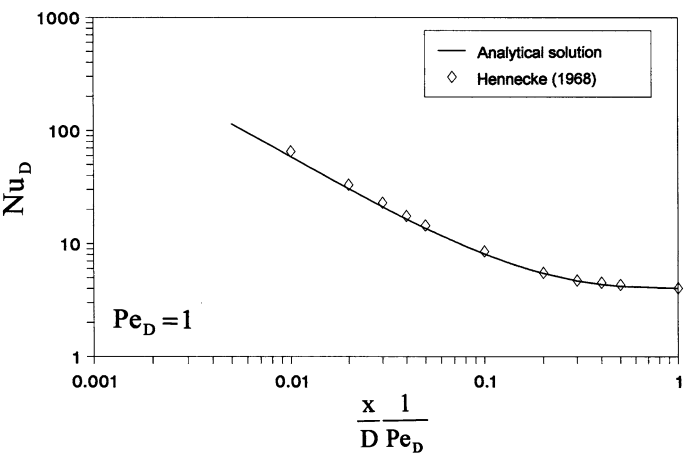


**Fig. 5.5** Distribution of the local Nusselt number for $\tilde{x} > 0$ and $Pe_D = 1$
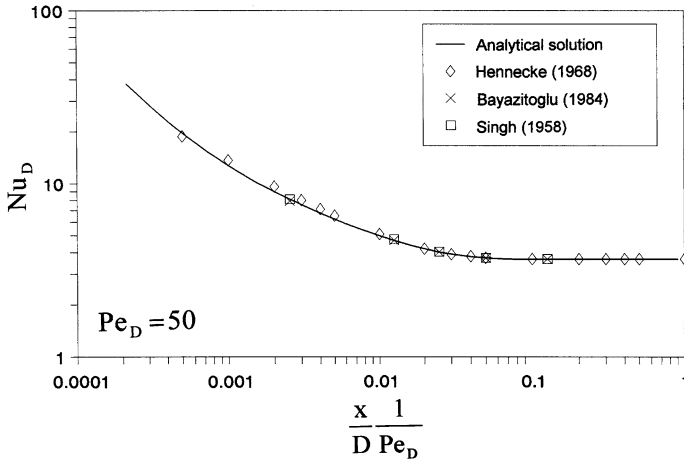
**Fig. 5.6** Distribution of the local Nusselt number for $\tilde{x} > 0$ and $Pe_D = 50$

In Eq. (5.55) the Nusselt number for the fully developed flow can be calculated by the asymptotic formulas from Michelsen and Villadsen (1974)

$$\overline{Nu}_\infty = \begin{cases} 4.1807(1 - 0.0439Pe_D), & Pe_D < 1.5 \\ 3.6568\left(1 + 1.227Pe_D^{-2}\right), & 5 < Pe_D < 50 \end{cases} \tag{5.56}$$

The constants for Eq. (5.55) have been determined by Weigand and Abdelmoula (2014) by a least squares method to

$$a = 0.1916Pe_D^{-1.022} + 0.005082 \tag{5.57}$$
$$b = -0.1166\exp(-0.05606\,Pe_D) - 0.8247$$
$$n = -0.2045Pe_D^{0.4364} + 2.18$$
$$c = 0$$

With this set of constants the local distribution of the Nusselt number can be calculated accurately for $Pe_D < 50$ where axial heat conduction within the fluid is of importance. Also for $\tilde{x} < 0$ a correlation has been developed by them for the local Nusselt number. For this the following constants can be used for $Pe_D < 50$

$$a = 0.2091\,Pe_D^{-0.8187} + 0.001857 \tag{5.58}$$
$$b = 0.002763\,Pe_D^{1.055} - 0.9649$$
$$n = 0.05287\,Pe_D^{1.02} + 1.794$$
$$c = 0$$

### Laminar Channel Flow

In order to investigate this case, the flow index $F$ in all the equations has to be set to 0. The first solution of this problem was obtained by Deavours (1974). He decomposed the eigenvalue problem for the parallel plate channel into a system of ordinary differential equations for which he proved the orthogonality of the eigenfunctions. As stated before, this case was also investigated by Weigand et al. (1993) with the

**Table 5.3**  Eigenvalues and constants for laminar channel flow

| $j$ | $Pe_D = 5$ | | $Pe_D = 10$ | |
|---|---|---|---|---|
| | $\lambda_j^+$ | $A_j^+$ | $\lambda_j^+$ | $A_j^+$ |
| 0 | 3.220469 | −0.376403 | 9.575077 | −0.230822 |
| 1 | 6.758122 | 0.202738 | 15.522013 | 0.192715 |
| 2 | 10.645334 | −0.124312 | 23.101943 | −0.121091 |
| 3 | 14.557251 | 0.089495 | 30.850355 | 0.087928 |
| 4 | 18.476438 | −0.069885 | 38.648148 | −0.068971 |
| 5 | 22.398690 | 0.057315 | 46.467380 | 0.056719 |
| 6 | 26.322503 | −0.048575 | 54.297781 | −0.048157 |
| 7 | 30.247224 | 0.042147 | 62.134735 | 0.041837 |
| 8 | 34.172509 | −0.037220 | 69.975845 | −0.036981 |
| 9 | 38.098175 | 0.033325 | 77.819763 | 0.033135 |
| 10 | 42.024105 | −0.030167 | 85.665658 | −0.030013 |
| 11 | 45.950232 | 0.027556 | 93.513006 | 0.027428 |
| 12 | 49.876499 | −0.025361 | 101.361442 | −0.025253 |
| 13 | 53.802882 | 0.023489 | 109.210726 | 0.023398 |
| 14 | 57.729349 | −0.021875 | 117.060670 | −0.021796 |
| $j$ | $-\lambda_j^-$ | $A_j^-$ | $-\lambda_j^-$ | $A_j^-$ |
| 0 | 1.192001 | 0.897756 | 1.580670 | 1.044165 |
| 1 | 5.139142 | −0.222463 | 8.989775 | −0.232941 |
| 2 | 9.062116 | 0.130123 | 16.748478 | 0.132737 |
| 3 | 12.984172 | −0.092272 | 24.547406 | −0.093479 |
| 4 | 16.907540 | 0.071518 | 32.366159 | 0.072234 |
| 5 | 20.831909 | −0.058393 | 40.195993 | −0.058873 |
| 6 | 24.756940 | 0.049341 | 48.032482 | 0.049686 |
| 7 | 28.682423 | −0.042719 | 55.873251 | −0.042979 |
| 8 | 32.608218 | 0.037664 | 63.716909 | 0.037868 |
| 9 | 36.534242 | −0.033679 | 71.562614 | −0.033843 |
| 10 | 40.460433 | 0.030456 | 79.409807 | 0.030592 |
| 11 | 44.386753 | −0.027797 | 87.258131 | −0.027910 |
| 12 | 48.313173 | 0.025564 | 95.107316 | 0.025661 |
| 13 | 52.239673 | −0.023664 | 102.957190 | −0.023747 |
| 14 | 56.166236 | 0.022026 | 110.807606 | 0.022098 |

$Pe_D = 5$ and $Pe_D = 10$

**Table 5.4** Nusselt number for the fully developed flow, $Nu_\infty^-$, compared to predictions by Ash

| $Pe_D$ | $Nu_\infty^-$ (Eq. (5.54)) | $Nu_\infty^-$ Ash (see Shah and London 1978) | $Nu_\infty^-$ Nguyen (1992) |
|---|---|---|---|
| 0.02352 | 8.1141 | 8.1144 | |
| 0.4444 | 8.0644 | 8.0644 | |
| 0.6508 | 8.0416 | 8.0416 | |
| 1.0576 | 7.9997 | 7.9998 | |
| 1.4368 | 7.9640 | 7.9640 | |
| 2 | 7.9165 | | 7.9164 |
| 5 | 7.7471 | | 7.7468 |
| 9.97 | 7.6310 | 7.6310 | |
| 50 | 7.5457 | | 7.5456 |
| 69.78 | 7.5432 | 7.5408 | |
| 100 | 7.5419 | | 7.5407 |
| 1000 | 7.5407 | | 7.5407 |

See Shah and London (1978) and Nguyen (1992)

analytical method presented here. Table 5.3 shows eigenvalues and constants for two different Peclet numbers. Similar to the circular pipe case (Table 5.1), it can be seen from Table 5.3 that the positive eigenvalues increase dramatically with growing values of the Peclet number. This shows again that the effect of the axial heat conduction in the fluid diminishes with growing values of the Peclet number. Values of the Nusselt number for fully developed channel flow, $Nu_\infty^-$, have also been reported in literature. Table 5.4 shows a comparison between the analytical predicted values and calculations of Ash (see Shah and London 1978) and Nguyen (1992). The values are ranging from $Pe_D = 0.02352$ up to $Pe_D = 1000$ and show a very good agreement between the presented analytical solution and literature data. It can be seen that the Nusselt number for the fully developed flow increases with decreasing values of the Peclet number. This behaviour is very similar to the results shown in the previous section for the circular pipe.

The temperature distribution at the centreline of the fluid is depicted in Fig. 5.7. By comparing Fig. 5.7 with Fig. 5.3 for the circular pipe, it can be seen that the axial heat conduction effect within the fluid has very similar effects for the two geometries. In addition, it can be seen that for very low values of the Peclet number the temperature at $\tilde{x} = 0$ is lowered because of axial heat conduction effects within the flow. Figure 5.8 shows the distribution of the local Nusselt number for $Pe_D = 4$ and $\tilde{x} > 0$. The Nusselt number is compared to calculated values of Agrawal (1960). Agrawal (1960) determined for $\tilde{x} > 0$ and $\tilde{x} \leq 0$ two independent series solutions, which then have been matched at $\tilde{x} = 0$. This approach resulted in a complicated expression for the Nusselt number. From Fig. 5.8, it can be seen that both calculations are in good agreement for $\tilde{x} \geq 0.1$. However, for smaller values of $\tilde{x}$, the values given by Agrawal (1960) are much lower than the Nusselt numbers predicted here. The reason for this behaviour is caused by the fact that Agrawal
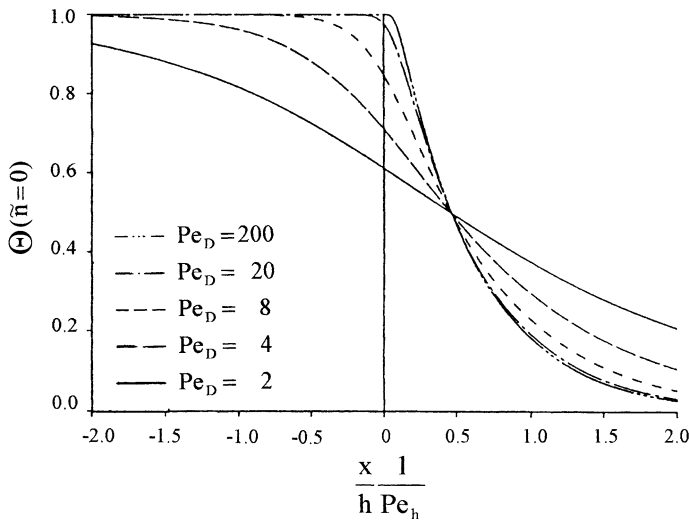
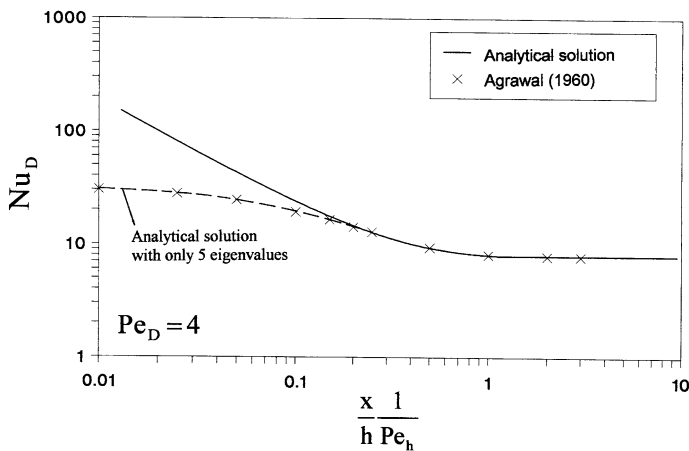**Fig. 5.7** Temperature distribution at the centerline of the parallel plate channel for different Peclet numbers



**Fig. 5.8** Distribution of the local Nusselt number for $Pe_D = 4$ ($\tilde{x} > 0$)

used only five eigenvalues for the prediction of the local Nusselt number. This is sufficient for larger values of the axial coordinate, but not for very small values of the axial coordinate.[2] For very small values of the axial coordinate, it can be seen

---

[2]If only the first five eigenvalues for the prediction of the Nusselt number are used with the present method, the predicted values are in close agreement with the ones by Agrawal (1960) (see Fig. 5.8).

from Fig. 5.8 that the Nusselt number can be approximated by $\mathrm{Nu}_D \propto \tilde{x}^{-|\beta|}$. This is in good agreement with predictions by Hennecke (1968) and by Kader (1971).

Also for the case of a laminar channel flow correlations for the local Nusselt number are available. This case has been investigated by Heji-Sheikh et al. (2008) and by Weigand and Abdelmoula (2014). Weigand and Abdelmoula have given the following correlations based on Eq. (5.55)

$$\frac{\mathrm{Nu}_D}{\mathrm{Nu}_\infty^-} = \left[\left(a\tilde{x}^{-b} + c\right)^n + 1\right]^{1/n} \tag{5.55}$$

In Eq. (5.55) the Nusselt number for the fully developed channel flow was prescribed for this case by Shah and London (1978)

$$\mathrm{Nu}_\infty^- = \begin{cases} 8.1142\left(1 - 0.030859\,\mathrm{Pe}_D + 0.0069436\,\mathrm{Pe}_D^2\right), & \mathrm{Pe}_D \ll 1 \\ 7.54\left(1 + 3.79Pe_D^{-2}\right), & \mathrm{Pe}_D > 1 \end{cases} \tag{5.59}$$

The constants for Eq. (5.55) have been determined by Weigand and Abdelmoula (2014) again by a least squares method to

$$\begin{aligned} a &= 0.09337\,\mathrm{Pe}_D^{-1.03} + 0.0002765 \\ b &= -0.1378\exp(-0.01963\mathrm{Pe}_D) - 0.8239 \\ n &= 1.802\,\mathrm{Pe}_D^{-0.057287} + 3.096 \times 10^{-6} \\ c &= 0 \end{aligned} \tag{5.60}$$

With this set of constants the local distribution of the Nusselt number can be calculated accurately for $\mathrm{Pe}_D < 50$ where axial heat conduction within the fluid is of importance. Also for $\tilde{x} < 0$ a correlation has been developed by them for the local Nusselt number. Here, the following constants can be used for $\mathrm{Pe}_D < 50$

$$\begin{aligned} a &= 0.08431\,\mathrm{Pe}_D^{-1.051} + 0.01392 \\ b &= 3.32410 \times 10^{-7}\mathrm{Pe}_D^{-5.128} - 0.9753 \\ n &= 0.007196\,\mathrm{Pe}_D^{2.045} + 1.821 \\ c &= 0 \end{aligned} \tag{5.61}$$

Figure 5.9 shows a comparison between the correlation of Weigand and Abdelmoula (2014), the one given by Haji-Sheikh et al. (2008) and the analytical solution. It can be seen that there is a good agreement between both correlations and the analytical solution. Please note also that the correlation by Haji-Sheikh et al. (2008) is only intended to approximate the Nusselt number for small axial values in the thermal entrance region. However, the correlation by Weigand and Abdelmoula (2014) has been developed to be valid for the whole thermal entrance region.
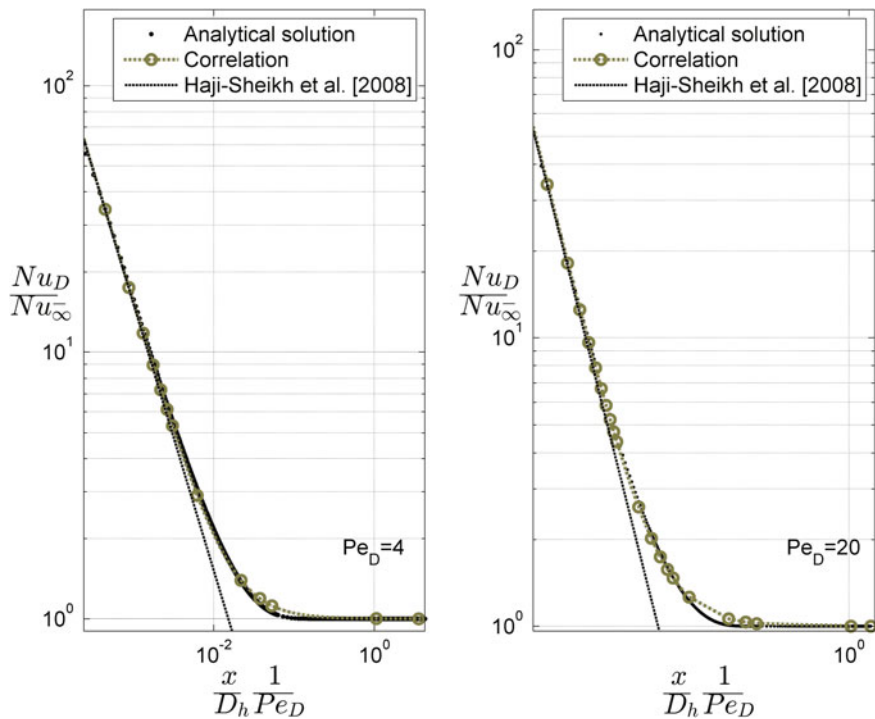
**Fig. 5.9** Comparison between correlations and analytical solution for a parallel plate channel with constant wall temperature and different Peclet numbers (Weigand and Abdelmoula 2014)

## 5.1.2 Heat Transfer in Turbulent Pipe and Channel Flows for Small Peclet Numbers

For the heat transfer in a turbulent duct flow, the functions $a_1$ and $a_2$ depend on the turbulent heat exchange in the flow. For the following analysis, the ratios $\varepsilon_{hx}/\varepsilon_{hr}$ and $\varepsilon_{hx}/\varepsilon_{hy}$ are set equal to one. This assumption has been made previously by Lee (1982) and Chieng and Launder (1980). Weigand et al. (2002) proved this assumption by solving Eq. (3.6) numerically by using a non-isotropic heat flux model for the heat transfer in a planar channel. They concluded that the above assumption is well justified for the applications considered here. Assuming that the ratio $\varepsilon_{hx}/\varepsilon_{hn}$ is equal to one, results in the fact that $a_1$ is equal to $a_2$ (see Eq. (5.8)). Since axial heat conduction effects in turbulent flows are only important if the Prandtl number is very small, the turbulent Prandtl number has to be calculated by adopting a model suitable for liquid metal flows (e.g. Eqs. (3.79)–(3.82)).

**Turbulent Pipe Flow**

If the flow index $F$ is set to one in the equations, the turbulent heat transfer in a pipe for a low Peclet number flow can be predicted. For the following calculations the

**Table 5.5** Eigenvalues and constants for turbulent pipe flow with Pr = 0.001

| $j$ | $\mathrm{Re}_D = 5000$ | | $\mathrm{Re}_D = 10{,}000$ | |
|---|---|---|---|---|
|     | $\lambda_j^+$ | $A_j^+$ | $\lambda_j^+$ | $A_j^+$ |
| 0 | 10.915 | −0.3959 | 33.569 | −0.2064 |
| 1 | 17.925 | 0.4220 | 45.293 | 0.3225 |
| 2 | 25.530 | −0.3748 | 59.584 | −0.3210 |
| 3 | 33.266 | 0.3354 | 74.598 | 0.3018 |
| 4 | 41.051 | −0.3049 | 89.896 | −0.2820 |
| 5 | 48.859 | 0.2810 | 105.33 | 0.2644 |
| 6 | 56.628 | −0.2617 | 120.85 | −0.2491 |
| 7 | 64.512 | 0.2458 | 136.41 | 0.2359 |
| 8 | 72.348 | −0.2324 | 152.01 | −0.2244 |
| 9 | 80.189 | 0.2209 | 167.63 | 0.2144 |
| $j$ | $-\lambda_j^-$ | $A_j^-$ | $-\lambda_j^-$ | $A_j^-$ |
| 0 | 3.305 | 1.2055 | 4.280 | 1.3923 |
| 1 | 10.626 | −0.6417 | 16.837 | −0.7376 |
| 2 | 18.337 | 0.4758 | 31.444 | 0.5281 |
| 3 | 26.127 | −0.3936 | 46.622 | −0.4262 |
| 4 | 33.947 | 0.3430 | 62.023 | 0.3653 |
| 5 | 41.779 | −0.3080 | 77.532 | −0.3242 |
| 6 | 49.617 | 0.2820 | 93.102 | 0.2943 |
| 7 | 57.460 | −0.2618 | 108.71 | −0.2713 |
| 8 | 65.305 | 0.2453 | 124.34 | 0.2530 |
| 9 | 73.152 | −0.2317 | 139.98 | 0.2380 |

turbulent Prandtl number model of Azer and Chao (1960) (see Eq. (3.82)) as well as the Kays and Crawford model (1993) (see Eqs. (3.79)–(3.81)) have been used. These two models have been found to give reliable answers for turbulent liquid metal flows. The reader is referred to Weigand (1996) or to Weigand et al. (1997) for comparisons between calculations and measurements for liquid metal flows in pipes with the above mentioned models for $\mathrm{Pr}_t$.

Eigenvalues and constants are shown in Table 5.5 for a Prandtl number of 0.001 and different values of the Reynolds number. It can be seen from Table 5.5 that the positive eigenvalues increase rapidly with growing values of the Reynolds number. This shows again the decreasing influence of the axial heat conduction within the flow.

Figure 5.10 shows the distribution of the Nusselt number for fully developed flow ($Nu_\infty^-$) as a function of the Peclet number for Pr = 0.022. The predicted values have been obtained by using different models for the turbulent Prandtl number. It can be seen that the two models give relatively similar results. The predicted values have been compared to experimental data from Sleicher et al. (1973) and Gilliland et al. (1951) (taken from Azer and Chao 1960). As it can be seen from Fig. 5.10, the agreement between experimental data and predictions is good.

Table 5.6 shows values of the Nusselt number $Nu_\infty^-$ for fully developed flow for different values of the Prandtl and Reynolds number. In addition, the table contains

**Fig. 5.10** Nusselt number of
the fully developed flow
($\overline{\mathrm{Nu}}_\infty$) as a function of the
Peclet number for Pr = 0.022
(Weigand et al. 1997)
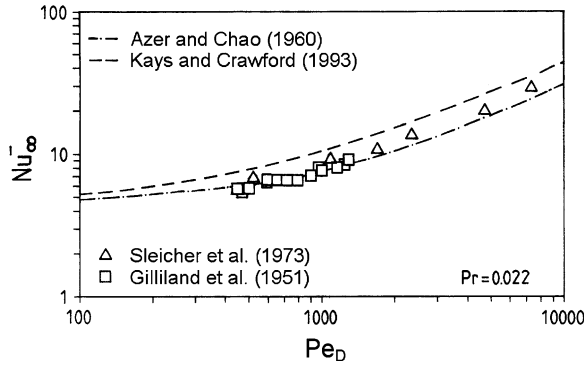
the relative deviation of the Nusselt number for a parabolic calculation $\Delta E = \left(\mathrm{Nu}_{\mathrm{elliptic}} - \mathrm{Nu}_{\mathrm{parabolic}}\right)/\mathrm{Nu}_{\mathrm{elliptic}}$.

From the entries in Table 5.6, it is obvious that axial heat conduction effects are not important for the fully developed flow ($x \rightarrow \infty$). Therefore, the influence of axial heat conduction on the Nusselt number for fully developed flow can be neglected with good accuracy. This may not be the case when the thermal entrance region is considered.

Figure 5.11 shows the relative error $\Delta E$ for the local Nusselt number by ignoring the axial heat conduction within the thermal entrance region. As mentioned before, the relative error is negligible for the fully developed flow ($\tilde{x} \rightarrow \infty$). However, it may be very large for small values of the axial coordinate. For example for $\mathrm{Pe}_D = 10$, the error will be about 30 % for $x/(D\,\mathrm{Pe}_D) = 0.01$ and for smaller values of the axial coordinate this error is even larger. This example illustrates that axial heat conduction effects may be important in the thermal entrance region, also for turbulent flows.

Figure 5.12 shows the local temperature field in the flow for two different values of the Peclet number. The increasing effect of the axial heat conduction in the flow

**Table 5.6** Nusselt number
for fully developed flow
($\overline{\mathrm{Nu}}_\infty$)

| Pr | 0.002 | 0.006 | 0.01 |
|---|---|---|---|
| $\mathrm{Re}_D$ | | | |
| 3000 | 8.370 (0.014) | 8.284 (0.003) | 8.277 (0.001) |
| 5000 | 8.518 (0.007) | 8.484 (0.001) | 8.497 (0.0004) |
| 10,000 | 8.760 (0.002) | 8.783 (0.0002) | 8.835 (0.0001) |
| 20,000 | 8.919 (0.0004) | 9.011 (0.0) | 9.149 (0.0) |
| 30,000 | 9.012 (0.0002) | 9.175 (0.0) | 9.408 (0.0) |

The values in brackets indicate the relative deviation $\Delta E = \left(\mathrm{Nu}_{\mathrm{elliptic}} - \mathrm{Nu}_{\mathrm{parabolic}}\right)/\mathrm{Nu}_{\mathrm{elliptic}}$ between an elliptic and a parabolic calculation
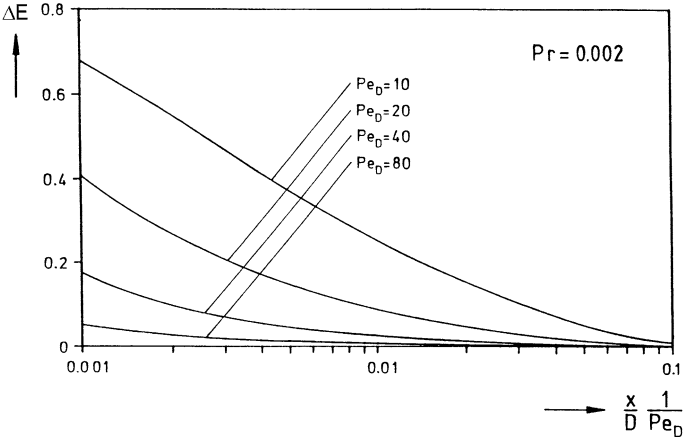
**Fig. 5.11** Relative error in the local Nusselt number by neglecting the axial heat conduction within the fluid (Weigand 1996)
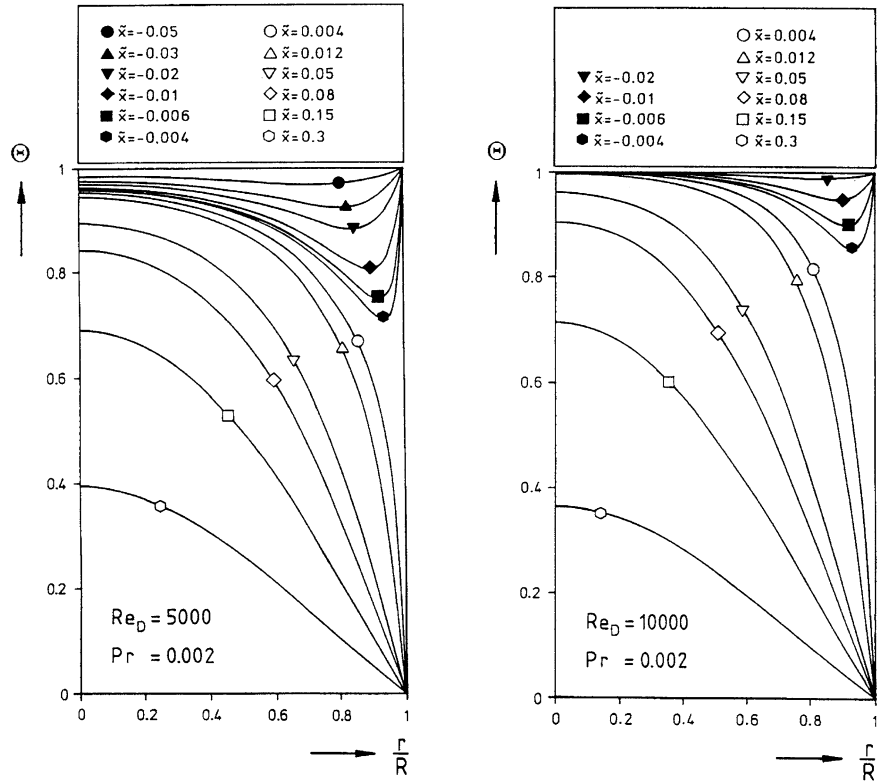


**Fig. 5.12** Temperature distribution for a thermally developing flow in a circular pipe (Weigand 1996)

for decreasing values of the Peclet number is clearly visible for small axial values. It is interesting to see how the region of influence of axial heat conduction for $\tilde{x} < 0$ increases for decreasing Peclet numbers. This shows again nicely the elliptic effect of the axial heat conduction within the flow. This also demonstrates that it would be not correct to prescribe for such a case just the temperature distribution at $\tilde{x} = 0$, because this is in fact part of the solution of the problem.

### Turbulent Flow in a Planar Channel

For flow and heat transfer in a parallel plate channel, the flow index $F$ in the preceding equations must be set to 0. The behaviour of the solutions, e.g. for the Nusselt number, is very similar to the one for the circular pipe and therefore is not be shown here. The reader is referred to Weigand (1996) and Weigand et al. (2002) for a detailed presentation of these results.

## 5.2 Heat Transfer for Constant Wall Heat Flux for $x \leq 0$ and $x > 0$

This case has been studied analytically by Papoutsakis et al. (1980b) for laminar, hydrodynamically fully developed pipe flow and by Weigand et al. (2001) for laminar and turbulent hydrodynamically fully developed pipe and channel flows. The geometry under consideration and the used coordinate system are shown in Fig. 5.13.

Similar to the considerations given in Sect. 5.1, we start with Eq. (5.3)

$$\rho c_p u(n) \frac{\partial T}{\partial x} = \frac{1}{r^F} \frac{\partial}{\partial n} \left[ r^F \left( k + \rho c_p \frac{\varepsilon_m}{Pr_t} \right) \frac{\partial T}{\partial n} \right] + \frac{\partial}{\partial x} \left[ \left( k + \rho c_p \frac{\varepsilon_m}{Pr_t} \right) \frac{\partial T}{\partial x} \right] \quad (5.3)$$
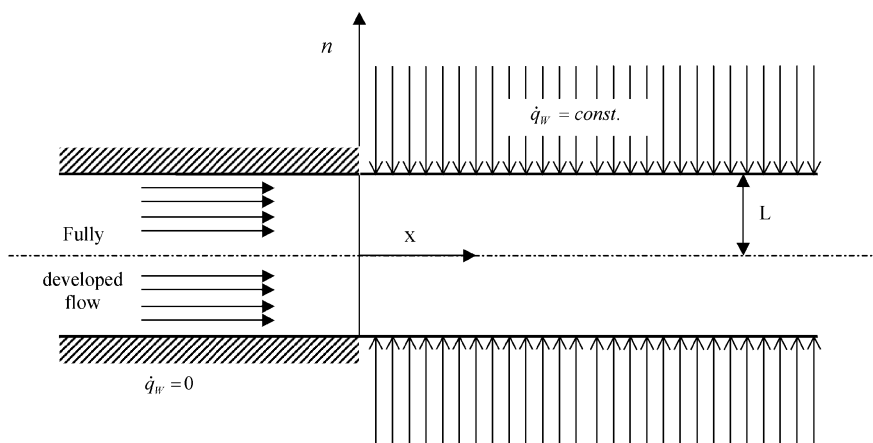


**Fig. 5.13** Geometrical configuration and coordinate system

This equation has to be solved together with the boundary conditions

$$n = 0 : \partial T / \partial n = 0, \tag{5.62}$$

$$n = L : x \leq 0 : \partial T / \partial n = 0,$$

$$x > 0 : \partial T / \partial n = \dot{q}_W / k,$$

$$\lim_{x \to -\infty} T = T_0$$

Introducing the following dimensionless quantities

$$\Theta = \frac{T - T_0}{\dot{q}_W L / k}, \tilde{x} = \frac{x}{L} \frac{1}{\mathrm{Pe}_L}, \tilde{u} = \frac{u}{\bar{u}}, \tilde{n} = \frac{n}{L}, \tilde{r} = \frac{r}{L} \tag{5.63}$$

$$\mathrm{Pe}_L = \mathrm{Re}_L \mathrm{Pr}, \mathrm{Re}_L = \frac{\bar{u} L}{\nu}, \mathrm{Pr} = \frac{\nu}{a}, \tilde{\varepsilon}_m = \frac{\varepsilon_m}{\nu}, \mathrm{Pr}_t = \frac{\varepsilon_m}{\varepsilon_{hn}}$$

into the energy equation (5.3) and into the boundary conditions, Eq. (5.62), results in

$$\tilde{u}(\tilde{n}) \frac{\partial \Theta}{\partial \tilde{x}} = \frac{1}{\mathrm{Pe}_L^2} \frac{\partial}{\partial \tilde{x}} \left[ a_1(\tilde{n}) \frac{\partial \Theta}{\partial \tilde{x}} \right] + \frac{1}{\tilde{r}^F} \frac{\partial}{\partial \tilde{n}} \left[ \tilde{r}^F a_2(\tilde{n}) \frac{\partial \Theta}{\partial \tilde{n}} \right] \tag{5.6}$$

with the boundary conditions

$$\tilde{x} \to -\infty : \Theta = 0 \tag{5.64}$$

$$\tilde{n} = 0 : \frac{\partial \Theta}{\partial \tilde{n}} = 0$$

$$\tilde{n} = 1 : \tilde{x} > 0 : \frac{\partial \Theta}{\partial \tilde{n}} = 1, \quad \tilde{x} \leq 0 : \frac{\partial \Theta}{\partial \tilde{n}} = 0$$

Similar to the procedure shown in Sect. 3.3, the temperature for the present case has been made dimensionless with the constant wall heat flux and the thermal conductivity of the fluid. The functions $a_1$ and $a_2$ are given by Eq. (5.8). The solution procedure for the energy equation for a constant heat flux at the wall is similar to the one for constant wall temperature. We are introducing again the axial energy flow through a cross-sectional area of height $\tilde{n}$ ($E(\tilde{x}, \tilde{n})$), given by Eq. (5.9). This results again in a system of partial differential equations, Eq. (5.10), with the solution vector $\vec{S}$ and the matrix operator $\underset{\sim}{L}$ defined by Eq. (5.11). The boundary conditions for the function $E(\tilde{x}, \tilde{n})$ can be derived from the definition of the axial energy flux, Eq. (5.9), by using Eq. (5.64). One obtains

$$\lim_{\tilde{x} \to -\infty} E = 0, \quad \tilde{n} = 0 : E = 0 \tag{5.65}$$

$$\tilde{n} = 1 : E = \begin{cases} 0, & -\infty < \tilde{x} \leq 0 \\ \tilde{x}, & \tilde{x} > 0 \end{cases}$$

For the inner product, the expression given by Eq. (5.14) can be used again. However, because of the changed boundary conditions, $D(\underset{\sim}{L})$ needs to be adapted

$$D(\underset{\sim}{L}) = \left\{ \vec{\Phi} \in H : \underset{\sim}{L}\vec{\Phi} \text{ (exists and) } \in H, \Phi_2(1) = \Phi_2(0) = 0 \right\} \qquad (5.66)$$

where the only change in Eq. (5.66) compared to Eq. (5.15) lies in the changed boundary condition that $\Phi_2(1) = 0$. For the eigenvalue problem one obtains again

$$\left[ \tilde{r}^F a_2(\tilde{n}) \Phi'_{j1} \right]' + \tilde{r}^F \left[ \frac{\lambda_j a_1(\tilde{n})}{Pe_L^2} - \tilde{u} \right] \lambda_j \Phi_{j1} = 0 \qquad (5.23)$$

but now with the boundary conditions

$$\Phi'_{j1}(0) = 0, \quad \Phi'_{j1}(1) = 0 \qquad (5.67)$$

Comparing the boundary conditions given by Eq. (5.67) for a constant wall heat flux to the ones for a constant wall temperature, it can be seen that only the boundary condition for $\tilde{n} = 1$ has been changed. The normalizing condition for the eigenfunctions, Eq. (5.25), can be used again. Similarly as for Eq. (5.26) it can be shown that an arbitrary vector $\vec{f}$ can be expanded into a series of eigenfunctions and the result is given by Eq. (5.30).

Since the expansion of an arbitrary vector in terms of eigenfunctions has already been developed, we focus directly on the solution of the system of partial differential equations given by Eq. (5.10). Because of the non-homogeneous boundary condition for the heat flux, the vector $\vec{S}$ does not belong to the domain $D(\underset{\sim}{L})$ given by Eq. (5.66). However, it can be shown that

$$\left\langle \underset{\sim}{L} \vec{S}, \vec{\Phi}_j \right\rangle = \left\langle \vec{S}, \underset{\sim}{L}\vec{\Phi}_j \right\rangle - \Phi_{j1}(1)E(\tilde{x}, 1) \qquad (5.68)$$

Note here the difference in this equation compared to Eq. (5.31). The last term on the right hand side of Eq. (5.68) is now a function of the axial coordinate and no longer a constant. Taking the inner product of both sides of Eq. (5.68) one obtains

$$\frac{\partial}{\partial \tilde{x}} \left\langle \vec{S}, \vec{\Phi}_j \right\rangle = \lambda_j \left\langle \vec{S}, \vec{\Phi}_j \right\rangle - \Phi_{j1}(1)E(\tilde{x}, 1) \qquad (5.69)$$

Equation (5.69) represents an ordinary differential equation for the expression $\langle \vec{S}, \vec{\Phi}_j \rangle$ and can be solved separately for positive and negative eigenvalues. This results in

$$\left\langle \vec{S}, \vec{\Phi}_j^- \right\rangle = -\Phi_{j1}^-(1) \int\limits_{-\infty}^{\tilde{x}} E(\tilde{x}, 1) \exp(\lambda_j^-(\tilde{x} - \bar{x})) d\bar{x} \qquad (5.70)$$

$$\left\langle \vec{S}, \vec{\Phi}_j^+ \right\rangle = \Phi_{j1}^+(1) \int\limits_{-\infty}^{\tilde{x}} E(\tilde{x}, 1) \exp(\lambda_j^+(\tilde{x} - \bar{x})) d\bar{x} \qquad (5.71)$$

After evaluating the integrals in Eqs. (5.70) and (5.71), the following result for the temperature distribution $\Theta$, which is the first vector component of $\vec{S}$, can be derived

$$\tilde{x} \leq 0 : \Theta(\tilde{x}, \tilde{n}) = \sum_{j=1}^{\infty} \frac{\Phi_{j1}^+(1)}{\left\| \vec{\Phi}_j^+ \right\|^2} \frac{\exp\left(\lambda_j^+ \tilde{x}\right)}{\lambda_j^{+2}} \Phi_{j1}^+(\tilde{n}) \qquad (5.72)$$

$$\tilde{x} > 0 : \Theta(\tilde{x}, \tilde{n}) = \sum_{j=0}^{\infty} \frac{\Phi_{j1}(1)}{\lambda_j^2 \left\| \vec{\Phi}_j \right\|^2} \Phi_{j1}(\tilde{n}) + \tilde{x} \sum_{j=0}^{\infty} \frac{\Phi_{j1}(1)}{\lambda_j \left\| \vec{\Phi}_j \right\|^2} \Phi_{j1}(\tilde{n}) \qquad (5.73)$$
$$- \sum_{j=0}^{\infty} \frac{\Phi_{j1}^-(1) \Phi_{j1}^-(\tilde{n})}{\lambda_j^{-2} \left\| \vec{\Phi}_j^- \right\|^2} \exp(\lambda_j^- \tilde{x})$$

The temperature distribution given above contains for $\tilde{x} > 0$ both negative and positive eigenfunctions. The expressions for the temperature field can be further simplified by replacing the first two terms in Eq. (5.73). This results (see Appendix D) in

$$\tilde{x} \leq 0 : \Theta(\tilde{x}, \tilde{n}) = \sum_{j=0}^{\infty} A_j^+ \exp\left(\lambda_j^+ \tilde{x}\right) \Phi_{j1}^+(\tilde{n}) \qquad (5.74)$$

$$\tilde{x} > 0 : \Theta(\tilde{x}, \tilde{n}) = \Psi(\tilde{n}) + (F+1)\tilde{x} - \sum_{j=0}^{\infty} A_j^- \Phi_{j1}^-(\tilde{n}) \exp(\lambda_j^- \tilde{x}) \qquad (5.75)$$

with the function $\Psi(\tilde{n})$ given by

$$\Psi(\tilde{n}) = \int\limits_0^{\tilde{n}} \frac{F+1}{\tilde{r}^F a_2(\bar{n})} \int\limits_0^{\bar{n}} \tilde{u}(s) \tilde{r}^F ds \, d\bar{n} + C_2 = \bar{\Psi}(\tilde{n}) + C_2 \qquad (5.76)$$

where

$$C_2 = \frac{(F+1)^2}{\mathrm{Pe}_L^2} \int\limits_0^1 \tilde{r}^F a_1(\tilde{n}) d\tilde{n} - (F+1) \int\limits_0^1 \tilde{r}^F \tilde{u}(\tilde{n}) \bar{\Psi}(\tilde{n}) \, d\tilde{n} \qquad (5.77)$$

The coefficients $A_j$ are defined by

$$A_j = \frac{\Phi_{j1}(1)}{\lambda_j^2 \left\| \vec{\Phi}_j \right\|^2} = -1 \Big/ \left[ \lambda_j^2 \frac{d}{d\lambda} \left( \frac{\Phi_{j1}'(1)}{\lambda} \right)_{\lambda=\lambda_j} \right] \qquad (5.78)$$

It is interesting to focus again on the differences in the solutions for the temperature field for the case of a constant wall temperature and for the case of a constant wall heat flux. For the case of a constant wall temperature, Eqs. (5.40) and (5.41) show that the temperature in the field changes like an exp-function for positive and negative values of the axial coordinate. Physically, this means that the fluid tries to achieve asymptotically the changed wall temperature after the temperature jump at $\tilde{x} = 0$. For the case of a constant heat flux at the wall, the temperature of the fluid will rise with increasing values of the axial coordinate. This is reflected by the second term on the right hand side of Eq. (5.75). The third term in Eq. (5.75) represents the response of the system to the change in the heat flux for $\tilde{x} = 0$, whereas the first term on the right hand side in Eq. (5.75) represents the shape of the fully developed temperature distribution, for large values of the axial coordinate. This behaviour is very similar to the one already discussed in Sect. 3.3. However, there is an important difference, which lies in the fact that the inlet temperature profile (at $\tilde{x} = 0$), for the case with axial heat conduction, is now part of the solution and no longer a boundary condition.

After the temperature distribution in the flow is known, the distribution of the bulk-temperature and the Nusselt number can be calculated from their definitions given by Eqs. (3.64) and (3.65). This results in

$$\tilde{x} \leq 0 : \Theta_b(\tilde{x}) = (F+1) \sum_{j=0}^{\infty} A_j^+ \exp\left(\lambda_j^+ \tilde{x}\right) \int\limits_0^1 \tilde{u} \tilde{r}^F \Phi_{j1}^+(\tilde{n}) \, d\tilde{n} \qquad (5.79)$$

$$\tilde{x} > 0 : \Theta_b(\tilde{x}) = \frac{(F+1)^2}{\mathrm{Pe}_L^2} \int\limits_0^1 \tilde{r}^F a_1(\tilde{n}) d\tilde{n} + (F+1)\tilde{x} \qquad (5.80)$$

$$- (F+1) \sum_{j=0}^{\infty} A_j^- \exp\left(\lambda_j^- \tilde{x}\right) \int\limits_0^1 \tilde{u} \tilde{r}^F \Phi_{j1}^-(\tilde{n}) d\tilde{n} +$$

$$\tilde{x} > 0 : \text{Nu}_D = -\frac{4}{(F+1)} \left\{ \frac{(F+1)^2}{\text{Pe}_L^2} \int_0^1 \tilde{r}^F a_1(\tilde{n}) d\tilde{n} - \Psi(1) \right. \tag{5.81}$$

$$- \sum_{j=0}^{\infty} A_j^- \exp\left(\lambda_j^- \tilde{x}\right)$$

$$\left. \left[ (F+1) \int_0^1 \tilde{u} \tilde{r}^F \Phi_{j1}^-(\tilde{n}) d\tilde{n} - \Phi_{j1}^-(1) \right] \right\}$$

Because of the applied boundary conditions of an adiabatic wall for $\tilde{x} \leq 0$, the Nusselt number has to be zero in this region.

### 5.2.1 Heat Transfer in Laminar Pipe and Channel Flows for Small Peclet Numbers

For a laminar flow, the functions $a_1$ and $a_2$ are equal to one. In addition, the velocity profile is given by a simple parabolic distribution, see Eqs. (3.1) and (3.2). For this simple case, the function $\Psi(\tilde{n})$, appearing in the temperature distribution, can be predicted analytically (see e.g. Papoutsakis et al. 1980b for pipe flow). For large values of the axial coordinate ($\tilde{x} \to \infty$), the temperature distribution for $\tilde{x} > 0$, Eq. (5.75), therefore simplifies to

*Pipe*

$$\Theta(\tilde{x}, \tilde{r}) = 2\tilde{x} + \tilde{r}^2 - \frac{\tilde{r}^4}{4} + \frac{2}{\text{Pe}_L^2} - \frac{7}{24} \tag{5.82}$$

*Planar Channel*

$$\Theta(\tilde{x}, \tilde{y}) = \tilde{x} + \frac{3}{4}\tilde{y}^2 - \frac{\tilde{y}^4}{12} + \frac{1}{\text{Pe}_L^2} - \frac{1}{7} \tag{5.83}$$

which is the temperature distribution of the fully developed flow. From Eqs. (5.82) and (5.83) one can see that the effect of axial heat conduction on the fully developed temperature profile is proportional to $1/Pe_L^2$.

*Laminar Pipe Flow*

In order to investigate this case, the flow index $F$ in all equations has to be set to one. This has been investigated by Papoutsakis et al. (1980b) for the case of a semi-infinite and also for a heated zone with finite length. Although they derived in their paper equations for the local Nusselt number distribution, only temperature distributions have been shown in their paper. Figure 5.14 shows the distribution of the bulk-temperature for various values of the Peclet number. This figure elucidates the
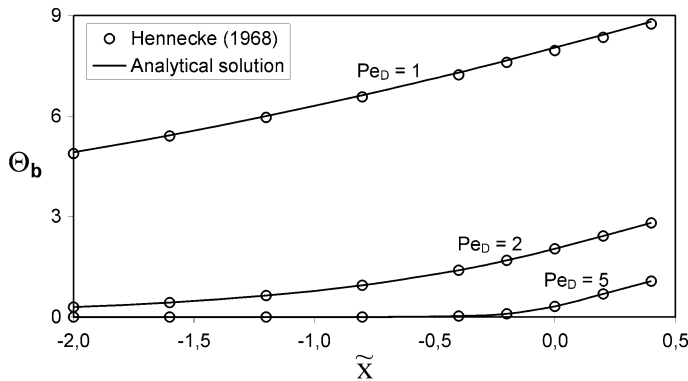
**Fig. 5.14** Distribution of the bulk-temperature for different values of the Peclet number (Weigand et al. 2001)

effect of axial heat conduction. It can be seen that for $Pe_D = 5$, the bulk-temperature is already zero for small distances upstream of $\tilde{x} = 0$. This is different for smaller Peclet numbers. For $Pe_D = 1$, one notices the large effect of the axial heat conduction in the fluid, resulting in finite values of $\Theta_b$ also far upstream of the entrance into the heating section. The analytically predicted values of the bulk-temperature have been compared with numerical predictions of Hennecke (1968) and very good agreement is found.

Figure 5.15 shows comparisons between present calculations of the local Nusselt number and predictions by Hsu (1971a), Nguyen (1992), Bilir (1992) and Hennecke (1968) for two different values of the Peclet number. As it can be seen from Fig. 5.15, the agreement between the present analytical calculations and the Nusselt number from other predictions is very good.

Figure 5.16 shows the distribution of the local Nusselt number for five different Peclet numbers (data taken from Nguyen 1992). As it can be seen from Fig. 5.16, the curves for the Nusselt numbers have an inflection point, i.e. $Nu_D$ increases with decreasing Peclet numbers. This phenomenon has been found by various workers, e.g. Hennecke (1968) and Hsu (1971a).

Weigand and Abdelmoula (2014) presented correlations for the local Nusselt number in the thermal entrance region for $\tilde{x} > 0$. These correlations have been based on the following expression for the local Nusselt number

$$\frac{Nu_D}{Nu_\infty^-} = [(a \; \exp(-b\tilde{x}^c))^n + 1]^{1/n} \tag{5.84}$$

This kind of expression has been extensively used in the past for correlating Nusselt number distributions in the thermal entrance region for constant wall heat flux boundary conditions (see e.g. Shah and London 1978). The value of $Nu_\infty^- = 4.36364$ according to Shah and London (1978). The constants in Eq. (5.84) have been determined by Weigand and Abdelmoula (2014) to
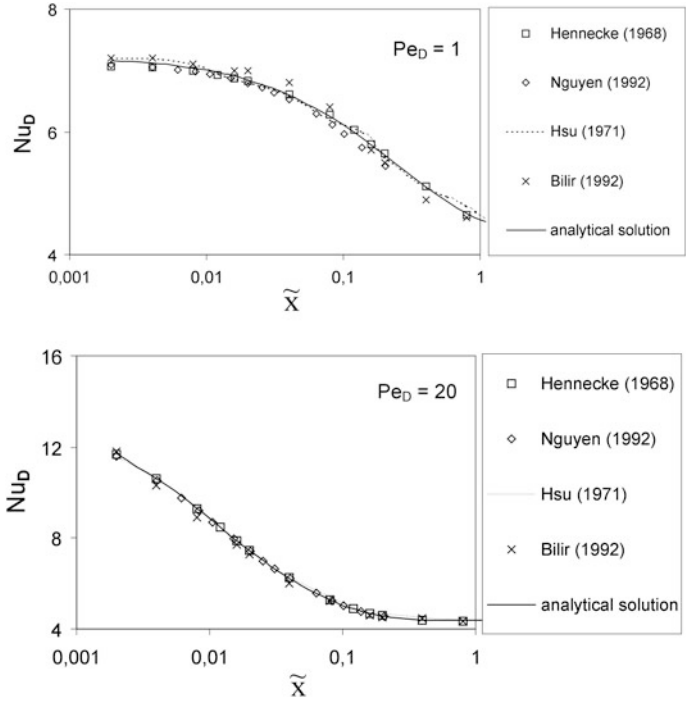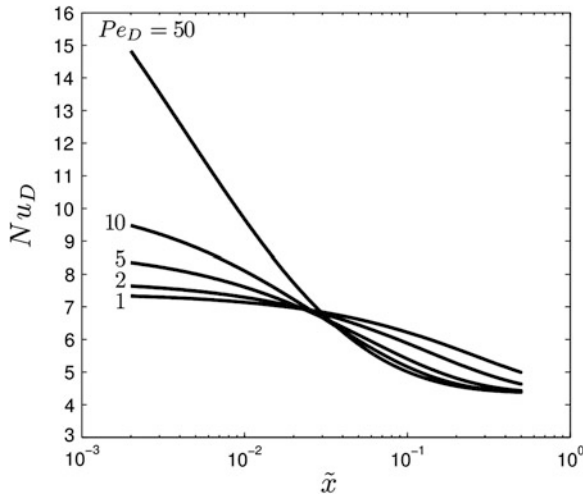
**Fig. 5.15** Distribution of the local Nusselt number for two different Peclet numbers

**Fig. 5.16** Local Nusselt numbers for pipe flow ($\dot{q}_W = \text{const.}$) and various $Pe_D$ (data taken from Nguyen 1992)

$$a = 1.257 \exp(-0.1 \, \text{Pe}_D) + 7.876 \times 10^{-4}$$
$$b = 95.55 \left( 1.002 - \exp\left(-0.05 \, \text{Pe}_D^{0.9528}\right) \right)$$
$$c = 0.3276 \exp\left(-0.02255 \, \text{Pe}_D^{0.9847}\right) + 0.3772 \tag{5.85}$$
$$n = 2.46 \exp\left(-0.5919 \, \text{Pe}_D^{0.4651}\right) + 0.1316$$

It is interesting to note that this correlation will work for arbitrary Peclet numbers. For larger Peclet numbers the distribution of the Nusselt number without axial heat conduction is obtained automatically.

### Laminar Channel Flow

In this case, the flow index $F$ has to be set to zero in all equations. Figure 5.17 shows typical temperature distributions $\Theta_W - \Theta$ for various axial locations. One clearly sees that already for $\tilde{x} < 0$ a temperature profile exists because of the axial heat conduction effects within the fluid. This profile is also present upstream of the start of the heating section. For larger values of the axial coordinate the fully developed temperature distribution, given by Eq. (5.83), is obtained asymptotically.

Also for this case a correlation for the local Nusselt number distribution has been derived by Weigand and Abdelmoula (2014). This correlation is based again on Eq. (5.84) using the following constants

$$a = 0.4538 \exp(-0.08085 \, \text{Pe}_D) - 0.01017 \exp(-0.02529 \, \text{Pe}_D) + 10^{-4}$$
$$b = 220(1.027 - \exp(-0.04062 \, \text{Pe}_D))$$
$$c = 0.2884 \exp\left(-0.01074 \, \text{Pe}_D^{1.084}\right) + 0.4364 \tag{5.86}$$
$$n = 0.6921 \exp\left(-0.1148 \, \text{Pe}_D^{0.7379}\right) + 0.1238$$

For this case $\text{Nu}_\infty^- = 8.2352941$ (see Shah and London 1978).

**Fig. 5.17** Temperature distribution $(\Theta_W - \Theta)$ for $\text{Pe}_D = 5$ and various axial positions
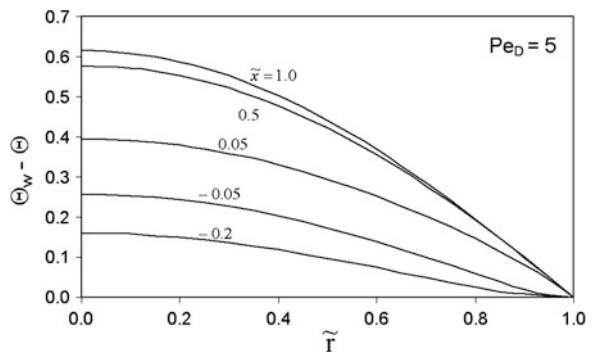
## 5.2.2 Heat Transfer in Turbulent Pipe and Channel Flows for Small Peclet Numbers

For a turbulent flow, the functions $a_1$ and $a_2$ are depending on the turbulent heat exchange in the flow. For the calculations, assuming a constant wall heat flux boundary condition, the ratio $\varepsilon_{hx}/\varepsilon_{hn}$ can be set to one and the models for the turbulent Prandtl number, explained in Sect. 5.1.2, can be used.

### Turbulent Pipe Flow

The general behaviour for turbulent pipe flow is similar to the one for laminar flow, even though radial mixing processes are enhanced by the turbulent fluctuations. Figure 5.18 shows distributions of the centerline temperature in the pipe for three different Peclet numbers and a Prandtl number of 0.001. For large Peclet number it can be seen that no heat is transferred upstream of $\tilde{x} = 0$. Therefore, this problem could be treated as parabolic. For lower values of the Peclet number, axial heat conduction effects start to change the centerline temperature upstream of $\tilde{x} = 0$. Because of the heat transferred upstream, the fluid temperature at the centerline increases to values larger than zero. Figure 5.19 shows a comparison between analytically predicted Nusselt numbers for the fully developed flow ($\overline{Nu}_\infty$) and experimental data of Fuchs (1973). It can be seen that the predictions are in good agreement with the experimental data.

Figure 5.20 shows the distribution of the local Nusselt number for different Peclet numbers and Pr = 0.001. It can be seen, that increasing values of the Peclet number result in enhanced turbulent mixing and, therefore, in increased values of the Nusselt numbers.
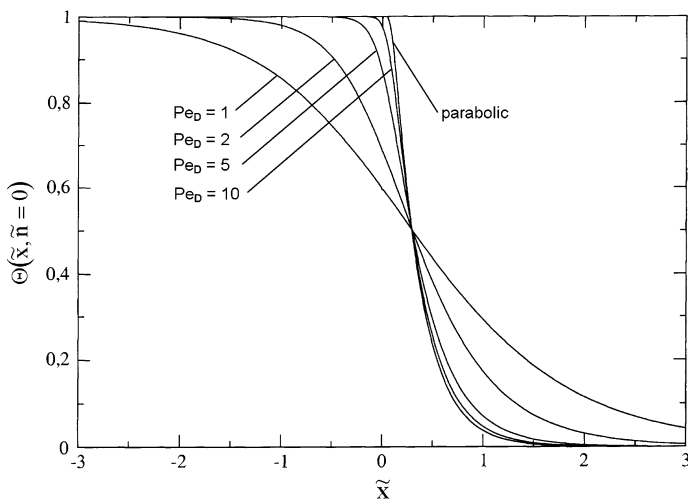


**Fig. 5.18** Temperature distribution at the pipe centerline for Pr = 0.001

**Fig. 5.19** Nusselt number for fully developed flow $(\overline{Nu}_\infty)$ as a function of the Reynolds number (adapted from Weigand et al. 1997)
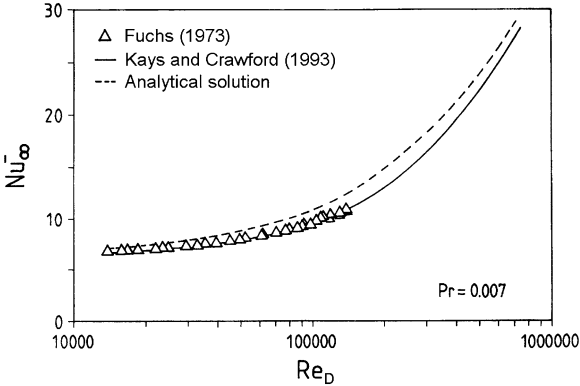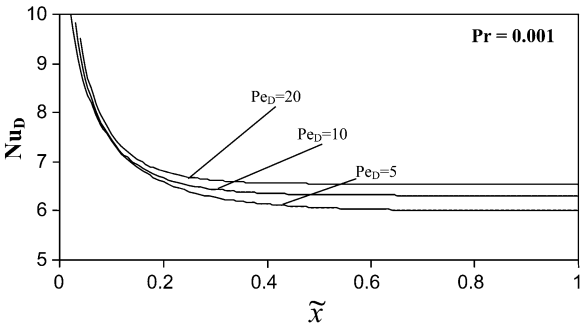
**Fig. 5.20** Variation of the local Nusselt number for different Peclet numbers and Pr = 0.001 (Weigand et al. 2001)

## Turbulent Channel Flow

For this case, the flow index $F$ has to be set to zero in all equations. Table 5.7 gives the first ten eigenvalues and constants for the turbulent flow in a parallel plate channel for Pr = 0.001 and for two different values of the Reynolds number.

As it can be seen from the entries in Table 5.7, the first non-zero negative eigenvalue $(\lambda_1^-)$ stays nearly constant for both Reynolds numbers. On the other side, it can be seen that the first non-zero positive eigenvalue $(\lambda_1^+)$ strongly increases with growing values of the Reynolds number. This shows again the decreasing importance of the effect of axial heat conduction with growing values of the Peclet number. This behaviour is very similar to the laminar flow case considered before.

**Table 5.7**  Eigenvalues and constants for turbulent channel flow with Pr = 0.001

| j | $\mathrm{Re}_D = 5000$ | | $\mathrm{Re}_D = 10{,}000$ | |
|---|---|---|---|---|
| | $\lambda_j^+$ | $A_j^+$ | $\lambda_j^+$ | $A_j^+$ |
| 0 | 0 | 0 | 0 | 0 |
| 1 | 100.72 | 2.9632E−4 | 353.45 | 4.0451E−7 |
| 2 | 179.41 | −2.0154E−3 | 622.30 | −1.9948E−05 |
| 3 | 197.87 | 4.1893E−3 | 690.36 | 2.7807E−04 |
| 4 | 223.14 | −3.9981E−3 | 729.86 | −9.6244E−04 |
| 5 | 255.70 | 2.9457E−3 | 766.13 | 1.3601E−03 |
| 6 | 290.88 | 2.2146E−3 | 817.95 | −1.2109E−03 |
| 7 | 327.40 | 1.7109E−3 | 878.26 | 1.0252E−03 |
| 8 | 364.69 | −1.3554E−3 | 943.31 | −8.7132E−04 |
| 9 | 402.47 | 1.0973E−3 | 1011.5 | 7.4558E−04 |
| 10 | 440.58 | −9.0511E−4 | 1081.8 | −6.4275E−04 |
| j | $-\lambda_j^-$ | $A_j^-$ | $-\lambda_j^-$ | $A_j^-$ |
| 0 | 0 | 0 | 0 | 0 |
| 1 | 10.31 | −1.7544E−1 | 10.82 | −1.8372E−1 |
| 2 | 34.50 | 4.2981E−2 | 40.14 | 4.7222E−2 |
| 3 | 65.28 | −1.8317E−2 | 83.48 | −2.0737E−2 |
| 4 | 99.21 | 9.8721E−3 | 136.53 | 1.1391E−2 |
| 5 | 134.85 | −6.0627E−3 | 196.11 | −7.0954E−3 |
| 6 | 171.53 | 4.0512E−3 | 260.15 | 4.7916E−3 |
| 7 | 208.88 | −2.8746E−3 | 327.31 | −3.4235E−3 |
| 8 | 246.68 | 2.1344E−3 | 396.72 | 2.5503E−3 |
| 9 | 284.80 | −1.6420E−3 | 467.82 | −1.9623E−3 |
| 10 | 323.14 | 1.2997E−3 | 540.18 | 1.5496E−3 |

## 5.3  Results for Heating Sections with a Finite Length

In the previous sections, we investigated the axial heat conduction effect for a hydrodynamically fully developed flow for a semi-infinite heating section. For this type of applications, the influence of the axial heat conduction scales very well with the Peclet number, and for flows with a Peclet number larger than 100 axial heat conduction effects can be neglected with good accuracy. Furthermore, for a hydrodynamically and thermally fully developed flow, the effect of axial heat conduction can normally be neglected with sufficient accuracy. However, the above given guidelines may not be applicable, if the length of the heating section decreases in size. It is quite obvious that axial heat conduction influences the heat transfer in a very short heated section also for larger values of the Peclet number. In addition, it should be noted that this type of problems can not be calculated correctly using the simplified energy equation (e.g. Eq. (3.14)), which is parabolic in nature. This is obvious because the parabolic nature of the simplified energy

equation permits that the end of the heating zone influences the conditions within the heating zone. The present section explains how the analytical method previously established can be adapted to this sort of problems. The resulting solutions are as simple and efficient to compute as the previously discussed solutions for the semi-infinite heating section.

### 5.3.1 Piecewise Constant Wall Temperature

This case has been investigated by Lauffer (2003) and Weigand and Lauffer (2004). The geometry under investigation is shown in Fig. 5.21. It can be seen that the wall temperature changes from $T_0$ to $T_W$ for $0 < x < x_1$. The length of the heating section is $x_1$.

The analysis presented in Sect. 5.1 can be used to solve the present problem. However, the boundary conditions have to be adapted and now are given by

$$n = L : T = T_0, x \leq 0, x \geq x_1, \tag{5.87}$$
$$T = T_W, 0 < x < x_1,$$
$$n = 0 : \partial T / \partial n = 0,$$
$$\lim_{x \to -\infty} T = T_o, \lim_{x \to +\infty} T = T_0$$

The changed boundary conditions result in a changed expression for the function $g(\tilde{x})$, which appears in Eqs. (5.36) and (5.37). If the integrals in Eqs. (5.36) and (5.37) are solved, the following temperature distribution in the fluid can be obtained (Lauffer 2003)
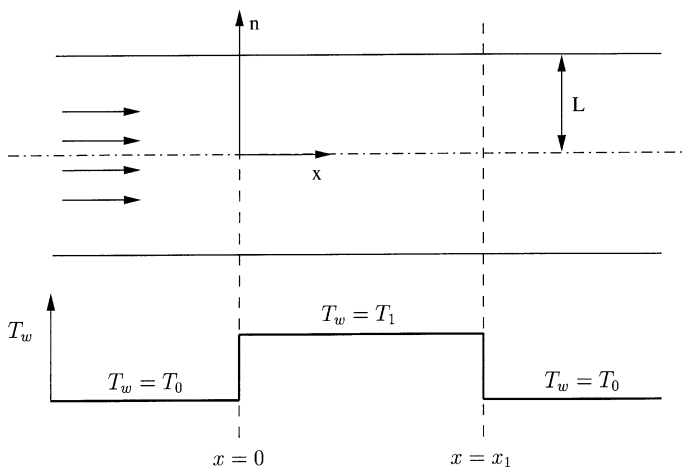


**Fig. 5.21** Geometry and boundary condition for a piecewise constant wall temperature

$$\tilde{x} \leq 0 : \Theta(\tilde{x}, \tilde{n}) = 1 + \sum_{j=0}^{\infty} A_j^+ \Phi_{j1}^+(\tilde{n}) \exp(\lambda_j^+ \tilde{x}) \left[ 1 - \exp(-\lambda_j^+ \tilde{x}_1) \right] \qquad (5.88)$$

$$0 < \tilde{x} < \tilde{x}_1 : \qquad\qquad\qquad\qquad\qquad\qquad\qquad\qquad\qquad\qquad (5.89)$$

$$\Theta(\tilde{x}, \tilde{n}) = - \sum_{j=0}^{\infty} A_j^- \Phi_{j1}^-(\tilde{n}) \exp\left( \lambda_j^- \tilde{x} \right) - \sum_{j=0}^{\infty} A_j^+ \Phi_{j1}^+(\tilde{n}) \exp\left( \lambda_j^+ (\tilde{x} - \tilde{x}_1) \right)$$

$$\tilde{x} \geq \tilde{x}_1 : \Theta(\tilde{x}, \tilde{n}) = 1 - \sum_{j=0}^{\infty} A_j^- \Phi_{j1}^-(\tilde{n}) \exp\left( \lambda_j^- \tilde{x} \right) \left[ 1 - \exp(-\lambda_j^- \tilde{x}_1) \right] \qquad (5.90)$$

where $\tilde{x}_1 = x_1/(L\mathrm{Pe}_L)$. From the above equations, it can be seen that for $\tilde{x}_1 \to \infty$ the results for the semi-infinite heating section are obtained, (see Eqs. (5.48) and (5.49)). Furthermore, it is interesting to note that for the case of a finite heated section the temperature distribution within the heating zone is influenced by positive and negative eigenvalues and eigenfunctions (see Eq. (5.89)). The distribution of the Nusselt number can be obtained from the definition of this quantity and the known temperature distribution given by Eqs. (5.88)–(5.90). This results in

$$\tilde{x} \leq 0 : \mathrm{Nu}_D = \frac{-4 \sum_{j=0}^{\infty} A_j^+ \Phi_{j1}'^+(1) \left[ \exp(\lambda_j^+ \tilde{x}) - \exp\left( \lambda_j^+ (\tilde{x} - \tilde{x}_1) \right) \right]}{4^F \sum_{j=0}^{\infty} A_j^+ \int_0^1 \Phi_{j1}^+(\tilde{n}) \tilde{u} \, \tilde{r}^F d\tilde{n} \left[ \exp(\lambda_j^+ \tilde{x}) - \exp\left( \lambda_j^+ (\tilde{x} - \tilde{x}_1) \right) \right]}$$
$$(5.91)$$

$$0 < \tilde{x} < \tilde{x}_1 :$$
$$\mathrm{Nu}_D = \frac{-4 \sum_{j=0}^{\infty} A_j^+ \Phi_{j1}'^+(1) - 4 \sum_{j=0}^{\infty} A_j^- \Phi_{j1}'^-(1) \exp(\lambda_j^- \tilde{x})}{N} \qquad (5.92)$$

$$N = 4^F \sum_{j=0}^{\infty} A_j^+ \int_0^1 \Phi_{j1}^+(\tilde{n}) \tilde{u} \, \tilde{r}^F d\tilde{n} \exp\left( \lambda_j^+ (\tilde{x} - \tilde{x}_1) \right) \qquad (5.93)$$

$$+ 4^F \sum_{j=0}^{\infty} A_j^- \int_0^1 \Phi_{j1}^-(\tilde{n}) \tilde{u} \, \tilde{r}^F d\tilde{n} \exp\left( \lambda_j^- \tilde{x} \right)$$

$$\tilde{x} \geq \tilde{x}_1 : \mathrm{Nu}_D = \frac{-4 \sum_{j=0}^{\infty} A_j^- \Phi_{j1}'^-(1) \left[ \exp(\lambda_j^- \tilde{x}) - \exp\left( \lambda_j^- (\tilde{x} - \tilde{x}_1) \right) \right]}{4^F \sum_{j=0}^{\infty} A_j^- \int_0^1 \Phi_{j1}^-(\tilde{n}) \tilde{u} \, \tilde{r}^F d\tilde{n} \left[ \exp(\lambda_j^- \tilde{x}) - \exp\left( \lambda_j^- (\tilde{x} - \tilde{x}_1) \right) \right]}$$
$$(5.94)$$

The above equations for the distribution of the Nusselt number reduce to the ones given by Eqs. (5.52) and (5.53) for the case of a semi-infinite heating zone $(\tilde{x}_1 \rightarrow \infty)$.

As mentioned before, the problem of a piecewise heated planar channel has been solved numerically by Weigand et al. (2002). Figure 5.22 shows a comparison between the analytically and numerically predicted distribution of the bulk-temperature (Lauffer 2003) for a turbulent flow and a length of the heated zone of $\tilde{x}_1 = 0.1$. It can be seen that the bulk-temperature tries to approach the wall temperature within the heated section. At the end of the heated section, the bulk-temperature decreases then towards the uniform temperature $T_0$. If the axial coordinate is scaled by the length of the heating zone $(\hat{x} = \tilde{x}/\tilde{x}_1)$, the effect of a changing length of the heating zone can be seen nicely.

Figure 5.23 shows the relative error between a parabolic and an elliptic calculation for $Pe_D = 10$ and a laminar flow through a circular pipe. It can be seen that near the start and the end of the heating section always a large deviation between the elliptic and the parabolic calculation exists. In these areas, the axial heat conduction in the fluid changes the temperature distribution substantially in the pipe and therefore the values of the Nusselt number are changed. If the heating zone decreases in length, axial heat conduction might be important throughout the full heated section. For such a situation, the complete energy equation has to be taken into account. This is clearly visible in Fig. 5.23. For the short heating section of $\tilde{x}_1 = 0.1$, the axial heat conduction in the flow results in a dramatic change of the temperature field, resulting in about 40 % relative error in the Nusselt number, even in the middle of the heated section.
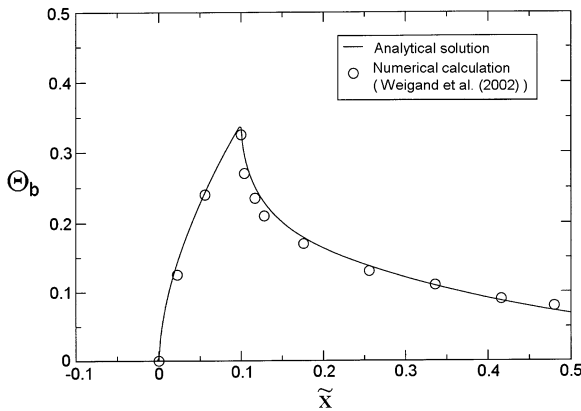


**Fig. 5.22** Comparison between a numerically and an analytically predicted distribution of the bulk-temperature for a turbulent flow in a parallel plate channel with turbulent internal flow $(Re_D = 40{,}000, Pr = 0.01, \tilde{x}_1 = 0.1)$
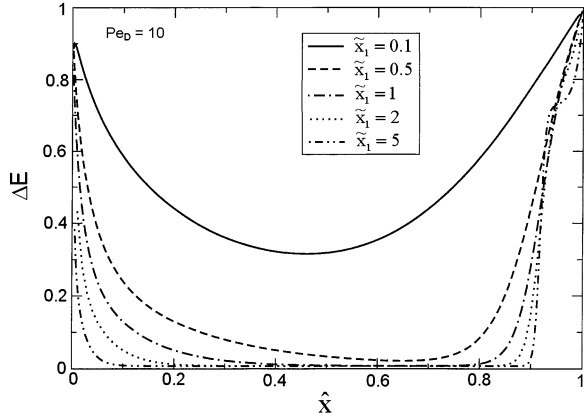
**Fig. 5.23** Relative error of the Nusselt number between elliptic and parabolic calculations for a laminar pipe flow ($Pe_D = 10$) with different length of the heating section

## 5.3.2 Piecewise Constant Wall Heat Flux

The case of a piecewise constant wall heat flux has been discussed by Papoutsakis et al. (1980b) and Weigand et al. (2001). The solution approach is very similar to the one outlined above for the piecewise constant wall temperature. The geometry and the boundary conditions under investigation are shown in Fig. 5.24.
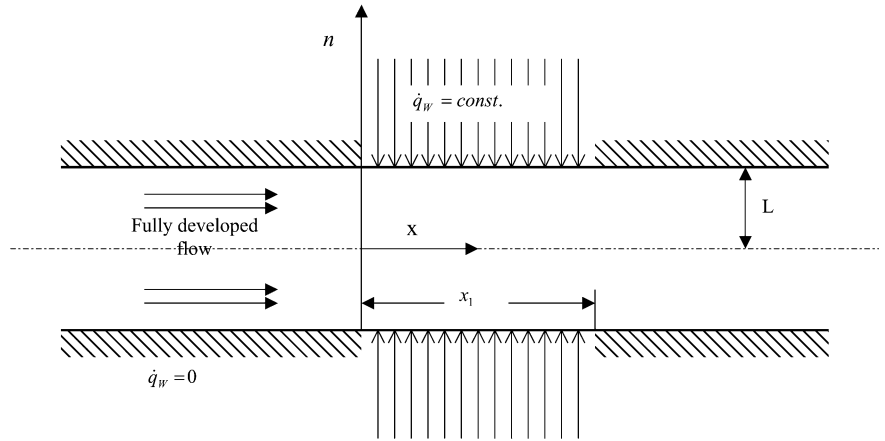


**Fig. 5.24** Geometrical configuration and boundary conditions

The boundary conditions given by Eq. (5.64) have to be changed according to

$$n = 0 : \frac{\partial T}{\partial n} = 0, \tag{5.95}$$

$$n = L : x \leq 0, x \geq x_1 : \frac{\partial T}{\partial n} = 0,$$

$$0 < x < x_1 : \frac{\partial T}{\partial n} = \frac{\dot{q}_w}{k}$$

$$\lim_{x \to -\infty} T = T_0$$

This results in a changed description of the boundary conditions for $E$. This means that Eq. (5.65) has to be replaced by

$$\lim_{\tilde{x} \to -\infty} E = 0, \quad \tilde{n} = 0 : E = 0 \tag{5.96}$$

$$\tilde{n} = 1 : E = \begin{cases} 0, & -\infty < \tilde{x} \leq 0 \\ \tilde{x}, & 0 < \tilde{x} < \tilde{x}_1 \\ \tilde{x}_1, & \tilde{x}_1 \leq \tilde{x} < \infty \end{cases}$$

This changed expression for $E(\tilde{x}, 1)$ has to be inserted into the integrals in Eqs. (5.70) and (5.71). These are, however, all the changes we need to do in order to solve this relatively complicated problem. Evaluating Eqs. (5.70) and (5.71) results in the following temperature distribution for this case (Weigand et al. 2001)

$$\tilde{x} \leq 0 : \Theta(\tilde{x}, \tilde{n}) = \sum_{j=0}^{\infty} \frac{\Phi_{j1}^+(1)}{\left\| \vec{\Phi}_j^+ \right\|^2} \frac{\exp\left(\lambda_j^+ \tilde{x}\right)}{\lambda_j^{+2}} \left[ 1 - \exp\left(-\lambda_j^+ \tilde{x}_1\right) \right] \Phi_{j1}^+(\tilde{n}) \tag{5.97}$$

$$0 < \tilde{x} < \tilde{x}_1 : \Theta(\tilde{x}, \tilde{n}) = \Psi(\tilde{n}) + (F+1)\tilde{x} - \sum_{j=0}^{\infty} A_j^- \Phi_{j1}^-(\tilde{n}) \exp\left(\lambda_j^- \tilde{x}\right) \tag{5.98}$$

$$- \sum_{j=0}^{\infty} A_j^+ \Phi_{j1}^+(\tilde{n}) \exp\left(\lambda_j^+ (\tilde{x} - \tilde{x}_1)\right)$$

$$\tilde{x} \geq \tilde{x}_1 : \Theta(\tilde{x}, \tilde{n}) = (F+1)\tilde{x}_1 + \sum_{j=0}^{\infty} A_j^- \Phi_{j1}^-(\tilde{n}) \left[ \exp\left(-\lambda_j^- \tilde{x}_1\right) - 1 \right] \exp\left(\lambda_j^- \tilde{x}\right)$$

$$\tag{5.99}$$

with the function $\Psi(\tilde{n})$ given by Eq. (5.76). Again the distribution of the bulk-temperature and the Nusselt number can be calculated from the definitions of these quantities and one finally obtains

$$\tilde{x} \leq 0: \ \Theta_b(\tilde{x}) = (F+1)\sum_{j=0}^{\infty} A_j^+ \left[1 - \exp\left(-\lambda_j^+ \tilde{x}_1\right)\right] \exp\left(\lambda_j^+ \tilde{x}\right) \int_0^1 \tilde{u}\tilde{r}^F \Phi_{j1}^+(\tilde{n})\, d\tilde{n}$$

$$(5.100)$$

$$0 < \tilde{x} < \tilde{x}_1: \ \Theta_b(\tilde{x}) = \frac{(F+1)^2}{\mathrm{Pe}_L^2} \int_0^1 \tilde{r}^F a_1(\tilde{n})d\tilde{n} + (F+1)\tilde{x} \qquad (5.101)$$

$$- (F+1)\sum_{j=0}^{\infty} A_j^- \exp\left(\lambda_j^- \tilde{x}\right) \int_0^1 \tilde{u}\tilde{r}^F \Phi_{j1}^-(\tilde{n})d\tilde{n}$$

$$- (F+1)\sum_{j=0}^{\infty} A_j^+ \exp\left(\lambda_j^+ (\tilde{x} - \tilde{x}_1)\right) \int_0^1 \tilde{u}\tilde{r}^F \Phi_{j1}^+(\tilde{n})d\tilde{n}$$

$$\tilde{x} \geq \tilde{x}_1:$$

$$\Theta_b = (F+1)\left\{\tilde{x}_1 - \sum_{j=0}^{\infty} A_j^- \left[\exp\left(-\lambda_j^- \tilde{x}_1\right) - 1\right] \exp\left(\lambda_j^- \tilde{x}\right) \int_0^1 \tilde{u}\tilde{r}^F \Phi_{j1}^-(\tilde{n})d\tilde{n}\right\}$$

$$(5.102)$$

The Nusselt number is zero for $\tilde{x} \leq 0$ and for $\tilde{x} \geq \tilde{x}_1$. For $0 < \tilde{x} < \tilde{x}_1$ the Nusselt number is given by

$$\mathrm{Nu}_D = -\frac{4}{(F+1)}\left\{\frac{(F+1)^2}{\mathrm{Pe}_L^2} \int_0^1 \tilde{r}^F a_1(\tilde{n})d\tilde{n} - \Psi(1)\right. \qquad (5.103)$$

$$- \sum_{j=0}^{\infty} A_j^- \exp\left(\lambda_j^- \tilde{x}\right) \left[(F+1)\int_0^1 \tilde{u}\tilde{r}^F \Phi_{j1}^-(\tilde{n})d\tilde{n} - \Phi_{j1}^-(1)\right]$$

$$\left. - \sum_{j=0}^{\infty} A_j^+ \exp\left(\lambda_j^+ (\tilde{x} - \tilde{x}_1)\right) \left[(F+1)\int_0^1 \tilde{u}\tilde{r}^F \Phi_{j1}^+(\tilde{n})d\tilde{n} - \Phi_{j1}^+(1)\right]\right\}^{-1}$$

## 5.4  Application of the Solution Method to Related Problems

The present method can be easily adapted to other related problems. Papoutsakis and Ramkrishna (1981) used the method for example for predicting the heat transfer in a capillary flow emerging from a reservoir. If source terms are present in the energy equation, the method can still provide a complete solution of the problem. The reader is referred to Weigand et al. (1993) for such an application of the method.

The method can also be used to solve related problems with other geometries. Weigand et al. (1997) and Weigand and Wrona (2003) used the method to solve the extended Graetz problem for laminar and turbulent flows inside concentric annuli for constant wall temperature as well as for piecewise constant wall heat flux boundary conditions. The geometry and the boundary conditions are shown in Fig. 5.25.
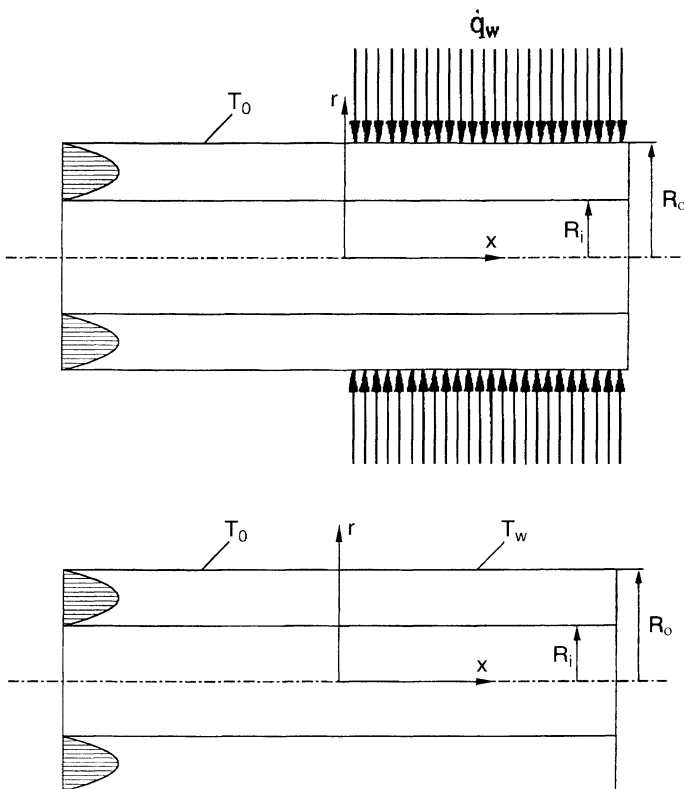


**Fig. 5.25**  Geometrical configuration and boundary conditions for the extended Graetz problem in a concentric annuli

If another geometry is investigated, the definition of the inner product, given by Eq. (5.14), needs to be adapted. For the heat transfer in concentric annuli it takes the form (see Weigand et al. 1997)

$$
\left\langle \vec{\Phi}, \vec{\Upsilon} \right\rangle = (1 - \chi) \int\limits_0^1 \left[ \begin{array}{c} \dfrac{a_1(\tilde{r})((1 - \chi)\tilde{r} + \chi)}{\mathrm{Pe}_D^2} \Phi_1(\tilde{r}) \Upsilon_1(\tilde{r}) \\[2ex] + \dfrac{\Phi_2(\tilde{r}) \Upsilon_2(\tilde{r})}{4(1 - \chi)^2 a_2(\tilde{r})((1 - \chi)\tilde{r} + \chi)} \end{array} \right] d\tilde{r} \qquad (5.104)
$$

where the following abbreviations have been used

$$
\chi = \frac{R_i}{R_o}, D = 2(R_o - R_i), \quad \tilde{r} = \frac{r - R_i}{R_o - R_i} \qquad (5.105)
$$

Figure 5.26 shows, as an example, one result for the heat transfer in a concentric annuli with a constant wall heat flux for laminar flow. The distribution of the Nusselt number is compared with an analytical solution by Hsu (1970), which has been constructed from two independent series solutions for $x < 0$ and $x > 0$. Both, the temperature distribution and the temperature gradient were then matched at $x = 0$ by constructing a pair of orthonormal functions from the eigenfunctions and using the Gram-Schmidt orthonormalization procedure. This method, therefore, was quite cumbersome for finding the solution of the problem. Compared to this solution, the present approach presents the analytical solution in a form, which is as simple as the one for the parabolic problem.



Fig. 5.26 Local Nusselt number for a concentric annulus with constant heat flux at the wall (Weigand and Wrona 2003)
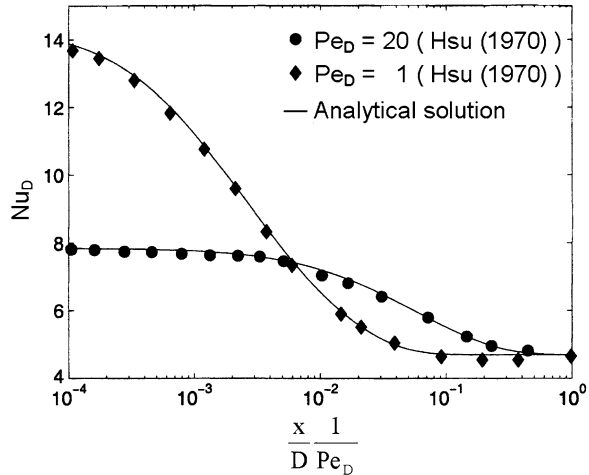
For more detailed explanations and for applications for turbulent flows inside concentric annuli the reader is referred to Weigand et al. (1997) and Weigand and Wrona (2003). Weigand and Eisenschmidt (2012) investigated the extended Graetz problem with piecewise constant wall temperatures at the outer wall for laminar and turbulent flows through a concentric annulus. For the inner cylinder two different temperature boundary conditions have been investigated; adiabatic or piecewise constant temperature variations. Similar as for pipe flows, it has been shown that the heating zone's length is an important parameter. A small length of the heating zone requires the consideration of axial heat conduction effects for nearly all Peclet numbers. As the heating zone gets smaller and smaller, the behaviour of the temperature field in the flow gets more and more effected by the finite length of the heating zone and elliptic effects cannot be ignored any longer.

Weigand and Gassner (2007) investigated the effect of a finite wall thickness on the heat transfer with taking axial heat conduction in the flow into account. An analytical solution with the method shown in this chapter has been obtained for a planar channel with a finite wall thickness. A piecewise constant temperature at the outer wall has been considered. The geometry and the coordinate system for this configuration is shown in Fig. 5.27.

In Fig. 5.27 it can be seen that the length of the higher wall temperature is $2\,l_1$. Figure 5.28 shows the temperature distribution $\Theta_W = (T_W - T_0)/(T_1 - T_0)$ for various values of the dimensionless wall thickness $\tilde{d} = d/h$. It can be seen that the temperature distribution at the inner wall cannot follow the outer prescribed piecewise constant temperature for larger values of the wall thickness.

The analytical solution has been compared to a numerical solution with FLUENT and good agreement has been found.

The above described method has also been used for the prediction of the thermally developing laminar flow of a dipolar fluid in a duct by Akyildiz and Bellout (2004). Dipolar fluids are the simplest example of a class of non-Newtonian fluids called multipolar fluids (see Bleustein and Green 1967 for a more detailed information about dipolar fluids).

**Fig. 5.27** Geometrical configuration and coordinate system (Weigand and Gassner 2007)
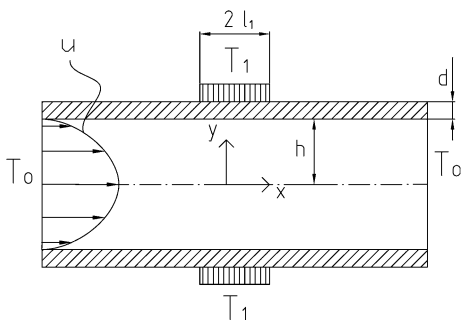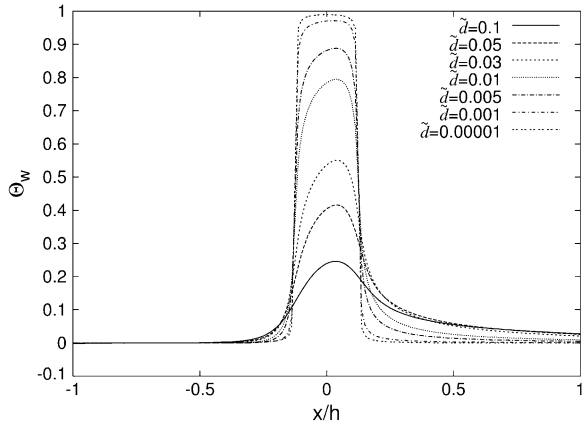
**Fig. 5.28** Wall temperature
distribution at the inner wall
for various values of the wall
thickness for $Re_D = 1000$,
$Pr = 0.005$, $l_1/l = 200$
(Weigand and Gassner 2007)



## Problems

5-1 Consider the flow and heat transfer in a planar channel with height $2h$. The
plates have a constant wall temperature $T_0$ for $x \leq 0$ and $T_W$ for $x > 0$. The
velocity profile of the laminar flow in the planar duct can be simplified to a
slug flow profile with $u = \bar{u} = \text{const}$. The velocity component in the $y$-
direction $v = 0$. All fluid properties can be considered to be constant. Axial
heat conduction in the flow cannot be neglected, because of small values of the
Peclet number. The temperature distribution in the fluid can be calculated from
the energy equation

$$u \frac{\partial T}{\partial x} = a \left( \frac{\partial^2 T}{\partial x^2} + \frac{\partial^2 T}{\partial y^2} \right)$$

with the boundary conditions

$$x = 0 : T = T_0$$

$$y = 0 : \frac{\partial T}{\partial y} = 0, \quad y = h : T = T_W$$

(a) Introduce the following dimensionless quantities

$$\tilde{x} = \frac{x}{h} \frac{a}{\bar{u}h} = \frac{x}{h} \frac{1}{Pe}, \tilde{y} = \frac{y}{h}, \Theta = \frac{T - T_W}{T_0 - T_W}$$

What is the resulting differential equation and the boundary conditions in
dimensionless form?

(b) Show that the above considered problem reduces in case of negligible
axial heat conduction in the fluid ($Pe \rightarrow \infty$) to Problem 3.3.

(c) Use the method of separation of variables to solve the given problem
($\Theta = f(\tilde{x})g(\tilde{y})$). What equations are obtained for the functions $f$ and $g$?

(d) Predict the complete solution for the temperature field.

(e) Compare the obtained temperature distribution with the one of Problem 3.3 for three different Peclet numbers (Pe = 0.1, 1, 2) for $x/h = 1$. What influence has the axial heat conduction on the temperature profile?

(f) Was it physically correct to prescribe a constant temperature distribution for $x = 0$? Explain your answer.

5-2 Problem 5-1 should now be solved with the method outlined in this chapter. The boundary condition for $x = 0 : T = T_0$ is replaced by

$$\lim_{x \to -\infty} T = T_0, \quad \lim_{x \to \infty} T = T_W$$

(a) Introduce the dimensionless quantities given in Problem 5.1. What is the resulting dimensionless differential equation and what are the boundary conditions?

(b) Split the problem into two first order partial differential equations by introducing a solution vector $\vec{S}$ consisting of the temperature and the axial energy flow. What system of differential equations is obtained? Show the associated eigenvalue problem and obtain its solution.

(c) Determine the complete solution of the problem.

(d) Compare your solution to the one of Problem 5.1 for $x/h = 1$ for different Peclet numbers. Explain your observations.

5-3 Consideration is given to the heat transfer in a concentric annulus which has constant temperatures at the inner and outer radii for $x \le 0$ and a temperature jump for $x > 0$ at the outer radius. Show from the definition of the inner product (Eq. (5.104)) that

$$\left\langle \vec{\Phi}, \underline{L} \tilde{\Upsilon} \right\rangle = \left\langle \underline{L} \vec{\Phi}, \tilde{\Upsilon} \right\rangle$$

5-4 Show for the heat transfer in a parallel plate channel that

$$\left\langle \vec{\Phi}_j, \vec{\Phi}_k \right\rangle = 0 \text{ for } \lambda_j \ne \lambda_k$$

by considering the eigenvalue problems

$$\underline{L} \vec{\Phi}_j = \lambda_j \vec{\Phi}_j \text{ and } \underline{L} \vec{\Phi}_k = \lambda_k \vec{\Phi}_k$$

for the case of a constant wall temperature.

5-5 Derive from Eqs. (5.76) and (5.77) the fully developed temperature distribution for large axial values for the case of laminar heat transfer in a pipe or a parallel plate channel with constant wall heat flux. Show that Eq. (5.82) is obtained in case of a circular pipe, whereas Eq. (5.83) is obtained for a parallel plate channel.

# Chapter 6
# Nonlinear Partial Differential Equations

In the previous chapters, we discussed the solution of linear partial differential equations. Special focus was given to the solution of internal heat transfer problems for duct flows. However, in most technical applications, problems are often described by nonlinear partial differential equations. For a lot of these applications, the equations have to be solved by numerical methods. In contrast to the large amount of literature dealing with the solution of linear partial differential equations, much less literature exists on the solution of nonlinear partial differential equations. One of the major difficulties arising in the solution of nonlinear problems is that we are no longer able to use the powerful superposition method for constructing solutions as for linear problems. Sometimes, the equations under consideration may be solved by using perturbation methods. An example on how to use this sort of method was shown in Chap. 4 for the solution of eigenvalue problems. In the present chapter, we do not discuss this solution approach. We will just look at one example on how to use a regular perturbation method to derive solutions for such problems. The interested reader is referred to the books of van Dyke (1964), Kevorkian and Cole (1981), Simmonds and Mann (1986), Aziz and Na (1984) and Schneider (1978) for many interesting applications of the perturbation method to fluid dynamics and heat transfer problems. In the following sections, we intend to provide a short overview on some selected solution methods for nonlinear partial differential equations occurring in heat transfer and fluid flow problems. The solution approaches discussed here include, for example, the method of separation of variables, the Kirchhoff transformation, and special solutions of the energy equation. However, the focal point of this chapter is on similarity solutions for the heat conduction and boundary layer equations. Here an overview is given on different methods and on how to determine these solutions. Similarity solutions are not only of importance because they may lead to analytical solutions of the underlying nonlinear partial differential equations, but also, because they play today an important role as excellent benchmark cases for testing computer codes.

## 6.1 The Method of Separation of Variables

This solution method can also be used for nonlinear partial differential equations. However, since we can not use the superposition principle to fulfill arbitrary boundary conditions, we have to find a solution which already satisfies the partial differential equation and the related boundary conditions. The method is explained for the flow and heat transfer on a rotating disk, which rotates with the constant angular velocity $\omega$ in a quiescent fluid. The geometry under investigation is depicted in Fig. 6.1.

Under the assumptions of angular symmetry for a laminar, incompressible flow with constant fluid properties and negligible viscous dissipation, the conservation equations in cylindrical coordinates can be written in the following form (see for example Schlichting 1982).
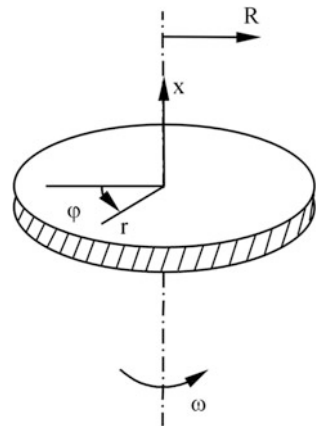
**Navier-Stokes Equations**

$$v\frac{\partial v}{\partial r} - \frac{w^2}{r} + u\frac{\partial v}{\partial x} = -\frac{1}{\rho}\frac{\partial p}{\partial r} + \frac{\mu}{\rho}\left[\frac{\partial^2 v}{\partial r^2} + \frac{\partial}{\partial r}\left(\frac{v}{r}\right) + \frac{\partial^2 v}{\partial x^2}\right] \tag{6.1}$$

$$v\frac{\partial w}{\partial r} + \frac{wv}{r} + u\frac{\partial w}{\partial x} = \frac{\mu}{\rho}\left[\frac{\partial^2 w}{\partial r^2} + \frac{\partial}{\partial r}\left(\frac{w}{r}\right) + \frac{\partial^2 w}{\partial x^2}\right] \tag{6.2}$$

$$v\frac{\partial u}{\partial r} + u\frac{\partial u}{\partial x} = -\frac{1}{\rho}\frac{\partial p}{\partial x} + \frac{\mu}{\rho}\left[\frac{\partial^2 u}{\partial r^2} + \frac{1}{r}\frac{\partial u}{\partial r} + \frac{\partial^2 u}{\partial x^2}\right] \tag{6.3}$$



**Fig. 6.1** Physical model and coordinate system for the rotating disk

**Continuity Equation**

$$\frac{\partial v}{\partial r} + \frac{v}{r} + \frac{\partial u}{\partial x} = 0 \tag{6.4}$$

**Energy Equation**

$$v\frac{\partial T}{\partial r} + u\frac{\partial T}{\partial x} = a\left(\frac{\partial^2 T}{\partial r^2} + \frac{1}{r}\frac{\partial T}{\partial r} + \frac{\partial^2 T}{\partial x^2}\right) \tag{6.5}$$

For the rotating disk, the velocity components $u$, $v$ and $w$ denote the flow in the $x$-, $r$- and $\varphi$-direction. Furthermore, we assume that the radius $R$ of the rotating disk is very large ($R \to \infty$), so that no boundary conditions have to be satisfied for a finite value of the radius.

The boundary conditions for the above equations are given by

$$\begin{array}{llll} x = 0: & u = 0, & v = 0, & w = r\omega, & T = T_W \\ x \to \infty: & & v = 0, & w = 0, & T = T_\infty \end{array} \tag{6.6}$$

No boundary condition is provided for $u(x \to \infty)$, because we only know that this quantity attains a finite value for $x \to \infty$.

As stated above, we consider an incompressible fluid with constant fluid properties. Therefore, the energy equation is decoupled from the momentum equations and the continuity equation. This means that we can first solve the momentum equations and subsequently the energy equation. Let us assume that the solution to Eqs. (6.1)–(6.4) can be represented by the products

$$\begin{aligned} v &= A(r)\,F(x) \\ w &= B(r)\,G(x) \\ u &= C(r)\,H(x) \end{aligned} \tag{6.7}$$

From the boundary conditions given by Eq. (6.6), one immediately obtains

$$w = B(r)\,G(0) = r\omega \tag{6.8}$$

From this equation it follows that $B(r) = B_1 r$, where $B_1$ is a constant. If we select this constant to be equal to $\omega$, it follows

$$w = r\omega\,G(x), \quad G(0) = 1 \tag{6.9}$$

After having gained some knowledge of the tangential velocity component $w$, let us now introduce the expressions given by Eq. (6.9) into the tangential component of the Navier-Stokes equations, Eq. (6.2). This results in

$$v\omega G(x) + vG(x)\omega + urG'(x)\omega = rG''(x)\omega r\mu/\rho \tag{6.10}$$

Introducing also Eq. (6.7) into Eq. (6.10) leads to

$$\begin{aligned} &\omega A(r)F(x)G(x) + \omega A(r)F(x)G(x) \\ &+ C(r)H(x)r\omega G'(x) = \omega rG''(x)\mu/\rho \end{aligned} \tag{6.11}$$

Comparing the left hand side of this equation to the right hand side, it is clear that Eq. (6.11) can only have a solution if the function $A(r) = A_1 r$ and $C(r) = C_1$. Selecting the arbitrary constants $A_1$ and $C_1$ leads to

$$\begin{aligned} A(r) &= r\omega \\ C(r) &= \sqrt{\omega\mu/\rho} \end{aligned} \tag{6.12}$$

This selection of constants guarantees that the functions $A$, $B$ and $C$ have the same dimensions. Summarizing, the velocity field is given by

$$\begin{aligned} v &= r\omega\, F(x) \\ w &= r\omega\, G(x) \\ u &= \sqrt{\omega\mu/\rho}\, H(x) \end{aligned} \tag{6.13}$$

Introducing the above expressions into the momentum equation in the $x$-direction results in

$$(\omega\mu/\rho)H(x)H'(x) = -\frac{1}{\rho}\frac{\partial p}{\partial x} + \mu/\rho\sqrt{\omega\mu/\rho}\, H''(x) \tag{6.14}$$

From Eq. (6.14) it follows that

$$\frac{\partial p}{\partial x} = p'(x) \rightarrow p = p(x) + I(r) \tag{6.15}$$

Furthermore, one sees from Eq. (6.14) that we can simplify this equation by introducing the following dimensionless coordinate

$$\eta = x\sqrt{\frac{\omega\rho}{\mu}} \tag{6.16}$$

Inserting Eqs. (6.15) and (6.16) into Eq. (6.14) results in

$$H(\eta)H'(\eta) = -\tilde{p}' + H''(\eta), \quad \tilde{p} = p/(\mu\omega) \tag{6.17}$$

where the prime in Eq. (6.17) indicates the differentiation with respect to $\eta$. Introducing Eq. (6.13) and Eqs. (6.15) and (6.16) into Eq. (6.1) gives

$$\omega^2 F^2 - \omega^2 G^2 + \sqrt{\omega\mu/\rho}\,\omega F' H - \mu/\rho\omega F'' = -\frac{1}{\rho}\frac{I'(r)}{r} \tag{6.18}$$

Because on the left hand side of this equation all quantities only depend on the axial coordinate, the right hand side of this equation can not be a function of $r$ and thus must be a constant. This leads to the following expression for the function $I(r)$

$$I(r) = C_1 \frac{r^2}{2} + C_2 \tag{6.19}$$

If we examine the pressure distribution for $\eta \to \infty$, the pressure needs to attain a uniform value. This means, that the constant $C_1$ in Eq. (6.19) must be zero. The constant $C_2$ can be included into $p(\eta)$ given by Eq. (6.15). Thus, all expressions for the velocity components and the pressure are known. Introducing Eqs. (6.13), (6.15) and (6.16) into Eqs. (6.1)–(6.4) and the associated boundary conditions, Eq. (6.6), results in the following set of ordinary differential equations, which has to be solved for obtaining the velocity distribution over the rotating disk

$$F^2 - G^2 + HF' = F'' \tag{6.20}$$

$$2FG + HG' = G'' \tag{6.21}$$

$$HH' = -\tilde{p}' + H'' \tag{6.22}$$

$$2F + H' = 0 \tag{6.23}$$

with the boundary conditions

$$\eta = 0 :\;\; F = 0,\, G = 1,\, H = 0 \tag{6.24}$$
$$\eta \to \infty : F = 0,\, G = 0$$

The above set of equations has been solved first by von Kármán (1921) by using an approximation method. Later Cochran (1934) presented a more accurate solution for the equations.

Figure 6.2 shows the distribution of the functions $F$, $G$ and $H$ as taken from data reported by Cochran (1934). From Fig. 6.2, it can be seen that the radial and circumferential velocity components decrease rapidly with increasing values of $\eta$, while the axial velocity component attains a finite value for large axial distances away from the rotating semi-infinite disk.
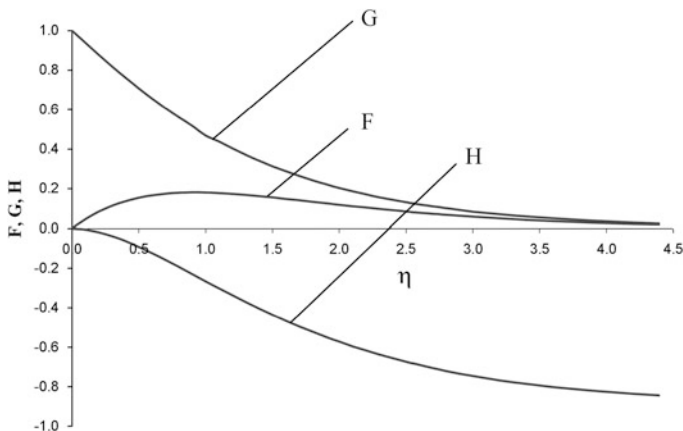
**Fig. 6.2** Velocity distribution on a rotating disk (graph compiled from data reported by Cochran 1934)

Let us now focus on the heat transfer problem for the rotating semi-infinite disk. Introducing the known velocity distribution, Eq. (6.13), and the dimensionless coordinate, Eq. (6.16), into the energy equation results in

$$\Theta'' = \text{Pr}\, H\, \Theta' \tag{6.25}$$

where the dimensionless temperature $\Theta$ is used, which is defined by

$$\Theta = \frac{T - T_\infty}{T_W - T_\infty} \tag{6.26}$$

Equation (6.25) has to be solved together with the following boundary conditions

$$\eta = 0 : \quad \Theta = 1 \tag{6.27}$$
$$\eta \to \infty : \Theta = 0$$

The heat transfer problem on a rotating disk has been investigated by Millsaps and Pohlhausen (1952) for Prandtl numbers in the range of 0.5–10 and by Sparrow and Gregg (1959) for a large range of different values of the Prandtl number (0.01, 0.1, 1, 10 and 100). Equation (6.25) has the general solution

$$\Theta = C_1 \int_0^\eta \exp\left( \text{Pr} \int_0^\xi H(\bar{\bar{\xi}}) d\bar{\bar{\xi}} \right) d\xi + C_2 \tag{6.28}$$

The constants $C_1$ and $C_2$ can be obtained by satisfying the boundary conditions according to Eq. (6.27). This results in

$$\Theta = 1 - \frac{\int_0^\eta \exp\left(\Pr \int_0^\xi H(\bar{\bar{\xi}})d\bar{\bar{\xi}}\right) d\xi}{\int_0^\infty \exp\left(\Pr \int_0^\xi H(\bar{\bar{\xi}})d\bar{\bar{\xi}}\right) d\xi} \tag{6.29}$$

Sparrow and Gregg (1959) investigated the asymptotic behavior of Eq. (6.29) for small and large values of the Prandtl number. This analysis is shown here in some detail, because it elucidates nicely the behavior of the heat transfer for extreme values of the Prandtl number.

Let us focus first on the case of very small molecular Prandtl numbers. Because the Prandtl number can be interpreted as the ratio of the thickness of the hydrodynamic to the thermal boundary layer (Kays et al. 2004), a very small value of the Prandtl number indicates that the thermal boundary layer is much thicker than the hydrodynamic boundary layer. This means that for very small Prandtl numbers a constant value of the velocity distribution can be used as a first guess in order to solve the convective heat transfer problem. Replacing therefore $H = H(\infty)$ in Eq. (6.25), this equation can be integrated easily. One obtains

$$\Pr \to 0 : \ \Theta = \exp(\Pr H(\infty)\eta), \quad H(\infty) = -0.88447 \tag{6.30}$$

The Nusselt number is defined by

$$\mathrm{Nu} = \frac{h \sqrt{\mu/(\rho\omega)}}{k} = \frac{-k\left(\frac{\partial T}{\partial x}\right)_{x=0} \sqrt{\mu/(\rho\omega)}}{k} = -\left(\frac{d\Theta}{d\eta}\right)_{\eta=0} \tag{6.31}$$

where, in Eq. (6.31), the quantity $\sqrt{\mu/(\rho\omega)}$ is used as length scale in the Nusselt number. Inserting Eq. (6.30) into Eq. (6.31) results in
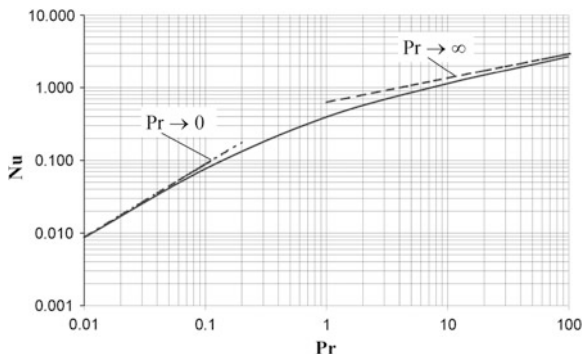
$$\Pr \to 0 : \ \mathrm{Nu} = 0.88447 \, \Pr \tag{6.32}$$

If the Prandtl number attains very large values, the thermal boundary layer is much thinner than the hydrodynamic boundary layer. This means that, in this case, the velocity distribution can be approximated by a Taylor series expansion of the velocity field around $\eta = 0$. This leads to

$$H = H(0) + H'(0)\eta + \frac{1}{2}H''(0)\eta^2 + \cdots \tag{6.33}$$

Since $H(0) = H'(0) = 0$, only the last term in Eq. (6.33) is retained. Inserting this expression into Eq. (6.29) results after integration in

$$\text{Pr} \to \infty : \Theta = 1 - \frac{\int_0^{\eta} \exp\left(\frac{1}{6}\text{Pr}\,H''(0)\xi^3\right) d\xi}{\int_0^{\infty} \exp\left(\frac{1}{6}\text{Pr}\,H''(0)\xi^3\right) d\xi} \tag{6.34}$$

For the Nusselt number, one obtains from Eqs. (6.34) and (6.31) (Sparrow and Gregg 1959)

$$\text{Pr} \to \infty : \text{Nu} = \frac{\left(-\text{Pr}H''(0)/6\right)^{1/3}}{\Gamma(4/3)} = 0.62048\,\text{Pr}^{1/3} \tag{6.35}$$

The distribution of the Nusselt number as a function of the Prandtl number, is shown in Fig. 6.3. The graph is based on calculated values of the Nusselt number from Sparrow and Gregg (1959). In this figure, the asymptotic distributions for small and large values of the Prandtl number are also plotted for comparison. It can be seen that there is a relatively good agreement between the asymptotic values and the numerically calculated Nusselt numbers for extreme values of the Prandtl number.

Before concluding the present example, it is noteworthy stressing once again, where the difference in applying the method of separation of variables to linear and nonlinear partial differential equation lies. The striking difference comes from the fact that the superposition approach can no longer successfully been used. This means that in contrast to Chaps. 2–5, boundary conditions can no longer be satisfied by adding up an infinite set of eigenfunctions.

## 6.2  Transformations Resulting in Linear Partial Differential Equations

For some nonlinear partial differential equations, it is possible to reduce them to linear partial differential equations by using special transformations. Some of these transformations are discussed in Ames (1965a), Schneider (1978), Schlichting (1982),

Loitsianki (1967), Carslaw and Jaeger (1992) and in Özisik (1968). For elucidating this type of solution approach, we discuss only one type of such a transformation. Consideration is given to the steady-state heat conduction within a two-dimensional region. The temperature field is described by the following heat conduction equation

$$\frac{\partial}{\partial x}\left(k(T)\frac{\partial T}{\partial x}\right) + \frac{\partial}{\partial y}\left(k(T)\frac{\partial T}{\partial y}\right) = 0 \tag{6.36}$$

The heat conductivity in Eq. (6.36) is assumed to depend on temperature, but not explicitly on the coordinates $x$, $y$. This is a good assumption, which is sufficiently accurate for a large number of engineering problems. Since the heat conductivity is a function of temperature, the above equation is nonlinear. However, if we define a new dependent variable in the form

$$\Omega = \int\limits_0^T \frac{k(\tilde{T})}{k_0}d\tilde{T} \tag{6.37}$$

where $k_0$ is a reference value of the thermal conductivity, Eq. (6.36) can be transformed into the linear Laplace equation

$$\frac{\partial^2\Omega}{\partial x^2} + \frac{\partial^2\Omega}{\partial y^2} = 0 \tag{6.38}$$

The transformation given by Eq. (6.37) is known in literature as the Kirchhoff transformation. The only problem arising with this transformation is that also the boundary conditions have to be in a suitable form, so that after introducing Eq. (6.37) also the boundary conditions are linear. If we assume constant temperature boundary conditions, the transformation given by Eq. (6.37) works perfectly well and the resulting equations are linear. The Kirchhoff transformation can also be applied to a much broader class of problems than the one shown above (see for example Carslaw and Jaeger 1992, Özisik 1968).

Let us consider one special example characterized by the following boundary conditions for Eq. (6.36)

$$T(0,y) = T_0, \quad T(l,y) = T_0 \tag{6.39}$$
$$T(x,0) = T_0, \quad T(x,l) = T_1$$

where $T_0$ and $T_1$ are constant temperatures. Let us further assume that the heat conductivity within the material is given by the following equation

$$k(T) = k_0\left(1 + C\frac{T - T_0}{T_1 - T_0}\right) \tag{6.40}$$

where $k_0$ and $C$ are known constants. Introducing the dimensionless quantities

$$\Theta = \frac{T - T_0}{T_1 - T_0}, \ \tilde{x} = \frac{x}{l}, \ \tilde{y} = \frac{y}{l} \tag{6.41}$$

into Eqs. (6.36) and (6.39) results in

$$\frac{\partial}{\partial \tilde{x}}\left(\frac{k(\Theta)}{k_0}\frac{\partial \Theta}{\partial \tilde{x}}\right) + \frac{\partial}{\partial \tilde{y}}\left(\frac{k(\Theta)}{k_0}\frac{\partial \Theta}{\partial \tilde{y}}\right) = 0 \tag{6.42}$$

with the boundary conditions

$$\begin{align}
\Theta(0, \tilde{y}) = 0, \quad \Theta(1, \tilde{y}) = 0 \\
\Theta(\tilde{x}, 0) = 0, \quad \Theta(\tilde{x}, 1) = 1
\end{align} \tag{6.43}$$

If we now apply the Kirchhoff transformation

$$\Omega = \int_0^\Theta \frac{k(\tilde{T})}{k_0}d\tilde{T} = \int_0^\Theta (1 + C\tilde{\Theta})\,d\tilde{\Theta} = \Theta + \frac{C}{2}\Theta^2 \tag{6.44}$$

to the Eqs. (6.42) and (6.43), we obtain

$$\frac{\partial^2 \Omega}{\partial \tilde{x}^2} + \frac{\partial^2 \Omega}{\partial \tilde{y}^2} = 0 \tag{6.45}$$

and the corresponding boundary conditions

$$\begin{align}
\Omega(0, \tilde{y}) = 0, \quad \Omega(1, \tilde{y}) = 0 \\
\Omega(\tilde{x}, 0) = 0, \quad \Omega(\tilde{x}, 1) = 1 + \frac{C}{2}
\end{align} \tag{6.46}$$

The above given problem for $\Omega$ can easily be solved by the method of separation of variables explained in Chap. 2. After obtaining the solution for the function $\Omega$, the temperature distribution for the nonlinear heat conduction problem can be calculated from Eq. (6.44) and is given by

$$\Theta = \frac{1}{C}\left(\sqrt{2C\Omega + 1} - 1\right) \tag{6.47}$$

The temperature distribution for this case is shown in Fig. 6.4. The left hand side shows the temperature distribution for $\tilde{y} = 0.5$, while the right hand side figure shows the one for $\tilde{x} = 0.5$. The figures contain temperature distributions for different values of the constant $C$, indicating increasing nonlinear effects of the solution with growing values of $C$.
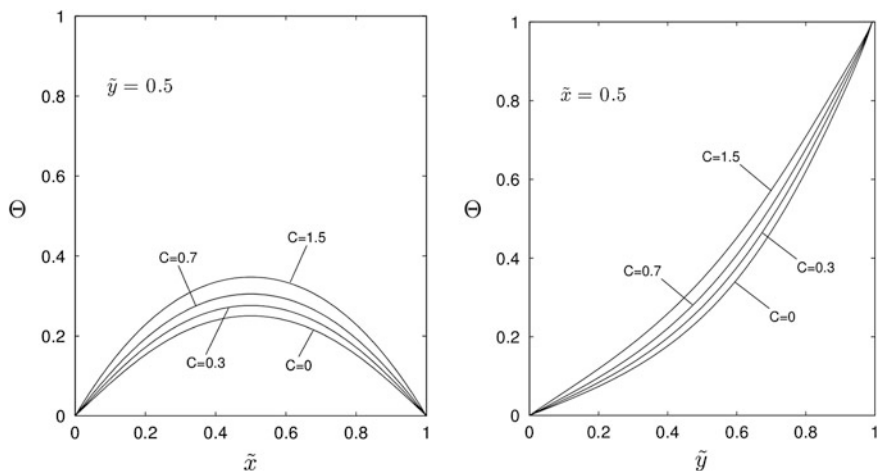
**Fig. 6.4** Temperature distribution in the plate for different values of $C$ (*left* for $\tilde{y} = 0.5$, *right* for $\tilde{x} = 0.5$)

In a lot of interesting engineering applications, like the one we investigate here, the effect of nonlinearity is relatively weak. This gives the chance to derive solutions for such problems by using perturbation methods. We do not want to go into detail into this method here. However, a simple application of a regular perturbation method for the problem under consideration will be shown in the following. For more details, the reader is referred to the books of van Dyke (1964), Kevorkian and Cole (1981), Simmonds and Mann (1986), Aziz and Na (1984) and Schneider (1978).

In order to do so, we assume that the parameter $C$ in Eq. (6.40) is small and we name this quantity $\varepsilon$. Thus, we obtain from Eq. (6.42)

$$\frac{\partial}{\partial \tilde{x}}\left((1 + \varepsilon\Theta)\frac{\partial\Theta}{\partial\tilde{x}}\right) + \frac{\partial}{\partial\tilde{y}}\left((1 + \varepsilon\Theta)\frac{\partial\Theta}{\partial\tilde{y}}\right) = 0 \qquad (6.48)$$

with the boundary conditions

$$\Theta(0, \tilde{y}) = 0, \quad \Theta(1, \tilde{y}) = 0 \qquad (6.43)$$
$$\Theta(\tilde{x}, 0) = 0, \quad \Theta(\tilde{x}, 1) = 1$$

Now, let us assume that we can expand the temperature in a series, given by

$$\Theta = \Theta_0 + \varepsilon\,\Theta_1 + \varepsilon^2\Theta_2 + \cdots \qquad (6.49)$$

Inserting this expression up to terms of the order $\varepsilon^2$ into Eqs. (6.48) and (6.43) results in

$$\frac{\partial}{\partial \tilde{x}}\left(\left(1+\varepsilon\left(\Theta_0+\varepsilon\,\Theta_1+\varepsilon^2\,\Theta_2\right)\right)\left(\frac{\partial \Theta_0}{\partial \tilde{x}}+\varepsilon\frac{\partial \Theta_1}{\partial \tilde{x}}+\varepsilon^2\frac{\partial \Theta_2}{\partial \tilde{x}}\right)\right) \tag{6.50}$$

$$+\frac{\partial}{\partial \tilde{y}}\left(\left(1+\varepsilon\left(\Theta_0+\varepsilon\,\Theta_1+\varepsilon^2\,\Theta_2\right)\right)\left(\frac{\partial \Theta_0}{\partial \tilde{y}}+\varepsilon\frac{\partial \Theta_1}{\partial \tilde{y}}+\varepsilon^2\frac{\partial \Theta_2}{\partial \tilde{y}}\right)\right)=0$$

and

$$\begin{aligned}
\Theta(0,\tilde{y})&=\Theta_0+\varepsilon\,\Theta_1+\varepsilon^2\Theta_2=0, & \Theta(1,\tilde{y})&=\Theta_0+\varepsilon\,\Theta_1+\varepsilon^2\Theta_2=0 \\
\Theta(\tilde{x},0)&=\Theta_0+\varepsilon\,\Theta_1+\varepsilon^2\Theta_2=0, & \Theta(\tilde{x},1)&=\Theta_0+\varepsilon\,\Theta_1+\varepsilon^2\Theta_2=1
\end{aligned} \tag{6.51}$$

From the boundary conditions, given by Eq. (6.51), it follows automatically that

$$\begin{aligned}
&\Theta_0(0,\tilde{y})=0, \quad \Theta_1(0,\tilde{y})=0, \quad \Theta_2(0,\tilde{y})=0, \\
&\Theta_0(1,\tilde{y})=0, \quad \Theta_1(1,\tilde{y})=0, \quad \Theta_2(1,\tilde{y})=0 \\
&\Theta_0(\tilde{x},0)=0, \quad \Theta_1(\tilde{x},0)=0, \quad \Theta_2(\tilde{x},0)=0, \\
&\Theta_0(\tilde{x},1)=1, \quad \Theta_1(\tilde{x},1)=0, \quad \Theta_2(\tilde{x},1)=0
\end{aligned} \tag{6.52}$$

One sees from Eq. (6.52) that all boundary conditions for $\Theta_1$, $\Theta_2$ are homogeneous, while the boundary conditions for $\Theta_0$ can be non-homogeneous. Ordering Eq. (6.51) for different powers of the perturbation quantity results in the following problems to solve. The problem of order $\varepsilon^0$ is given by

$$\varepsilon^0: \quad \frac{\partial^2 \Theta_0}{\partial \tilde{x}^2}+\frac{\partial^2 \Theta_0}{\partial \tilde{y}^2}=0 \tag{6.53}$$

with the boundary conditions

$$\begin{aligned}
\Theta_0(0,\tilde{y})&=0, \quad \Theta_0(1,\tilde{y})=0 \\
\Theta_0(\tilde{x},0)&=0, \quad \Theta_0(\tilde{x},1)=1
\end{aligned} \tag{6.54}$$

The problem of order $\varepsilon^1$ is given by

$$\varepsilon^1: \quad \frac{\partial^2 \Theta_1}{\partial \tilde{x}^2}+\frac{\partial^2 \Theta_1}{\partial \tilde{y}^2}=-\frac{\partial}{\partial \tilde{x}}\left(\Theta_0\frac{\partial \Theta_0}{\partial \tilde{x}}\right)-\frac{\partial}{\partial \tilde{y}}\left(\Theta_0\frac{\partial \Theta_0}{\partial \tilde{y}}\right) \tag{6.55}$$

with the boundary conditions

$$\begin{aligned}
\Theta_1(0,\tilde{y})&=0, \quad \Theta_1(1,\tilde{y})=0 \\
\Theta_1(\tilde{x},0)&=0, \quad \Theta_1(\tilde{x},1)=0
\end{aligned} \tag{6.56}$$

The problem of order $\varepsilon^2$ is finally given by

$$\varepsilon^2 : \quad \frac{\partial^2 \Theta_2}{\partial \tilde{x}^2} + \frac{\partial^2 \Theta_2}{\partial \tilde{y}^2} = -\frac{\partial}{\partial \tilde{x}} \left( \Theta_0 \frac{\partial \Theta_1}{\partial \tilde{x}} + \Theta_1 \frac{\partial \Theta_0}{\partial \tilde{x}} \right) - \frac{\partial}{\partial \tilde{y}} \left( \Theta_0 \frac{\partial \Theta_1}{\partial \tilde{y}} + \Theta_1 \frac{\partial \Theta_0}{\partial \tilde{y}} \right)$$

(6.57)

with the boundary conditions

$$\Theta_2(0, \tilde{y}) = 0, \quad \Theta_2(1, \tilde{y}) = 0$$
$$\Theta_2(\tilde{x}, 0) = 0, \quad \Theta_2(\tilde{x}, 1) = 0$$

(6.58)

From this set of equations, which has been derived, one sees clearly that the problem under consideration has been linearized by using the regular perturbation method. In addition, we notice that the homogeneous equation is repeated, while the problems for $\Theta_1$, $\Theta_2$ contain known terms on the right hand side of the equations. Thus, we can solve these equations by using again the methods from Chaps. 2 and 3.

The problem for $\Theta_0$ can easily been solved by using the method of separation of variables. One obtains

$$\Theta_0(\tilde{x}, \tilde{y}) = \frac{4}{\pi} \sum_{n=0}^{\infty} \frac{\sin((2n+1)\pi\tilde{x}) \; \sinh((2n+1)\pi\tilde{y})}{(2n+1) \sinh((2n+1)\pi)}$$

(6.59)

The solution for $\Theta_1$ needs to be constructed of the solution for the homogenous equation and a particular solution. The homogeneous solution is the same as for the problem for $\Theta_0$. For the particular solution we can assume

$$\Theta_{1p} = A_1 \Theta_0^2$$

(6.60)

The constant in Eq. (6.60) can be determined to be $A_1 = -1/2$. Thus, the solution of the problem is given by

$$\Theta_1 = \frac{1}{2} \Theta_0 - \frac{1}{2} \Theta_0^2$$

(6.61)

The problem for $\Theta_2$ can be solved in a similar way. Here we can assume a particular solution of the form

$$\Theta_{2p} = A_2 \Theta_0 \Theta_1$$

(6.62)

The constant can be determined to be $A_2 = -1$. Because this particular solution contains also the function $\Theta_1$, it automatically satisfies all boundary conditions and is the solution of the problem. Thus, the complete solution is given by

$$\Theta = \Theta_0 + \varepsilon \frac{1}{2} \left( \Theta_0 - \Theta_0^2 \right) - \varepsilon^2 \Theta_0 \Theta_1 + \cdots$$
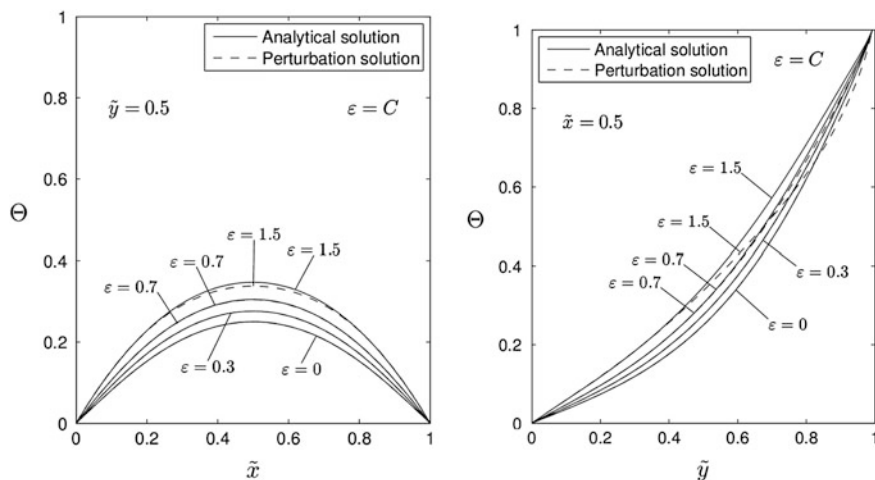
(6.63)

**Fig. 6.5** Comparison between the numerically predicted temperature distribution and the perturbation solution in the plate for different values of $\varepsilon = C$ (*left* for $\tilde{y} = 0.5$, *right* for $\tilde{x} = 0.5$)

Figure 6.5 shows a comparison between the numerical solution of the problem and the perturbation solution. One sees nicely that the perturbation solution gives very accurate solutions for $\varepsilon = C = 0.7$. Some deviations are visible for larger values of the perturbation parameter (e.g. $\varepsilon = C = 1.5$).

## 6.3 Functional Relations Between Dependent Variables

Sometimes it is possible to establish functional relations between different dependent variables. This can be very useful. In case of the flow and heat transfer in a boundary layer it may be used to relate the heat transfer coefficient to the friction factor.

### 6.3.1 Incompressible Flow over a Heated Flat Plate

In order to elucidate this method, let us investigate the simple problem of a flow over a flat plate. It is assumed that the flow is incompressible and that the fluid properties are constant. The plate surface is kept at a uniform temperature $T_W$, whereas the fluid far away from the wall moves with a constant velocity $u_\infty$ and has the constant temperature $T_\infty$. The problem under consideration is depicted in Fig. 6.6.
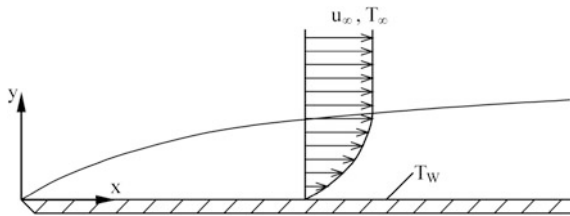
**Fig. 6.6** Flow and heat transfer over a flat plate

The problem can be described by the boundary layer equations (Kays et al. 2004) for a laminar flow with constant fluid properties

$$u\frac{\partial u}{\partial x} + v\frac{\partial u}{\partial y} = \frac{\mu}{\rho}\frac{\partial^2 u}{\partial y^2} \tag{6.64}$$

$$\frac{\partial u}{\partial x} + \frac{\partial v}{\partial y} = 0 \tag{6.65}$$

$$u\frac{\partial T}{\partial x} + v\frac{\partial T}{\partial y} = a\frac{\partial^2 T}{\partial y^2} \tag{6.66}$$

with the boundary conditions

$$\begin{aligned} y = 0: &\quad u = 0, \quad v = 0, \quad T = T_W \\ y \to \infty: &\quad u = u_\infty, \qquad\qquad\; T = T_\infty \end{aligned} \tag{6.67}$$

By comparing Eq. (6.64) to Eq. (6.66), it can be seen that both equations have a very similar structure. Introducing the following dimensionless quantities

$$\tilde{u} = \frac{u}{u_\infty}, \; \tilde{v} = \frac{v}{u_\infty}, \; \tilde{x} = \frac{x}{\delta}, \; \tilde{y} = \frac{y}{\delta}, \; \Theta = \frac{T - T_W}{T_\infty - T_W} \tag{6.68}$$

into Eqs. (6.64)–(6.67), where $\delta$ denotes a length scale, one obtains

$$\tilde{u}\frac{\partial \tilde{u}}{\partial \tilde{x}} + \tilde{v}\frac{\partial \tilde{u}}{\partial \tilde{y}} = \frac{\mu}{\rho u_\infty \delta}\frac{\partial^2 \tilde{u}}{\partial \tilde{y}^2} \tag{6.69}$$

$$\frac{\partial \tilde{u}}{\partial \tilde{x}} + \frac{\partial \tilde{v}}{\partial \tilde{y}} = 0 \tag{6.70}$$

$$\tilde{u}\frac{\partial \Theta}{\partial \tilde{x}} + \tilde{v}\frac{\partial \Theta}{\partial \tilde{y}} = \frac{a}{u_\infty \delta}\frac{\partial^2 \Theta}{\partial \tilde{y}^2} \tag{6.71}$$

with the boundary conditions

$$\tilde{y} = 0: \quad \tilde{u} = 0, \tilde{v} = 0, \quad \Theta = 0 \tag{6.72}$$
$$\tilde{y} \to \infty: \quad \tilde{u} = 1, \qquad \Theta = 1$$

If we finally assume that the Prandtl number of the fluid is 1, which means that $a = \mu/\rho$ (which is a good assumption for all gases), one can see that the structure of Eq. (6.69) is identical to the one of Eq. (6.71). In addition, the boundary conditions for $\tilde{u}$ and $\Theta$ are the same. This means that both equations must have the same solution. Thus,

$$\Theta = \tilde{u}, \quad \frac{T - T_W}{T_\infty - T_W} = \frac{u}{u_\infty} \tag{6.73}$$

Because the Prandtl number is equal to 1, the thickness of the hydrodynamic and the thermal boundary layer is the same in size. Equation (6.73) states the simple fact that the non-dimensional velocity profile in the boundary layer has in this case the same shape as the non-dimensional temperature profile. Equation (6.73) is a very useful equation, because it can be used to establish a relation between the friction factor and the heat transfer coefficient at the surface.

In order to show this, we will first predict the heat flux at the surface

$$\dot{q}_W = -k \left( \frac{\partial T}{\partial y} \right)_W = -k \left( \frac{\partial T}{\partial u} \right) \left( \frac{\partial u}{\partial y} \right)_W = -\frac{k(T_\infty - T_w)}{u_\infty} \left( \frac{\partial u}{\partial y} \right)_W \tag{6.74}$$

Introducing the friction factor $c_f$ defined as

$$c_f = \frac{2\tau_W}{\rho u_\infty^2} = \mu \left( \frac{\partial u}{\partial y} \right)_W \frac{2}{\rho u_\infty^2} \tag{6.75}$$

results in

$$\dot{q}_W = \frac{k(T_W - T_\infty)}{\mu} \frac{c_f}{2} \rho u_\infty \tag{6.76}$$

If we finally introduce the definition of the Nusselt number, based on the plate length $L$

$$\mathrm{Nu}_L = \frac{hL}{k} = \frac{\dot{q}_W L}{k(T_\infty - T_W)} \tag{6.77}$$

into the above equation, one obtains

$$\frac{\mathrm{Nu}_L}{\mathrm{Re}_L \, \mathrm{Pr}} = \mathrm{St} = \frac{c_f}{2} \tag{6.78}$$

Equation (6.78) states the interesting fact that the knowledge of the friction factor is sufficient for predicting the heat transfer for the above case. This relation is known as the Reynolds analogy in convective heat transfer. It is traditionally derived for a turbulent flow with $Pr = 1$ and $Pr_t = 1$ (see for example Kays et al. 2004). The equation can be used in order to obtain an approximate value of the heat transfer coefficient by simply using the known friction factor.

### 6.3.2 Compressible Flow over a Flat, Heated Plate

Having established a direct relation between the friction factor and the heat transfer coefficient, one could ask whether similar expressions between the temperature field and the velocity field exist also for compressible flows. This is indeed the case and the following analysis should serve as another example for establishing functional dependences between dependent variables. Let us consider the case of a compressible flow over a flat plate. The equations describing the laminar flow and heat transfer in this situation are the compressible boundary layer equations (Kays et al. 2004; Schlichting 1982; Jischa 1982). For the case of no axial pressure gradient ($dp/dx = 0$) in the flow, these equations are given by

$$\frac{\partial}{\partial x}(\rho u) + \frac{\partial}{\partial y}(\rho v) = 0 \tag{6.79}$$

$$\rho\left(u\frac{\partial u}{\partial x} + v\frac{\partial u}{\partial y}\right) = \frac{\partial}{\partial y}\left(\mu\frac{\partial u}{\partial y}\right) \tag{6.80}$$

$$\rho c_p\left(u\frac{\partial T}{\partial x} + v\frac{\partial T}{\partial y}\right) = \frac{\partial}{\partial y}\left(k\frac{\partial T}{\partial y}\right) + \mu\left(\frac{\partial u}{\partial y}\right)^2 \tag{6.81}$$

In addition to the conservation equations, we have to prescribe for a compressible flow also a relation between $p$, $\rho$ and $T$. This is accomplished by the thermal state equation. If we assume that the fluid can be treated as an ideal gas, one has

$$p = \rho R T \tag{6.82}$$

The above equations have to be solved together with the boundary conditions

$$y = 0: \quad u = 0, \quad v = 0, \quad T = T_W \tag{6.83}$$
$$y \to \infty: \quad u = u_\infty, \quad T = T_\infty$$

For a compressible flow, Eqs. (6.79)–(6.82) are strongly coupled by the varying density. As in the case of an incompressible flow, we are looking for a functional relationship of the form

$$T = f(u) \tag{6.84}$$

Inserting Eq. (6.84) into the energy equation, Eq. (6.81), results in

$$\rho c_p \frac{dT}{du} \left( u \frac{\partial u}{\partial x} + v \frac{\partial u}{\partial y} \right) = \frac{\partial}{\partial y} \left( k \frac{\partial u}{\partial y} \frac{dT}{du} \right) + \mu \left( \frac{\partial u}{\partial y} \right)^2 \tag{6.85}$$

This equation can be further simplified by using Eq. (6.80) and one obtains

$$c_p \frac{dT}{du} \frac{\partial}{\partial y} \left( \mu \frac{\partial u}{\partial y} \right) = \frac{\partial}{\partial y} \left( k \frac{\partial u}{\partial y} \frac{dT}{du} \right) + \mu \left( \frac{\partial u}{\partial y} \right)^2 \tag{6.86}$$

Performing all differentiations on the right hand side of Eq. (6.86) leads to

$$c_p \frac{dT}{du} \frac{\partial}{\partial y} \left( \mu \frac{\partial u}{\partial y} \right) = \frac{dT}{du} \frac{\partial}{\partial y} \left( k \frac{\partial u}{\partial y} \right) + k \frac{d^2 T}{du^2} \left( \frac{\partial u}{\partial y} \right)^2 + \mu \left( \frac{\partial u}{\partial y} \right)^2 \tag{6.87}$$

Rearranging gives

$$\frac{dT}{du} \left( c_p \frac{\partial}{\partial y} \left( \mu \frac{\partial u}{\partial y} \right) - \frac{\partial}{\partial y} \left( k \frac{\partial u}{\partial y} \right) \right) = \left( \frac{\partial u}{\partial y} \right)^2 \left( k \frac{d^2 T}{du^2} + \mu \right) \tag{6.88}$$

Let us now assume that $c_p$ is constant. Then we introduce the Prandtl number ($\mathrm{Pr} = \mu c_p / k$) into Eq. (6.88). This leads to

$$\frac{dT}{du} \left( \frac{\partial}{\partial y} \left( k \mathrm{Pr} \frac{\partial u}{\partial y} \right) - \frac{\partial}{\partial y} \left( k \frac{\partial u}{\partial y} \right) \right) = \left( \frac{\partial u}{\partial y} \right)^2 \left( k \frac{d^2 T}{du^2} + \mu \right) \tag{6.89}$$

For $\mathrm{Pr} = 1$, Eq. (6.89) simplifies drastically and one obtains

$$k \frac{d^2 T}{du^2} + \mu = 0 \tag{6.90}$$

Equation (6.90) is an ordinary differential equation, which can be integrated easily. Adapting the solution to the boundary conditions given by Eq. (6.83) leads to

$$\frac{T - T_W}{T_\infty - T_W} = \frac{u}{u_\infty} + \frac{u_\infty^2}{2 c_p (T_\infty - T_W)} \frac{u}{u_\infty} \left( 1 - \frac{u}{u_\infty} \right) \tag{6.91}$$

Equation (6.91) shows nicely that the linear dependence between temperature and velocity, see Eq. (6.73), is now replaced by a nonlinear relationship. For small velocities, the quadratic term on the right hand side of Eq. (6.91) can be neglected and one obtains again Eq. (6.73). However, if we rewrite Eq. (6.91) using the stagnation temperatures instead of static temperatures, which means

$$T_0 = T + \frac{1}{2}\frac{u^2}{c_p}, \quad T_{0\infty} = T_\infty + \frac{1}{2}\frac{u_\infty^2}{c_p}, \quad T_{0W} = T_W \tag{6.92}$$

one obtains again

$$\frac{T_0 - T_{0W}}{T_{0\infty} - T_{0W}} = \frac{u}{u_\infty} \tag{6.93}$$

This is an extension of the similarity between the velocity distribution and the temperature distribution given by Eq. (6.73). For a more detailed discussion of this case, the reader is referred to Schlichting (1982) and Loitsianki (1967).

## 6.4  Similarity Solutions

In the following section, we are interested in "similar solutions" of nonlinear partial differential equations. Mathematically speaking, similarity solutions of partial differential equations appear when the number of independent variables can be reduced by a transformation of these variables. If we focus on the important case of a partial differential equation with two independent variables, this means that an ordinary differential equation is obtained after the transformation.

Similarity solutions play an important role in boundary layer theory and also in heat conduction. For example, in boundary layer theory, similarity solutions can be obtained for some cases if the physical problem under consideration is lacking a characteristic length or a characteristic time scale (e.g. the boundary layer on a semi-infinite plate with zero pressure gradient). In such cases, the nonlinear partial differential equations for the boundary layer are reduced to nonlinear ordinary differential equations. There are several books dealing with similarity solutions and the different methods to obtain them. The reader is referred for example to Hansen (1964), Ames (1965a), Schneider (1978), Dewey and Gross (1967) and Özisik (1968) for detailed discussions on similarity solutions. Basically, there are three main classes of methods for obtaining similarity solutions (Hansen 1964). These three methods are explained in the following section for a simple heat conduction problem. Subsequently, we analyse similarity solutions for different boundary layer problems.

## 6.4.1  Similarity Solutions for a Transient Heat Conduction Problem

Consider one-dimensional transient heat conduction in a semi-infinite solid. The body has a uniform initial temperature $T_0$. For $t \geq 0$, the wall temperature is set to the constant temperature $T_W$. The properties of the solid are assumed to be constant. The problem is described by the heat conduction equation for the solid

$$\rho c \frac{\partial T}{\partial t} = \frac{\partial}{\partial x}\left(k\frac{\partial T}{\partial x}\right) \tag{6.94}$$

with the boundary conditions

$$
\begin{aligned}
t = 0 &: \quad T = T_0 \\
x = 0 &: \quad T = T_W, \quad x \to \infty : \quad T = T_0
\end{aligned}
\tag{6.95}
$$

The problem under consideration is depicted in Fig. 6.7. Of course, Eq. (6.94) represents a linear partial differential equation and can be solved also with other methods. However, the simplicity of this equation makes it a good candidate to explain the different methods for obtaining similarity solutions, before considering more complicated problems.

### 6.4.1.1 Methods Based on Dimensional Analysis

The dimensional analysis is a powerful method, which can be used for all physical applications. The method is based on the fact, that all physical quantities have units, which can be split into "basic units". These basic units could be, for example, the ones used in the SI-system with the units: Length $L$ (m), mass $M$ (kg), time $\tau$ (s), temperature $\vartheta$(K), species amount $N$ (mol), current strength $I$ (A) and light strength $S$ (cd). The density for example has the unit mass $M$ divided by length cubed $L^3$, which can be denoted by $[ML^{-3}]$. The velocity, as a second example, has the unit length $L$ divided by time $\tau$, which can be denoted by $[L\tau^{-1}]$.

In general, one can say that for any problem there is always the task to express a physical quantity $p_1$ as a function of other physical quantities $p_2, p_3, \ldots, p_n$, where $n$ is the number of physical variables needed to describe the problem under consideration (Görtler 1975; Spurk 1992; Simon and Weigand 2006). This means that a relation

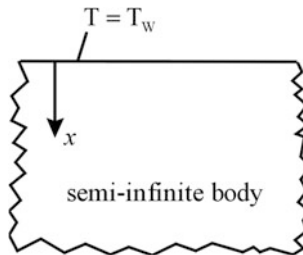$$f(p_1, p_2, \ldots, p_n) = 0 \tag{6.96}$$



**Fig. 6.7**  Transient heat conduction in a semi-infinite solid

can be established. Each of the physical variables $p_j$ has units, which can be constructed from the basic units stated above. This means that the dimension of the variable $p_j$, denoted by $[p_j]$, is given by

$$[p_j] = \prod_{i=1}^{m}(X_i)^{a_{ij}} \tag{6.97}$$

where $X_i$ denotes one of the basic units powered by the exponent $a_{ij}$. For the above example of the density, $p_1$, and the velocity, $p_2$, one has

$$\begin{aligned}
[\rho] &= M^1 L^{-3}, \quad a_{11} = 1, \quad a_{21} = -3 \\
[v] &= L^1 \tau^{-1}, \quad a_{22} = 1, \quad a_{32} = -1
\end{aligned} \tag{6.98}$$

Since every physical process must be independent of the arbitrary units used, the relation given by Eq. (6.96) can be reduced to a relationship between dimensionless quantities $\Pi_j$, so that.

$$f(\Pi_1, \Pi_2, \ldots, \Pi_d) = 0 \tag{6.99}$$

where $d$ is the number of dimensionless products. These dimensionless quantities are products of the physical quantities, which means

$$\Pi = \prod_{j=1}^{n}(p_j)^{b_j} \tag{6.100}$$

with the dimension

$$[\Pi] = 1 = \prod_{j=1}^{n}[p_j]^{b_j} \tag{6.101}$$

Inserting Eq. (6.97) into Eq. (6.101) leads to

$$[\Pi] = 1 = \prod_{j=1}^{n}\prod_{i=1}^{m}(X_i)^{a_{ij}b_j} \tag{6.102}$$

In Eq. (6.102) the coefficients $a_{ij}$ are known and the exponents $b_j$ have to be determined, so that the equation is satisfied. This is always possible, if the system of equations

$$\sum_{j=1}^{n} a_{ij}b_j = 0 \tag{6.103}$$

has nontrivial solutions for the $n$ unknown coefficients $b_j$. The coefficient matrix $a_{ij}$ is also known as the dimension matrix.

The equivalence between Eqs. (6.96) and (6.99) is known in literature as the "Buckingham theorem" or as the "Pi theorem" (Görtler 1978; Spurk 1992; Simon and Weigand 2006). This theorem gives also a relation between the number of physical variables involved, $n$, and the number of independent dimensionless quantities, $d$, according to

$$d = n - r \qquad (6.104)$$

where $r$ is the rank of the dimension matrix.

Let us now focus again on the problem of finding similarity solutions for Eqs. (6.94) and (6.95). The physical quantities involved in the problem are: $\rho$, $c$, $k$, $T_0$, $T_W$, $T$, $t$, $x$. This means that we can construct the dimension matrix (Table 6.1) where the units for the heat conductivity $k$ [W m$^{-1}$ K$^{-1}$] and for the specific heat $c$ [J kg$^{-1}$ K$^{-1}$] have been expressed in basic units. Note that, in the dimension matrix, we have used only temperature differences. This is because of the fact, that temperature differences are needed for the heat transfer.

The rank of the dimension matrix, given by Table 6.1, $r = 4$, which implies that the number of dimensionless products is $d = n - r = 7 - 4 = 3$. However, upon inspection of Eq. (6.94), one notices that the quantities $\rho$, $c$, $k$ do not appear independently in this equation. Because of this, they can be lumped together to build the heat diffusivity $a = k/(\rho c)$. By doing so, the dimension matrix simplifies to as shown in Table 6.2.

In this matrix, no entries appear for the mass $M$, so that the rank of this matrix is only 3. This means that we can construct 2 dimensionless quantities. By doing so, one obtains as in Table 6.3.

**Table 6.1** Dimension matrix for the transient heat conduction problem

|       | $\rho$ | $c$ | $k$ | $T - T_0$ | $T_0 - T_W$ | $t$ | $x$ |
|-------|------|-----|-----|-----------|-------------|-----|-----|
| $L$   | $-3$ | 2   | 1   | 0         | 0           | 0   | 1   |
| $M$   | 1    | 0   | 1   | 0         | 0           | 0   | 0   |
| $\tau$ | 0   | $-2$ | $-3$ | 0        | 0           | 1   | 0   |
| $\vartheta$ | 0 | $-1$ | $-1$ | 1     | 1           | 0   | 0   |

**Table 6.2** Simplified dimension matrix for the transient heat conduction problem

|       | $a$ | $T - T_0$ | $T_0 - T_W$ | $t$ | $x$ |
|-------|-----|-----------|-------------|-----|-----|
| $L$   | 2   | 0         | 0           | 0   | 1   |
| $M$   | 0   | 0         | 0           | 0   | 0   |
| $\tau$ | $-1$ | 0        | 0           | 1   | 0   |
| $\vartheta$ | 0 | 1      | 1           | 0   | 0   |

**Table 6.3** Dimension matrix with dimensional groups

|   | $x/\sqrt{at}$ | $(T - T_0)/(T_W - T_0)$ | $T_0 - T_W$ | $t$ | $x$ |
|---|---|---|---|---|---|
| $L$ | 0 | 0 | 0 | 0 | 1 |
| $M$ | 0 | 0 | 0 | 0 | 0 |
| $\tau$ | 0 | 0 | 0 | 1 | 0 |
| $\vartheta$ | 0 | 0 | 1 | 0 | 0 |

This means that the solution of the current problem must have the functional form

$$\frac{T - T_0}{T_W - T_0} = f\left(\frac{x}{\sqrt{at}}\right) \tag{6.105}$$

Introducing the new coordinate

$$\eta = \frac{x}{\sqrt{at}} \tag{6.106}$$

into Eqs. (6.94) and (6.95), results in the ordinary differential equations

$$\Theta'' + \frac{1}{2}\eta\Theta' = 0 \tag{6.107}$$

where the prime denotes differentiation with respect to the coordinate $\eta$. The boundary conditions for this equation are

$$\begin{aligned} \eta = 0: \quad & \Theta = 1 \\ \eta \to \infty: \ & \Theta = 0 \end{aligned} \tag{6.108}$$

Equation (6.108) shows nicely that the two boundary conditions for $t = 0$ and for $x \to \infty$ given by Eq. (6.95) have been replaced by one boundary condition for $\eta \to \infty$. Equation (6.107) together with the boundary conditions given by Eq. (6.108) can be integrated and one finally obtains

$$\Theta = 1 - \frac{1}{\sqrt{\pi}} \int_0^\eta \exp\left(-\frac{\bar{\eta}^2}{4}\right) d\bar{\eta} \tag{6.109}$$

### 6.4.1.2 Group-Theory Methods

This method for obtaining similarity solutions has been suggested by Birkhoff (1948) and has been investigated extensively by Morgan (1951), Müller and Matschat (1962), Aimes (1965a, b). The method implies that the search for

similarity solutions for a system of partial differential equations is equivalent to the determination of the invariant solutions of these equations under a particular parameter group of transformation. A set of similarity variables, which are invariants of the group, is obtained by solving a set of simultaneous algebraic equations.

Suppose $\Gamma$ is a set of $N$ partial differential equations given by

$$\Gamma : \psi_j(x_i, y_j) = 0, \quad i = 1, 2, 3, ..., M \tag{6.110}$$
$$j = 1, 2, 3, ..., N$$

where $x_i$, $i = 1, 2, 3, \ldots, M$ are the independent and $y_j$, $j = 1, 2, 3, \ldots, N$ are the dependent variables. Now we are considering a one-parameter group $G_1$ with the non-zero real parameter $A$, whose elements are given by

$$\bar{x}_i = A^{\gamma_i} x_i \tag{6.111}$$
$$\bar{y}_j = A^{\kappa_j} y_j$$

In Eq. (6.111) $A$ is a nonzero real number, called the parameter of transformation, and the exponents $\gamma_i$, $\kappa_j$ have to be determined from the requirement that the system of partial differential equations, given by Eq. (6.110), is absolutely invariant under the transformation given by Eq. (6.111). This means that

$$\psi_j(x_i, y_j) = \psi_j(\bar{x}_i, \bar{y}_j) \tag{6.112}$$

After applying the transformation to the partial differential equations, one obtains a set of simultaneous algebraic equations for determining the unknown coefficients $\gamma_i$ and $\kappa_j$. More detailed information on this method can be found in the literature mentioned above.

Let us illustrate the method by obtaining similarity solutions for the Eqs. (6.94) and (6.95). We assume a linear transformation for the dependent and independent variables in Eq. (6.94) of the form

$$\bar{x} = A^{\gamma_1} x, \ \bar{t} = A^{\gamma_2} t \tag{6.113}$$
$$\bar{T} = A^{\kappa_1} T$$

As noted before $\gamma_1$, $\gamma_2$, $\kappa_1$ are constants and the quantity $A$ is called the parameter of the transformation. Solving the above given equation for $A$ gives

$$A = \left(\frac{\bar{x}}{x}\right)^{1/\gamma_1} = \left(\frac{\bar{t}}{t}\right)^{1/\gamma_2} = \left(\frac{\bar{T}}{T}\right)^{1/\kappa_1} \tag{6.114}$$

Introducing the quantities given by Eq. (6.113) into Eq. (6.94) results in

$$A^{\gamma_2 - \kappa_1} \rho c \frac{\partial \bar{T}}{\partial \bar{t}} = A^{2\gamma_1 - \kappa_1} \frac{\partial}{\partial \bar{x}} \left( k \frac{\partial \bar{T}}{\partial \bar{x}} \right) \qquad (6.115)$$

Comparing Eq. (6.115) to Eq. (6.94) shows clearly that the partial differential equation does not get altered by the transformation if

$$\kappa_1 - \gamma_2 = \kappa_1 - 2\gamma_1 \qquad (6.116)$$

This equation leads immediately to the result that $\gamma_2 = 2\gamma_1$, whereas nothing can be said about $\kappa_1$. This is obvious, because the differential equation is linear and therefore every exponent for the temperature drops out. Introducing the relationship between $\gamma_1$ and $\gamma_2$ into Eq. (6.114), it can be seen that the coordinates should be related in the following way in order to guarantee similarity solutions

$$\left( \frac{\bar{x}}{x} \right)^{1/\gamma_1} = \left( \frac{\bar{t}}{t} \right)^{1/2\gamma_1} \Rightarrow \bar{\eta} = \frac{x}{\sqrt{t}} \qquad (6.117)$$

This new coordinate can be made dimensionless by using $a = k/(\rho c)$ and one obtains the similarity coordinate given by Eq. (6.106)

$$\eta = \frac{x}{\sqrt{at}} \qquad (6.106)$$

Introducing again the dimensionless temperature $\Theta = (T - T_0)/(T_W - T_0)$ leads after performing the change of variables in Eq. (6.115), to the ordinary differential Eq. (6.107) with boundary conditions given by Eq. (6.108).

### 6.4.1.3 Separation of Variables and the Method of the Free Variable

Both methods are strongly related to each other. We have already seen in Sect. 6.1 how the method of separation of variables can be used in order to find a solution for partial differential equations. Here we want to investigate the method of the free variable (see also Schneider (1978)). For this method, we simply transform the coordinates in Eq. (6.94) according to

$$\tau = t \qquad (6.118)$$
$$\eta = x\,g(t)$$

The new variable $\eta$ contains the unknown function $g(t)$. This variable is the free variable, which gave the method its name. In order to use the method for obtaining similarity solutions for Eqs. (6.94) and (6.95), we introduce the dimensionless temperature distribution $\Theta = (T - T_0)/(T_W - T_0)$ into these equations. This results in

$$\frac{\partial \Theta}{\partial t} = a \frac{\partial^2 \Theta}{\partial x^2} \tag{6.119}$$

with the boundary conditions

$$
\begin{aligned}
t = 0 : \quad & \Theta = 0 \\
x = 0 : \quad & \Theta = 1, x \to \infty : \Theta = 0
\end{aligned}
\tag{6.120}
$$

Introducing the new coordinates defined in Eq. (6.118) into the partial differential Eq. (6.119) results in

$$\frac{\eta}{g(\tau)} g'(\tau) \frac{d\Theta}{d\eta} = a\, g^2(\tau) \frac{d^2\Theta}{d\eta^2} \tag{6.121}$$

where the prime denotes differentiation with respect to $\tau$. In Eq. (6.121) we have assumed that $\Theta$ depends only on $\eta$. This assumption is suggested by the form of the boundary conditions given by Eq. (6.120). Equation (6.121) reduces to an ordinary differential equation, if the dependence on time drops out of this equation. This is satisfied, if

$$\frac{g'(\tau)}{g^3(\tau)} = \text{const.} \tag{6.122}$$

From this equation we can calculate $g(\tau)$

$$g(\tau) = 1/\sqrt{C_1 + a\tau} \tag{6.123}$$

The constant $C_1$ in Eq. (6.123) can be set to zero, because it only shifts the time origin and we are only interested in one solution of Eq. (6.123). Introducing Eq. (6.123) with $C_1 = 0$ into Eq. (6.121) leads to

$$\Theta'' + \frac{1}{2}\eta\, \Theta' = 0 \tag{6.124}$$

which is identical to Eq. (6.107).

## 6.4.2 Similarity Solutions of the Boundary Layer Equations for Laminar Free Convection Flow on a Vertical Flat Plate

After discussing the fundamentals of the different methods for a very simple example, the present section investigates similarity solutions of the boundary layer

**Fig. 6.8** Free convection flow along a vertical flat plate
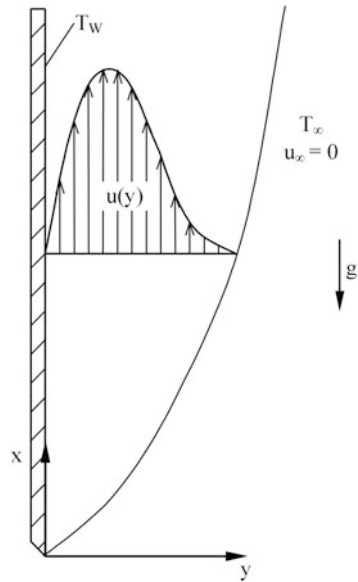


equations for laminar, incompressible, free convection flow on a vertical flat wall. The reader is referred to Jaluria (1980) and Ede (1967) for detailed discussions on this topic. Similarity solutions for this type of application have been obtained for example by Ostrach (1953), which are in very good agreement with measurements performed by Schmidt and Beckmann (1930).

The geometry as well as the velocity distribution for the free convection on a vertical flat plate is shown in Fig. 6.8.

The free convection flow is driven by the temperature difference between the wall and the free-stream. It is assumed that the Boussinesq approximation can be applied. This means that the density difference can be replaced by a simplified equation of state and that variable property effects can be neglected, except for the density in the momentum equation (see for example Jaluria (1980)).

In the following equations, $g$ is the gravitational acceleration and $\beta$ denotes the thermal volumetric expansion coefficient, defined by

$$\beta = \frac{1}{\rho} \left( \frac{\partial \rho}{\partial T} \right)_p \tag{6.125}$$

The continuity Eq. (6.64) can automatically be satisfied by introducing a stream-function, defined by

$$u = \frac{\partial \Psi}{\partial y}, \quad v = -\frac{\partial \Psi}{\partial x} \tag{6.126}$$

This leads to the following set of partial differential equations

$$\frac{\partial \Psi}{\partial y}\frac{\partial^2 \Psi}{\partial x \partial y} - \frac{\partial \Psi}{\partial x}\frac{\partial^2 \Psi}{\partial y^2} = g\beta(T_W - T_\infty)\Theta + \frac{\mu}{\rho}\frac{\partial^3 \Psi}{\partial y^3} \tag{6.127}$$

$$\frac{\partial \Psi}{\partial y}\frac{\partial \Theta}{\partial x} - \frac{\partial \Psi}{\partial x}\frac{\partial \Theta}{\partial y} = a\frac{\partial^2 \Theta}{\partial y^2} \tag{6.128}$$

with the boundary conditions

$$
\begin{array}{llll}
y = 0: & \partial\Psi/\partial y = 0, & \partial\Psi/\partial x = 0, & \Theta = 1 \\
y \to \infty: & \partial\Psi/\partial y = 0, & & \Theta = 0
\end{array} \tag{6.129}
$$

and the dimensionless temperature

$$\Theta = \frac{T - T_\infty}{T_W - T_\infty} \tag{6.130}$$

### 6.4.2.1 Group-Theory Method

The group-theory method has been used, for example, by Ames (1965a) and by Cebeci and Bradshaw (1984) for obtaining similarity solutions for the boundary layer equations for forced convection flows. Here we want to investigate the free convection on a vertical flat plate by using the linear transformation

$$
\begin{array}{ll}
\bar{x} = A^{\gamma_1}x, & \bar{\Psi} = A^{\kappa_1}\Psi \\
\bar{y} = A^{\gamma_2}y, & \bar{\Theta} = A^{\kappa_2}\Theta
\end{array} \tag{6.131}
$$

for the dependent and independent variables. From Eq. (6.131) one obtains

$$\left(\frac{\bar{x}}{x}\right)^{1/\gamma_1} = \left(\frac{\bar{y}}{y}\right)^{1/\gamma_2} = \left(\frac{\bar{\Psi}}{\Psi}\right)^{1/\kappa_1} = \left(\frac{\bar{\Theta}}{\Theta}\right)^{1/\kappa_2} = A \tag{6.132}$$

Introducing the linear transformation, given by Eq. (6.131), into the Eqs. (6.127) and (6.128) results in

$$A^{\gamma_1+2\gamma_2-2\kappa_1}\frac{\partial \bar{\Psi}}{\partial \bar{y}}\frac{\partial^2 \bar{\Psi}}{\partial \bar{x}\partial \bar{y}} - A^{\gamma_1+2\gamma_2-2\kappa_1}\frac{\partial \bar{\Psi}}{\partial \bar{x}}\frac{\partial^2 \bar{\Psi}}{\partial \bar{y}^2} \tag{6.133}$$

$$= g\beta(T_W - T_\infty)A^{-\kappa_2}\,\bar{\Theta} + A^{3\gamma_2-\kappa_1}\frac{\mu}{\rho}\frac{\partial^3 \bar{\Psi}}{\partial \bar{y}^3}$$

$$A^{\gamma_1+\gamma_2-\kappa_1-\kappa_2}\frac{\partial \bar{\Psi}}{\partial \bar{y}}\frac{\partial \bar{\Theta}}{\partial \bar{x}} - A^{\gamma_1+\gamma_2-\kappa_1-\kappa_2}\frac{\partial \bar{\Psi}}{\partial \bar{x}}\frac{\partial \bar{\Theta}}{\partial \bar{y}} = aA^{2\gamma_2-\kappa_2}\frac{\partial^2 \bar{\Theta}}{\partial \bar{y}^2} \tag{6.134}$$

If one requires that the differential equations are completely invariant to the proposed linear transformations, the following coupled algebraic equations are obtained

$$\gamma_1 + 2\gamma_2 - 2\kappa_1 = -\kappa_2 \tag{6.135}$$
$$3\gamma_2 - \kappa_1 = -\kappa_2$$
$$\gamma_1 + \gamma_2 - \kappa_1 - \kappa_2 = 2\gamma_2 - \kappa_2$$

Under the assumption that the exponent $\gamma_1 \neq 0$, a ratio $\gamma = \gamma_2/\gamma_1$ can be defined. Thus, one obtains from Eq. (6.135) the following relations

$$\gamma = \frac{\gamma_2}{\gamma_1}, \; \frac{\kappa_1}{\gamma_1} = 1 - \gamma, \; \frac{\kappa_2}{\gamma_1} = 1 - 4\gamma \tag{6.136}$$

Introducing Eq. (6.136) into Eq. (6.132) results in

$$\eta = \frac{y}{x^\gamma}, \;\; \Psi = x^{1-\gamma}F(\eta), \;\; \Theta = x^{1-4\gamma}G(\eta) \tag{6.137}$$

with the yet unknown coefficient $\gamma$. However, if one introduces the expression for the temperature into the boundary conditions, Eq. (6.129), one obtains

$$\begin{aligned} \eta = 0: & \quad x^{1-4\gamma}G(0) = 1 \\ \eta \to \infty: & \quad x^{1-4\gamma}G(\infty) = 0 \end{aligned} \tag{6.138}$$

From the boundary condition for $\eta \to \infty$ it can be seen that $G(\infty) = 0$. From the second boundary condition for $\eta = 0$ it is obvious that the exponent $\gamma$ must be 1/4. Inserting this value of $\gamma$ into Eq. (6.137) yields

$$\eta = \frac{y}{x^{1/4}}, \;\; \Psi = x^{3/4}F(\eta), \;\; \Theta = G(\eta) \tag{6.139}$$

Transforming the individual terms in Eqs. (6.127)–(6.129) results in

$$\left(\frac{\partial\Psi}{\partial y}\right)_x = x^{1/2}F'(\eta), \;\; \left(\frac{\partial\Psi}{\partial x}\right)_y = \frac{3}{4}x^{-1/4}F(\eta) - \frac{1}{4}x^{-1/4}\eta F'(\eta), \tag{6.140}$$

$$\left(\frac{\partial^2\Psi}{\partial y^2}\right)_x = x^{1/4}F''(\eta), \;\; \left(\frac{\partial^2\Psi}{\partial x \partial y}\right) = \frac{1}{2}x^{-1/2}F'(\eta) - \frac{1}{4}x^{-1/2}\eta F'(\eta),$$

$$\left(\frac{\partial^3\Psi}{\partial y^3}\right)_x = F'''(\eta)$$

where a prime in Eq. (6.140) indicates a differentiation with respect to the similarity coordinate $\eta$. Inserting these expressions into Eqs. (6.127)–(6.129) results with $v = \mu/\rho$ in

$$-\frac{1}{2}\left(F'(\eta)\right)^2 + \frac{3}{4}F(\eta)F''(\eta) + vF'''(\eta) + g\beta(T_W - T_\infty)G(\eta) = 0 \qquad (6.141)$$

$$\frac{3}{4}F(\eta)G'(\eta) + a\,G''(\eta) = 0 \qquad (6.142)$$

with the boundary conditions

$$\begin{array}{llll} \eta = 0: & F(0) = 0, & F'(0) = 0, & G(0) = 1 \\ \eta \to \infty: & F'(\infty) = 0, & & G(\infty) = 0 \end{array} \qquad (6.143)$$

Introducing finally the following dimensionless quantities

$$\tilde{\eta} = \frac{y}{x^{1/4}}\left(\frac{g\beta(T_W - T_\infty)}{v^2}\right)^{1/4} = \eta\left(\frac{g\beta(T_W - T_\infty)}{v^2}\right)^{1/4}$$
$$F = \left(g\beta(T_W - T_\infty)v^2\right)^{1/4}\tilde{F} \qquad (6.144)$$

into Eqs. (6.141)–(6.143) results in

$$-\frac{1}{2}\left(\tilde{F}'(\tilde{\eta})\right)^2 + \frac{3}{4}\tilde{F}(\tilde{\eta})\tilde{F}''(\tilde{\eta}) + \tilde{F}'''(\tilde{\eta}) + \tilde{G}(\tilde{\eta}) = 0 \qquad (6.145)$$

$$\frac{3}{4}\mathrm{Pr}\,\tilde{F}(\tilde{\eta})G'(\tilde{\eta}) + G''(\tilde{\eta}) = 0 \qquad (6.146)$$

$$\begin{array}{llll} \tilde{\eta} = 0: & \tilde{F}(0) = 0, & \tilde{F}'(0) = 0, & \tilde{G}(0) = 1 \\ \tilde{\eta} \to \infty: & \tilde{F}'(\infty) = 0, & & \tilde{G}(\infty) = 0 \end{array} \qquad (6.147)$$

### 6.4.2.2   The Method of the Free Variable

Let us now investigate the same problem, Eqs. (6.127)–(6.129), with the method of the free variable. Therefore, we introduce the new coordinates, defined by

$$\begin{aligned} \xi &= x \\ \eta &= y\,g(x) \end{aligned} \qquad (6.148)$$

In addition, we assume that the stream-function can be prescribed by the following expression

$$\Psi = H(\xi) F(\eta) \tag{6.149}$$

Introducing the new coordinates Eq. (6.148) and the stream-function, given by Eq. (6.149), into Eqs. (6.127)–(6.129) results in

$$(F')^2 (H'g(\xi) + Hg'(\xi))Hg(\xi) - FF''g^2(\xi)HH' \tag{6.150}$$
$$= vg^3(\xi)HF''' + g\beta(T_W - T_\infty)\Theta$$

$$a\,\Theta'' + F\left(\frac{H'}{g(\xi)}\right)\Theta' = 0 \tag{6.151}$$

with the boundary conditions

$$\begin{aligned}
\eta = 0: \quad & F = 0, \quad F' = 0, \quad \Theta = 1 \\
\eta \to \infty: \quad & F' = 0, \quad\quad\quad\quad \Theta = 0
\end{aligned} \tag{6.152}$$

In order to reduce Eqs. (6.150) and (6.151) to a set of ordinary differential equations, the dependence on the coordinate $\xi$ has to drop out from these equations. This leads to the fact that the following ordinary differential equations have to be satisfied

$$\begin{aligned}
Hg(H'g + Hg') &= C_1 \\
g^2 HH' &= C_2 \\
g^3 H &= C_3 \\
\frac{H'}{g} &= C_4
\end{aligned} \tag{6.153}$$

where $C_1$, $C_2$, $C_3$ and $C_4$ are constants. The four differential equations, given by Eq. (6.153) have to be linearly dependent on each other so that the two functions $H$ and $g$ can be determined. If we divide, for example, the second relation in Eq. (6.153) by the third one, the fourth relation is obtained. If we eliminate $H$ and $H'$ in the second relation using the third and the fourth relations, one obtains

$$C_3 C_4 = C_2 \tag{6.154}$$

Introducing the third and the fourth relations into the first one results in the following ordinary differential equation for the unknown function $g$

$$\frac{g'}{g^5} = \left(\frac{C_1}{C_3^2} - \frac{C_4}{C_3}\right) \tag{6.155}$$

This ordinary differential equation has the solution

$$g = (B_1\xi + B_2)^{-1/4} \tag{6.156}$$

where $B_1$ and $B_2$ are constants. The constant $B_2$ can be set to zero, because it only shifts the origin of the $\xi$-coordinate. For the function $H$ one obtains from Eq. (6.153)

$$H = B_3 \xi^{3/4} \tag{6.157}$$

Introducing Eqs. (6.156) and (6.157) into the Eqs. (6.148) and (6.149), one obtains for the similarity coordinate and for the stream-function

$$\eta = \frac{y}{x^{1/4}}, \quad \Psi = x^{3/4} F(\eta) \tag{6.158}$$

This are the same expressions which have been derived by using the group-theory method (see Eq. (6.139)).

## 6.4.3 Similarity Solutions of the Compressible Boundary Layer Equations

As a further example, we want to consider the compressible boundary layer equations for laminar, forced convection flow over a flat plate. Similarity solutions for compressible flows have been investigated e.g. by Li and Nagamatsu (1953, 1955). A good overview on this subject is provided e.g. by Schlichting (1982). For a compressible, laminar flow, the boundary layer equations take the form (Kays et al. 2004)

$$\frac{\partial}{\partial x}(\rho u) + \frac{\partial}{\partial y}(\rho v) = 0 \tag{6.79}$$

$$\rho u \frac{\partial u}{\partial x} + \rho v \frac{\partial u}{\partial y} = -\frac{dp}{dx} + \frac{\partial}{\partial y}\left(\mu \frac{\partial u}{\partial y}\right) \tag{6.159}$$

$$\rho c_p \left(u \frac{\partial T}{\partial x} + v \frac{\partial T}{\partial y}\right) = u \frac{dp}{dx} + \frac{\partial}{\partial y}\left(k \frac{\partial T}{\partial y}\right) + \mu \left(\frac{\partial u}{\partial y}\right)^2 \tag{6.160}$$

As it can be seen from the system of Eqs. (6.79), (6.159) and (6.160), they are strongly coupled by the density. In addition, the fluid properties may no longer be considered constant, because of the high velocities under consideration. It can be assumed that the dynamic viscosity can be approximated by

$$\frac{\mu(T)}{\mu(T_{ref})} = \left(\frac{T}{T_{ref}}\right)^{\omega}, \quad 0.5 \leq \omega \leq 1 \tag{6.161}$$

where $T_{ref}$ is a reference temperature. The density is related to the pressure and the temperature by a thermal state equation and we assume that the fluid under consideration can be considered as an ideal gas.

$$\rho = \frac{p}{RT} \tag{6.162}$$

In addition, we assume that $c_p$ is constant.

For the compressible flow, it is preferable to introduce the specific total enthalpy into the boundary layer equations. The specific total enthalpy is defined for a boundary layer flow ($v \ll u$) by

$$h_0 = c_p T + \frac{1}{2}\left(u^2 + v^2\right) = c_p T + \frac{1}{2}u^2 \tag{6.163}$$

Introducing the specific total enthalpy into the energy Eq. (6.160) results in

$$\rho\left(u\frac{\partial h_0}{\partial x} + v\frac{\partial h_0}{\partial y}\right) = \frac{\partial}{\partial y}\left(\mu\frac{Pr-1}{Pr}u\frac{\partial u}{\partial y}\right) + \frac{\partial}{\partial y}\left(\frac{\mu}{Pr}\frac{\partial h_0}{\partial y}\right) \tag{6.164}$$

The set of partial differential Eqs. (6.79), (6.159) and (6.164) has to be solved together with Eqs. (6.161) and (6.162) and the following boundary conditions

$$x = 0 : u, v, h_0 \quad \text{given} \tag{6.165}$$
$$y = 0 : u = v = 0, \quad h_0 = h_W$$
$$y \to \infty : u = u_\infty(x), \quad h_0 = h_{0\infty}$$

It is convenient to introduce a stream-function into the boundary layer equations defined by

$$\rho u = \frac{\partial \Psi}{\partial y}, \quad \rho v = -\frac{\partial \Psi}{\partial x} \tag{6.166}$$

In addition, the following new coordinates are introduced

$$\zeta = \rho_\infty u_\infty \int_0^y \frac{\rho}{\rho_\infty}d\bar{y} \tag{6.167}$$

$$\xi = \int_0^x \rho_\infty u_\infty \eta_\infty d\bar{x}$$

The introduction of the coordinate transformation results in the fact that the partial differential equations, which describe the momentum and energy transport in the boundary layer, take a similar structure as those for an incompressible fluid (see

Schlichting 1982, Loitsianki 1967). The change of coordinates given by Eq. (6.167) is known in literature as the Illingworth-Stewardson transformation.

After introducing the stream-function and carrying out the coordinate transformation, one obtains the following two partial differential equations from Eqs. (6.159) and (6.164)

$$\frac{1}{u_\infty}\frac{du_\infty}{d\xi}\left(\frac{\partial\Psi}{\partial\zeta}\right)^2 + \frac{\partial\Psi}{\partial\zeta}\frac{\partial^2\Psi}{\partial\xi\partial\zeta} - \frac{\partial\Psi}{\partial\xi}\frac{\partial^2\Psi}{\partial\zeta^2} = \frac{\rho_\infty}{\rho}\frac{1}{u_\infty}\frac{du_\infty}{d\xi} + \frac{\partial}{\partial\zeta}\left[Ch\frac{\partial^2\Psi}{\partial\zeta^2}\right] \quad (6.168)$$

$$\frac{\partial\Psi}{\partial\zeta}\frac{\partial\phi}{\partial\xi} - \frac{\partial\Psi}{\partial\xi}\frac{\partial\phi}{\partial\zeta} = \frac{u_\infty^2}{h_{0\infty}}\frac{\partial}{\partial\zeta}\left(\frac{\text{Pr}-1}{\text{Pr}}Ch\frac{\partial\Psi}{\partial\zeta}\frac{\partial^2\Psi}{\partial\zeta^2}\right) + \frac{\partial}{\partial\zeta}\left(\frac{Ch}{\text{Pr}}\frac{\partial\phi}{\partial\zeta}\right) \quad (6.169)$$

where the following abbreviations have been used

$$Ch = \frac{\rho\mu}{\rho_\infty\mu_\infty}, \quad \text{Pr} = \frac{\mu c_p}{k}, \quad \phi = \frac{h_0}{h_{0\infty}} \quad (6.170)$$

The quantity $Ch$, which appears in the above equations, is called the Chapman-Rubesin parameter. This parameter can be described as a function of temperature by inserting Eqs. (6.161) and (6.162) into Eq. (6.170). One obtains ($p = p_\infty$)

$$Ch = \frac{p}{RT}\frac{RT_\infty}{p_\infty}\left(\frac{T}{T_\infty}\right)^\omega = \left(\frac{T}{T_\infty}\right)^{\omega-1}, \ 0.5 \le \omega \le 1 \quad (6.171)$$

The Eqs. (6.168) and (6.169) have to be solved together with the following boundary conditions

$$\xi = 0 : \Psi, \phi \qquad\qquad \text{given} \qquad\qquad (6.172)$$
$$\zeta = 0 : \frac{\partial\Psi}{\partial\xi} = 0, \qquad \frac{\partial\Psi}{\partial\zeta} = 0, \qquad \phi = \phi_W$$
$$\zeta \to \infty : \qquad\qquad \frac{\partial\Psi}{\partial\zeta} = 1, \qquad \phi = 1$$

After expressing the conservation equations in a suitable form, the question whether the above given set of partial differential equations has similar solutions can be addressed. This can be done by using the method of the free variable. Therefore, we are going to introduce the new variables

$$\bar{x} = \xi \qquad\qquad (6.173)$$
$$\eta = \zeta\, w_1(\xi)$$

into the Eqs. (6.168) and (6.169) and into the boundary conditions, Eq. (6.172). The function $w_1(\xi)$ is unknown and is determined during the solution process.

Performing the change of coordinates results in

$$\frac{1}{u_\infty}\frac{du_\infty}{d\bar{x}}\left(\frac{\partial\Psi}{\partial\eta}\right)^2 + \frac{w_1'}{w_1}\left(\frac{\partial\Psi}{\partial\eta}\right)^2 + \frac{\partial\Psi}{\partial\eta}\frac{\partial^2\Psi}{\partial\bar{x}\partial\eta} - \frac{\partial\Psi}{\partial\bar{x}}\frac{\partial^2\Psi}{\partial\eta^2} \tag{6.174}$$

$$= \frac{\rho_\infty}{\rho}\frac{1}{w_1^2}\frac{1}{u_\infty}\frac{du_\infty}{d\bar{x}} + w_1\frac{\partial}{\partial\eta}\left(Ch\frac{\partial^2\Psi}{\partial\eta^2}\right)$$

$$\frac{\partial\Psi}{\partial\eta}\frac{\partial\phi}{\partial\bar{x}} - \frac{\partial\Psi}{\partial\bar{x}}\frac{\partial\phi}{\partial\eta} = w_1^3\frac{u_\infty^2}{h_{0\infty}}\frac{\partial}{\partial\eta}\left(\frac{\mathrm{Pr}-1}{\mathrm{Pr}}Ch\frac{\partial\Psi}{\partial\eta}\frac{\partial^2\Psi}{\partial\eta^2}\right) + w_1\frac{\partial}{\partial\eta}\left(\frac{Ch}{\mathrm{Pr}}\frac{\partial\phi}{\partial\eta}\right) \tag{6.175}$$

with the boundary conditions

$$\bar{x} = 0 : \Psi, g \text{ are given} \tag{6.176}$$

$$\eta = 0 : \frac{\partial\Psi}{\partial\eta} = 0, \ \frac{\partial\Psi}{\partial\bar{x}} = 0, \ \ \phi = \phi_W$$

$$\eta \to \infty : w_1(\bar{x})\frac{\partial\Psi}{\partial\eta} = 1, \ \ \ \phi = 1$$

After introducing the new coordinates, it may now be assumed that the stream-function can be expressed by the following product

$$\Psi = w_2(\bar{x})f(\eta) \tag{6.177}$$

The expression given by Eq. (6.177) is obvious from the boundary condition for the stream-function for $\eta \to \infty$.

The enthalpy function $\phi$ is assumed to depend only on $\eta$. Introducing the assumed expressions for $\Psi$ and $\phi$ into the boundary conditions, one obtains

$$\eta = 0 : f(0) = 0, \ f'(0) = 0 \tag{6.178}$$

$$\phi(0) = \phi_W$$

$$\eta \to \infty : w_1(\bar{x})w_2(\bar{x})f'(\infty) = 1$$

$$\phi(\infty) = 1$$

From Eq. (6.178) one obtains immediately that $w_1(\bar{x})\,w_2(\bar{x})$ has to be a constant in order to satisfy the boundary condition for $\eta \to \infty$. This can be achieved, if we set for example

$$w_2(\bar{x}) = \frac{1}{w_1(\bar{x})} \tag{6.179}$$

which leads to the following expression for the stream-function

$$\Psi = \frac{f(\eta)}{w_1(\bar{x})} \tag{6.180}$$

Introducing the expressions for the stream-function and the temperature into the Eqs. (6.174) and (6.175) results in the following differential equations

$$\frac{1}{w_1^2}\frac{1}{u_\infty}\frac{du_\infty}{d\bar{x}}(f')^2+\frac{w_1'}{w_1^3}ff''=\frac{\rho_\infty}{\rho}\frac{1}{w_1^2}\frac{1}{u_\infty}\frac{du_\infty}{d\bar{x}}+(Chf'')' \tag{6.181}$$

$$\frac{w_1'}{w_1^3}f\phi'=\frac{u_\infty^2}{h_{0\infty}}\left(\frac{Pr-1}{Pr}Chf'f''\right)'+\left(\frac{Ch}{Pr}\phi'\right)' \tag{6.182}$$

In order to obtain similarity solutions for these two equations, the dependence on $\bar{x}$ in the equations must cancel out. This is only possible, if

$$\frac{w_1'}{w_1^3}=\text{const.} \tag{6.183}$$

Equation (6.183) can simply be integrated and one result of this equation is

$$w_1=\frac{1}{\sqrt{2\bar{x}}} \tag{6.184}$$

Introducing Eq. (6.184) into the Eqs. (6.181) and (6.182) results in

$$(Chf'')'+\frac{2\bar{x}}{u_\infty}\frac{du_\infty}{d\bar{x}}\left(\frac{\rho_\infty}{\rho}-(f')^2\right)+ff''=0 \tag{6.185}$$

$$\left(\frac{Ch}{Pr}\phi'\right)'+f\phi'+\frac{u_\infty^2}{h_{0\infty}}\left(\frac{Pr-1}{Pr}Chf'f''\right)=0 \tag{6.186}$$

These two coupled ordinary differential equations have to be solved together with the following boundary conditions

$$\eta=0: \quad f(0)=0, \quad f'(0)=0, \quad \phi(0)=\phi_W \tag{6.187}$$
$$\eta\to\infty: \qquad\qquad f'(\infty)=1, \quad \phi(\infty)=1$$

In order to guarantee that the Eqs. (6.185) and (6.186) are a set of ordinary differential equations, any dependence on $\bar{x}$ must cancel out from these equations. This fact leads to the following restrictions on the coefficients in these equations:

1. The Prandtl number must be a constant or has to depend only on $\eta$. This is not a strong restriction, because, e.g. for air, the Prandtl number is approximately a constant for a large temperature range.
2. The Chapman-Rubesin parameter $Ch$ must be a constant or should only be a function of $\eta$. This is no real restriction, as can be seen from Eq. (6.171). For the viscosity law considered here, this is always satisfied.

3. The density ratio $\rho_\infty/\rho$ has to be constant or a function of $\eta$ only. Because we considered an ideal gas, we obtain from Eq. (6.162) that

$$\frac{\rho_\infty}{\rho} = \frac{T}{T_\infty} \tag{6.188}$$

4. The expression

$$\frac{2\bar{x}}{u_\infty}\frac{du_\infty}{d\bar{x}} = \beta = \text{const.} \tag{6.189}$$

has to be constant. This is possible if the external flow speed $u_\infty = $ const., or in general if $u_\infty = C_1\bar{x}^m$.
5. Finally, one has to require that the expression

$$\frac{u_\infty^2}{h_{0\infty}} = 2\left(1 + \frac{2}{(\kappa - 1)\text{Ma}_\infty^2}\right)^{-1} \tag{6.190}$$

has to be constant, or the Prandtl number must be equal to one. For most gases the assumption that $\text{Pr} = 1$ is quite reasonable. If this is not the case, it is required that either the Mach number is constant or that the Mach number is high enough, so that $u_\infty^2/h_{0\infty}$ can be approximated by 2.

The similarity Eqs. (6.185) and (6.186) have first been obtained by Cohen and Reshotko (1956) (see also Eckert and Drake (1987), Jischa (1982)).

### 6.4.3.1 Flow and Temperature Distribution for a Flat Plate

As an illustration of the preceding analysis we consider a flow over a flat plate. The free stream velocity $u_\infty = $ const. and the dynamic viscosity is described by

$$\frac{\mu(T)}{\mu(T_{ref})} = \frac{T}{T_{ref}} \tag{6.191}$$

This leads to the fact that the Chapman-Rubesin parameter $Ch = 1$ and the Eqs. (6.185) and (6.186) simplify to

$$f''' + ff'' = 0 \tag{6.192}$$

$$K(f'f'')' + \vartheta'' + \text{Pr}f\vartheta' = 0 \tag{6.193}$$

with the abbreviations

$$\vartheta = \frac{\phi - \phi_W}{1 - \phi_W}, \quad K = \frac{2(\mathrm{Pr} - 1)}{1 - \phi_W}\left(1 + \frac{2}{(\kappa - 1)Ma_\infty^2}\right)^{-1} \tag{6.194}$$

The Eqs. (6.192) and (6.193) have to be integrated with the boundary conditions

$$\begin{array}{llll}
\eta = 0: & f(0) = 0, & f'(0) = 0, & \vartheta(0) = 0 \\
\eta \to \infty: & f'(\infty) = 1, & & \vartheta(\infty) = 1
\end{array} \tag{6.195}$$

Under these assumptions, the momentum equation reduces to the Blasius equation (see Prandtl 1935, Schlichting 1982). The energy equation can be solved by standard methods and the final result is given by

$$\vartheta = 1 - \frac{\int_\eta^\infty (f'')^{\mathrm{Pr}} d\bar\eta}{\int_0^\infty (f'')^{\mathrm{Pr}} d\bar\eta} + K \int_0^\infty (f'')^{\mathrm{Pr}} \int_0^t (f'')^{-\mathrm{Pr}} (f'f'')' d\bar\eta dt \tag{6.196}$$

$$\times \left\{ \frac{\int_\eta^\infty (f'')^{\mathrm{Pr}} d\bar\eta}{\int_0^\infty (f'')^{\mathrm{Pr}} d\bar\eta} - \frac{\int_\eta^\infty (f'')^{\mathrm{Pr}} \int_0^t (f'')^{-\mathrm{Pr}} (f'f'')' d\bar\eta dt}{\int_0^\infty (f'')^{\mathrm{Pr}} \int_0^t (f'')^{-\mathrm{Pr}} (f'f'')' d\bar\eta dt} \right\}$$

## Problems

6-1  Consider the heat conduction in a rectangular flat plate. The plate has a heat conductivity which depends only on temperature. The problem can be described by the following equation

$$\frac{\partial}{\partial x}\left(k(T)\frac{\partial T}{\partial x}\right) + \frac{\partial}{\partial y}\left(k(T)\frac{\partial T}{\partial y}\right) = 0$$

where the heat conductivity is assumed to be given by the following equation

$$k(T) = k_0\left(\frac{T}{T_0}\right)$$

where $k_0$, $T_0$ are constant reference values.

(a)  Investigate first the case of a constant heat conductivity $k = k_0$. Show by insertion, that if $T_1$ and $T_2$ are both solutions of the heat conduction equation, then also $C_1 T_1 + C_2 T_2$ is a solution of the equation ($C_1$ and $C_2$ are arbitrary constants).

(b)  Consider now the case of a temperature dependent heat conductivity. Show that if two solutions of the problem have been found ($T_1$ and $T_2$), the sum of them $T_1 + T_2$ is not necessarily a solution of the problem.

6-2 Consider the one dimensional transient heat conduction in a slab ($0 \le x \le L$). The slab is initially at a constant temperature $T_0$. For $t > 0$ the boundary condition are: at $x = 0$, the slab is insulated and at $x = L$, it is kept at a constant temperature $T_W$. The problem under consideration is described by the following equation

$$\rho c \frac{\partial T}{\partial t} = \frac{\partial}{\partial x}\left(k\frac{\partial T}{\partial x}\right)$$

with the boundary conditions

$$t = 0 : \quad T = T_0$$
$$x = 0 : \quad \frac{\partial T}{\partial x} = 0$$
$$x = L : \quad T = T_W$$

The heat conductivity of the solid is assumed to depend on temperature in the form

$$k = k_0(1 + C(T - T_0))$$

However, the heat diffusivity $a = k/(\rho c)$ can be taken as constant.

(a) Apply the Kirchhoff transformation to the above equations and show that the resulting heat conduction equation reduces to a linear equation if the heat diffusivity is assumed constant.
(b) Solve the transformed problem by using the method of separation of variables.
(c) What is the solution of the original problem?

6-3 Consider the partial differential equation

$$\tilde{y}\frac{\partial \Theta}{\partial \tilde{x}} = \frac{\partial^2 \Theta}{\partial \tilde{y}^2}$$

with the boundary conditions

$$\tilde{x} = 0 : \quad \Theta = 1$$
$$\tilde{y} = 0 : \quad \Theta = 0$$
$$\tilde{y} \to \infty : \quad \Theta = 1$$

For this problem, similarity solutions can be obtained with the method of the free variable.

(a) Introduce the new variables

$$\xi = \tilde{x}$$
$$\eta = \tilde{y}\,g(\tilde{x})$$
$$\Theta = \Theta(\eta)$$

into the differential equation. What is the resulting equation (please remember that $\Theta$ depends only on $\eta$)?

(b) Which ordinary differential equation has to be satisfied for the function $g(\tilde{x})$, so that similarity solutions are possible?

(c) Solve the ordinary differential equation for $g$ and determine the similarity coordinate.

(d) Determine the solution for the above given problem.

6-4 Consider the transient heat conduction in a semi-infinite body. The body contains a heat source. At the surface of the body, a time dependent temperature is applied. The process can be described by the following nonlinear partial differential equation

$$\rho c \frac{\partial T}{\partial t} = k \frac{\partial^2 T}{\partial x^2} + F(T,t)e^{-x/\sqrt{t}}$$

with boundary conditions

$$x = 0: \quad T = T_W(t)$$
$$x \to \infty: \quad T = T_0$$
$$t = 0: \quad T = T_0$$

All properties ($\rho$, $c$, $k$) of the material can be considered constant. Investigate under which circumstances similarity solutions of the above equation are possible, assuming the similarity variable is given by $\eta = Cx/\sqrt{t}$, $C = $ const.

(a) Introduce the dimensionless temperature $\Theta = (T - T_0)/(T_W(t) - T_0)$ into the above equation and boundary conditions.

(b) Determine the constant $C$ in the similarity variable from dimensional reasoning, so that $\eta$ is dimensionless.

(c) Consider now the case $F(T, t) = 0$. Perform the coordinate transformation and show that similarity solutions are possible for the boundary conditions under consideration.

(d) Consider now the case $T_W = $ const. Determine for this case the form of the function $F(T, t)$, for which similarity solutions are possible employing the similarity variable suggested above.

6-5   Consider the flow over a flat plate with an external pressure gradient. The flow
      is incompressible and all fluid properties are constant. The problem is
      described by the incompressible boundary layer equations given by

$$\frac{\partial u}{\partial x} + \frac{\partial v}{\partial y} = 0$$

$$u\frac{\partial u}{\partial x} + v\frac{\partial u}{\partial y} = -\frac{1}{\rho}\frac{dp}{dx} + \frac{\mu}{\rho}\frac{\partial^2 u}{\partial y^2}$$

with boundary conditions

$$\begin{aligned} y = 0: \quad & u = v = 0 \\ y \to \infty: \quad & u = u_\infty(x) \end{aligned}$$

The pressure gradient in the momentum equation is linked to the free-stream
acceleration by

$$-\frac{1}{\rho}\frac{dp}{dx} = u_\infty\frac{du_\infty}{dx}$$

(a) Introduce a stream-function into the momentum equation, so that the
    continuity equation is automatically satisfied. Express the boundary
    conditions in terms of the stream-function. What are the resulting
    equations?
(b) Investigate the equations obtained above by using the group-theory
    method. What is the similarity coordinate and how has the stream-
    function to look like so that similarity solutions are possible? What
    ordinary differential equation can be obtained for the modified stream-
    function?
(c) Investigate the problem under (b) once again using the method of the free
    variable. Can you verify the results obtained under (b)?

6-6   Consider the one dimensional transient heat conduction in a semi-infinite
      solid. The temperature distribution can be described by the following
      equations

$$\frac{\partial T}{\partial t} = a\frac{\partial}{\partial x}\left[\left(1 + b\left(\frac{T - T_0}{T_W - T_0}\right)\right)\frac{\partial T}{\partial x}\right]$$

$$\begin{aligned} t = 0: \quad & T = T_0 \\ x = 0: \quad & T = T_W \\ x \to \infty: \quad & T = T_0 \end{aligned}$$

where the heat diffusivity $a$ can be considered to be constant. The temperatures $T_0$ and $T_W$ and the value $b$ are constant.

(a) Introduce a suitable dimensionless temperature into the above equations.
(b) For this problem, similarity solutions can be obtained using the method of the free variable. Introduce the new coordinate $\eta = x^2 g(t)$ into the heat conduction equation under the assumption that the dimensionless temperature only depends on the similarity coordinate. What ordinary differential equation has to be satisfied for the function $g(t)$? What similarity coordinate is obtained? Determine the similarity solution of the problem.

6-7 On a Sunday afternoon a professor thinks at home about the question, if similarity solutions exist for the following problem: A sphere, which is very large and can be considered to be half-infinite in size, is hollow ($r = r_1$). At the beginning the sphere has a constant temperature $T = T_0$ everywhere. Then, suddenly the temperature at $r = r_1$ is changed to $T = T_1$ for $t > 0$. For very large radii, the temperature of the sphere stays always at $T_0$. All properties of the sphere ($\rho$, $c$, $k$) are constant. The temperature distribution in the sphere can be calculated by solving the heat conduction equation. This equation is given in spherical coordinates by

$$\rho c \frac{\partial T}{\partial t} = \frac{k}{r^2} \frac{\partial}{\partial r}\left(r^2 \frac{\partial T}{\partial r}\right) + \frac{k}{r^2 \sin\psi} \frac{\partial}{\partial \psi}\left(\sin\psi \frac{\partial T}{\partial \psi}\right)$$

$$+ \frac{k}{r^2 \sin\psi} \frac{\partial}{\partial \varphi}\left(\frac{\partial T}{\partial \varphi}\right) + \dot{q}_{i0}$$

In this equation $r$ is the radial coordinate, $\varphi$, $\psi$ denote the tangential and azimuthal coordinates. The term $\dot{q}_{i0}$ denotes sources or sinks in the domain.

(a) Simplify the heat conduction equation under the assumption of one-dimensional transient heat conduction.
(b) Introduce the dimensionless temperature $\Theta = (T - T_0)/(T_1 - T_0)$ into the energy equation and formulate the boundary conditions for $r = r_1$ and for $r \to \infty$.
(c) Please now support the professor in searching for similarity solutions for this differential equation. For this, introduce

$$\tau = t$$
$$\eta = rg(\tau)$$

into the equation and derive an equation for $\Theta = f(\eta)$.
(d) Which condition has to be satisfied for $g(\tau)$, so that self-similar solutions can be obtained for this problem? Derive now the ordinary differential equation for $\Theta(\eta)$. Insert in this equation the substitution $z = \eta^2 \Theta'$ and derive a solution for the problem.

6-8. Consideration is given to a planar channel subjected to a laminar internal flow. The velocity profile is hydrodynamically fully developed. The fluid, which is flowing through the channel, has a very high Prandtl number, $\Pr \gg 1$. The flow enters the channel with a constant temperature $T_0$. At the axial position $x \geq 0$, the wall temperature of the channel is set to the higher value $T = T_1$ and heat transfer takes place between the wall and the fluid. In the following the temperature distribution should be calculated for $x \geq 0$. The flow is assumed to be incompressible and the fluid properties $(\rho,\ \lambda,\ c_p,\ \eta)$ are assumed to be constant. The velocity distribution for the hydrodynamically fully developed flow is given by

$$u = 2\bar{u}\left(1 - \left(\frac{y}{h}\right)^2\right), \quad v = 0$$

In this equation $\bar{u}$ denotes the mean inlet velocity into the channel. The orthogonal velocity component $v$ is equal to zero. The temperature profile in the flow can be calculated from the energy equation

$$\rho c_p u(y)\frac{\partial T}{\partial x} = \lambda\left(\frac{\partial^2 T}{\partial x^2} + \frac{\partial^2 T}{\partial y^2}\right)$$

together with the boundary conditions

$$x = 0 : T = T_0 = \text{const.}$$
$$y = h : T = T_0 \quad \text{for } x < 0, \quad T = T_1 \quad \text{for } x \geq 0$$

(a) Introduce the following quantities

$$\Theta = \frac{T - T_0}{T_1 - T_0}, \quad \tilde{x} = \frac{x}{h}\frac{1}{Pe_h}, \quad \tilde{y} = \frac{y}{h}, \quad Pe_h = Re_h\,\Pr, \quad Re_h = \frac{\bar{u}h}{\nu}, \quad \Pr$$
$$= \frac{\nu}{a}, \quad \tilde{u} = \frac{u}{\bar{u}}$$

into the energy equation and transform the energy equation in non-dimensionless form.

(b) Which term can be neglected in the energy equation if the Peclet number $Pe_h$ is very large? Neglect this term and give the resulting equation.

In order to derive now an approximation for large Prandtl numbers, one should proceed as follows.

(c) For $\Pr \to \infty$ the thermal boundary layer is much thinner than the hydrodynamic boundary layer. Because of this fact a linear approximation should be derived for the velocity distribution $\tilde{u}$, which is valid near

the wall. For this a wall coordinate $\tilde{y}_W = y_W/h = 1 - \tilde{y}$ should be considered and the velocity distribution has to be expressed as a function of this coordinate: $\tilde{u} = f(\tilde{y}_W)$. In order to do so, neglect all quadratic terms in the velocity distribution.

(d) Introduce the new wall coordinate $\tilde{y}_W$ and the velocity distribution from (c) into the energy equation from (b). What is obtained?

(e) For the equation developed under (d) a similarity solution should be obtained. Thus, introduce the new coordinates

$$\xi = \tilde{x}$$
$$\eta = \tilde{y}_W h(\tilde{x})$$

into the energy equation and assume that $\Theta = f(\eta)$. What equation can be obtained and what condition has to be satisfied for the function $h(\tilde{x})$, so that the equation has self-similar solutions.

(f) Solve the ordinary differential equation and determine the temperature distribution by using the boundary conditions $\eta = 0 : \Theta = 0, \ \eta \to \infty : \Theta = 1$.

(g) Determine finally the Nusselt number at the wall of the channel. For this the Nusselt number shall be defined as

$$\mathrm{Nu} = \frac{-\frac{\partial T}{\partial y}\big|_{y=h} h}{(T_1 - T_0)}$$

What dependence has Nu on the axial coordinate?

# Appendix A
# The Fully Developed Velocity Profile
# for Turbulent Duct Flows

This appendix discusses the hydrodynamically fully developed velocity profile for pipe and channel flows. The geometry under consideration is shown in Fig. A.1.

For the flow in a parallel plate channel, the velocity components in the $x$-, $y$- and $z$-direction are $u$, $v$ and $w$, whereas for the flow in a circular pipe, the velocity components $u$, $v$ and $w$ denote the flow in the $x$-, $r$- and $\varphi$- direction.

We restrict our considerations to an incompressible flow with constant fluid properties. The Reynolds averaged Navier-Stokes equations and the continuity equation are given for a flow in a parallel plate channel by Kays et al. (2004).

## *Parallel Plate Channel*

$$\rho\left(u\frac{\partial u}{\partial x}+v\frac{\partial u}{\partial y}\right)=-\frac{\partial p}{\partial x}+\mu\left(\frac{\partial^2 u}{\partial x^2}+\frac{\partial^2 u}{\partial y^2}\right)-\rho\frac{\partial\overline{(u'u')}}{\partial x}-\rho\frac{\partial\overline{(u'v')}}{\partial y} \qquad (A.1)$$

$$\rho\left(u\frac{\partial v}{\partial x}+v\frac{\partial v}{\partial y}\right)=-\frac{\partial p}{\partial y}+\mu\left(\frac{\partial^2 v}{\partial x^2}+\frac{\partial^2 v}{\partial y^2}\right)-\rho\frac{\partial\overline{(u'v')}}{\partial x}-\rho\frac{\partial\overline{(v'v')}}{\partial y} \qquad (A.2)$$

$$\frac{\partial u}{\partial x}+\frac{\partial v}{\partial y}=0 \qquad (A.3)$$

For the flow in a circular pipe with rotational symmetry, the equations are given by Kays et al. (2004).

## *Pipe*

$$\rho\left(u\frac{\partial u}{\partial x}+v\frac{\partial u}{\partial r}\right)=-\frac{\partial p}{\partial x}+\frac{\mu}{r}\frac{\partial}{\partial r}\left(r\frac{\partial u}{\partial r}\right)+\mu\frac{\partial^2 u}{\partial x^2} \qquad (A.4)$$

$$-\frac{\rho}{r}\frac{\partial}{\partial r}\left(r\overline{u'v'}\right)-\rho\frac{\partial}{\partial x}\left(\overline{u'u'}\right)$$

Parallel Plate Channel                    Pipe
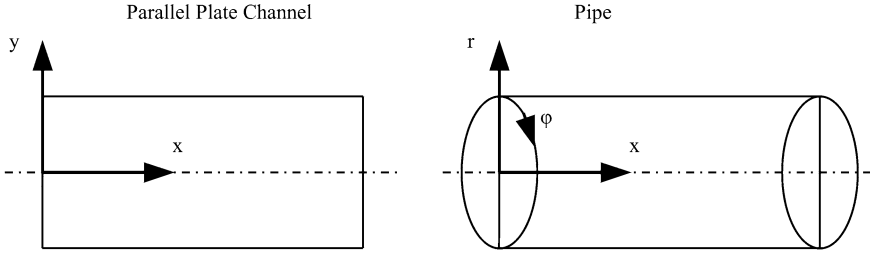
Fig. A.1 Geometry and coordinate system

$$\rho\left(u\frac{\partial v}{\partial x}+v\frac{\partial v}{\partial r}\right)=-\frac{\partial p}{\partial r}+\frac{\mu}{r}\frac{\partial}{\partial r}\left(r\frac{\partial v}{\partial r}\right)+\mu\frac{\partial^2 v}{\partial x^2} \tag{A.5}$$

$$-\frac{\rho}{r}\frac{\partial}{\partial r}\left(r\overline{v'v'}\right)-\rho\frac{\partial}{\partial x}\left(\overline{u'v'}\right)-\rho\frac{\overline{w'w'}}{r}$$

$$\frac{\partial u}{\partial x}+\frac{1}{r}\frac{\partial}{\partial r}(rv)=0 \tag{A.6}$$

For a hydrodynamically fully developed flow, the axial velocity component does not change (by definition) with the axial position and therefore $\partial u/\partial x$ is zero. If we introduce this result into the continuity Eq. (A.3) or (A.6), we obtain that the radial velocity component $v$ is equal to zero and the continuity equation is then automatically satisfied. The fact that $v = 0$ for the fully developed flow is obvious, as a non-zero velocity component $v$ would lead automatically to a change in the axial velocity component for different axial positions. Introducing these results into the above given equations results in.

## *Parallel Plate Channel*

$$0=-\frac{\partial p}{\partial x}+\mu\frac{d^2 u}{dy^2}-\rho\frac{d\overline{(u'v')}}{dy} \tag{A.7}$$

$$0=-\frac{\partial p}{\partial y}-\rho\frac{d\left(\overline{v'v'}\right)}{dy} \tag{A.8}$$

## *Pipe*

$$0=-\frac{\partial p}{\partial x}+\frac{\mu}{r}\frac{d}{dr}\left(r\frac{du}{dr}\right)-\frac{\rho}{r}\frac{d}{dr}\left(r\overline{u'v'}\right) \tag{A.9}$$

$$0 = -\frac{\partial p}{\partial r} - \frac{\rho}{r}\frac{d}{dr}\left(r\overline{v'v'}\right) - \rho\frac{\overline{w'w'}}{r} \tag{A.10}$$

The above equations have to be solved together with the following boundary conditions:

### Parallel Plate Channel

$$y = 0 : \frac{du}{dy} = 0, \tag{A.11}$$
$$y = h : u = 0$$

### Pipe

$$r = 0 : \frac{du}{dr} = 0, \tag{A.12}$$
$$r = R : u = 0$$

In the above equations, the partial derivatives for the axial velocity component and the turbulent stresses have been replaced by total derivatives, because the functions are only dependent on the coordinate orthogonal to the flow direction.

The equations describing the hydrodynamically fully developed flow in the parallel plate channel and in the pipe are quite similar, as it can be seen by comparing Eq. (A.7) with (A.9) and Eq. (A.8) with (A.10). They can be written in a condensed form by using a flow superscript $F$. For the flow in a parallel plate channel $F = 0$, whereas for the flow in a pipe $F = 1$. This results in the following equations:

$$0 = -\frac{\partial p}{\partial x} + \frac{1}{r^F}\frac{d}{dn}\left[r^F\left(\mu\frac{du}{dn} - \rho\overline{u'v'}\right)\right] \tag{A.13}$$

$$0 = \rho\left[\frac{d\overline{(v')^2}}{dn} + F\left(\frac{\overline{(v')^2} - \overline{(w')^2}}{r}\right)\right] + \frac{\partial p}{\partial n} \tag{A.14}$$

with the boundary conditions.

$$n = 0 : \frac{du}{dn} = 0, \tag{A.15}$$
$$n = L : u = 0$$

In these equations, $n$ denotes the coordinate orthogonal to the flow direction ($n = r$ for the flow in a pipe and $n = y$ for the flow in a parallel plate channel). The

quantity $L = R$ (pipe radius) for pipe flow and $L = h$ (half channel height) for the flow in a parallel plate channel.

The Eqs. (A.13) and (A.14) are solved together with the boundary conditions given by Eq. (A.15). Equation (A.14) can directly be integrated and results in

$$
p = p_W(x) - \rho \overline{(v')^2} + \rho F \int_r^R \frac{\overline{(v')^2} - \overline{(w')^2}}{\bar{r}} d\bar{r} \tag{A.16}
$$

Equation (A.16) shows nicely that the pressure in the direction orthogonal to the main flow changes across the duct due to the presence of the turbulent stresses. For a parallel plate channel, the change in pressure is only caused by the normal turbulent stress, whereas for pipe flow also the difference between the normal turbulent stresses in radial and circumferential direction causes an additional change. Differentiating Eq. (A.16) with respect to $x$ leads to

$$
\frac{\partial p}{\partial x} = \frac{\partial p_W}{\partial x}
$$

because the turbulent stresses only depend on the coordinate orthogonal to the flow direction.

For the flows considered here through a pipe or a parallel plate channel, the mass flow rate is constant and the integral form of the mass continuity equation leads to

$$
\bar{u} L^{(F+1)} = (F + 1) \int_0^L u r^F dn \tag{A.17}
$$

where $\bar{u}$ denotes the mean axial velocity in the duct. The above given equation determines the yet unknown pressure gradient in axial direction ($\partial p / \partial x$ is a constant for the hydrodynamically fully developed flow). In order to solve Eq. (A.13), the turbulent shear stress $-\rho \overline{u'v'}$ has to be related to the mean flow field. This can be done using a simple mixing length model. The use of the simple mixing length model is adequate for this type of flows (Cebeci and Bradshaw 1984). However, for more complicated flows, like the flow through a pipe with cyclic constrictions, mixing length models may lead to inaccurate answers. The reader is referred to Reynolds (1974), Launder (1988) or Kays et al. (2004) for a review of more advanced turbulence models. Using the mixing length model, the turbulent shear stress can be written as

$$
-\overline{u'v'} = \varepsilon_m \frac{du}{dn} \tag{A.18}
$$

with the eddy viscosity $\varepsilon_m$ given by

$$\varepsilon_m = l^2 \left| \frac{du}{dn} \right| \tag{A.19}$$

The mixing length $l$ has been measured by Nikuradse (1932) for pipe flows. He obtained the interesting result that $l$ does not depend on the Reynolds number for $Re_D > 10^5$. The mixing length distribution can be approximated by Schlichting (1982).[1]

$$\frac{l}{L} = 0.14 - 0.08 \left( \frac{n}{L} \right)^2 - 0.06 \left( \frac{n}{L} \right)^4 \tag{A.20}$$

Near the wall, the mixing length distribution, according to Eq. (A.20), approaches the one given by Prandtl (see Schlichting 1982).

$$l = \kappa(L - n), \quad \kappa = 0.4 \tag{A.21}$$

Close to the wall, the turbulent fluctuations are damped out and, below a certain dimensionless distance away from the wall, the turbulent fluctuations are zero. In order to use the mixing length distribution throughout the whole calculation region, it is convenient to modify the expression by using a damping function. This guarantees that the mixing length tends to zero within the laminar sublayer. Cebeci and Bradshaw (1984) modified the mixing length distribution, given by Eq. (A.20), with the van Driest damping term (van Driest 1956). This leads to

$$\frac{l}{L} = \left[ 0.14 - 0.08 \left( \frac{n}{L} \right)^2 - 0.06 \left( \frac{n}{L} \right)^4 \right] \left\{ 1 - \exp\left( -\frac{y^+}{26} \right) \right\} \tag{A.22}$$

with the abbreviations

$$y^+ = \frac{y_W u_\tau}{\nu}, \quad u_\tau = \sqrt{\frac{|\tau_W|}{\rho}}, \quad y_W = (L - n) \tag{A.23}$$

Introducing Eq. (A.18) into Eq. (A.13) results in an ordinary differential equation for the axial velocity component

$$0 = -\frac{\partial p_W}{\partial x} + \frac{1}{r^F} \frac{d}{dn} \left[ r^F \left( \mu \frac{du}{dn} + \rho l^2 \frac{du}{dn} \left| \frac{du}{dn} \right| \right) \right] \tag{A.24}$$

---

[1]Zagustin and Zagustin (1969) developed theoretically a formula for the mixing length distribution in a pipe by solving the conservation equation for the turbulent energy. Their mixing length distribution is also in good agreement with the measurements of Nikuradse (1932).
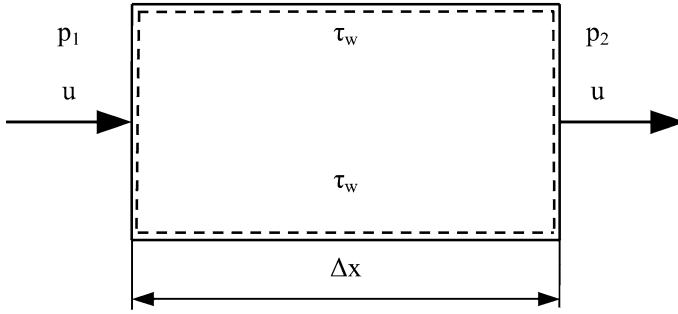
**Fig. A.2** Force balance for a small duct element

This equation has to be solved together with the boundary conditions given by Eq. (A.15). The axial pressure gradient $\partial p_W / \partial x$ can be replaced by the shear stress velocity $u_\tau$. In order to do this, let us consider the forces acting on a small duct element (shown in Fig. A.2).

Equating the forces acting on the small duct element shown in Fig. A.2 results in:

$$(p_1 - p_2)\, \pi R^2 = \tau_W 2\pi R \Delta x, \quad \text{Pipe} \tag{A.25}$$

$$(p_1 - p_2)\, 2h = \tau_W 2 \Delta x, \quad \text{Parallel Plates} \tag{A.26}$$

From the above two equations, one obtains the following relation between the pressure gradient and the wall shear stress

$$-\frac{\partial p}{\partial x} = \frac{\tau_W (F+1)}{L} = \frac{u_\tau^2 \rho (F+1)}{L} \tag{A.27}$$

Introducing this result and the following dimensionless quantities into Eq. (A.24)

$$\tilde{r} = \frac{r}{L}, \quad \tilde{n} = \frac{n}{L}, \quad u^+ = \frac{u}{u_\tau}, \quad \tilde{l} = \frac{l}{L}, \quad \mathrm{Re}_\tau = \frac{u_\tau L}{\nu} \tag{A.28}$$

results in the following ordinary differential equation for the axial velocity component.

$$-\mathrm{Re}_\tau \tilde{r}^F (F+1) = \frac{d}{d\tilde{n}} \left[ \tilde{r}^F \left( \frac{du^+}{d\tilde{n}} - \tilde{l}^2 \mathrm{Re}_\tau \left( \frac{du^+}{d\tilde{n}} \right)^2 \right) \right] \tag{A.29}$$

Integration of this equation and application of the boundary condition $du^+/d\tilde{n} = 0$ for $\tilde{n} = 0$ results in

$$-\mathrm{Re}_\tau \tilde{n} = \frac{du^+}{d\tilde{n}} - \tilde{l}^2 \mathrm{Re}_\tau \left(\frac{du^+}{d\tilde{n}}\right)^2 \tag{A.30}$$

After solving for the unknown velocity gradient one obtains from Eq. (A.30).

$$\frac{du^+}{d\tilde{n}} = \frac{-2\tilde{n}\mathrm{Re}_\tau}{1 + \sqrt{1 + 4\tilde{n}\tilde{l}^2\mathrm{Re}_\tau^2}} \tag{A.31}$$

This ordinary differential equation has to be solved numerically together with the boundary condition that $u^+ = 0$ for $\tilde{n} = 1$. In addition, the continuity equation in integral form, Eq. (A.17), has to be satisfied. This equation reads after introducing the dimensionless quantities according to Eq. (A.28).

$$\frac{\mathrm{Re}_L}{\mathrm{Re}_\tau} = (F + 1) \int_0^1 u^+ \tilde{r}^F d\tilde{n}, \quad \mathrm{Re}_L = \frac{\bar{u}L}{v} \tag{A.32}$$

For a selected Reynolds number $\mathrm{Re}_L$, a value for $\mathrm{Re}_\tau$ has to be estimated. After this, Eq. (A.31) is solved numerically and the resulting velocity distribution is inserted into Eq. (A.32). From Eq. (A.32) a new value for $\mathrm{Re}_\tau$ is obtained and the iteration is carried on up to the point, where both Eqs. (A.31) and (A.32) are satisfied.

Figure A.3 shows a comparison between predicted and measured velocity profiles in a planar channel and in a pipe.

It can be seen that the application of the simple mixing length model leads to quite satisfactory results for the fully developed flow in a pipe and in a parallel plate channel.

Note that also the hydrodynamic developing flow in a duct can be predicted as well by using a modified mixing length model. The reader is referred for more details to Cebeci and Chang (1978) and Cebeci and Bradshaw (1984).

Antonia and Kim (1991) compared calculations based on a mixing length model for hydrodyamically fully developed flow in a channel with experiments and also with direct numerical simulations (DNS). They found good agreement between their calculations and the DNS data.

After establishing a simple calculation method for the hydrodynamically fully developed flow, the *universality of the velocity profiles* for turbulent pipe flows is addressed next. As it can be seen from Eq. (A.13), the total shear stress $\tau_{rx}$ for the pipe flow consists of a molecular part and of the turbulent shear stress:

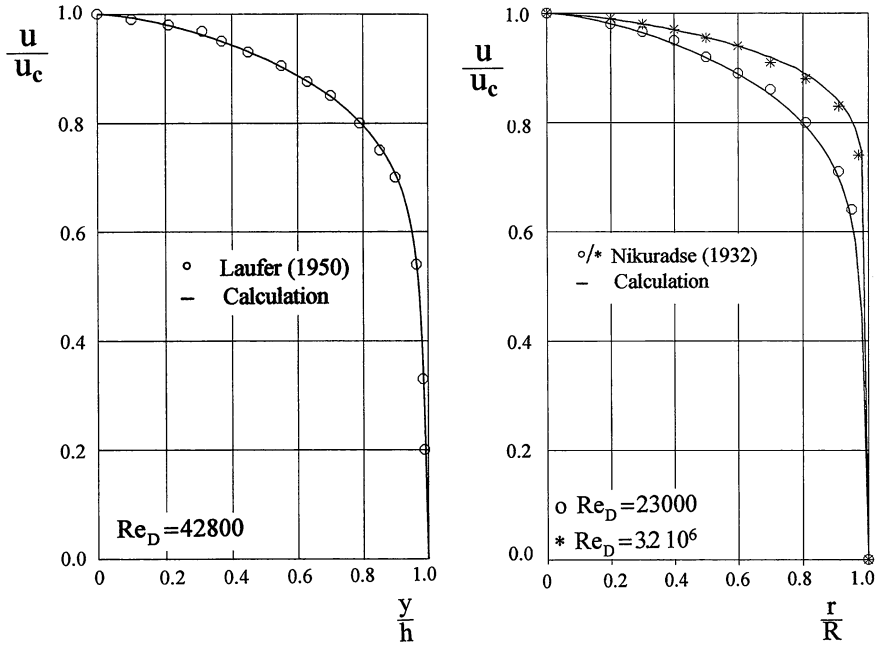$$\tau_{rx} = (\mu + \rho\varepsilon_m)\frac{du}{dr} \tag{A.33}$$

**Fig. A.3** Fully developed velocity profiles in a planar channel and in a pipe

After integrating Eq. (A.13) it can be seen that the total shear stress $\tau_{rx}$ varies linearly across the pipe. With this result, one obtains from Eq. (A.33)

$$\frac{du^+}{dy^+} = \frac{\tau_{rx}/\tau_W}{1 + \dfrac{\varepsilon_m}{\nu}} = \frac{1 - y_W/R}{1 + \dfrac{\varepsilon_m}{\nu}} \tag{A.34}$$

where $y_W = R - r$. Equation (A.34) has been the basis for many considerations for turbulent pipe flows, which led finally to approximations for the fully developed turbulent velocity distribution. In the following section, we describe mainly the work of Reichhardt (1951) on this topic.

## *The Law of the Wall*

Near the wall, the eddy viscosity distribution $\varepsilon_m$ can be approximated relatively easy from experimental data. Nikuradse (1932) derived from his experimental results the following approximation for $\varepsilon_m$

$$\frac{\varepsilon_m}{\nu} = \kappa y^+, \quad y^+ = \frac{y_W u_\tau}{\nu} \tag{A.35}$$

Introducing Eq. (A.35) into Eq. (A.34) and integrating the resulting expression for the region close to the wall ($y_W/R \ll 1$ and $y^+ \gg 1$) results in

$$u^+ = \frac{1}{\kappa} \ln y^+ + c \tag{A.36}$$

The logarithmic velocity distribution in Eq. (A.36) has been derived under various assumptions by Prandtl (1925) and von Kármán (1939). It is a very important result for turbulent flows, because of the universality of this velocity distribution for various turbulent flow fields. From Eq. (A.35), it can be seen that this equation looses its meaning, if we consider values of $y^+$ very close to the wall, as for $y^+ < 11$ the turbulent exchange in the viscous sublayer of the flow tends to zero. In order to overcome this difficulty, Reichardt (1951) developed the following distribution for the eddy viscosity near the wall.

$$\frac{\varepsilon_m}{\nu} = \kappa \left( y^+ - y_1^+ \arctan\left(\frac{y^+}{y_1^+}\right) \right), \quad y_1^+ = 11 \tag{A.37}$$

This function goes to zero for $y^+ \to 0$. For larger values of $y^+$, Eq. (A.37) approaches continuously Eq. (A.35). Introducing Eq. (A.37) into Eq. (A.34) and integrating, results after restricting again to the region close to the wall ($y_W/R \ll 1$ and $y^+ \gg 1$) in

$$u^+ = 2.5 \ln(1 + \kappa y^+) + 7.8 \left[ 1 - \exp\left(-\frac{y^+}{y_1^+}\right) - \left(\frac{y^+}{y_1^+}\right) \exp\left(-\frac{y^+}{3}\right) \right] \tag{A.38}$$

Equation (A.38) compares favorably with experimental data in the near wall region (see Reichardt 1951).

## The Core Region

In the central part of the pipe, all distributions have to be symmetric to $\tilde{r} = 0$. Therefore, it is useful to analyze this area with Eq. (A.34) after introducing the radial coordinate instead of the wall coordinate. Furthermore, the molecular viscosity can be neglected compared to the turbulent eddy viscosity in the denominator of Eq. (A.34). This leads to

$$\frac{du^+}{d\tilde{r}} = \frac{\tilde{r}}{\text{Re}_\tau \dfrac{\varepsilon_m}{v}} \tag{A.39}$$

In the central region of the pipe, the eddy viscosity can be approximated according to Reichhardt (1951) by

$$\frac{\varepsilon_m}{v} = Re_\tau \frac{\kappa}{3}\left(\frac{1}{2} + \tilde{r}^2\right)\left(1 - \tilde{r}^2\right) \tag{A.40}$$

Equation (A.40) was found to be in good agreement with experimental data. If we introduce Eq. (A.40) into Eq. (A.39) and integrate, the following result for the velocity distribution is obtained

$$\frac{u_C - u}{u_\tau} = \frac{1}{\kappa}\ln\left(\frac{1 + 2\tilde{r}^2}{1 - \tilde{r}^2}\right) \tag{A.41}$$

where $u_C$ denotes the maximum velocity in the pipe at $\tilde{r} = 0$. Equation (A.41) is valid throughout the flow area, except the region close to the wall, where the molecular viscosity plays an important role (Reichhardt 1951).

## *An Approximate Velocity Distribution for the Whole Flow Field*

Based on the two approximate velocity distributions, Eq. (A.38) and Eq. (A.41), Reichhardt (1951) developed an approximate velocity distribution, which is valid throughout the flow area.

$$u^+ = \frac{1}{\kappa}\ln\left\{(1 + \kappa y^+)\frac{\frac{3}{2}(1 + \tilde{r})}{1 + 2\tilde{r}^2}\right\} + C_1\left[1 - \exp\left(-\frac{y^+}{y_1^+}\right) - \left(\frac{y^+}{y_1^+}\right)\exp\left(-\frac{y^+}{3}\right)\right] \tag{A.42}$$

with the constant $C_1 = 5.5 - 1/\kappa \ln \kappa$. Equation (A.42) agrees very well with experimental results of Nikuradse (1932) and Reichhardt (1940).

During the past 90 years, a large number of different expressions for the universal velocity distribution in a pipe have been developed by different researchers. All equations are based on slightly different assumptions for the eddy viscosity distribution in the pipe and all the equations describe more or less accurately the hydrodynamically fully developed velocity distribution.

Table A.1 gives an overview over several different expressions for the velocity distribution in the pipe.

Strictly speaking, the above derived universal velocity distribution is only valid for large Reynolds numbers $(\text{Re}_D > 10^5)$. However, it was found that they

**Table A.1** Universal velocity profiles for hydrodynamically fully developed duct flows

| References | Functional dependence $u^+ = f(y^+)$ | Validity range |
|---|---|---|
| Prandtl (1910) | $u^+ = y^+$ | $0 \leq y^+ \leq 11.5$ |
| Taylor (1916) | $u^+ = 2.5 \ln y^+ + 5.5$ | $y^+ > 11.5$ |
| von Kármán (1939) | $u^+ = y^+$ | $0 \leq y^+ \leq 5$ |
| | $y^+ = 5 \ln y^+ - 3.05$ | $5 < y^+ \leq 30$ |
| | $u^+ = 2.5 \ln y^+ + 5.5$ | $y^+ > 30$ |
| Reichhardt (1951) | $u^+ = 2.5 \ln(1 + \kappa y^+) + 7.8\,(1 - \exp(y^+/y_1^+)$ $- (y^+/y_1^+) \exp(y^+/3))$ | for all $y^+$ |
| Deissler (1954) | $u^+ = \int_0^{y^+} \dfrac{d\hat{y}}{1 + n^2 u^+ \hat{y}[1 - \exp(-n^2 n^+ \hat{y})]}, \quad n = 0.124$ | $0 \leq y^+ \leq 26$ |
| | $u^+ = 2.78 \ln y^+ + 3.8$ | $y^+ > 26$ |
| Rannie (1956) | $u^+ = 14.53 \tanh(y^+/14.53)$ | $0 \leq y^+ \leq 27.5$ |
| | $u^+ = 2.5 \ln y^+ + 5.5$ | $y^+ > 27.5$ |
| Spalding (1961) | $y^+ = u^+ + 0.1108\,[\exp(0.4u^+) - 1 - 0.4u^+$ $- (0.4u^+)^2/2! - (0.4u^+)^3/3! - (0.4u^+)^4/4!]$ | for all $y^+$ |
| Notter and Schleicher (1971) | $u^+ = \frac{1}{0.091} \tan^{-1}(0.091 y^+)$ | $0 \leq y^+ \leq 45$ |
| | $u^+ = 5.1 + 2.5 \ln y^+$ | $45 \leq y^+ < \bar{y}_W$ $\bar{y}_W = 0.15$ |
| | $\frac{u - u_C}{\bar{u}} = -\sqrt{\frac{c_f}{8}} f(\bar{y}_W)$ | $0.15 < \bar{y}_W \leq 1$ |
| Kays and Crawford (1993) | $u^+ = y^+$ | $0 \leq y^+ < 5$ |
| | $u^+ = 5 \ln y^+ - 3.05$ | $5 \leq y^+ < 30$ |
| Reichhard (1951) | $u^+ = 5.5 + 2.5 \ln\left[ y^+ \frac{1.5(1+\tilde{n})}{1+2\tilde{n}} \right]$ | $y^+ \geq 30$ |
| Mirushina and Ogisio (1970) | $u^+ = \dfrac{1}{6A^{2/3}} \left( A^{1/3} + \dfrac{1}{\mathrm{Re}_\tau} \right) \ln \left| \dfrac{\left( y^+ + 1/A^{1/3} \right)^3}{y^{+3} + 1/A} \right|$ $+ \dfrac{1}{\sqrt{3} A^{2/3}} \left( A^{1/3} - \dfrac{1}{\mathrm{Re}_\tau} \right) \times \tan^{-1} \left( \dfrac{2y^+ - 1/A^{1/3}}{\sqrt{3} A^{1/3}} + \dfrac{\pi}{6} \right)$ | $0 \leq y^+ \leq y_1^+$ |
| | $u^+ = 2.5 \ln y^+ + 5.5$ | $y_1^+ < y^+ \leq y_2^+$ |
| | $u^+ = \dfrac{y^+ - y_2^+}{1 + 0.07 \mathrm{Re}_\tau} \left( 1 - \dfrac{y^+ + y_2^+}{2\mathrm{Re}_\tau} \right) + 2.5 \ln y_2^+ + 5.5,$ $y_2^+ = 0.23 \mathrm{Re}_\tau$ | $y_2^+ < y^+ \leq \mathrm{Re}_\tau$ |
| | $A(y_1^+)^3 = 0.4 y_1^+ \left( 1 - \dfrac{y_1^+}{\mathrm{Re}_\tau} \right) - 1, \quad y_1^+ = 26.3$ | |

approximate very well the velocity distribution also for much lower Reynolds numbers. Rothfus et al. (1958) and Dwyer (1965) showed that the influence of the Reynolds number on the universal velocity distribution $u^+ = f(y^+)$ can be incorporated by using the following quantities

$$y^{++} = y^+ / \left(\frac{\bar{u}}{u_C}\right)_{\text{Pipe}}, \quad u^{++} = u^+ / \left(\frac{\bar{u}}{u_C}\right)_{\text{Pipe}} \tag{A.43}$$

In addition, Rothfus et al. (1958) and Dwyer (1965) were able to show that the modified velocity distribution $u^{++} = f(y^{++})$ can also be applied to the flow in a parallel channel and in a concentric circular annulus. The agreement between experimental data and the velocity distribution $u^{++} = f(y^{++})$ given by Rothfus et al. (1958) for a wide range of Reynolds numbers is good.

# Appendix B
# The Fully Developed Velocity Profile in an Axially Rotating Pipe

In the following appendix, the hydrodynamically fully developed velocity profile for a turbulent flow in an axially rotating pipe is discussed. The geometry under consideration is shown in Fig. B.1.

For the flow in the axially rotating pipe, the velocity components $u$, $v$ and $w$ denote the flow in the $x$-, $r$- and $\varphi$-direction.

For the following analysis, we restrict our considerations to an incompressible flow with constant fluid properties. The Reynolds averaged Navier-Stokes equations and the continuity equation, assuming rotational symmetry, are given for example by Rothe (1994).

$$\rho\left(\frac{\partial(uu)}{\partial x}+\frac{1}{r}\frac{\partial(ruv)}{\partial r}\right)=-\frac{\partial p}{\partial x}+\frac{\mu}{r}\frac{\partial}{\partial r}\left(r\frac{\partial u}{\partial r}\right)+\mu\frac{\partial^2 u}{\partial x^2} \qquad \text{(B.1)}$$
$$-\frac{\rho}{r}\frac{\partial}{\partial r}\left(r\overline{u'v'}\right)-\rho\frac{\partial}{\partial x}\left(\overline{u'u'}\right)$$

$$\rho\left(\frac{\partial(uv)}{\partial x}+\frac{1}{r}\frac{\partial(rvv)}{\partial r}-\frac{w^2}{r}\right)=-\frac{\partial p}{\partial r}+\frac{\mu}{r}\frac{\partial}{\partial r}\left(r\frac{\partial v}{\partial r}\right)+\mu\frac{\partial^2 v}{\partial x^2}-\frac{v}{r^2} \qquad \text{(B.2)}$$
$$-\frac{\rho}{r}\frac{\partial}{\partial r}\left(r\overline{v'v'}\right)-\rho\frac{\partial}{\partial x}\left(\overline{u'v'}\right)-\rho\frac{\overline{w'w'}}{r}$$

$$\rho\left(\frac{\partial(uw)}{\partial x}+\frac{1}{r}\frac{\partial(rvw)}{\partial r}+\frac{vw}{r}\right)=\frac{\mu}{r}\frac{\partial}{\partial r}\left(r\frac{\partial w}{\partial r}\right)+\mu\frac{\partial^2 w}{\partial x^2}-\frac{w}{r^2} \qquad \text{(B.3)}$$
$$-\frac{\rho}{r}\frac{\partial}{\partial r}\left(r\overline{v'w'}\right)-\rho\frac{\partial}{\partial x}\left(\overline{u'w'}\right)-\rho\frac{\overline{v'w'}}{r}$$

$$\frac{\partial u}{\partial x}+\frac{1}{r}\frac{\partial}{\partial r}(rv)=0 \qquad \text{(B.4)}$$

For a hydrodynamically fully developed flow, the axial velocity component does not change with the axial position and, therefore, $\partial u/\partial x$ is zero. If we introduce this result into the continuity Eq. (B.4), we obtain the result that the radial velocity component $v$ is equal to zero and the continuity equation is automatically satisfied if

**Fig. B.1** Geometry and coordinate system (Reich and Beer 1989)
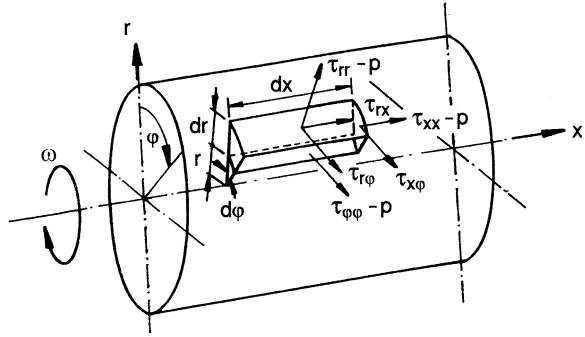


$u = f(r)$. The fact that $v = 0$ for the fully developed flow is obvious, because a non-zero velocity component $v$ would lead automatically to a change in the axial velocity component for different axial positions. Introducing this results into the above given equations result in

$$-\rho \frac{w^2}{r} = -\frac{\partial p}{\partial r} - \frac{\rho}{r} \frac{\partial}{\partial r} \left( r \overline{v'v'} \right) + \rho \frac{\overline{w'w'}}{r} \tag{3.103}$$

$$0 = \frac{1}{r^2} \frac{\partial}{\partial r} \left( \mu \, r^3 \frac{\partial}{\partial r} \left( \frac{w}{r} \right) - \rho \, r^2 \, \overline{v'w'} \right) \tag{3.104}$$

$$0 = \frac{\partial p}{\partial x} + \frac{1}{r} \frac{\partial}{\partial r} \left( \mu r \frac{\partial u}{\partial r} - \rho r \overline{u'v'} \right) \tag{3.105}$$

with the boundary conditions

$$r = 0 : w = 0, \; v = 0, \; \frac{\partial u}{\partial r} = 0 \tag{3.106}$$

$$r = R : w = w_W, \; u = 0, \; v = 0$$

As mentioned in Chap. 3, experimental data show that the tangential velocity distribution is universal and can be approximated by Eq. (3.102).

$$\frac{w}{w_W} = \left( \frac{r}{R} \right)^2 \tag{3.102}$$

Figure 3.14 shows the tangential velocity distribution for different rotation rates N as well as for different Reynolds numbers. From Fig. 3.14, it is obvious that Eq. (3.102) is a very good approximation for the tangential velocity distribution. The axial velocity distribution $u(r)$ can be calculated from Eq. (3.105). In order to do so, the turbulent shear stress in this equation has to be related to the mean velocity gradients. This can be done by using a mixing length model according to
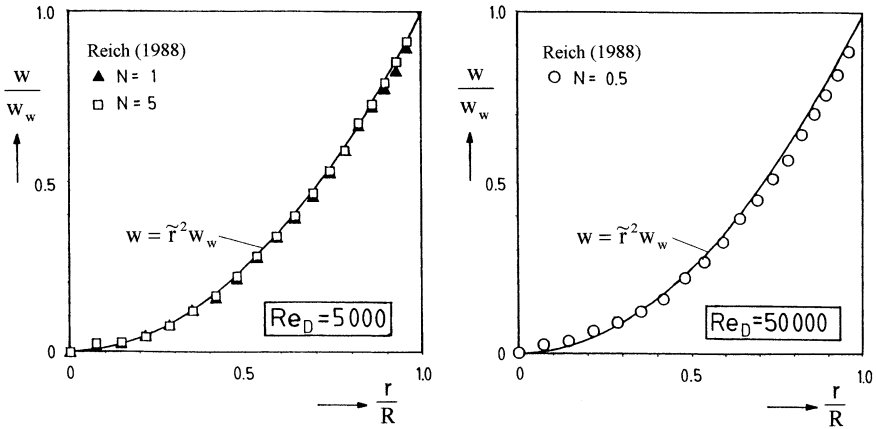
**Fig. 3.14** Tangential velocity distribution (Reich and Beer 1989)

Koosinlin et al. (1975). This results in the following expression for the turbulent shear stress

$$\rho \overline{u'v'} = \rho\, l^2 \left[ \left( \frac{\partial u}{\partial r} \right)^2 + \left( r \frac{\partial}{\partial r} \left( \frac{w}{r} \right) \right)^2 \right]^{1/2} \frac{\partial u}{\partial r} = \varepsilon_m \rho \frac{\partial u}{\partial r} \tag{3.107}$$

where the mixing length distribution $l$ is given by (Reich and Beer (1989)).

$$\frac{l}{l_0} = \left( 1 - \frac{1}{6} \mathrm{Ri} \right)^2 \tag{3.108}$$

The mixing length distribution $l_0$ is the one for a non-rotating pipe (see Appendix A, Eq. (A.22)). The Richardson number in Eq. (3.108) describes the effect of pipe rotation on the turbulent motion and is defined as

$$\mathrm{Ri} = \frac{2 \dfrac{w}{r^2} \dfrac{\partial}{\partial r}(wr)}{\left( \dfrac{\partial u}{\partial r} \right)^2 + \left( r \dfrac{\partial}{\partial r} \left( \dfrac{w}{r} \right) \right)^2} \tag{3.109}$$

Without rotation, Ri = 0, there exists a fully developed turbulent pipe flow. If Ri > 0, i.e. for an axially rotating pipe with a radially growing tangential velocity, the centrifugal forces suppress the turbulent fluctuations and the mixing length decreases. If we introduce the expression for the turbulent shear stress Eq. (3.107) and Eq. (3.102) into Eq. (3.105), we obtain the following nonlinear ordinary differential equation after integration.

$$0 = \tilde{l}^2 \left[ \left( \frac{du^+}{d\tilde{r}} \right)^2 + \left( \tilde{r} N \frac{Re_D}{2Re_\tau} \right)^2 \right]^{1/2} \left( \frac{du^+}{d\tilde{r}} \right) + \frac{1}{Re_\tau} \left( \frac{du^+}{d\tilde{r}} \right) + \tilde{r} \qquad (B.5)$$

where the following dimensionless quantities have been used

$$\tilde{r} = \frac{r}{R}, \ \tilde{l} = \frac{l}{R}, \ u^+ = \frac{u}{u_\tau}, \ u_\tau = \sqrt{|\tau_W|/\rho}, \qquad (B.6)$$

$$Re_\tau = \frac{u_\tau R}{\nu}, \ Re_D = \frac{\bar{u} D}{\nu}, \ N = \frac{w_W}{\bar{u}}$$

In Eq. (B.5), the partial differentials have been replaced by ordinary differentials, because the axial velocity is only a function of the radial coordinate. Equation (B.5) is a strongly nonlinear ordinary differential equation and has to be solved with the boundary condition

$$u^+(\tilde{r} = 1) = 0 \qquad (B.7)$$

Equation (B.5) together with Eq. (B.7) can now be solved in the following way: for a given value of the Reynolds number $Re_D$, a value of the shear stress Reynolds number $Re_\tau$ is assumed. After this, Eq. (B.5) can be integrated numerically so that the boundary condition according to Eq. (B.7) is fulfilled. After the integration, the continuity equation in integral form

$$\frac{Re_D}{4Re_\tau} = \int_0^1 u^+ \tilde{r} d\tilde{r} \qquad (B.8)$$

has to be satisfied. If Eq. (B.8) is not satisfied, a new value for $Re_\tau$ can be calculated from the equation. After some iteration, the desired velocity profile is obtained. The resulting axial velocity distribution is shown in Fig. 3.15.

As it can be seen from Fig. 3.15, the agreement between the experimental data and the numerical predictions is good.

For turbulent flow in a non-rotating pipe, it is well known that the axial velocity profile can be described by an universal velocity profile, given by

$$\frac{u_C - u}{u_\tau} = f(\tilde{r}) \qquad (B.9)$$

In this equation, $u_C$ denotes the axial velocity in the pipe center. The velocity law is valid over a large portion of the pipe radius and the function $f$ is not dependent on the Reynolds number. If one examines Eq. (B.5) in more detail, one sees that only one quantity describes the influence of the rotation on the velocity field. This quantity is
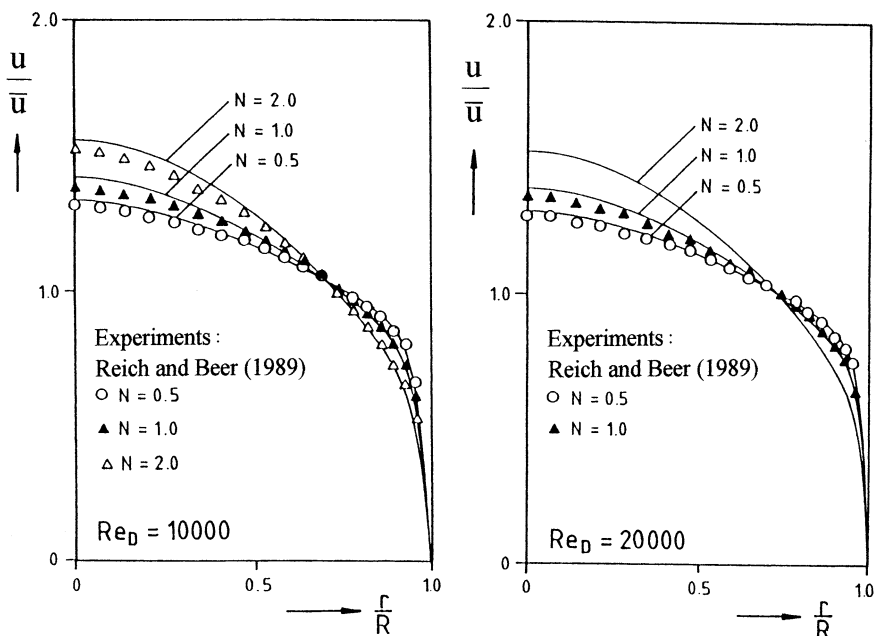
**Fig. 3.15** Axial velocity distribution as a function of the rotation rate N (Reich and Beer 1989)

$$Z = N \frac{\text{Re}_D}{2\text{Re}_\tau} = N / \sqrt{\frac{c_f}{8}} \tag{B.10}$$

From Eq. (B.10), it can be seen that the parameter Z involves the rotation rate N and the coefficient of friction loss $c_f$. The rotation rate N characterizes the effect of rotation on the axial mean velocity in the rotating pipe. The additional term $\sqrt{c_f/8}$ takes into account the variation in the shape of the axial velocity profile at the pipe wall and, therefore, includes the effect of different pressure losses in the pipe section due to rotation.

Figure B.2 shows the functional relationship between Z and $\text{Re}_D$ for various N. It can be seen that for a given value of N, the quantity Z increases with increasing values of the flow-rate Reynolds number. This is caused by the decreasing value of the friction factor with growing values of $\text{Re}_D$.

If we assume in Eq. (B.5) to be far away from the wall so that $1/\text{Re}_\tau du^+/d\tilde{r}$ is sufficiently small to be neglected in comparison with all other terms in this equation, we can hope to find an universal velocity law for the core region if the mixing length is only a function of $\tilde{r}$ and Z. From the above assumption, it is clear that the following analysis is only valid if N does not approach infinity. In this latter case, the whole pipe cross section is influenced by the viscous forces and the axial velocity distribution tends to the one for laminar pipe flow (Hagen-Poiseuille flow)

**Fig. B.2** Rotation parameter Z as a function of the flow-rate Reynolds number with N as parameter (Weigand and Beer 1994)
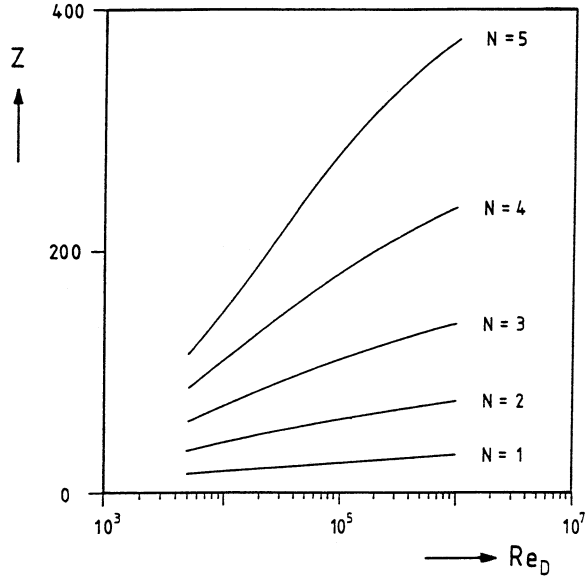
$$\frac{u}{\bar{u}} = 2\left(1 - \tilde{r}^2\right) \tag{B.11}$$

This behavior is caused by the vanishing turbulent shear stress with increasing rotation rate N. If we now exclude extremely large values of N and introduce the dimensionless quantities defined in Eq. (B.6), we obtain from Eq. (3.109) for the Richardson number,

$$\text{Ri} = \frac{6\tilde{r}^2 Z^2}{\left(\dfrac{\partial u^+}{\partial \tilde{r}}\right)^2 + (\tilde{r}Z)^2} \tag{B.12}$$

The mixing length distribution is given by Eq. (3.108).

Because the mixing length only depends on the radial coordinate and the Richardson number, it follows from Eq. (B.5) that the velocity profile in the core region must have an universal character. Figure B.3 shows the distribution of the axial velocity for various values of Z. It can be seen that the velocity profiles are universal. There is only a difference in the profiles for different Reynolds numbers near the wall ($\tilde{r} \simeq 1$), where the viscous forces play an important role.

In order to derive an approximation for the axial velocity distribution, we follow the work of Reichardt (1951) for the non-rotating pipe and subdivide the flow area ($0 \leq \tilde{r} \leq 1$) into two parts: a near wall region and a part, which contains the rest of the flow area. Reichardt (1951) developed, for the turbulent flow in a non-rotating pipe, an approximation for the velocity distribution which is valid for the whole
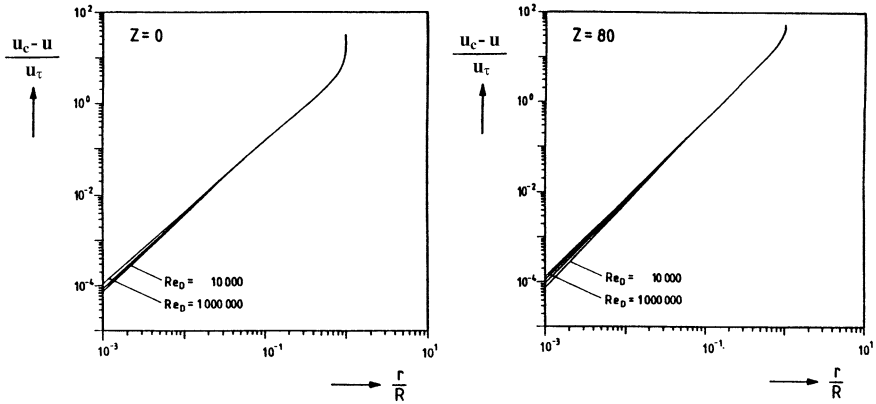
**Fig. B.3** Axial velocity distribution for various values of the rotation rate Z and different $Re_D$ (Weigand and Beer 1994)

flow area. This is also the aim for the case of turbulent flow in an axially rotating pipe. For more details on this subject, the reader is referred to Weigand and Beer (1994).

## The Velocity Distribution in the Core Region

If one plots the velocity distribution of Fig. B.3 in a diagram containing logarithmic axis, one obtains for the velocity distribution

$$\frac{u_C - u}{u_\tau} = A\,\tilde{r}^B \tag{B.13}$$

where $A$ and $B$ are depending on Z

$$A(Z) = \sqrt{0.06052\,Z^2 + 5.4\,Z + 25.705}, \tag{B.14}$$
$$B(Z) = 1.55 + 0.338[1 - \exp(-0.0553\,Z)]$$

For Z = 0 (non-rotating pipe), the velocity distribution given by the Eqs. (B.13) and (B.14) is identical to the one reported by Darcy (1858). Figure B.4 shows a comparison between the numerically predicted axial velocity distribution and the approximation given by Eqs. (B.13) and (B.14). It can be seen that Eqs. (B.13) and (B.14) approximate the velocity profile very well for $\tilde{r} \leq 0.7$. For larger values of $\tilde{r}$, larger deviations can be noticed.
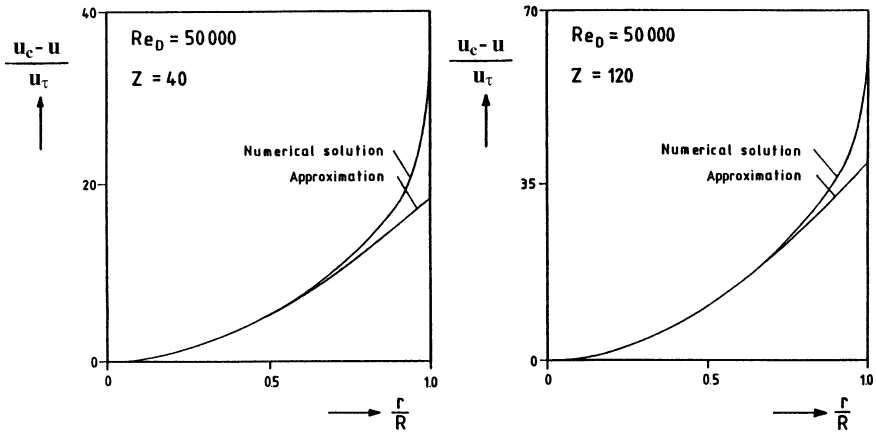
**Fig. B.4** Comparison between numerical solution and the approximation for the axial velocity in the core region (Weigand and Beer 1994)

## The Velocity Distribution in the Near Wall Region

It is well known that the velocity distribution near the wall in a non-rotating pipe has a logarithmic distribution given by

$$u^+ = \frac{1}{\kappa} \ln y^+ + c \tag{A.36}$$

where $\kappa$ and $c$ are constants and $y^+$ is the dimensionless distance from the wall, given by Eq. (A.23). In an axially rotating pipe, the turbulent fluctuations are suppressed by centrifugal forces. Furthermore, the area, where the velocity profile is still logarithmic in shape, decreases with increasing rotation rates. This fact is shown in Fig. B.5 and has been observed in DNS calculations by Eggels and Nieuwstadt (1993) and by Orlandi and Fatica (1995). However, Weigand and Beer (1994) obtained an approximation formula for the velocity distribution in the near wall region, which includes the effect of relaminarization due to system rotation.

This equation is given by (for more details the reader is referred to Weigand and Beer 1994)

$$u^+ = \frac{1}{\kappa_1} \ln(1 + \kappa_1 y^+) + 7.8 \left[ \frac{\mathrm{Re}_\tau}{(\mathrm{Re}_\tau)_0} \left( 1 - \exp\left(\frac{y^+}{y_1^+}\right) - \left(\frac{y^+}{y_1^+}\right) \exp(-by^+) \right) \right] \tag{B.15}$$
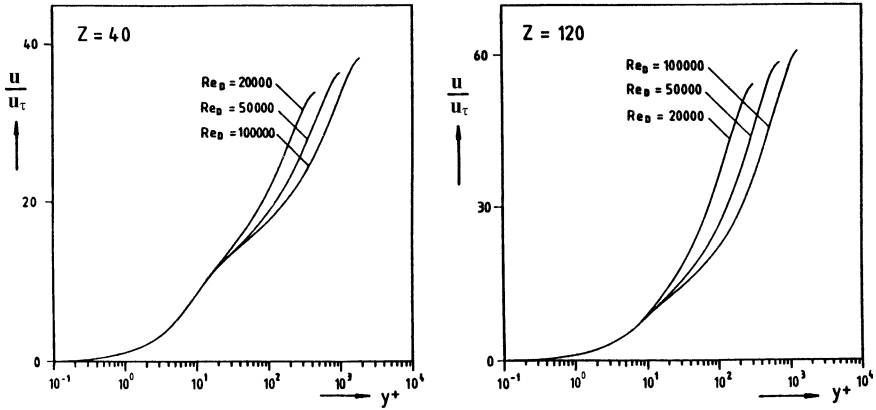
**Fig. B.5** Axial velocity distribution $u/u_\tau$ as a function of the wall coordinate $y^+$ for two different values of Z (Weigand and Beer 1994)

with the quantities

$$y_1^+ = y_{10} \frac{\mathrm{Re}_\tau}{(\mathrm{Re}_\tau)_0}, \quad y_{10} = 11 \tag{B.16}$$

$$\kappa_1 = \kappa \left( \frac{\mathrm{Re}_\tau}{(\mathrm{Re}_\tau)_0} \right) \Bigg/ \left[ \left( \frac{Z}{\mathrm{Re}_\tau} \right)^2 + 1 \right]^{3.5}, \quad \kappa = 0.4$$

$$b = \frac{1}{3} \sqrt{\frac{\kappa_1}{\kappa}}$$

In the equations above $(\mathrm{Re}_\tau)_0$ denotes the shear-stress Reynolds number for the non-rotating pipe. As it can be seen from Eq. (B.15), the velocity distribution in the near wall region is influenced by a term containing the influence of the system rotation on the wall shear stress. Figure B.6 shows the good agreement between the approximation given above and the numerical solution of the problem.

## An Approximation Formula for the Whole Region of the Pipe

Strictly speaking, the two equations given above for the axial velocity distribution are only valid in the near wall region and in the core region. However, the two solutions can be combined to one single relation, as shown by Weigand and Beer (1994). They obtained

**Fig. B.6** Comparison between numerical solution and the approximation for $u/u_\tau$ in the near wall region (Weigand and Beer 1994)
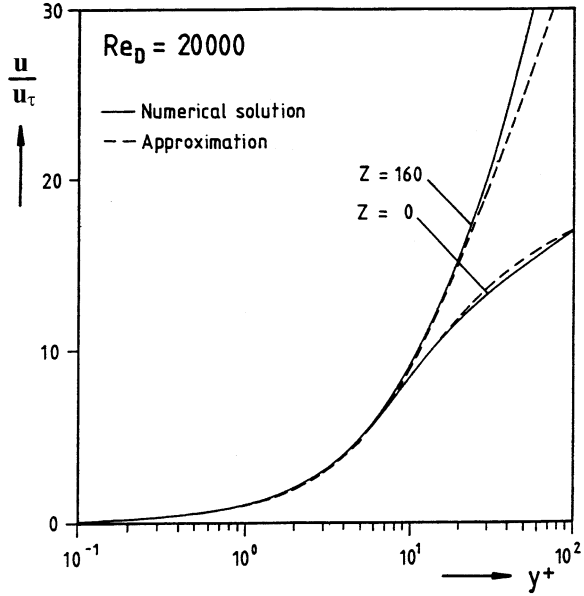


$$u^+ = \left\{ \frac{1}{\kappa_1} \ln(1 + \kappa_1 y^+) + 7.8 \left[ \frac{Re_\tau}{(Re_\tau)_0} \left( 1 - \exp\left(\frac{y^+}{y_1^+}\right) - \left(\frac{y^+}{y_1^+}\right) \exp(-by^+) \right) \right] \right\} \quad (B.17)$$

$$\{\exp(a_1(1 - \tilde{r}))\} + \left\{ \frac{u_C}{u_\tau} - A\tilde{r}^B \right\} \{1 - \exp(a_1(1 - \tilde{r}))\}$$

with $a_1 = 5(Re_\tau)_0/Re_\tau$. From the continuity equation in integral form, one can finally obtain a functional dependence between the shear-stress velocity and the maximum velocity in the pipe center

$$\frac{u_C}{u_\tau} = \frac{Re_D}{2Re_\tau} + \frac{2A}{2 + B} \quad (B.18)$$

Figure B.7 elucidates the influence of the rotation parameter Z on the axial velocity distribution for two different flow-rate Reynolds numbers. It can be seen that increasing Z tends to relaminarize the flow. The axial velocity profiles tend to approach the parabolic distribution of the Hagen-Poiseuille flow for growing values of Z. Furthermore, it can be seen that the above obtained equation for the axial velocity approximates very well the numerical calculation.

If the approximation is used in Fig. 3.15 instead of the numerical solution, no noticeable difference can be seen.

Finally, it should be noted here that the effect of pipe rotation is very much different if a laminar flow enters the axially rotating pipe. In contrast to the previous
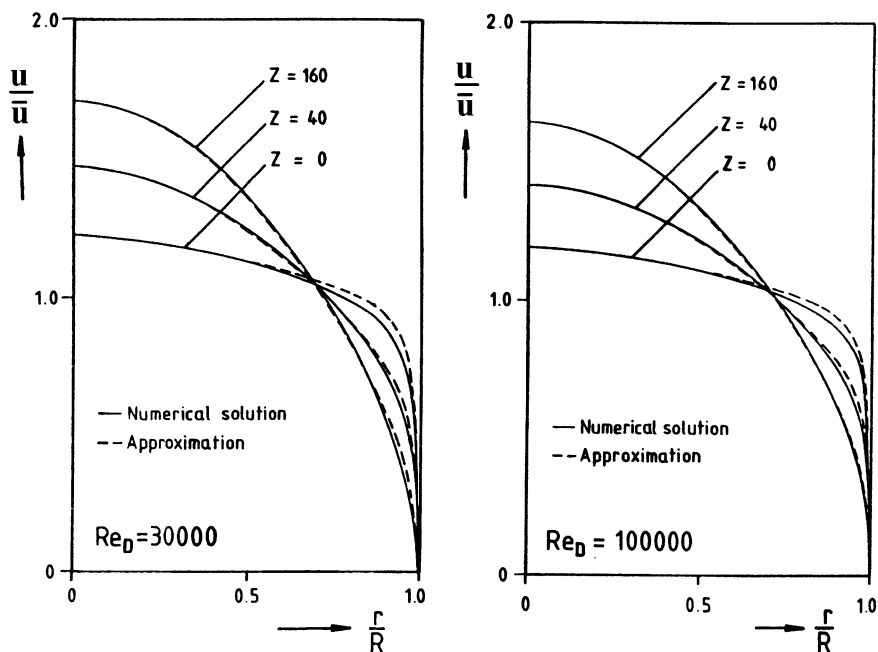
**Fig. B.7** Influence of a variation of the rotation parameter Z on the shape of the axial velocity profile (Weigand and Beer 1994)

discussions, the rotation causes for a laminar inlet flow a destabilization of the flow, even so the flow rate Reynolds number is much smaller than 2000. Mackrodt (1971) found that a laminar pipe flow is only stable against circumferential disturbances if the Reynolds numbers are below the limits $Re_{\varphi} = 53.92$ and $Re_D = 165.76$. The reader is referred to the papers of Murakami and Kikuyama (1980), Kikuyama et al. (1983), Reich et al. (1989) and Weigand and Beer (1992b) for a more detailed discussion of this subject.

# Appendix C
# A Numerical Solution Method
# for Eigenvalue Problems

During the analytical solution process for the thermal entrance problems in pipe and channel flows, a linear partial differential equation of the kind

$$\tilde{u}(\tilde{n})\frac{\partial\Theta}{\partial\tilde{x}} = \frac{1}{\tilde{r}^F}\frac{\partial}{\partial\tilde{n}}\left[\tilde{r}^F a_2(\tilde{n})\frac{\partial\Theta}{\partial\tilde{n}}\right] \tag{3.19}$$

has to be solved. If we consider a step change in the wall temperature, the boundary conditions for this partial differential equation are given by

$$\tilde{x} = 0 : \Theta(0,\tilde{n}) = 1 \tag{3.17}$$

$$\tilde{n} = 0 : \left.\frac{\partial\Theta}{\partial\tilde{n}}\right|_{\tilde{n}=0} = 0$$

$$\tilde{n} = 1 : \Theta(\tilde{x},1) = 0$$

The solution of the above given problem has been derived in Chap. 3 and is given by

$$\Theta = \sum_{j=0}^{\infty} A_j \Phi_j(\tilde{n}) \exp\left(-\lambda_j^2 \tilde{x}\right) \tag{3.55}$$

In the following, one possible numerical solution procedure for the eigenvalue problems discussed in Chaps. 3 and 4 will be presented. As it has been demonstrated, the solution of the energy equation can be obtained for these problems as a sum of eigenfunctions. In order to determine the temperature distribution, the eigenfunctions and the related eigenvalues have to be predicted. For the above given problem Eqs. (3.17) and (3.19) the eigenfunctions are the solutions of the following ordinary differential equation

$$\tilde{r}^F \tilde{u}(\tilde{n})\lambda_j^2 \Phi_j(\tilde{n}) + \left[\tilde{r}^F a_2(\tilde{n})\Phi_j'(\tilde{n})\right]' = 0 \tag{3.25}$$

with the boundary conditions

$$\Phi_j'(0) = 0 \tag{3.26}$$
$$\Phi_j(1) = 0$$

The flow index $F$ in Eq. (3.25) has to be set to one for the heat transfer in pipe flows and to zero for the heat transfer in a parallel plate channel.

Eigenvalue problems, like the one given by the Eqs. (3.25) and (3.26), can normally only be solved numerically, because the coefficients in the differential equation are complicated functions of the coordinate $\tilde{n}$. This is the case for the velocity distribution $\tilde{u}(\tilde{n})$ and also for the function

$$a_2(\tilde{n}) = 1 + \frac{\mathrm{Pr}}{\mathrm{Pr}_t}\tilde{\varepsilon}_m(\tilde{n}) \tag{C.1}$$

One efficient method to solve these eigenvalue problems is by using a Runge-Kutta method. This approach will be explained now in detail: In order to solve the Eqs. (3.25) and (3.26) by a Runge-Kutta method, we transform the second-order ordinary differential equation into a system of two first-order ordinary differential equation. Introducing the new function

$$\chi_j = \tilde{r}^F a_2(\tilde{n})\, \Phi_j' \tag{C.2}$$

into Eq. (3.25) results in the following system of ordinary differential equations

$$\begin{pmatrix} \Phi_j' \\ \chi_j' \end{pmatrix} = \begin{pmatrix} \chi_j/(\tilde{r}^F a_2(\tilde{n})) \\ -\tilde{r}^F \tilde{u}\, \lambda_j^2 \Phi_j \end{pmatrix} = \begin{pmatrix} 0 & (\tilde{r}^F a_2)^{-1} \\ -\tilde{r}^F \tilde{u}\, \lambda_j^2 & 0 \end{pmatrix} \begin{pmatrix} \Phi_j \\ \chi_j \end{pmatrix} \tag{C.3}$$

In order to solve the system of equations given by Eq. (C.3) with a Runge-Kutta method, the problem has to be considered as an initial value problem. Therefore, we provide an additional normalizing condition for the eigenfunctions according to

$$\Phi_j(0) = 1 \tag{C.4}$$

Using an arbitrary normalizing condition does not change the solution of the problem, because in Eq. (3.55) all the individual eigenfunctions are multiplied by constants. This means that the value prescribed by Eq. (C.4) will only influence the value of the constants $A_j$ in Eq. (3.55).

The algorithm for the Runge-Kutta method for solving a system of ordinary differential equations is relatively simple (see for example Törnig 1979). The system of differential equations, given by Eq. (C.3), is now solved together with the two initial conditions

$$\Phi_j(0) = 1$$
$$\chi_j(0) = 0 \qquad\qquad (C.5)$$

This will be done by using a guessed value of the eigenvalue $\lambda_a^2$. Examining the boundary condition for the eigenfunction for $\tilde{n} = 1$ ($\Phi_j(1) = 0$) shows, if the guessed value $\lambda_a^2$ is an eigenvalue of the problem under consideration. If $\lambda_a^2$ is not an eigenvalue, the calculation procedure will be continued with a different guessed value $\lambda_b^2 > \lambda_a^2$. This procedure, which is known in literature as a shooting method, will be continued up to the point when a change in sign appears for $\Phi_j(1)$. If this is the case, an eigenvalue has been found in the interval $\left[\lambda_a^2, \lambda_b^2\right]$. This eigenvalue can then be predicted to whatever accuracy is desired, by successively halving the interval. This means that the eigenvalue can finally be predicted with the accuracy

$$\Phi_j(1) \le \varepsilon \qquad\qquad (C.6)$$

where it is normally accurate enough to set $\varepsilon = 10^{-6}$. The here discussed procedure is illustrated in Fig. C.1.

The number of zero-points of the eigenfunctions $\Phi_j$ increases linearly with growing values of $j$. This means that higher eigenfunctions strongly oscillate and that it is difficult to capture exactly the shape of the eigenfunctions for larger $j$ by a numerical method. In Chap. 4, we have investigated an analytical methods for predicting such eigenfunctions for large values of $j$. However, if the number of grid points used to resolve the interval [0, 1] in the numerical prediction is large enough, also higher eigenfunctions and eigenvalues can be predicted accurately. For this normally 1000–2000 grid points have shown to be sufficient.

## C.1 Numerical Tools

On the internet web page, given in the preface, the reader will find several useful programs (executables and source codes) for the prediction and animation of thermal entrance heat transfer problems.
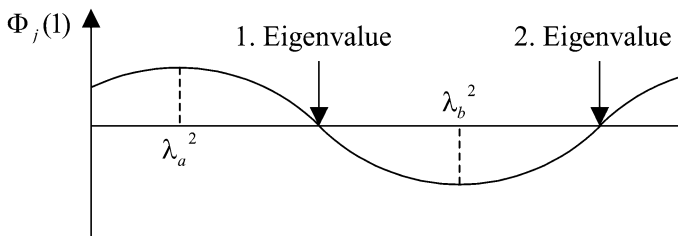


**Fig. C.1** Numerical prediction of the eigenvalues

The programs for predicting thermal entrance problems in a parallel plate channel will be explained here in more detail, because for these programs also the source code is provided on the web page.

## *Vel2dch*

This program (Velocity-Profile-2D-Channel), which is written in FORTRAN, predicts the hydrodynamically fully developed velocity profile for a laminar or turbulent channel flow. The underlying equations, which are solved, are discussed in detail in Appendix A. At the start of the program the reader is asked to provide a Reynolds number for the channel flow. If a value for the Reynolds number, based on the hydraulic diameter is provided, which is smaller than 2000, the program automatically calculates the velocity profile for a laminar channel flow (see Eq. (3.2)).

In addition to the solution of the hydrodynamically fully developed velocity profile, the program also predicts the function given by Eq. (C.1) and the fully developed temperature distribution in case of a constant wall heat flux. For the turbulent heat diffusivity, the turbulent Prandtl number model by Weigand et al. (1997a) is used. For laminar flow, the function $a_2(\tilde{n}) = 1$, and the fully developed temperature distribution is given by Eq. (5.83) (for $\text{Pe}_L \to \infty$). This program serves as an input generator to the program *Temp2dch* (Temperature-Distribution-2D-Channel), which solves the energy equation for the thermal entrance problem in a parallel plate channel.

## *Temp2dch*

This program, which is also written in FORTRAN, predicts the temperature distribution and the Nusselt number for a hydrodynamically fully developed flow. The underlying equations are discussed in detail in Chap. 3. Solutions of the energy equation are provided for the case of constant wall temperature and for the case of constant wall heat flux. The program uses the velocity distribution, the function $a_2(\tilde{y})$ and the fully developed temperature profile (which is only needed in case of a constant wall heat flux boundary condition) from the program *Vel2dch*. The calculation of the eigenvalues is done by using a Runge-Kutta method and follows the approach outlined in the first part of this appendix.

## *Visualization of Results*

After executing the above described programs, several data files are generated, which can be visualized by freeware programs as explained on the previous mentioned web page. The output files contain all main interesting calculated quantities like temperature profiles (line plots and the development of the profiles as a function of axial coordinate), Nusselt number distribution, and so on.

All the programs provided on the internet page have been rewritten from older FORTRAN programs in order to be more user friendly. The author has used similar programs for a long time and a lot of comparisons have been made over time between predicted eigenvalues, constants, Nusselt number distributions and literature data. This includes comparisons for pipe flow with Shah (1975), Shah and London (1978), Papoutsakis et al. (1980a) (with axial heat conduction), comparisons for parallel plate channels with Brown (1960), Deavours (1974), Shah and London (1978) and for the case of circular annuli with Lundberg et al. (1963) and with Hsu (1970) (with axial heat conduction).

Table C.1 shows a comparison of some predictions with values reported by Shah (1975) for a laminar flow in a parallel plate channel with constant wall temperature. It can be seen that the present calculations are in excellent agreement with the values of Shah (1975). This is interesting, because Shah (1975) obtained for $x/(D\mathrm{Pe}_D) \leq 10^{-4}$ the values for the Nusselt number from an extended Leveque solution.[2]

In addition, this sort of programs have been compared against numerical predictions for pipe flows (for example Hennecke 1968) and for circular annuli (Fuller and Samuels 1971). Some of the above mentioned comparisons have already been shown in Chaps. 3 and 4. The reader will find it relatively straight forward to extend the programs provided on the above given web page to the case of pipe flow and flow in circular annuli. Also the extension to solve eigenvalue problems for situations, where the axial heat conduction cannot be ignored, is relatively easy.

## One Example

On the web-page the reader will find also some example calculations and a documentation in order to show how to use the programs. In addition also some comparisons between the programs and literature data are provided. One simple example, which could be used as a start, in order to get used to the programs, could be to compute the laminar heat transfer for a slug-flow velocity profile. Here one can develop very easily a complete analytical solution. Let us assume that

$$\tilde{u}(\tilde{y}) = 1 \tag{C.7}$$

---

[2]The series solution for the temperature field and for the Nusselt number, which have been obtained in Chap. 3, are converging very slowly for $\tilde{x} \to 0$. Leveque (1928) developed an approximation for the temperature field for very small values of $\tilde{x}$. He approximated the velocity profile, within the very thin thermal boundary layer by $\tilde{u} = 1 - \tilde{n}$. By doing so, the energy equation has a similarity solution (see Chap. 6). This solution can be used as long as the thermal boundary layer thickness is very thin $(x/(D\mathrm{Pe}_D) \leq 10^{-3})$. The reader is also referred to Worsoe-Schmitt (1967) and to Kader (1971), where also solutions of this kind are reported for the extended Graetz problem (with axial heat conduction).

**Table C.1** Comparison of local Nusselt numbers for the thermal entrance region in a parallel plate channel with laminar internal flow and constant wall temperature

| $x/(D\mathrm{Pe}_D)$ | $\mathrm{Nu}_D$ (Shah 1975) | $\mathrm{Nu}_D$ (own calculation) |
|---|---|---|
| 0.000001 | 122.943 | 122.7618 |
| 0.000003 | 85.187 | 85.2384 |
| 0.000005 | 71.830 | 71.8536 |
| 0.000006 | 67.589 | 67.6069 |
| 0.000007 | 64.200 | 64.2141 |
| 0.000008 | 61.403 | 61.4139 |
| 0.000009 | 59.037 | 59.0463 |
| 0.00001 | 56.999 | 57.0064 |
| 0.00003 | 39.539 | 39.5402 |
| 0.00005 | 33.379 | 33.3791 |
| 0.0001 | 26.560 | 26.5600 |
| 0.0005 | 15.830 | 15.8300 |
| 0.001 | 12.822 | 12.8217 |
| 0.005 | 8.5166 | 8.5166 |
| 0.01 | 7.7405 | 7.7405 |
| 0.05 | 7.5407 | 7.5407 |
| 0.1 | 7.5407 | 7.5407 |

This could be the case for a laminar flow of a liquid metal with a very low Prandtl number. Inserting Eq. (C.7) into the energy equation (3.15) results in

$$\frac{\partial \Theta}{\partial \tilde{x}} = \frac{\partial^2 \Theta}{\partial \tilde{y}^2} \tag{C.8}$$

Let us now consider constant wall temperature boundary conditions according to Eq. (3.17). Then we obtain for the planar channel

$$\tilde{x} = 0 : \Theta(0, \tilde{y}) = 1 \tag{3.17}$$
$$\tilde{y} = 0 : \left.\frac{\partial \Theta}{\partial y}\right|_{\tilde{y}=0} = 0$$
$$\tilde{y} = 1 : \Theta(\tilde{x}, 1) = 0$$

The solution of Eq. (C.8) together with the boundary conditions given by Eq. (3.17) can easily been obtained by the method of separation of variables and one gets

$$\Theta = \sum_{j=0}^{\infty} A_j \cos(\lambda_j \tilde{y}) \exp(-\lambda_j^2 \tilde{x}) \tag{C.9}$$

**Table C.2** Comparison between analytically predicted eigenvalues and calculated eigenvalues by using the program *Temp2dch*

| Nr. | $(\lambda_j^2)_{\text{analytical}}$ | $(\lambda_j^2)_{\text{numerical}}$ | Rel. error |
|---|---|---|---|
| 0 | 2.4674012 | 2.4674009 | $<10^{-7}$ |
| 1 | 22.206611 | 22.206608 | $<10^{-7}$ |
| 2 | 61.685031 | 61.685022 | $<10^{-7}$ |
| 3 | 120.90266 | 120.90264 | $<10^{-7}$ |
| 4 | 199.85950 | 199.85947 | $<10^{-7}$ |
| 5 | 298.55555 | 298.55551 | $<10^{-7}$ |
| 6 | 416.99081 | 416.99075 | $<10^{-7}$ |
| 7 | 555.16528 | 555.16520 | $<10^{-7}$ |
| 8 | 890.73185 | 890.73172 | $<10^{-7}$ |

with the quantities

$$A_j = \frac{2\sin(\lambda_j)}{\lambda_j}, \ \lambda_j = \frac{(2j+1)\pi}{2}, \ j = 0, 1, 2, \ldots \qquad (C.10)$$

The uniform velocity profile given by Eq. (C.7) can easily been modified in the input file for the program *Temp2dch* by setting all values for the velocity profile to one.

A comparison between the analytical predicted eigenvalues and the numerical calculated values is reported in Table C.2. It can be seen that there is an excellent agreement between the numerically predicted values and the exact solution.

The same sort of accuracy can also be achieved for the constants $A_j$. A comparison between numerically predicted values and the exact solution is given in Table C.3.

More examples can be found on the previous mentioned web-page.

Please note that the provided programs on the web-page are for educational use only. They should not be used for any commercial applications. Furthermore, the author does not take any warranty for any results produced by the programs.

**Table C.3** Comparison between analytically predicted constants $A_j$ and numerically calculated values by using the program *Temp2dch*

| Nr. | $(A_j)_{\text{analytical}}$ | $(A_j)_{\text{numerical}}$ | Rel. error |
|---|---|---|---|
| 0 | 1.2732395 | 1.2732395 | $<5 \ 10^{-8}$ |
| 1 | –0.42441317 | –0.42441313 | $<10^{-7}$ |
| 2 | 0.25464790 | 0.25464783 | $<3 \ 10^{-7}$ |
| 3 | –0.18189136 | –0.18189125 | $<7 \ 10^{-7}$ |
| 4 | 0.14147106 | 0.14147091 | $<2 \ 10^{-6}$ |
| 5 | –0.11574905 | –0.11574887 | $<2 \ 10^{-6}$ |
| 6 | 0.097941501 | 0.097941291 | $<3 \ 10^{-6}$ |
| 7 | –0.084882634 | –0.084882391 | $<3 \ 10^{-6}$ |
| 8 | 0.074896442 | 0.074896166 | $<4 \ 10^{-6}$ |

# Appendix D
# Detailed Derivation of Certain Properties of the Method for Solving the Extended Graetz Problems

In the following appendix, certain properties of the method explained in Chap. 5 are derived in detail. Where necessary, the derivation is shown for the two different boundary conditions considered in Chap. 5: constant wall temperature and constant wall heat flux.

## D.1 Symmetry of the Matrix Operato L

We start our considerations by showing that the matrix operator $L$ is a symmetric operator in the Hilbert space $H = H_1 \oplus H_2$, where $H_1$ is the space containing all functions $f(\tilde{n})$ in [0, 1] for which the integral

$$\int_0^1 f^2(\tilde{n})\, \tilde{r}^F a_1(\tilde{n}) d\tilde{n} < \infty \tag{D.1}$$

holds. $H_2$ is the space of all functions $b(\tilde{n})$ in [0, 1] for which Eq. (D.2) holds

$$\int_0^1 \frac{b^2(\tilde{n})}{\tilde{r}^F a_2(\tilde{n})} d\tilde{n} < \infty \tag{D.2}$$

Now it can be shown, that the matrix operator $L$, given by Eq. (5.11), is symmetric with respect to the inner product defined by Eq. (5.14). We assume that the two vectors $\vec{\Phi}$, $\vec{\Upsilon}$ belong to $D(L)$, which is defined for a given wall temperature by Eq. (5.15) and for a given wall heat flux by Eq. (5.66). This means that we have to show, that

$$\left\langle \vec{\Phi}, L\vec{\Upsilon} \right\rangle = \left\langle L\vec{\Phi}, \vec{\Upsilon} \right\rangle \tag{5.16}$$

Equation (5.16) can be proven by inserting the expressions $L\vec{\Phi}$ and $L\vec{\Upsilon}$ into the definition of the inner product according to Eq. (5.14). This results in

$$\left\langle \vec{\Phi}, L\vec{\Upsilon} \right\rangle = \int\limits_0^1 \left[ \frac{\tilde{u}\,\tilde{r}^F}{Pe_L} \Phi_1(\tilde{n})\,\Upsilon_1(\tilde{n}) - \Phi_1(\tilde{n})\Upsilon_2'(\tilde{n}) + \Phi_2(\tilde{n})\,\Upsilon_1'(\tilde{n}) \right] d\tilde{n} \qquad (5.17)$$

$$\left\langle L\vec{\Phi}, \vec{\Upsilon} \right\rangle = \int\limits_0^1 \left[ \frac{\tilde{u}\,\tilde{r}^F}{Pe_L} \Phi_1(\tilde{n})\,\Upsilon_1(\tilde{n}) - \Phi_2'(\tilde{n})\Upsilon_1(\tilde{n}) + \Phi_1'(\tilde{n})\,\Upsilon_2(\tilde{n}) \right] d\tilde{n} \qquad (5.18)$$

Subtracting Eq. (5.18) from Eq. (5.17) results after integration in

$$\left\langle \vec{\Phi}, L\vec{\Upsilon} \right\rangle - \left\langle L\vec{\Phi}, \vec{\Upsilon} \right\rangle = \Phi_2(1)\Upsilon_1(1) - \Phi_2(0)\Upsilon_1(0) \qquad (5.19)$$
$$- \Phi_1(1)\Upsilon_2(1) + \Phi_1(0)\Upsilon_2(0)$$

The resulting expression on the right hand side of Eq. (5.19) is zero for the case of a given wall temperature because $\Phi_1(1) = \Upsilon_1(1) = 0$, as well as for the case of a given wall heat flux boundary condition, because $\Phi_2(1) = \Upsilon_2(1) = 0$. For both boundary conditions $\Phi_2(0) = \Upsilon_2(0) = 0$ because of the assumed symmetry of the eigenfunctions.

## D.2 The Eigenfunctions Constitute a Set of Orthogonal Functions

Next, we show that the eigenfunctions given in Chap. 5 constitute a set of orthogonal functions. Consider the two eigenfunctions $\vec{\Phi}_j$ and $\vec{\Phi}_k$ together with the related eigenvalues $\lambda_j$ and $\lambda_k$. From Eq. (5.20) one obtains:

$$\begin{aligned} L\vec{\Phi}_j &= \lambda_j\vec{\Phi}_j \\ L\vec{\Phi}_k &= \lambda_k\vec{\Phi}_k \end{aligned} \qquad (D.3)$$

with the boundary conditions.

### *Constant Wall Temperature*

$$\Phi_{j1}'(0) = \Phi_{k1}'(0) = 0, \quad \Phi_{j1}(1) = \Phi_{k1}(1) = 0 \qquad (D.4)$$

### Constant Wall Heat Flux

$$\Phi'_{j1}(0) = \Phi'_{k1}(0) = 0, \quad \Phi'_{j1}(1) = \Phi'_{k1}(1) = 0 \tag{D.5}$$

By taking the inner product (defined by Eq. (5.14)) of Eq. (D.3), one obtains (note, that from Eq. (5.14) follows that $\left\langle \vec{\Phi}_j, \vec{\Phi}_k \right\rangle = \left\langle \vec{\Phi}_k, \vec{\Phi}_j \right\rangle$)

$$\left\langle L\vec{\Phi}_j, \vec{\Phi}_k \right\rangle - \left\langle \vec{\Phi}_j, L\vec{\Phi}_k \right\rangle = \left( \lambda_j - \lambda_k \right) \left\langle \vec{\Phi}_j, \vec{\Phi}_k \right\rangle \tag{D.6}$$

In the last paragraph, it has been shown that the operator $L$ is a symmetric operator in the Hilpert space. This means that Eq. (5.16) is valid

$$\left\langle \vec{\Phi}, L\vec{\Upsilon} \right\rangle = \left\langle L\vec{\Phi}, \vec{\Upsilon} \right\rangle \tag{5.16}$$

where $\vec{\Phi}$ and $\vec{\Upsilon}$ can be replaced by $\vec{\Phi}_j$ and $\vec{\Phi}_k$. Then it follows immediately from Eq. (D.6) that

$$0 = \left( \lambda_j - \lambda_k \right) \left\langle \vec{\Phi}_j, \vec{\Phi}_k \right\rangle \tag{D.7}$$

From this equation, one can conclude that

$$\left\langle \vec{\Phi}_j, \vec{\Phi}_k \right\rangle = \begin{cases} 0 & \text{for } \lambda_j \neq \lambda_k \\ \left\| \vec{\Phi}_j \right\|^2 & \text{for } \lambda_j = \lambda_k \end{cases} \tag{D.8}$$

Equation (D.8) shows that the eigenfunctions constitute a set of orthogonal functions for the inner product defined according to Eq. (5.14).

## D.3 A Detailed Derivation of Eqs. (5.31) and (5.68)

Because of the non-homogeneous boundary conditions, the vector $\vec{S}$ does not belong to the domain $D\left(L\right)$ given by Eq. (5.15) (for constant wall temperature boundary conditions) or by Eq. (5.66) (for constant wall heat flux boundary conditions). However, it can be shown that Eq. (5.31) and Eq. (5.68) hold.

$$\left\langle L\vec{S}, \vec{\Phi}_j \right\rangle = \left\langle \vec{S}, L\vec{\Phi}_j \right\rangle + \Phi_{j2}(1)\, g(\tilde{x}) \tag{5.31}$$

$$\left\langle L\vec{S}, \vec{\Phi}_j \right\rangle = \left\langle \vec{S}, L\vec{\Phi}_j \right\rangle - \Phi_{j1}(1) E(\tilde{x}, 1) \tag{5.68}$$

These two equations can be derived in the following way: from the definition of the inner product by Eq. (5.14) one obtains

$$\left\langle L\vec{S},\, \vec{\Phi}_j \right\rangle = \int_0^1 \left[ \frac{\tilde{u}\,\tilde{r}^F}{Pe_L}\, \Phi_{j1}\,(\tilde{n})\, S_1(\tilde{n}) - \Phi_{j1}(\tilde{n})\, S_2'(\tilde{n}) + \Phi_{j2}\,(\tilde{n})\, S_1'(\tilde{n}) \right] d\tilde{n} \quad \text{(D.9)}$$

$$\left\langle \vec{S},\, L\vec{\Phi}_j \right\rangle = \int_0^1 \left[ \frac{\tilde{u}\,\tilde{r}^F}{Pe_L}\, \Phi_{j1}(\tilde{n})\, S_1(\tilde{n}) - \Phi_{j2}'(\tilde{n}) S_1(\tilde{n}) + \Phi_{j1}'(\tilde{n})\, S_2(\tilde{n}) \right] d\tilde{n} \quad \text{(D.10)}$$

where the prime denotes the derivative with respect to $\tilde{n}$. From these two equations one obtains

$$\left\langle L\vec{S},\, \vec{\Phi}_j \right\rangle = \left\langle \vec{S},\, L\vec{\Phi}_j \right\rangle + \Phi_{j2}(1)\, S_1(1) - \Phi_{j2}(0)\, S_1(0) + \quad \text{(D.11)}$$
$$- \Phi_{j1}(1) S_2(1) + \Phi_{j1}(0) S_2(0)$$

where the solution vector $\vec{S}$ was defined in Eq. (5.11) by

$$\vec{S} = \begin{bmatrix} \Theta(\tilde{x},\tilde{n}) \\ E(\tilde{x},\tilde{n}) \end{bmatrix} \quad \text{(D.12)}$$

Therefore, Eq. (D.11) can also be written as

$$\left\langle L\vec{S},\, \vec{\Phi}_j \right\rangle = \left\langle \vec{S},\, L\vec{\Phi}_j \right\rangle + \Phi_{j2}(1)\, \Theta(\tilde{x}, 1) - \Phi_{j2}(0)\, \Theta(\tilde{x}, 0) \quad \text{(D.13)}$$
$$- \Phi_{j1}(1) E(\tilde{x}, 1) + \Phi_{j1}(0) E(\tilde{x}, 0)$$

For the case of a constant wall temperature, the boundary conditions are given by

$$\Phi_{j1}'(0) = 0, \quad \Phi_{j1}(1) = 0, \quad \text{(D.14)}$$
$$\left. \frac{\partial \Theta}{\partial \tilde{n}} \right|_{\tilde{n}=0} = 0, \quad \Theta(\tilde{x}, 1) = \text{given}$$

In addition, it follows from Eq. (5.22) that $\Phi_{j2}(0) = 0$ and from the definition of the function $E$ by Eq. (5.9) it follows that $E(\tilde{x}, 0) = 0$. Therefore, Eq. (D.13) simplifies for the case of a given wall temperature to

$$\left\langle L\vec{S},\, \vec{\Phi}_j \right\rangle = \left\langle \vec{S},\, L\vec{\Phi}_j \right\rangle + \Phi_{j2}(1)\, \Theta(\tilde{x}, 1) \quad \text{(D.15)}$$

If now $\Theta(\tilde{x}, 1)$ is replaced by the boundary condition according to Eq. (5.7), Eq. (5.31) is obtained.

For the case of a given wall heat flux, the boundary conditions are given by

$$\Phi'_{j1}(0) = 0, \quad \Phi'_{j1}(1) = 0, \tag{D.16}$$

$$\left.\frac{\partial \Theta}{\partial \tilde{n}}\right|_{\tilde{n}=0} = 0, \quad \left.\frac{\partial \Theta}{\partial \tilde{n}}\right|_{\tilde{n}=1} = \text{given}$$

Recalling that $\Phi_{j2}(0) = 0$ and $E(\tilde{x}, 0) = 0$, one obtains from Eq. (D.13), by considering that $\Phi_{j2}(1) = 0$ for the case of a prescribed wall heat flux, Eq. (5.68)

$$\left\langle L\vec{S}, \vec{\Phi}_j \right\rangle = \left\langle \vec{S}, L\vec{\Phi}_j \right\rangle - \Phi_{j1}(1)E(\tilde{x}, 1) \tag{5.68}$$

## D.4 Simplification of the Expression for the Temperature Distribution (for Constant Wall Temperature)

In Eq. (5.42) we used the result that

$$-\sum_{j=0}^{\infty} \frac{\Phi_{j2}^{-}(1)\,\Phi_{j1}^{-}(\tilde{n})}{\lambda_j^{-}\,\left\|\vec{\Phi}_j^{-}\right\|^2} - \sum_{j=0}^{\infty} \frac{\Phi_{j2}^{+}(1)\,\Phi_{j1}^{+}(\tilde{n})}{\lambda_j^{+}\,\left\|\vec{\Phi}_j^{+}\right\|^2} = 1 \tag{5.42}$$

This expression can be derived in the following way. We start by expanding a vector $\vec{f} = (1, 0)^T$ according to Eq. (5.29). This results in

$$\begin{pmatrix} 1 \\ 0 \end{pmatrix} = \sum_{j=0}^{\infty} \frac{\left\langle \vec{f}, \vec{\Phi}_j \right\rangle}{\left\|\vec{\Phi}_j\right\|^2} \vec{\Phi}_j(\tilde{n}) \tag{D.17}$$

The expression $\left\langle \vec{f}, \vec{\Phi}_j \right\rangle$ can now be evaluated from Eq. (5.14) which results in

$$\left\langle \vec{f}, \vec{\Phi}_j \right\rangle = \int_0^1 \left[ \frac{a_1(\tilde{n})\,\tilde{r}^F}{\text{Pe}_L^2} \cdot 1 \cdot \Phi_{j1}(\tilde{n}) \right] d\tilde{n} \tag{D.18}$$

From this equation, one obtains for the first vector component of Eq. (D.17)

$$1 = \sum_{j=0}^{\infty} \frac{\Phi_{j1}}{\left\|\vec{\Phi}_j\right\|^2} \int_0^1 \frac{a_1(\tilde{n})\tilde{r}^F \Phi_{j1}}{\text{Pe}_L^2} d\tilde{n} \tag{D.19}$$

Now the integral in Eq. (D.19) can be rewritten. First, one can replace the integrand by using Eq. (5.21). This results in

$$\int_0^1 \frac{a_1(\tilde{n})\tilde{r}^F \Phi_{j1}}{Pe_L^2} d\tilde{n} = \frac{1}{\lambda_j} \left\{ \int_0^1 \tilde{u}\tilde{r}^F \Phi_{j1} d\tilde{n} - \Phi_{j2}(1) \right\} \tag{D.20}$$

The integral on the right hand side of Eq. (D.20) can be expressed as

$$\frac{1}{\lambda_j} \int_0^1 \tilde{u}\tilde{r}^F \Phi_{j1} d\tilde{n} = \frac{1}{\lambda_j} \left( \Phi_{j1} \int_0^{\tilde{n}} \tilde{u}\tilde{r}^F d\tilde{n} \right) \Bigg|_0^1 - \frac{1}{\lambda_j} \int_0^1 \Phi_{j1}' \left( \int_0^{\tilde{n}} \tilde{u}\tilde{r}^F d\hat{n} \right) d\tilde{n} \tag{D.21}$$

Evaluating the first expression on the right hand side of Eq. (D.21) shows that this term is zero. If one further replaces $\Phi_{j1}'$ by Eq. (5.22), one obtains

$$-\frac{1}{\lambda_j} \int_0^1 \Phi_{j1}' \left( \int_0^{\tilde{n}} \tilde{u}\tilde{r}^F d\hat{n} \right) d\tilde{n} = -\int_0^1 \frac{\Phi_{j2}}{\tilde{r}^F a_2} \left( \int_0^{\tilde{n}} \tilde{u}\tilde{r}^F d\hat{n} \right) d\tilde{n} = -\int_0^1 \Phi_{j2}\, \gamma(\tilde{n})\, d\tilde{n} \tag{D.22}$$

If one replaces now the integral in Eq. (D.19) one obtains

$$1 = -\sum_{j=0}^{\infty} \frac{\Phi_{j1}(\tilde{n})}{\left\| \vec{\Phi}_j \right\|^2} \int_0^1 \Phi_{j2}\, \gamma(\tilde{n}) d\tilde{n} - \sum_{j=0}^{\infty} \frac{\Phi_{j1}(\tilde{n})\Phi_{j2}(1)}{\left\| \vec{\Phi}_j \right\|^2} \tag{D.23}$$

In order to show that this expression is identical to Eq. (5.42), one has to show that the first sum on the right hand side of this equation is zero. Expanding the vector $\vec{f} = (0,\ \gamma(\tilde{n})\tilde{r}^F a_2)^T$ into a series, one obtains for the first vector component

$$0 = \sum_{j=0}^{\infty} \frac{\Phi_{j1}}{\left\| \vec{\Phi}_j \right\|^2} \int_0^1 \gamma(\tilde{n})\, \Phi_{j2}\, d\tilde{n} \tag{D.24}$$

Equation (D.24) shows that the first sum in Eq. (D.23) is zero and one obtains therefore

$$1 = -\sum_{j=0}^{\infty} \frac{\Phi_{j1}(\tilde{n})\Phi_{j2}(1)}{\left\| \vec{\Phi}_j \right\|^2} \tag{D.25}$$

If we distinguish explicitly between positive and negative eigenfunctions in Eq. (D.25), we obtain Eq. (5.42).

## D.5 Simplification of the Expression for the Temperature Distribution (for Constant Wall Heat Flux)

For the case of a prescribed wall heat flux, we can simplify Eq. (5.73) by replacing the first two terms in this equation. In the following section, it will be explained how this can be done. The first term in Eq. (5.73) to be replaced is

$$\sum_{j=0}^{\infty} \frac{\Phi_{j1}(1)}{\lambda_j^2 \left\| \vec{\Phi}_j \right\|^2} \Phi_{j1}(\tilde{n}) \tag{D.26}$$

We start our considerations by expanding the vector $\vec{f} = (1,0)^T$ into a series. For the first vector component one obtains

$$1 = \sum_{j=0}^{\infty} \frac{\Phi_{j1}}{\left\| \vec{\Phi}_j \right\|^2} \int_0^1 \frac{a_1(\tilde{n}) \tilde{r}^F \Phi_{j1}}{\text{Pe}_L^2} d\tilde{n} \tag{D.19}$$

The integral in the above equation can be rewritten by using Eq. (5.23). This results in

$$\int_0^1 \frac{a_1(\tilde{n}) \tilde{r}^F \Phi_{j1}}{\text{Pe}_L^2} d\tilde{n} = -\frac{1}{\lambda_j^2} \int_0^1 \frac{d}{d\tilde{n}} \left[ \tilde{r}^F a_2(\tilde{n}) \Phi_{j1}' \right] d\tilde{n} + \frac{1}{\lambda_j} \int_0^1 \tilde{u} \tilde{r}^F \Phi_{j1} d\tilde{n} \tag{D.27}$$

Carrying out the integrations in the above equation, it can be seen that the first integral is zero for the case of a prescribed wall heat flux and one obtains

$$1 = \sum_{j=0}^{\infty} \frac{\Phi_{j1}(\tilde{n})}{\lambda_j \left\| \vec{\Phi}_j \right\|^2} \int_0^1 \tilde{u} \tilde{r}^F \Phi_{j1}(\tilde{n}) d\tilde{n} \tag{D.28}$$

The integral in Eq. (D.28) can be further rewritten by partial integration. This results in

$$1 = \sum_{j=0}^{\infty} \frac{\Phi_{j1}(\tilde{n})}{\lambda_j \left\| \vec{\Phi}_i \right\|^2} \frac{\Phi_{j1}(1)}{F+1} - \sum_{j=0}^{\infty} \frac{\Phi_{j1}(\tilde{n})}{\lambda_j \left\| \vec{\Phi}_j \right\|^2} \int_0^1 \Phi_{j2}(\tilde{n}) \omega(\tilde{n}) d\tilde{n} \tag{D.29}$$

$$\omega(\tilde{n}) = \frac{1}{\tilde{r}^F a_2(\tilde{n})} \int_0^{\tilde{n}} \tilde{u} \, \tilde{r}^F d\bar{n}$$

In order to obtain an expression for Eq. (D.26), the second term on the right hand side of Eq. (D.29) needs to be evaluated. Expanding the vector $\vec{f} = (0, \omega(\tilde{n})\tilde{r}^F a_2(\tilde{n}))^T$ into a series results in

$$\begin{pmatrix} 0 \\ \omega(\tilde{n})\tilde{r}^F a_2(\tilde{n}) \end{pmatrix} = \sum_{j=0}^{\infty} \frac{\langle \vec{f}, \vec{\Phi}_j \rangle}{\left\| \vec{\Phi}_j \right\|^2} \vec{\Phi}_j(\tilde{n}) = \sum_{j=0}^{\infty} \frac{\vec{\Phi}_j(\tilde{n})}{\left\| \vec{\Phi}_j \right\|^2} \int_0^1 \omega(\tilde{n}) \Phi_{j2} d\tilde{n} \qquad (D.30)$$

Taking the first vector component of Eq. (D.30) shows that the second term on the right hand side of Eq. (D.29) is zero and we obtain for the expression given by Eq. (D.26)

$$\sum_{j=0}^{\infty} \frac{\Phi_{j1}(1)}{\lambda_j \left\| \vec{\Phi}_j \right\|^2} \Phi_{j1}(\tilde{n}) = F + 1 \qquad (D.31)$$

In addition, we want to derive an analytical expression for the first sum on the right hand side of Eq. (5.73):

$$\sum_{j=0}^{\infty} \frac{\Phi_{j1}(1)}{\lambda_j^2 \left\| \vec{\Phi}_j \right\|^2} \Phi_{j1}(\tilde{n}) \qquad (D.32)$$

If we put $\tilde{x} \to \infty$ in Eq. (5.73), we obtain the fully developed temperature distribution in the duct with a prescribed heat flux at the wall. Using Eq. (D.31) this distribution can be written as

$$\tilde{x} \to \infty : \Theta_\infty(\tilde{x}, \tilde{n}) = \sum_{j=0}^{\infty} \frac{\Phi_{j1}(1)}{\lambda_j^2 \left\| \vec{\Phi}_j \right\|^2} \Phi_{j1}(\tilde{n}) + \tilde{x}(F + 1) \qquad (D.33)$$

As it can be seen from Eq. (D.33) this temperature distribution contains a term, which is linearly increasing in $\tilde{x}$ and a term, which is a function of $\tilde{n}$. Therefore, Eq. (D.33) might be written as

$$\tilde{x} \to \infty : \Theta_\infty(\tilde{x}, \tilde{n}) = \Psi(\tilde{n}) + \tilde{x}(F + 1) \qquad (D.34)$$

The function $\Psi(\tilde{n})$, appearing in Eq. (D.34), is not known. However, this function can easily been obtained by inserting Eq. (D.34) into the energy equation (5.6) and solving the resulting ordinary differential equation for $\Psi(\tilde{n})$. One finally gets

$$\Psi(\tilde{n}) = \int_0^{\tilde{n}} \frac{F+1}{\tilde{r}^F a_2(\bar{n})} \int_0^{\bar{n}} \tilde{u}(s)\tilde{r}^F ds d\bar{n} + C_2 = \bar{\Psi}(\tilde{n}) + C_2 \qquad (D.35)$$

The constant $C_2$, which appears in the above equation, can be obtained from a global energy balance. This might be done by evaluating Eq. (5.9) for the case of a thermally fully developed flow $(\tilde{x} \to \infty)$ for the whole flow domain $E(\tilde{n} = 1, \tilde{x} \to \infty)$. By considering the boundary conditions for the function $E$, given by Eq. (5.65), one obtains

$$\tilde{x} \to \infty : E(1, \tilde{x}) = \tilde{x} = \int\limits_0^1 \left[ \tilde{u}\, \Theta_\infty - \frac{1}{\mathrm{Pe}_L^2} a_1(\bar{n}) \frac{\partial \Theta_\infty}{\partial \tilde{x}} \right] \tilde{r}^F d\bar{n} \qquad (D.36)$$

Inserting the temperature distribution given by Eq. (D.34) into Eq. (D.36) results in

$$\int\limits_0^1 \tilde{u}\, \tilde{n}^F \Psi(\tilde{n}) d\tilde{n} = \frac{(F+1)}{\mathrm{Pe}_L^2} \int\limits_0^1 a_1(\tilde{n})\, \tilde{r}^F d\tilde{n} \qquad (D.37)$$

Comparing Eq. (D.37) with Eq. (D.35) results in the following expression for the constant $C_2$

$$C_2 = \frac{(F+1)^2}{\mathrm{Pe}_L^2} \int\limits_0^1 a_1(\tilde{n})\, \tilde{r}^F d\tilde{n} - (F+1) \int\limits_0^1 \tilde{u}\, \tilde{r}^F \bar{\Psi}(\tilde{n}) d\tilde{n} \qquad (D.38)$$

$$\bar{\Psi}(\tilde{n}) = \int\limits_0^{\tilde{n}} \frac{F+1}{\tilde{r}^F a_2(\tilde{n})} \int\limits_0^{\tilde{n}} \tilde{u}\, \tilde{r}^F ds d\bar{n} \qquad (D.39)$$

From this equation one finally obtains for the sum, Eq. (D.32),

$$\sum_{j=0}^\infty \frac{\Phi_{j1}(1)}{\lambda_j^2 \left\| \vec{\Phi}_j \right\|^2} \Phi_{j1}(\tilde{n}) = \Psi(\tilde{n}) = \bar{\Psi}(\tilde{n}) + C_2 \qquad (D.40)$$

It should be noted here that the above analytical expressions, Eqs. (D.26) and (D.32), transform into the expressions developed by Papoutsakis et al. (1980), if we consider the simplified case of a laminar pipe flow $(F = 1, a_1 = a_2 = 1, \tilde{u} = 2(1 - \tilde{n}^2))$. For this case one obtains

$$\sum_{j=0}^\infty \frac{\Phi_{j1}(\tilde{n}) \Phi_{j1}(1)}{\lambda_j \left\| \vec{\Phi}_j \right\|^2} = 2 \qquad (D.41)$$

and

$$\sum_{j=0}^{\infty} \frac{\Phi_{j1}(1)\Phi_{j1}(\tilde{n})}{\lambda_j^2 \left\|\vec{\Phi}_j\right\|^2} = \tilde{n}^2 - \frac{\tilde{n}^4}{4} + \frac{8}{Pe_D^2} - \frac{7}{24} \tag{D.42}$$

These expressions have also been given in Eq. (5.82). For the case of a planar channel, Eq. (5.83) is obtained.

# D.6 The Vector Norm $\left\|\vec{\Phi}_j\right\|^2$

In this section, some interesting results about the vector norm $\left\|\vec{\Phi}_j\right\|^2$ are presented. The vector norm is defined by inserting the eigenvector into Eq. (5.14). This results in

$$\left\|\vec{\Phi}_j\right\|^2 = \left\langle \vec{\Phi}_j,\, \vec{\Phi}_j \right\rangle = \int\limits_0^1 \left[ \frac{a_1(\tilde{n})\,\tilde{r}^F}{Pe_L^2}\,\Phi_{j1}^2(\tilde{n}) + \frac{\Phi_{j2}^2(\tilde{n})}{a_2(\tilde{n})\,\tilde{r}^F} \right] d\tilde{n} \tag{D.43}$$

First, we establish a connection between the vector norm and the derivative of the eigenfunction with respect to the eigenvalue (see Eqs. (5.46) and (5.78)). This connection is important because it allows us to evaluate the constants in the temperature distribution very easily. Therefore, we consider two vectors $\vec{\Phi}_j$ and $\vec{\Phi}$ which both satisfy Eq. (5.20). This results in

$$L\vec{\Phi}_j = \lambda_j\vec{\Phi}_j \tag{D.44}$$
$$L\vec{\Phi} = \lambda\,\vec{\Phi}$$

The eigenvector $\vec{\Phi}_j$ satisfies both boundary conditions at $\tilde{n} = 0$ and $\tilde{n} = 1$, whereas the vector $\vec{\Phi}$ satisfies the boundary condition at $\tilde{n} = 0$ and only in the limit $\lambda \to \lambda_j$ the boundary condition at $\tilde{n} = 1$.

If we now apply the inner product, given by Eq. (5.14), to Eq. (D.44), we obtain

$$\left\langle L\vec{\Phi}_j, \vec{\Phi} \right\rangle - \left\langle \vec{\Phi}_j, L\vec{\Phi} \right\rangle = (\lambda_j - \lambda)\left\langle \vec{\Phi}_j, \vec{\Phi} \right\rangle \tag{D.45}$$

The expression on the left hand side of Eq. (D.45) can be evaluated to be

$$\left\langle L\vec{\Phi}_j, \vec{\Phi} \right\rangle - \left\langle \vec{\Phi}_j, L\vec{\Phi} \right\rangle = \left[ \Phi_{j1}\Phi_2 - \Phi_{j2}\Phi_1 \right]\big|_0^1 \tag{D.46}$$

Because $\Phi_{j2}(0) = \Phi_2(0) = 0$ one obtains from Eq. (D.45)

$$\left\langle \vec{\Phi}_j, \vec{\Phi} \right\rangle = \frac{\Phi_{j1}(1)\Phi_2(1, \lambda) - \Phi_{j2}(1)\Phi_1(1, \lambda)}{\lambda_j - \lambda} \tag{D.47}$$

If we evaluate Eq. (D.47) for the limiting case when $\lambda \to \lambda_j$, $\vec{\Phi} \to \vec{\Phi}_j$ we obtain

$$\lim_{\lambda \to \lambda_j} \left\langle \vec{\Phi}_j, \vec{\Phi} \right\rangle = \left\| \vec{\Phi}_j \right\|^2 = \lim_{\lambda \to \lambda_j} \frac{\Phi_{j1}(1)\Phi_2(1, \lambda) - \Phi_{j2}(1)\Phi_1(1, \lambda)}{\lambda_j - \lambda} \tag{D.48}$$

Before evaluating the expression on the right hand side of Eq. (D.48), the wall boundary conditions for $\tilde{n} = 1$ need to be specified.

## *Constant Wall Temperature:* $\Phi_{j1}(1) = 0$

Inserting this boundary condition into Eq. (D.48) one obtains

$$\lim_{\lambda \to \lambda_j} \left\langle \vec{\Phi}_j, \vec{\Phi} \right\rangle = \left\| \vec{\Phi}_j \right\|^2 = \lim_{\lambda \to \lambda_j} \left\{ -\Phi_{j2}(1)\frac{\Phi_1(1, \lambda)}{\lambda_j - \lambda} \right\} \tag{D.49}$$

If $\lambda \to \lambda_j$ is introduced into the Eq. (D.49), the expression on the right hand side leads to 0/0 and can be evaluated by the rule of L'Hospital. One obtains Eq. (5.46)

$$\left\| \vec{\Phi}_j \right\|^2 = -\Phi_{j2}(1)\frac{d\Phi_{j1}(1, \lambda)}{d\lambda}\bigg|_{\lambda = \lambda_j} \tag{5.46}$$

## *Constant Wall Heat Flux:* $\Phi_{j2}(1) = 0$

For this case one obtains from Eq. (D.48)

$$\lim_{\lambda \to \lambda_j} \left\langle \vec{\Phi}_j, \vec{\Phi} \right\rangle = \left\| \vec{\Phi}_j \right\|^2 = \lim_{\lambda \to \lambda_j} \frac{\Phi_{j1}(1)\Phi_2(1, \lambda)}{\lambda_j - \lambda} \tag{D.50}$$

Using the rule of L'Hospital to evaluate the term on the right hand side results in

$$\left\| \vec{\Phi}_j \right\|^2 = \Phi_{j1}(1)\frac{d\Phi_{j2}(1, \lambda)}{d\lambda}\bigg|_{\lambda = \lambda_j} \tag{D.51}$$

In Eq. (D.51) the vector component $\Phi_2$ can be replaced by using Eq. (5.22) at the wall. This leads to

$$\left\|\vec{\Phi}_j\right\|^2 = \Phi_{j1}(1) \frac{d}{d\lambda} \left(\frac{\Phi'_{j1}(1, \lambda)}{\lambda}\right)\bigg|_{\lambda=\lambda_j} \tag{D.52}$$

Finally, for the case of a constant wall temperature, Eq. (5.45) is derived

$$\left\|\vec{\Phi}_j\right\|^2 = -\frac{1}{\lambda_j} \int_0^1 \tilde{r}^F \tilde{u} \, \Phi_{j1}^2 d\tilde{n} + \frac{2}{\text{Pe}_L^2} \int_0^1 \tilde{r}^F a_1(\tilde{n}) \Phi_{j1}^2 d\tilde{n} \tag{5.45}$$

In order to obtain this equation, we start from Eq. (D.43)

$$\left\|\vec{\Phi}_j\right\|^2 = \left\langle \vec{\Phi}_j, \, \vec{\Phi}_j \right\rangle = \int_0^1 \left[ \frac{a_1(\tilde{n}) \tilde{r}^F}{\text{Pe}_L^2} \Phi_{j1}^2(\tilde{n}) + \frac{\Phi_{j2}^2(\tilde{n})}{a_2(\tilde{n}) \tilde{r}^F} \right] d\tilde{n} \tag{D.43}$$

For Eq. (D.43), one can rewrite the second term in the integral by using Eq. (5.22). This results in

$$\int_0^1 \frac{\Phi_{j2}^2(\tilde{n})}{a_2(\tilde{n}) \tilde{r}^F} d\tilde{n} = \frac{1}{\lambda_j} \int_0^1 \Phi_{j2} \Phi'_{j1} d\tilde{n} \tag{D.53}$$

The first term in the integral of Eq. (D.43) can be rewritten by using Eq. (5.21)

$$\int_0^1 \frac{a_1(\tilde{n}) \tilde{r}^F}{\text{Pe}_L^2} \Phi_{j1}^2(\tilde{n}) d\tilde{n} = \frac{1}{\lambda_j} \int_0^1 \left( \tilde{u} \tilde{r}^F \Phi_{j1}^2 - \Phi_{j1} \Phi'_{j2} \right) d\tilde{n} \tag{D.54}$$

Introducing Eqs. (D.53) and (D.54) into Eq. (D.43) gives

$$\left\|\vec{\Phi}_j\right\|^2 = \frac{1}{\lambda_j} \int_0^1 \left[ \tilde{u} \tilde{r}^F \Phi_{j1}^2(\tilde{n}) + \Phi'_{j1} \Phi_{j2} - \Phi_{j1} \Phi'_{j2} \right] d\tilde{n} \tag{D.55}$$

and after partial integration (with the boundary conditions $\Phi_{j2}(0) = \Phi_{j1}(1) = 0$) one obtains from Eq. (D.55)

$$\left\|\vec{\Phi}_j\right\|^2 = \frac{1}{\lambda_j} \int_0^1 \tilde{u} \tilde{r}^F \Phi_{j1}^2(\tilde{n}) d\tilde{n} - \frac{2}{\lambda_j} \int_0^1 \Phi_{j1} \Phi'_{j2} \, d\tilde{n} \tag{D.56}$$

The second integral in Eq. (D.56) can now be modified by using Eq. (5.22)

$$-\frac{2}{\lambda_j}\int_0^1 \Phi_{j1}\Phi'_{j2}\,d\tilde{n} = -\frac{2}{\lambda_j}\int_0^1 \tilde{u}\tilde{r}^F\Phi_{j1}^2 d\tilde{n} + \frac{2}{\lambda_j}\int_0^1 \frac{a_1\tilde{r}^F}{\mathrm{Pe}_L^2}\Phi_{j1}^2 d\tilde{n} \qquad (D.57)$$

Inserting Eq. (D.57) into Eq. (D.56) results in Eq. (5.45).

# Appendix E
# Short Solutions of the Chapter Problems

The following appendix provides short solutions to the problems given at the end of each chapter. For more detailed solutions the reader is referred to the solution manual. This manual can be found on the web-page of the book (see preface to the second edition).

## Chapter 1

### Problem 1-1

(a) linear, homogeneous partial differential equation of order 2
(b) linear, non-homogeneous partial differential equation of order 2
(c) linear, non-homogeneous partial differential equation of order 4
(d) non-linear, non-homogeneous second order partial differential equation.
(e) quasi-linear, non-homogeneous partial differential equation of second order.

### Problem 1-2

(a) The problem can be split in the following two problems

$$\frac{\partial^2 \Theta}{\partial \tilde{x}^2} + \frac{\partial^2 \Theta_1}{\partial \tilde{y}^2} = 0$$

with the boundary conditions

$$\Theta_1(0, \tilde{y}) = 0$$
$$\Theta_1(1, \tilde{y}) = \sin(\pi \tilde{y})$$
$$\Theta_1(\tilde{x}, 0) = 0$$
$$\Theta_1(\tilde{x}, 1) = 0$$

and

$$\frac{\partial^2 \Theta_2}{\partial \tilde{x}^2} + \frac{\partial^2 \Theta_2}{\partial \tilde{y}^2} = 0$$

with the boundary conditions

$$\Theta_2(0, \tilde{y}) = 0$$
$$\Theta_2(1, \tilde{y}) = 0$$
$$\Theta_2(\tilde{x}, 0) = 0$$
$$\Theta_2(\tilde{x}, 1) = \sin(3\pi\tilde{x})$$

(b) Adding up the two problems results is: $\Theta = \Theta_1 + \Theta_2$

$$\frac{\partial^2\Theta_1}{\partial\tilde{x}^2} + \frac{\partial^2\Theta_1}{\partial\tilde{y}^2} + \frac{\partial^2\Theta_2}{\partial\tilde{x}^2} + \frac{\partial^2\Theta_2}{\partial\tilde{y}^2} = \frac{\partial^2\Theta}{\partial\tilde{x}^2} + \frac{\partial^2\Theta}{\partial\tilde{y}^2} = 0$$

For the boundary conditions one obtains

$$\Theta(0, \tilde{y}) = \Theta_1(0, \tilde{y}) + \Theta_2(0, \tilde{y}) = 0$$
$$\Theta(1, \tilde{y}) = \Theta_1(1, \tilde{y}) + \Theta_2(1, \tilde{y}) = \sin(\pi\tilde{y})$$
$$\Theta(\tilde{x}, 0) = \Theta_1(\tilde{x}, 0) + \Theta_2(\tilde{x}, 0) = 0$$
$$\Theta(\tilde{x}, 1) = \Theta_1(\tilde{x}, 1) + \Theta_2(\tilde{x}, 1) = \sin(3\pi\tilde{x})$$

(c) By inserting the expressions below for $\Theta_1$ and $\Theta_2$ into the partial differential equations and the boundary conditions, it can easily be shown that the expressions satisfy the related equations.

### Problem 1-3

(a) One obtains the solution: $\Theta_1 = \tilde{x} + \tilde{y}$
(b) For $\tilde{y} = 1 - \tilde{x}$ one obtains: $\Theta_1 = 1$. This does not satisfy the original boundary condition at $\tilde{y} = 1 - \tilde{x}$.
(c) $\Theta_2$ needs to be obtained in the triangular region with the boundary conditions

$$\begin{array}{lll} \tilde{x} = 0 : & \Theta_2 = 0, & 0 < \tilde{x} < 1 \\ \tilde{y} = 0 : & \Theta_2 = 0, & 0 < \tilde{y} < 1 \\ \tilde{y} = 1 - \tilde{x} : & \Theta_2 = \tilde{x} - \tilde{x}^2 \end{array}$$

(d) For this function one obtains $\Theta_2 = \tilde{x}\tilde{y}$. Thus, the complete solution of the problem is given by: $\Theta = \Theta_1 + \Theta_2 = \tilde{x} + \tilde{y} + \tilde{x}\tilde{y}$

# Chapter 2

## Problem 2-1

(a) A = 4, B = 5/2, C = 1, the equation is of hyperbolic type
(b) From the characteristic equations we obtain the two characteristics

$$y - x = C_1 = \xi$$

$$y - \frac{x}{4} = C_2 = \eta$$

(c) The standard form of the partial differential equation is

$$\frac{\partial^2 u}{\partial \xi \partial \eta} = \frac{1}{3}\frac{\partial u}{\partial \eta} - \frac{8}{9}$$

(d) The general solution is given by

$$u = g(\eta)\exp(\xi/3)\frac{8}{3}\eta + f(\xi)$$

where g and f are arbitrary functions.

**Problem 2-2**

(a) Inserting $u = F(x)G(y)$ into the equation results in

$$-x\frac{F''}{F} - \frac{1}{2}\frac{F'}{F} = -y\frac{G''}{G} - A(x,y)\frac{G'}{G} = \text{const.}$$

From this equation, one can conclude that

$$A(x,y) = f(y)$$

(b) $A = -x$, $B = 0$, $C = y$ and $B^2 - AC = 4xy$
This shows that the partial differential equation has the following type

| | | |
|---|---|---|
| $y > 0$: | $x < 0$: | elliptic |
| $y > 0$: | $x > 0$: | hyperbolic |
| $y < 0$: | $x < 0$: | hyperbolic |
| $y < 0$: | $x > 0$: | elliptic |
| $x = 0$ or | $y = 0$: | parabolic |

(c) The characteristics are given by

$$\xi = 2(y^{1/2} - x^{1/2}), \quad \eta = 2(y^{1/2} + x^{1/2})$$

With $A(x, y) = -1/2$, and after introducing the characteristic coordinates, the partial differential equation can be transformed into

$$\frac{\partial^2 u}{\partial \xi \partial \eta} - \frac{1}{(\xi + \eta)}\left(\frac{\partial u}{\partial \eta} + \frac{\partial u}{\partial \eta}\right) = 0$$

## Problem 2-3

(a)  $A = 1$, $B = 5/2$, $C = 4$

$B^2 - AC = 25/4 - 4 = 9/4 > 0$. Thus, the equation is of hyperbolic type

(b)  The characteristics are given by

$$\xi = y - 4x, \quad \eta = y - x$$

(c)  Introducing the new coordinates into the partial differential equation results in

$$-9\frac{\partial^2 u}{\partial \xi \partial \eta} + 10\frac{\partial u}{\partial \xi} + 10\frac{\partial u}{\partial \eta} = \sin(-1/3(\xi - \eta))$$

## Problem 2-4

(a)  We are introducing the following dimensionless quantities

$$\tilde{x} = \frac{x}{a}, \tilde{y} = \frac{y}{b}, \; \Theta = \frac{T - T_1}{T_1}$$

into the partial differential equation and into the boundary conditions.
This results in

$$\frac{\partial^2 \Theta}{\partial \tilde{x}^2} + \left(\frac{a}{b}\right)^2 \frac{\partial^2 \Theta}{\partial \tilde{y}^2} = 0$$

This problem has to be solved together with the following boundary conditions

$$\Theta(0, \tilde{y}) = 0$$
$$\Theta(1, \tilde{y}) = \sin^3(2\pi\tilde{y})$$
$$\Theta(\tilde{x}, 0) = 0$$
$$\Theta(\tilde{x}, 1) = 0$$

(b)  Introducing the following expression for the temperature field

$$\Theta(\tilde{x}, \tilde{y}) = F(\tilde{x})G(\tilde{y})$$

results in the following distribution for the temperature

$$\Theta(\tilde{x}, \tilde{y}) = \frac{3}{4\sinh(2\pi a/b)}\sinh(\frac{2\pi a}{b}\tilde{x})\sin(2\pi\tilde{y})$$
$$- \frac{1}{4\sinh(6\pi a/b)}\sinh(\frac{6\pi a}{b}\tilde{x})\sin(6\pi\tilde{y})$$

**Problem 2-5**

(a) Introducing the dimensionless quantities into the partial differential equation and into the boundary conditions results in

$$\frac{\partial \Theta}{\partial \tilde{t}} = \frac{\partial^2 \Theta}{\partial \tilde{x}^2}$$

and the following boundary conditions

$$\tilde{t} = 0 : \Theta = 1$$

$$\tilde{x} = 0 : \text{Bi}_G \, \Theta(0, \tilde{t}) - \left.\frac{\partial \Theta}{\partial \tilde{x}}\right|_{\tilde{x}=0} = 0$$

$$\tilde{x} = 1 : \text{Bi}_C(\Theta(0, \tilde{t}) - \Theta_C) + \left.\frac{\partial \Theta}{\partial \tilde{x}}\right|_{\tilde{x}=1} = 0, \quad \Theta_C = \frac{T_C - T_G}{T_i - T_G}$$

(b) The temperature distribution shall be split into the steady-state temperature distribution and into the transient part: $\Theta = \Theta_s + \Theta_t$, whereas the steady-state temperature is obtained from

$$\frac{\partial^2 \Theta_s}{\partial \tilde{x}^2} = 0$$

with the boundary conditions

$$\tilde{x} = 0 : \text{Bi}_G \, \Theta_s(0) - \left.\frac{\partial \Theta_s}{\partial \tilde{x}}\right|_{\tilde{x}=0} = 0$$

$$\tilde{x} = 1 : \text{Bi}_C \, (\Theta_s(1) - \Theta_C) + \left.\frac{\partial \Theta_s}{\partial \tilde{x}}\right|_{\tilde{x}=1} = 0$$

For the transient temperature distribution the following problem has to be solved

$$\frac{\partial \Theta_t}{\partial \tilde{t}} = \frac{\partial^2 \Theta_t}{\partial \tilde{x}^2}$$

with the boundary conditions

$$\tilde{t} = 0 : \Theta_t = 1 - \Theta_s$$

$$\tilde{x} = 0 : \text{Bi}_G \, \Theta_t(0, \tilde{t}) - \left.\frac{\partial \Theta_t}{\partial \tilde{x}}\right|_{\tilde{x}=0} = 0$$

$$\tilde{x} = 1 : \text{Bi}_C \, \Theta_t(1, \tilde{t}) + \left.\frac{\partial \Theta_t}{\partial \tilde{x}}\right|_{\tilde{x}=1} = 0$$

(c) Solving for the steady-state temperature distribution in the slab results in

$$\Theta_s(\tilde{x}) = \frac{\Theta_C Bi_C}{Bi_G(1 + Bi_C) + Bi_C}(1 + Bi_G\tilde{x})$$

(d) The temperature distribution for the transient part is given by

$$\Theta_t = \sum_{n=1}^{\infty} C_n \left\{ \cos(\lambda_n\tilde{x})\frac{Bi_G}{\lambda_n}\sin(\lambda_n\tilde{x}) \right\} \exp(-\lambda_n^2\tilde{t})$$

The unknown coefficients $C_n$ can be evaluated by applying the solution to the boundary condition for $\tilde{t} = 0$

$$A + B\tilde{x} = \sum_{n=1}^{\infty} C_n \left\{ \cos(\lambda_n\tilde{x}) + \frac{Bi_G}{\lambda_n}\sin(\lambda_n\tilde{x}) \right\} = \sum_{n=1}^{\infty} C_n X_n(\tilde{x}), \ \tilde{t} = 0$$

From this equation, the unknown constants can be determined to be

$$C_n = \frac{\int_0^1 (A + B\tilde{x})X_n(\tilde{x})\mathrm{d}\tilde{x}}{\int_0^1 X_n^2(\tilde{x})\mathrm{d}\tilde{x}}$$

The complete solution of the problem is finally given by summing up the transient part and the steady-state solution.

**Problem 2-6**

(a) We introduce the following dimensionless quantities

$$\tilde{x} = \frac{x}{l}, \quad \tilde{t} = \frac{at}{l^2}, \quad \Theta = \frac{T - T_1}{T_2 - T_1}$$

into the partial differential equation and the boundary conditions. This results in

$$\frac{\partial\Theta}{\partial\tilde{t}} = \frac{\partial^2\Theta}{\partial\tilde{x}^2} + \tilde{x}B$$
$$\Theta(0, \tilde{x}) = \tilde{x} - 1$$
$$\Theta(\tilde{t}, 0) = 0$$
$$\Theta(\tilde{t}, 1) = 1$$

(b) In order to solve the above given problem, the problem will be split into two simpler problems. The first one will give the steady-state solution of the

problem, while the second problem will focus on the transient behaviour. Thus, the solution will be given by $\Theta = \Theta_s + \Theta_t$

First problem

$$\frac{\partial^2 \Theta_s}{\partial \tilde{x}^2} = -\tilde{x}B$$

$$\Theta_s(0) = 0$$

$$\Theta_s(1) = 1$$

Second problem

$$\frac{\partial \Theta_t}{\partial \tilde{t}} = \frac{\partial^2 \Theta_t}{\partial \tilde{x}^2}$$

$$\Theta_t(0, \tilde{x}) = \tilde{x} - 1 - \Theta_s(\tilde{x})$$

$$\Theta_t(\tilde{t}, 0) = 0$$

$$\Theta_t(\tilde{t}, 1) = 0$$

(c) The solution of the steady-state problem can easily be obtained:

$$\Theta_s(\tilde{x}) = \frac{1}{6}B(\tilde{x} - \tilde{x}^3) + \tilde{x}$$

For the second problem, the following partial differential equation has to be solved

$$\frac{\partial \Theta_t}{\partial \tilde{t}} = \frac{\partial^2 \Theta_t}{\partial \tilde{x}^2}$$

$$\Theta_t(0, \tilde{x}) = \tilde{x} - 1 - \Theta_s(\tilde{x}) = \frac{1}{6}B(\tilde{x}^3 - \tilde{x}) - 1$$

$$\Theta_t(\tilde{t}, 0) = 0$$

$$\Theta_t(\tilde{t}, 1) = 0$$

One obtains as solution for this problem

$$\Theta_t = \sum_{n=1}^{\infty} D_n \sin(n\pi\tilde{x}) \exp(-(n\pi)^2 \tilde{t})$$

$$D_n = \frac{\int_0^1 \left(\frac{1}{6}B(\tilde{x}^3 - \tilde{x}) - 1\right) \sin(n\pi\tilde{x}) d\tilde{x}}{\int_0^1 \sin^2(n\pi\tilde{x}) d\tilde{x}}$$

**Problem 2-7**

(a) In case of rotational symmetry, the derivatives with respect to $\partial/\partial\varphi$ and $\partial/\partial\Psi$ are identical to zero. This leads to

$$\rho c \frac{\partial T}{\partial t} = \frac{k}{r^2} \frac{\partial}{\partial r} \left( r^2 \frac{\partial T}{\partial r} \right) + \dot{q}_{i0}$$

The boundary conditions are given by

$$t = 0 : T = T_i$$
$$r = R : T = T_0$$
$$r = 0 : T = finite$$

(b) Introducing the new function $T(r,t) = U(r,t)/r$ results in

$$\frac{\partial U}{\partial t} = a \frac{\partial^2 U}{\partial r^2} + r \frac{\dot{q}_{i0}}{\rho c}$$

with the resulting boundary conditions

$$t = 0 : U = T_i r$$
$$r = R : U = T_0 R$$
$$r = 0 : U = 0$$

(c) Introducing the following dimensionless quantities

$$\tilde{r} = \frac{r}{R}, \tilde{t} = \frac{at}{R^2}, \Theta = \frac{U}{RT_0} - \frac{r}{R}$$

leads to

$$\frac{\partial\Theta}{\partial\tilde{t}} = \frac{\partial^2\Theta}{\partial\tilde{r}^2} + \tilde{r}\tilde{q}_i, \quad \tilde{q}_i = \frac{\dot{q}_{i0}R^2}{kT_0}$$
$$\tilde{t} = 0 : \Theta \frac{T_i}{T_0}\tilde{r} = \tilde{r}$$
$$\tilde{r} = 1 : \Theta = 0$$
$$\tilde{r} = 0 : \Theta = 0$$

(d) We split the solution into a transient part and into a steady-state part.

$$\Theta = \Theta_s + \Theta_t$$

For the two temperature distributions, the following equations have to be solved

$$\frac{\partial^2 \Theta_s}{\partial \tilde{r}^2} = -\tilde{r}\tilde{q}_i$$

$$\tilde{r} = 1 : \Theta_s = 0$$

$$\tilde{r} = 0 : \Theta_s = 0$$

$$\frac{\partial \Theta_t}{\partial \tilde{r}} = \frac{\partial^2 \Theta_t}{\partial \tilde{r}^2}$$

$$\tilde{t} = 0 : \Theta = \frac{T_i}{T_0}\tilde{r} - \tilde{r} - \Theta_s(\tilde{r})$$

$$\tilde{r} = 1 : \Theta = 0$$

$$\tilde{r} = 0 : \Theta = 0$$

The solution of the steady-state temperature distribution is given by

$$\Theta_s = -\frac{\tilde{q}_i}{6}\left(\tilde{r}^3 - \tilde{r}\right)$$

The method of separation of variables leads for the second problem to

$$\Theta_t = \sum_{n=1}^{\infty} A_n \sin(n\pi\tilde{r}) \exp(-(n\pi)^2\tilde{t})$$

where the constants $A_n$ have to be determined by satisfying the boundary condition for $\tilde{t} = 0$. This leads to

$$A_n = \frac{\int_0^1 \sin(n\pi\tilde{r})\left\{\frac{T_i}{T_0}\tilde{r} - \tilde{r} - \Theta_s(\tilde{r})\right\}d\tilde{r}}{\int_0^1 \sin^2(n\pi\tilde{r})}$$

Thus, the complete solution is given by

$$\Theta = \frac{\tilde{q}_i}{6}\left(\tilde{r}^3 - \tilde{r}\right) + \sum_{n=1}^{\infty} A_n \sin(n\pi\tilde{r}) \exp(-(n\pi)^2\tilde{t})$$

(e) The temperature distribution is given by

$$\frac{T(\tilde{r},\tilde{t})}{T_0} = 1 + \tilde{r}^{-1}\left\{\frac{\tilde{q}_i}{6}\left(\tilde{r}^3 - \tilde{r}\right) + \sum_{n=1}^{\infty} A_n \sin(n\pi\tilde{r}) \exp(-(n\pi)^2\tilde{t})\right\}$$

**Problem 2-8**

(a) Using the given characteristics leads to

$$\bar{A} = 4A - 2B + C = 0$$
$$\bar{C} = 4A + 2B + C = 0$$

From these equations one obtains with $A = 1$: $B = 0$, $C = -4$. Thus, one obtains for the partial differential equation

$$\frac{\partial^2 u}{\partial x^2} - 4\frac{\partial^2 u}{\partial y^2} = -8xy$$

(b) The coefficient $B^*$ in the given equation, can be calculated from Eq. (2.17) to be

$$\bar{B} = A\frac{\partial \xi}{\partial x}\frac{\partial \eta}{\partial x} + B\left(\frac{\partial \xi}{\partial x}\frac{\partial \eta}{\partial y} + \frac{\partial \xi}{\partial y}\frac{\partial \eta}{\partial x}\right) + C\frac{\partial \xi}{\partial y}\frac{\partial \eta}{\partial y}$$
$$= -8 - 8 = -16$$

(c) The general solution of the equation is given by

$$u(\xi, \eta) = -\frac{1}{48}\xi^3 \eta + \frac{1}{48}\eta^3 \xi + f(\xi) + g(\eta)$$

**Problem 2-9**

(a) For $m = 0$, the equation is parabolic, for $m < 0$ the equation is of elliptic type and for $m > 0$ the equation is of hyperbolic type. For $m = 0$ one obtains

$$\frac{\partial^2 u}{\partial x^2} = 2xy$$

(b) The general solution of this equation can be found by twice integrating the equation. One obtains

$$u = \frac{1}{3}x^3 y + h(y) + g(y)x$$

(c) The solution of the problem is given by

$$u = \frac{1}{3}x^3 y + y^2 + yx$$

# Chapter 3

## Problem 3-1

(a) In order to show that the eigenvalue problem is self-adjoint and positive definite, we have to show that

$$\langle v, w \rangle = \langle w, v \rangle, \quad (v, w) = (w, v) \tag{3.32}$$

$$\langle v, v \rangle > 0, \quad (v, v) > 0 \tag{3.33}$$

are satisfied. We insert the expressions into the definitions

$$\langle v, w \rangle = -\int_0^1 vw'' d\tilde{n} = -\int_0^1 v''w \, d\tilde{n} = \langle w, v \rangle$$

$$\Rightarrow \int_0^1 (vw'' - wv'')d\tilde{n} = \int_0^1 (vw' - wv')' d\tilde{n} = (vw' - wv')|_0^1 = 0$$

$$(v, w) = \int_0^1 vw d\tilde{n} = \int_0^1 wv d\tilde{n} = (w, v)$$

and see that this is fulfilled. In order to show that the problem is also positive definite, one has to show that

$$\langle v, v \rangle > 0, \quad (v, v) > 0 \tag{3.33}$$

which leads to

$$\langle v, v \rangle = -\int_0^1 vv'' d\tilde{n} = -(vv')|_0^1 + \int_0^1 v'v' d\tilde{n} = \int_0^1 (v')^2 d\tilde{n} > 0,$$

$$(v, v) = \int_0^1 v^2 d\tilde{n} > 0 \tag{3.33}$$

(b) We consider the two eigenvalue problems

$$Y_n'' + \lambda_n^2 Y_n = 0$$
$$Y_m'' + \lambda_m^2 Y_m = 0$$

The first equation will be multiplied by $Y_m$ and the second equation with $Y_n$. This leads after subtraction and integration between zero and one to

$$\int\limits_0^1 Y_n'' Y_m d\tilde{n} - \int\limits_0^1 Y_n'' Y_n d\tilde{n} = -(\lambda_n^2 - \lambda_m^2) \int\limits_0^1 Y_m Y_n d\tilde{n}$$

$$\Rightarrow 0 = -(\lambda_n^2 - \lambda_m^2) \int\limits_0^1 Y_m Y_n d\tilde{n}$$

(c) The solution of the problem is given by

$$Y_j(\tilde{n}) = \cos(\lambda_j \tilde{n}), \quad \lambda_j = j\pi, \ j = 1, 2, 3, \ldots$$

## Problem 3-2

Show that the following eigenvalue problem is self-adjoint and positive definite

$$\left(1 + \tilde{y}^2\right)\lambda_n \Phi_n + \Phi_n'' = 0$$
$$\Phi_n(0) = \Phi_n(1) = 0$$

In order to show that the eigenvalue problem is self-adjoint, we have to show that

$$\langle v, w \rangle = \langle w, v \rangle, \quad (v, w) = (w, v) \tag{3.32}$$

We insert the expressions in the definitions

$$\langle v, w \rangle = -\int\limits_0^1 vw'' d\tilde{n} = -\int\limits_0^1 v'' w \, d\tilde{n} = \langle w, v \rangle$$

$$\Rightarrow \int\limits_0^1 (vw'' - wv'') d\tilde{n} = \int\limits_0^1 (vw' - wv')' d\tilde{n} = (vw' - wv')|_0^1 = 0$$

$$(v, w) = \int\limits_0^1 v(1 + \tilde{n}^2) w d\tilde{n} = \int\limits_0^1 wv(1 + \tilde{n}^2) d\tilde{n} = (w, v)$$

and see that this is fulfilled. In order to show that the problem is also positive definite, one has to show that

$$\langle v, v \rangle > 0, \quad (v, v) > 0 \tag{3.33}$$

which leads to

$$\langle v, v \rangle = -\int_0^1 vv''\,d\tilde{n} = -(vv')|_0^1 + \int_0^1 v'v'\,d\tilde{n} = \int_0^1 (v')^2\,d\tilde{n} > 0,$$

(3.33)

$$(v, v) = \int_0^1 (1 + \tilde{n}^2)v^2\,d\tilde{n} > 0$$

Show that the following eigenvalue problem is self-adjoint and positive definite

$$\tilde{r}R_n'' + R_n' + \lambda_n^2 \tilde{r} R_n = 0$$
$$R'(0) = R(1) = 0$$

Let us first rewrite the problem

$$-\left(\tilde{r}R_n'\right)' = \lambda_n^2 \tilde{r} R_n$$
$$R'(0) = R(1) = 0$$

Thus

$$L[v] = -\frac{d}{d\tilde{r}}\left(\tilde{r}\frac{dv}{d\tilde{r}}\right)$$

$$M[v] = \tilde{r}v, \quad \bar{\lambda}_n = \lambda_n^2$$

See the proof shown in Chap. 3.
Show that the following eigenvalue problem is self-adjoint and positive definite

$$\left(1 - \tilde{x}^2\right)Y_n'' - 2\tilde{x}Y_n' + \lambda_n(\lambda_n + 1)Y_n = 0$$
$$Y_n(0) = Y_n(1) = 0$$

Let us first rewrite the problem

$$-\left[\left(1 - \tilde{x}^2\right)Y_n'\right] = \lambda_n(\lambda_n + 1)Y_n$$
$$Y_n(0) = Y_n(1) = 0$$

Thus

$$L[v] = -\frac{d}{d\tilde{x}}\left((1 - \tilde{x})\frac{dv}{d\tilde{x}}\right)$$
$$M[v] = v, \quad \bar{\lambda}_n = \lambda_n(\lambda_n + 1)$$

See the proof shown in Chap. 3.

## Problem 3-3

(a) Introducing the dimensionless quantities results in

$$\frac{\partial \Theta}{\partial \tilde{x}} = \frac{\partial^2 \Theta}{\partial \tilde{y}^2}$$

with the boundary conditions

$$\tilde{x} = 0 : \Theta = 1$$

$$\tilde{y} = 0 : \frac{\partial \Theta}{\partial \tilde{y}} = 0, \quad \tilde{y} = 1 : \Theta = 0$$

(b) Inserting the expression $\Theta = f(\tilde{x})g(\tilde{y})$ into the partial differential equation results in

$$\frac{f'}{f} = \frac{g''}{g} = -\lambda^2$$

(c) Solving these ordinary differential equations results in

$$f(\tilde{x}) = C_1 \exp(-\lambda^2 \tilde{x})$$
$$g(\tilde{y}) = C_2 \cos(\lambda \tilde{y}) + C_3 \sin(\lambda \tilde{y})$$

(d) For the temperature field one obtains

$$\Theta = \sum_{n=1}^{\infty} A_n \cos(\lambda_n \tilde{y}) \exp(-\lambda_n^2 \tilde{x})$$

with

$$A_n = \frac{\int_0^1 \cos(\lambda_n \tilde{y}) d\tilde{y}}{\int_0^1 \cos^2(\lambda_n \tilde{y}) d\tilde{y}} = \frac{2 \sin \lambda_n}{\lambda_n + \sin \lambda_n \cos \lambda_n}; \quad \lambda_n = \frac{2n - 1}{2} \pi; \quad n = 1, 2, 3, \ldots$$

## Problem 3-4

(a) The energy equation for this problem is given in dimensionless form (by using the following dimensionless quantities)

$$\tilde{x} = \frac{x}{h} \frac{a}{\bar{u}h} = \frac{x}{h} \frac{1}{\mathrm{Re}_h \, \mathrm{Pr}}, \quad \tilde{y} = \frac{y}{h}, \quad \Theta = \frac{T - T_0}{\dot{q}_w h/k}, \quad \tilde{u} = \frac{u}{\bar{u}} = \frac{3}{2}(1 - \tilde{y}^2)$$

by

$$\tilde{u}\frac{\partial \Theta}{\partial \tilde{x}} = \frac{\partial^2 \Theta}{\partial \tilde{y}^2}$$

with the boundary conditions

$$\tilde{x} = 0 : \Theta = 1$$

$$\tilde{y} = 0 : \frac{\partial \Theta}{\partial \tilde{y}} = 0, \quad \tilde{y} = 1 : \frac{\partial \Theta}{\partial \tilde{y}} = -1$$

Because the temperature distribution for large axial values should be calculated, the boundary condition for $\tilde{x} = 0$ can not be satisfied and will be omitted. Carrying out an energy balance as given by Eq. (3.122) for the present case results in

$$-\tilde{x} = \int_0^1 \tilde{u}\Theta \, dy$$

From this equation we see that the temperature distribution for large axial values has the form

$$\Theta = C_1\tilde{x} + \Psi(\tilde{y})$$

Thus, the temperature distribution for large axial values is given by

$$\Theta = -\tilde{x} - \frac{3}{4}\tilde{y}^2 + \frac{1}{8}\tilde{y}^4 + \frac{39}{280}$$

(b) The Nusselt number for the fully developed flow can be calculated by using the above given temperature distribution

$$\text{Nu}_D = \frac{D\frac{\partial T}{\partial y}\big|_{y=0}}{T_W - T_b} = \frac{\frac{-\dot{q}_w}{k}(4h)}{T_W - T_b} = \frac{-4}{\Theta(\tilde{x}, 1) - \Theta_b}$$

The bulk-temperature is given in dimensionless form by

$$\Theta_b = \int_0^1 \tilde{u}\Theta d\tilde{y} = -\tilde{x}$$

Inserting the above temperature distribution and the distribution for the bulk-temperature into the definition of the Nusselt number leads to

$$\mathrm{Nu}_D = \frac{4}{17/35} = \frac{140}{17} = 8.2353$$

(c) In order to obtain the solution for the complete problem, we split the temperature distribution into two parts

$$\Theta = \Theta_1 + \Theta_2$$

Here, $\Theta_1$ is the temperature distribution for large axial values, which already has been obtained. For $\Theta_2$ we have to solve the following problem

$$\tilde{u}\frac{\partial\Theta_2}{\partial\tilde{x}} = \frac{\partial^2\Theta_2}{\partial\tilde{y}^2}$$

with the boundary conditions

$$\tilde{x} = 0: \quad \Theta_2 = -\Theta_1(\tilde{x} = 0)$$

$$\tilde{y} = 0: \quad \frac{\partial\Theta_2}{\partial\tilde{y}} = 0, \qquad \tilde{y} = 1: \quad \frac{\partial\Theta_2}{\partial\tilde{y}} = 0$$

Using the method of separation of variables, one obtains for $\Theta_2$

$$\Theta_2 = \sum_{j=0}^{\infty} A_j\Phi_j(\tilde{y})\exp(-\lambda_j^2\tilde{x}), \quad A_j = \frac{-\int_0^1 \Theta_1(\tilde{x} = 0)\Theta_j\tilde{u}d\tilde{y}}{\int_0^1 \Theta_j^2\tilde{u}d\tilde{y}}$$

Thus

$$\Theta = -\tilde{x} + \frac{1}{8}\tilde{y}^4 - \frac{3}{4}\tilde{y}^2 + \sum_{j=0}^{\infty} A_j\Theta_j(\tilde{y})\exp(-\lambda_j^2\tilde{x})$$

## Problem 3-5

(a) Simplifying the energy equation for this problem leads after introduction of the following dimensionless quantities

$$\tilde{y} = \frac{y}{h}, \; \tilde{x} = \frac{x}{h}, \tilde{u} = \frac{u}{u_\infty}, \; \Theta = \frac{T - T_0}{\dot{q}_w h/k}$$

to

$$(1 - \tilde{y})\frac{\partial \Theta}{\partial \tilde{x}} = \frac{1}{\text{Pe}_h}\left(\frac{\partial^2 \Theta}{\partial \tilde{x}^2} + \frac{\partial^2 \Theta}{\partial \tilde{y}^2}\right), \quad \text{Pe}_h = \frac{u_\infty h}{a}$$

with the boundary conditions

$$\tilde{y} = 0 : \frac{\partial \Theta}{\partial \tilde{y}} = 0$$

$$\tilde{y} = 1 : \frac{\partial \Theta}{\partial \tilde{y}} = -1$$

(b) The integral energy balance takes the following form after inserting the dimensionless quantities

$$-\tilde{x}\frac{1}{\text{Pe}_h} = \int_0^1 (1 - \tilde{y})\Theta \, dy$$

From this equation we see that the temperature distribution for large axial values has the form

$$\Theta = C_1 \tilde{x} + \Psi(\tilde{y})$$

(c) Inserting this expression into the partial differential equation and into the boundary conditions results in

$$\Theta = \frac{-2}{\text{Pe}_h}\tilde{x} - \tilde{y}^2 + \frac{1}{3}\tilde{y}^3 + \frac{2}{15}$$

(d) The Nusselt number can be calculated from its definition

$$|\text{Nu}_h| = \left|\frac{h\frac{\partial T}{\partial y}\big|_{y=h}}{T(y=0) - T(y=h)}\right| = \left|\frac{\frac{-\dot{q}_w}{k}h}{T(y=0) - T(y=h)}\right|$$

$$= \frac{1}{\Theta(\tilde{y}=0) - \Theta(\tilde{y}=1)}$$

Using the temperature distribution which has been calculated above, one obtains

$$|\text{Nu}_h| = \frac{3}{2}$$

**Problem 3-6**

(a)  The energy equation and the boundary conditions are given by

$$\rho c_p u(y)\frac{\partial T}{\partial x} = \lambda \frac{\partial^2 T}{\partial y^2}$$

$$y = 0 : \frac{\partial T}{\partial y} = 0, \ \text{adiabatic wall}$$

$$y = t_F : -\lambda \frac{\partial T}{\partial y} = \dot{q}_s = \text{const.}$$

$$x = 0 : T = T_0$$

(b)  Introducing the above given dimensionless quantities leads to

$$\tilde{u}\frac{\partial \Theta}{\partial \tilde{x}} = \frac{\partial^2 \Theta}{\partial \tilde{y}^2}$$

$$\tilde{y} = 0 : \frac{\partial \Theta}{\partial \tilde{y}} = 0, \quad \tilde{y} = 1 : -\frac{\partial \Theta}{\partial \tilde{y}} = 1,$$

$$\tilde{x} = 0 : \Theta = 0$$

(c)  Carrying out an energy balance similar to the one in Sect. 3.3.2 one obtains

$$-\tilde{x} = \int_0^1 \tilde{u}\Theta d\tilde{y}$$

The temperature distribution is given by

$$\Theta = -\frac{3}{2}\tilde{x} + \Psi(\tilde{r})$$

with

$$\Psi = -\frac{1}{2}\tilde{y}^3 + \frac{1}{8}\tilde{y}^4 + \frac{39}{280}$$

(d)  The Nusselt number is defined by (see Eq. 3.64)

$$Nu_D = \frac{D\frac{\partial T}{\partial y}\big|_{y=t_F}}{T(y=t_F) - T_b}, \quad D = 2t_F$$

Introducing the dimensionless quantities results in

$$Nu_D = \frac{2}{\Theta(\tilde{y} = 1) - \Theta_b} = \frac{280}{33}$$

(e) The complete solution can be obtained as a sum of two parts

$$\Theta = \Theta_1 + \Theta_2$$

where $\Theta_1$ denotes the already predicted solution for large axial values. The describing equation for $\Theta_2$ is given by

$$\tilde{u}\frac{\partial \Theta_2}{\partial x} = \frac{\partial^2 \Theta_2}{\partial \tilde{y}^2}$$

$$\tilde{y} = 0 : \frac{\partial \Theta_2}{\partial \tilde{y}} = 0, \quad \tilde{y} = 1 : -\frac{\partial \Theta_2}{\partial \tilde{y}} = 1$$

$$\tilde{x} = 0 : \Theta_2 = -\Theta_1$$

Using the method of separation of variables one obtains

$$\Theta_2 = \sum_{j=0}^{\infty} A_j \Phi_j(\tilde{y}) \exp\left(-\lambda_j^2 \tilde{x}\right)$$

$$A_j = \frac{-\int_0^1 \Theta_1(\tilde{x} = 0)\Phi_j \tilde{u} d\tilde{y}}{\int_0^1 \Phi_j^2 \tilde{u} d\tilde{y}}$$

The complete solution of the problem is given by $\Theta = \Theta_1 + \Theta_2$.

**Problem 3-7**

(a) The eigenvalue problem is self-adjoint, if $\langle v, w \rangle = \langle w, v \rangle$, $(v, w) - (w, v)$
The second condition

$$(v, w) = \int_0^1 v r^2 w dr = \int_0^1 w r^2 v dr = (w, v)$$

is satisfied. The first condition leads to $\langle v, w \rangle - \langle w, v \rangle = 0$. This leads to

$$\int_0^1 w \frac{d}{dr}\left(r^2 \frac{dv}{dr}\right) - v \frac{d}{dr}\left(r^2 \frac{dw}{dr}\right) dr = \int_0^1 \left[wr^2 v' - vr^2 w'\right]' dr = 0$$

Evaluating the above given integral gives

$$\left[wr^2v' - vr^2w'\right]_0^1 = w(1)v'(1) - v(1)w'(1) = 0$$

Thus, the problem is self-adjoint. In order to show that the problem is also positive definite, one has to show that $\langle v, v \rangle$ and $(v, v) > 0$

$$(v, v) = \int_0^1 v^2 r^2 dr > 0$$

$$\langle v, v \rangle = -\int_0^1 v \frac{d}{dr}\left(r^2 \frac{dr}{dr}\right) dr = \int_0^1 v' r^2 v' dr > 0$$

(b) It can be shown that the eigenfunctions form an orthogonal set of functions

$$\lambda_j^2 - \lambda_i^2 \int_0^1 \Phi_i M[\Phi_i] d\tilde{n} = 0$$

Using the operator from above, one finally obtains

$$\int_0^1 r^2 \Phi_i \Phi_j d\tilde{n} = 0, \quad \text{for } i \neq j$$

(c) $f(r) = 1$ should be developed in a series:

$$f(r) = 1 = \sum_{j=0}^{\infty} A_j \Phi_j(r)$$

From Eq. (3.54) one obtains

$$A_j = \frac{\int_0^1 r^2 1 \Phi_j(r) dr}{\int_0^1 r^2 \Phi_j^2(r) dr}$$

(d) Inserting $\Phi_n = h_n/r$ into the eigenvalues problem results in

$$h_n'' + \lambda_n^2 h_n = 0$$

The boundary conditions transform to

$$r \to 0 : r^2 \left( \frac{1}{r} h_n \right)' = 0, \quad -h_n + r h'_n = 0$$

$$r = 1 : h_n = 0$$

(e) From the solution of the above given eigenvalue problem one obtains

$$h_n = C_1 \cos(\lambda_n r) + C_1 \sin(\lambda_n r)$$

From the boundary condition for $r \to 0$ it follows that $C_{1n} = 0$. From the second boundary condition for $r = 1$ follows that

$$0 = C_{2n} \sin(\lambda), \quad \lambda_n = n\pi, \quad n = 1, 2, 3, \ldots$$

Thus, the eigenfunctions are given by

$$h_n = C_n \sin(\lambda_n r), \quad \Phi_n = \frac{1}{r} C_n \sin(\lambda_n r)$$

(f) The constants in (c) have been given by

$$A_j = \frac{\int_0^1 r^2 \, 1 \, \Phi_j(r) dr}{\int_0^1 r^2 \Phi_j^2(r) dr} = \frac{\frac{-1}{\lambda_j}(-1)^n}{\frac{1}{2}}$$

Evaluating the integrals leads to

$$1 = \sum_{j=1}^{\infty} \left( 2 \frac{-(-1)}{j\pi} \right) \frac{1}{r} \sin(j\pi r)$$

# Chapter 4

## Problem 4-1

It might be more convenient to show that from Eqs. (4.11) and (4.12) the above given problem can be obtained. Let us start with Eqs. (4.11) and (4.12)

$$\frac{d^2 \vartheta}{d\xi^2} + \left[ k^2 - w(\xi) \right] \vartheta = 0 \tag{4.11}$$

$$\xi = 0 : \vartheta(0) = 0$$
$$\xi = \pi : \vartheta(\pi) = 0 \tag{4.12}$$

with the quantities

$$G = \frac{1}{\pi} \int_0^1 \sqrt{\frac{\tilde{u}}{2a_2}} d\bar{r}, \quad k = \sqrt{2}\lambda_j G, \quad \xi = \frac{1}{G} \int_0^{\bar{r}} \sqrt{\frac{\tilde{u}}{2a_2}} d\bar{r} \qquad (4.9)$$

$$\vartheta = \left(\frac{\tilde{r}^2 a_2 \tilde{u}}{2}\right)^{1/4} \Phi_j, \quad w(\xi) = \left(\frac{\tilde{r} a_2 \tilde{u}}{2}\right)^{-1/4} \frac{d^2}{d\xi^2} \left(\frac{\tilde{r}^2 a_2 \tilde{u}}{2}\right)^{1/4} \qquad (4.10)$$

For the second derivative of the new quantity $\vartheta$ one obtains

$$\frac{d^2\vartheta}{d\xi^2} = \frac{\frac{d\xi}{d\bar{r}}\frac{d^2\vartheta}{d\bar{r}^2} - \frac{d^2\xi}{d\bar{r}^2}\frac{d\vartheta}{d\bar{r}}}{\left(\frac{d\xi}{d\bar{r}}\right)^3}$$

with the expressions

$$\frac{d\xi}{d\xi} = \frac{1}{G}\sqrt{\frac{\tilde{u}}{2a_2}}, \frac{d^2\xi}{d\tilde{r}^2} = \frac{1}{2G}\left(\frac{\tilde{u}}{2a_2}\right)^{-1/2}\frac{d}{d\tilde{r}}\left(\frac{\tilde{u}}{2a_2}\right)$$

$$\frac{d\vartheta}{d\tilde{r}} = \frac{d}{dr}\left(\left(\frac{\tilde{r}^2 a_2 \tilde{u}}{2}\right)^{1/4}\Phi_j\right) = \Phi_j \frac{d}{d\tilde{r}}\left(\frac{\tilde{r}^2 a_2 \tilde{u}}{2}\right)^{1/4} + \left(\frac{\tilde{r}^2 a_2 \tilde{u}}{2}\right)^{1/4}\frac{d\Phi_j}{d\tilde{r}}$$

Using the abbreviation

$$b = \left(\frac{\tilde{r}^2 a_2 \tilde{u}}{2}\right)$$

one obtains

$$\frac{d^2\vartheta}{d\tilde{r}^2} = \frac{d}{d\tilde{r}}\frac{d\vartheta}{d\tilde{r}} = \frac{d\Phi_j}{d\tilde{r}}\frac{db^{1/4}}{d\tilde{r}} + \Phi_j\frac{d^2 b^{1/4}}{d\tilde{r}^2} + \frac{db^{1/4}}{d\tilde{r}}\frac{d\Phi_j}{d\tilde{r}} + b^{1/4}\frac{d^2\Phi_j}{d\tilde{r}^2}$$

From the above equations we obtain

$$\frac{d^2\vartheta}{d\tilde{\xi}^2} = \left\{2\frac{d\Phi_j}{d\tilde{r}}\frac{db^{1/4}}{d\tilde{r}} + \Phi_j\frac{d^2 b^{1/4}}{d\tilde{r}^2} + \frac{db^{1/4}}{d\tilde{r}}\frac{d\Phi_j}{d\tilde{r}}\right\} \Big/ \left(\frac{1}{G^2}\frac{\tilde{u}}{2a_2}\right)$$

$$- \frac{1}{2G}\left(\frac{\tilde{u}}{2a_2}\right)^{-1/2}\frac{d}{d\tilde{r}}\left(\frac{\tilde{u}}{2a_2}\right)\left\{\Phi_j\frac{d}{d\tilde{r}}\left(\frac{\tilde{r}^2 a_2 \tilde{u}}{2}\right)^{1/4} + \left(\frac{\tilde{r}^2 a_2 \tilde{u}}{2}\right)^{1/4}\frac{d\Phi_j}{d\tilde{r}}\right\}$$

$$\bullet \frac{1}{\frac{1}{G^3}\frac{\tilde{u}}{2a_2}\sqrt{\frac{\tilde{u}}{2a_2}}}$$

For the term $k^2 \vartheta$ one obtains

$$k^2 \vartheta = 2\lambda_j^2 G^2 b^{1/4} \Phi$$

and for $w(\xi)\vartheta$ one obtains

$$w(\xi)\vartheta = \Phi_j \frac{d^2 b^{1/4}}{d\xi^2}$$

This expression can be calculated similar to $d^2\vartheta/d\xi^2$ and one obtains

$$w(\xi)\vartheta = \Phi_j \frac{d^2 b^{1/4}}{d\tilde{r}^2} \Bigg/ \left(\frac{1}{G}\sqrt{\frac{\tilde{u}}{2a_2}}\right)^2 - \frac{1}{2}\frac{d}{d\tilde{r}}\left(\frac{\tilde{u}}{2a_2}\right)\frac{db^{1/4}}{d\tilde{r}}\Phi_j \Bigg/ \left(\frac{1}{G}\frac{\tilde{u}}{2a_2}\right)^2$$

Now inserting all above calculated terms into the eigenvalue problem for $\vartheta$ leads by recognizing that

$$a_2 = 1, \tilde{u} = 2\left(1 - \tilde{r}^2\right)$$

to the eigenvalue problem

$$\frac{d}{d\tilde{r}}\left[\tilde{r}\frac{d\Phi}{d\tilde{r}}\right] + \tilde{r}2(1 - \tilde{r}^2)\Phi_j = 0$$

**Problem 4-2**

This problem is solved by the computer code provided on the internet. Please have a look at the manual and at the calculated examples.

# Chapter 5

**Problem 5-1**

(a) Introducing the dimensionless quantities results in

$$\frac{\partial \Theta}{\partial \tilde{x}} = \frac{1}{Pe^2}\frac{\partial^2 \Theta}{\partial \tilde{x}^2} + \frac{\partial^2 \Theta}{\partial \tilde{y}^2}$$

with the boundary conditions

$$\tilde{x} = 0 : \Theta = 1$$

$$\tilde{y} = 0 : \frac{\partial \Theta}{\partial \tilde{y}} = 0$$

$$\tilde{y} = 1 : \Theta = 0$$

(b) For the case $Pe \to \infty$, the first term on the right hand side of the partial differential equation drops out and we obtain Problem 3.3.

(c) Inserting the expression $\Theta = f(\tilde{x})g(\tilde{y})$ into the partial differential equation and the boundary conditions results in the following ordinary differential equation

$$\frac{f'}{f} - \frac{1}{Pe^2}\frac{f''}{f} = -\lambda^2, \quad \frac{g''}{g} = -\lambda^2$$

(d) The temperature distribution is given by

$$\Theta = \sum_{n=1}^{\infty} D_n \cos(\lambda_n \tilde{y}) \exp(-C_{2n}\tilde{x})$$

with

$$D_n = \frac{2\sin(\lambda_n)}{\lambda_n + \sin(\lambda_n)\cos(\lambda_n)}; \quad \lambda_n = \frac{2n-1}{2}\pi; \quad n = 1, 2, 3, \ldots$$

(e) For small Peclet numbers the temperature distribution is changed because of the axial heat conduction effect within the flow.

(f) It was not physically correct to apply a boundary condition for $x = 0$, because the effect of axial heat conduction will normally influence this temperature profile. Therefore, it is only correct to prescribe a boundary condition for the temperature for $\tilde{x} \to -\infty$ in case of axial heat conduction effects.

## Problem 5-2

(a) Introducing the dimensionless quantities results in

$$\frac{\partial \Theta}{\partial \tilde{x}} = \frac{1}{Pe^2}\frac{\partial^2 \Theta}{\partial \tilde{x}^2} + \frac{\partial^2 \Theta}{\partial \tilde{y}^2}$$

with the boundary conditions

$$\lim_{\tilde{x}\to\infty} : \Theta = 1, \quad \lim_{\tilde{x}\to\infty} : \Theta = 0$$

$$\tilde{y} = 0 : \frac{\partial \Theta}{\partial \tilde{y}} = 0$$

$$\tilde{y} = 1 : \Theta = 0, \tilde{x} > 0 \quad \text{and} \quad \tilde{y} = 1 : \Theta = 1, \tilde{x} < 0$$

(b) The axial energy flow is given for the present problem by

$$E = \int_0^{\tilde{y}} \left[\Theta - \frac{1}{Pe^2}\frac{\partial \Theta}{\partial \tilde{x}}\right] d\bar{n}$$

With this definition, the following system of partial differential equations can be obtained

$$\frac{\partial}{\partial \tilde{x}} \vec{S}(\tilde{x}, \tilde{n}) = \underset{\sim}{L} \vec{S}(\tilde{x}, \tilde{n})$$

where the solution vector $\vec{S}$ and the matrix operator $\underset{\sim}{L}$ are defined by

$$\vec{S} = \begin{bmatrix} \Theta(\tilde{x}, \tilde{n}) \\ E(\tilde{x}, \tilde{n}) \end{bmatrix}, \qquad \underset{\sim}{L} = \begin{bmatrix} Pe^2 & -Pe^2 \frac{\partial}{\partial \tilde{y}} \\ \frac{\partial}{\partial \tilde{y}} & 0 \end{bmatrix}$$

The associated eigenvalue problem is given by

$$\Phi_{j1}'' + \left[ \frac{\lambda_j}{Pe^2} - 1 \right] \lambda_j \Phi_{j1} = 0$$

This equation has to be solved together with the homogenous boundary conditions

$$\Phi_{j1}'(0) = 0, \quad \Phi_{j1}(1) = 0$$

This eigenvalues problem has the solution

$$\Phi_{j1} = A_{j1} \cos(\gamma_j \tilde{y}), \quad \gamma_j = \sqrt{\frac{\lambda_j^2}{Pe^2} - \lambda_j} = \frac{2j-1}{2}\pi, \quad j = 1, 2, 3, \ldots$$

From the above relationship between $\gamma_j$ and the eigenvalues $\lambda_j$, the eigenvalues can be obtained

$$\lambda_j^+ = \frac{Pe^2}{2} + \sqrt{\gamma_j^2 + \left(\frac{Pe}{2}\right)^2}, \qquad \gamma_j = \frac{2j-1}{2}\pi, j = 1, 2, 3, \ldots$$

$$\lambda_j^- = \frac{Pe^2}{2} - \sqrt{\gamma_j^2 + \left(\frac{Pe}{2}\right)^2}$$

(c) The complete solution for the temperature field is given by Eqs. (5.41) and (5.43), where the above predicted eigenfunctions and eigenvalues have to be used

$$\tilde{x} \le 0 : \Theta(\tilde{x}, \tilde{y}) = 1 + \sum_{j=0}^{\infty} \frac{\Phi_{j2}^+(1)\Phi_{j1}^+(\tilde{y})}{\lambda_j^+ \left\| \Phi_j^+ \right\|^2} \exp\left(\lambda_j^+ \tilde{x}\right)$$

$$\tilde{x} > 0 : \Theta(\tilde{x}, \tilde{y}) = \sum_{j=0}^{\infty} \frac{\Phi_{j2}^-(1)\Phi_{j1}^-(\tilde{y})}{\lambda_j^- \left\| \Phi_j^- \right\|^2} \exp\left(\lambda_j^- \tilde{x}\right)$$

(d) Comparing the solution to the one of Problem 5.1 shows that for small Peclet numbers there is a substantial difference in the temperature field for $x/h = 1$. This is caused by the different boundary conditions used for both problems.

## Problem 5-3

The matrix operator $L$ is given for the heat transfer in a concentric annulus by (see also Weigand et al. 1993).

$$L = \begin{bmatrix} \frac{Pe_D^2 \tilde{u}(\tilde{r})}{a_1(\tilde{r})} & -\frac{Pe_D^2}{a_1(\tilde{n})[(1-\chi)\tilde{r}+\chi]}\frac{\partial}{\partial \tilde{r}} \\ a_2(\tilde{n})[(1-\chi)\tilde{r}+\chi]4(1-\chi)\frac{\partial}{\partial \tilde{r}} & 0 \end{bmatrix}$$

Using Eq. (5.93) and the above given definition of the matrix operator, one obtains

$$\left\langle \Phi, \overrightarrow{L\Upsilon} \right\rangle = (1-\chi)\int_0^1 \begin{bmatrix} \frac{a_1((1-\chi)\tilde{r}+\chi)}{Pe_D^2}\Phi_1\left\{\frac{\tilde{u}Pe_D^2}{a_1}\Upsilon_1 - \frac{Pe_D^2\Upsilon_2'}{a_1(1-\chi)((1-\chi)\tilde{r}+\chi)}\right\} + \\ \frac{\Phi_2}{4(1-\chi)^2 a_2(\tilde{r})((1-\chi)\tilde{r}+\chi)}4(1-\chi)a_2(\tilde{r})((1-\chi)\tilde{r}+\chi)\Upsilon_1' \end{bmatrix} d\tilde{r}$$

$$\left\langle \overrightarrow{L\Phi}, \overrightarrow{\Upsilon} \right\rangle = (1-\chi)\int_0^1 \begin{bmatrix} \frac{a_1((1-\chi)\tilde{r}+\chi)}{Pe_D^2}\Upsilon_1\left\{\frac{\tilde{u}Pe_D^2}{a_1}\Phi_1 - \frac{Pe_D^2\Phi_2'}{a_1(1-\chi)((1-\chi)\tilde{r}+\chi)}\right\} + \\ \frac{\Upsilon_2}{4(1-\chi)^2 a_2(\tilde{r})((1-\chi)\tilde{r}+\chi)}4(1-\chi)a_2(\tilde{r})((1-\chi)\tilde{r}+\chi)\Phi_1' \end{bmatrix} d\tilde{r}$$

Subtracting both equations, results in

$$\left\langle \overrightarrow{\Phi}, \overrightarrow{L\Upsilon} \right\rangle - \left\langle \overrightarrow{L\Phi}, \overrightarrow{\Upsilon} \right\rangle = -\int_0^1 (\Phi_1\Upsilon_2' + \Phi_1\Upsilon_1' + \Phi_2\Upsilon_1' + \Phi_1\Upsilon_2')d\tilde{r}$$

After carrying out the integration, the results is obtained that

$$\left\langle \overrightarrow{\Phi}, L\tilde{\Upsilon} \right\rangle = \left\langle L\overrightarrow{\Phi}, \tilde{\Upsilon} \right\rangle$$

## Problem 5-4

Multiplying the above eigenvalue problems by $\overrightarrow{\Phi}_j$ and $\overrightarrow{\Phi}_k$ respectively and taking the inner product results in Eq. (D.6)

$$\left\langle L\overrightarrow{\Phi}_j, \overrightarrow{\Phi}_k \right\rangle - \left\langle \overrightarrow{\Phi}_j, L\overrightarrow{\Phi}_k \right\rangle = (\lambda_j - \lambda_k)\left\langle \overrightarrow{\Phi}_j, \overrightarrow{\Phi}_k \right\rangle \qquad (D.6)$$

The left hand side is given by

$$\left\langle L\overrightarrow{\Phi}_j, \overrightarrow{\Phi}_k \right\rangle - \left\langle \overrightarrow{\Phi}_j, L\overrightarrow{\Phi}_k \right\rangle = \int_0^1 \begin{bmatrix} -\Phi_{k1}(\tilde{n})\Phi_{j2}'(\tilde{n}) + \Phi_{j1}(\tilde{n})\Phi_{k2}'(\tilde{n}) \\ +\Phi_{k2}(\tilde{n})\Phi_{j1}'(\tilde{n}) - \Phi_{j2}(\tilde{n})\Phi_{k1}'(\tilde{n}) \end{bmatrix} d\tilde{n}$$

Carrying out the integration gives

$$\left\langle \underset{\sim}{L}\overrightarrow{\Phi}_j, \overrightarrow{\Phi}_k \right\rangle - \left\langle \overrightarrow{\Phi}_j, \underset{\sim}{L}\overrightarrow{\Phi}_k \right\rangle = \Phi_{j1}\Phi_{k2} - \Phi_{j2}\Phi_{k1}\big|_0^1$$

Because we are considering the case of a uniform wall temperature

$$\Phi_{j2}(0) = \Phi_{k2}(0) = 0, \quad \Phi_{j1}(1) = \Phi_{k1}(1) = 0$$

This shows by considering Eq. (D.6) that $\left\langle \overrightarrow{\Phi}_j, \overrightarrow{\Phi}_k \right\rangle = 0$ for $\lambda_j \neq \lambda_k$.

## Problem 5-5

For laminar pipe flow, we have to solve

$$\Psi(\tilde{r}) = \int_0^{\tilde{r}} \frac{2}{r} \int_0^{\tilde{r}} 2(1 - s^2)s\,ds\,d\bar{n} + C_2 = \bar{\Psi}(\tilde{r}) + C_2$$

where

$$C_2 = \frac{4}{\mathrm{Pe}_L^2} \int_0^1 \tilde{n}\,d\tilde{n} - 2\int_0^1 \tilde{n}2(1 - \tilde{n}^2)\bar{\Psi}(\tilde{n})\,d\tilde{n}$$

Solving the integral, one obtains for $\bar{\Psi}$

$$\bar{\Psi}(\tilde{r}) = 2\int_0^{\tilde{r}} \left( \bar{r} - \frac{1}{2}\bar{r}^3 \right) d\bar{r} = \tilde{r}^2 - \frac{1}{4}\tilde{r}^4$$

For $C_2$ one obtains

$$C_2 = \frac{2}{\mathrm{Pe}_L^2} - \frac{7}{24}$$

For the temperature distribution for the fully developed flow we obtain Eq. (5.82)

$$\Theta(\tilde{x}, \tilde{r}) = 2\tilde{x} + \tilde{r}^2 - \frac{\tilde{r}^4}{4} + \frac{2}{\mathrm{Pe}_L^2} - \frac{7}{24} \tag{5.82}$$

For the laminar flow between parallel plates, one has to solve

$$\Psi(\tilde{n}) = \int_0^{\tilde{n}} \int_0^{\tilde{n}} \frac{3}{2}(1 - s^2)\,ds\,d\bar{n} + C_2 = \bar{\Psi}(\tilde{n}) + C_2 \tag{5.76}$$

where

$$C_2 = \frac{1}{Pe_L^2} \int_0^1 1 d\tilde{n} - \int_0^1 \frac{3}{2}(1 - \tilde{n}^2)\bar{\Psi}(\tilde{n})d\tilde{n} \tag{5.77}$$

Integrating the above equations leads to Eq. (5.83).

## Chapter 6

### Problem 6-1

(a) For the case of a constant heat conductivity, the equation simplifies to

$$\frac{\partial^2 T}{\partial x^2} + \frac{\partial^2 T}{\partial y^2} = 0$$

$T_1$ and $T_2$ are both solutions of this equation. If we insert $C_1 T_1 + C_2 T_2$ we obtain

$$C_1 \left\{ \frac{\partial^2 T_1}{\partial x^2} + \frac{\partial^2 T_1}{\partial y^2} \right\} + C_2 \left\{ \frac{\partial^2 T_2}{\partial x^2} + \frac{\partial^2 T_2}{\partial y^2} \right\} = 0$$

This shows that also the sum of the solutions $C_1 T_1 + C_2 T_2$ is a solution of the linear equation.

(b) Now we are considering the nonlinear problem:

$$\frac{\partial}{\partial x}\left( T\frac{\partial T}{\partial x} \right) + \frac{\partial}{\partial y}\left( T\frac{\partial T}{\partial y} \right) = 0$$

We know that $T_1$ and $T_2$ are both solutions of this equation. If we insert $C_1 T_1 + C_2 T_2$ we obtain

$$C_1 C_2 \frac{\partial}{\partial x}\left( T_1 \frac{\partial T_2}{\partial x} \right) + C_1 C_2 \frac{\partial}{\partial x}\left( T_2 \frac{\partial T_1}{\partial y} \right)$$
$$+ C_1 C_2 \frac{\partial}{\partial y}\left( T_1 \frac{\partial T_2}{\partial y} \right) + C_1 C_2 \frac{\partial}{\partial y}\left( T_2 \frac{\partial T_1}{\partial y} \right) = 0$$

This shows that the sum of the two solutions **is not** a solution of the nonlinear problem under consideration.

## Problem 6-2

(a) Introducing dimensionless quantities defined by

$$\tilde{x} = \frac{x}{h}, \ \tilde{t} = \frac{ta}{L^2}, \ a = \frac{k}{\rho c}, \ \Theta = \frac{T - T_W}{T_0 - T_W}$$

and applying the Kirchhoff transformation

$$\Omega = \int_0^\Theta \frac{k}{k_0} d\tilde{T} = \int_0^\Theta (1 + C(T_0 - T_W)(\tilde{\Theta} - 1)) d\tilde{\Theta}$$

$$= \Theta + C(T_0 - T_W)\left(\frac{\Theta^2}{2} - \Theta\right)$$

results in

$$\frac{\partial \Omega}{\partial \tilde{t}} = \frac{\partial^2 \Omega}{\partial \tilde{x}^2}$$

with the boundary conditions

$$\tilde{t} = 0: \ \Omega = 1 - \frac{C}{2}(T_0 - T_W)$$

$$\tilde{x} = 0: \ \frac{\partial \Omega}{\partial \tilde{x}} = 0$$

$$\tilde{x} = 1: \ \Omega = 0$$

(b) Using the method of separation of variables, the solution for this problem is given by

$$\Omega = \sum_{n=1}^\infty C_n \cos(\lambda_n \tilde{x}) \exp(-\lambda_n^2 \tilde{t}), \quad \lambda_n = \frac{2n - 1}{2}\pi, \ n = 1, 2, 3, \ldots$$

$$C_n = \frac{\int_0^1 \left(1 - \frac{1}{2}C(T_0 - T_W)\right)\cos(\lambda_n \tilde{x}) d\tilde{x}}{\int_0^1 \cos^2(\lambda_n \tilde{x}) d\tilde{x}}$$

(c) The solution of the original problem can be obtained from the relationship between $\Omega$ and $\Theta$. Thus

$$\Theta = \frac{1}{C(T_0 - T_W)}\left\{ \sqrt{2\Omega C(T_0 - T_W) + (1 - C(T_0 - T_W))^2} - (1 - C(T_0 - T_W)) \right\}$$

## Problem 6-3

(a) Introducing the new variables into the partial differential equation results in

$$\eta^2 g'(\xi) \frac{d\Theta}{d\eta} = g^4(\xi) \frac{d\Theta}{d\eta^2}$$

(b) In order that the above equation is an ordinary equation for the temperature, the function $g(\xi)$ has to satisfy the following equation

$$\frac{g'(\xi)}{g^4(\xi)} = \text{const.}$$

(c) Solving the above given ordinary differential equation gives

$$g(\xi) = \frac{1}{(C_1\xi + C_2)^{1/3}}$$

In this equation there are two arbitrary constants $C_1$ and $C_2$. Selecting $C_1 = 3$ and $C_2 = 0$ gives finally

$$g(\xi) = \frac{1}{(3\xi)^{1/3}}, \quad \eta = \frac{\tilde{y}}{(3\xi)^{1/3}}$$

(d) The solution is given by

$$\Theta = \frac{\int_0^\eta \exp(-1/3\bar{\eta}^3)d\bar{\eta}}{\int_0^\eta \exp(-1/3\bar{\eta}^3)d\bar{\eta}}$$

## Problem 6-4

(a) Introducing the dimensionless temperature into the partial differential equation and into the boundary conditions results in

$$\rho c \left\{ \frac{\partial\Theta}{\partial t} + \Theta \frac{1}{(T_W(t) - T_0)} \frac{dT_W}{dt} \right\} = k \frac{\partial^2\Theta}{\partial x^2} + \frac{F(T,t)}{(T_W(t) - T_0)} e^{-x/\sqrt{t}}$$

$$\Theta(x = 0, t) = 1, \quad \Theta(x \to \infty, t) = 0$$

$$\Theta(x, t = 0) = 0$$

(b) The constant can be determined by dimensional reasoning, so that the similarity coordinate is dimensionless

$$\eta = \frac{Cx}{\sqrt{t}}, \quad \eta = \frac{x}{\sqrt{at}}, \quad C = \frac{1}{\sqrt{a}}$$

(c) Introducing the similarity variable into the differential equation gives for the case $F(T,t) = 0$

$$-\frac{1}{2}\eta\frac{d\Theta}{d\eta} + \Theta\frac{t}{T_W(t) - T_0}\frac{dT_W}{dt} = \frac{d^2\Theta}{d\eta^2}$$

From this equation, we see that similarity solutions are only possible if

$$\frac{t}{T_W(t) - T_0}\frac{dT_W}{dt} = \text{const.}, \quad T_W(t) - T_0 = Dt^\alpha$$

(d) For the case $T_W = \text{const.}$ we obtain

$$-\frac{1}{2}\eta\frac{d\Theta}{d\eta} = \frac{d^2\Theta}{d\eta^2} + \frac{F(\Theta,t)}{T_W - T_0}\exp(-\eta/C)$$

This equation can only have similarity solutions, if the function $F(\Theta,t)$ depends only on $\Theta$ and not on $t$.

## Problem 6-5

(a) Introducing a stream function, defined by

$$u = \frac{\partial\Psi}{\partial y}, \quad v = -\frac{\partial\Psi}{\partial x}$$

results in

$$\frac{\partial\Psi}{\partial y}\frac{\partial^2\Psi}{\partial x\partial y} - \frac{\partial\Psi}{\partial x}\frac{\partial^2\Psi}{\partial y^2} = u_\infty\frac{du_\infty}{dx} + v\frac{\partial^3\Psi}{\partial y^3}$$

with the boundary conditions

$$y = 0: \quad \frac{\partial\Psi}{\partial x} = \frac{\partial\Psi}{\partial y} = 0$$

$$y \to \infty: \quad \frac{\partial\Psi}{\partial y} = u_\infty(x)$$

(b) The problem should be investigated by using the group-theory method. For this we introduce

$$x = A^{\alpha_1}\bar{x}, \; y = A^{\alpha_2}\bar{y}$$
$$\Psi = A^{\alpha_3}\bar{\Psi}, \; u_\infty = A^{\alpha_4}\bar{u}_\infty$$

and obtain

$$A^{2\alpha_3 - \alpha_1 - 2\alpha_2} \left( \frac{\partial \bar{\Psi}}{\partial \bar{y}} \frac{\partial^2 \bar{\Psi}}{\partial \bar{x} \partial \bar{y}} - \frac{\partial \bar{\Psi}}{\partial \bar{x}} \frac{\partial^2 \bar{\Psi}}{\partial \bar{y}^2} \right) = A^{2\alpha_3 - \alpha_1} u_\infty \frac{du_\infty}{d\alpha} + \nu A^{2\alpha_4 - 3\alpha_2} \frac{\partial^3 \bar{\Psi}}{\partial \bar{y}^3}$$

All exponents of $A$ have to be the same, which means that

$$2\alpha_3 - \alpha_1 - 2\alpha_2 = 2\alpha_4 - \alpha_1 = \alpha_3 - 3\alpha_2$$

From this equation, we obtain

$$A = \left( \frac{x}{\bar{x}} \right)^{\frac{1}{\alpha_1}} = \left( \frac{y}{\bar{y}} \right)^{\frac{1}{\alpha_2}} = \left( \frac{\Psi}{\bar{\Psi}} \right)^{\frac{1}{\alpha_3}} = \left( \frac{u_\infty}{\bar{u}_\infty} \right)^{\frac{1}{\alpha_4}}$$

Now we can establish a relation between the old and the new quantities and obtain the similarity variables

$$\eta = \frac{y}{x^\alpha}, \quad f(\eta) = \frac{\Psi}{x^{1-\alpha}}, \quad h(\eta) = \frac{u_\infty}{x^{1-2\alpha}} = \text{const.}$$

Using the expression $u_\infty / x^{1-2\alpha} = C$ one finally obtains

$$\eta \sqrt{\frac{u_\infty}{xC}} y, \quad \Psi = \sqrt{x u_\infty C} f(\eta), \quad C = \nu$$

where the constant C has been selected to be equal to the kinematic viscosity in order to get the correct dimension for the stream-function ($\eta$ and $f$ being dimensionless). Introducing the above given expressions into the partial differential equation for the stream-function, one finally obtains

$$f''' + \frac{m+1}{2} ff'' + m \left[ 1 - (f')^2 \right] = 0$$
$$\bar{\eta} = 0 : f = f' = 0$$
$$\bar{\eta} \to \infty : f' = 1$$

(c) We reconsider the problem by using the method of the free variable. Therefore, we introduce the new coordinates

$$\xi = x$$
$$\bar{\eta} = y g(x)$$

For the stream-function, we introduce

$$\Psi = G(\xi) \bar{f}(\bar{\eta})$$

Introducing the stream-function into the boundary conditions results in

$$\bar{\eta} = 0: \quad G'(\xi)\bar{f}(0) = 0, \quad G(\xi)g(\xi)\bar{f}'(0) = 0$$
$$\bar{\eta} \to \infty: G(\xi)g(\xi)\bar{f}'(\infty) = u_\infty(\xi)$$

From this equation, we obtain

$$\bar{\eta} = 0: \quad \bar{f}(0) = 0, \quad \bar{f}'(0) = 0$$
$$\bar{\eta} \to \infty: \bar{f}'(\infty) = 1 \text{ and } G(\xi) = \frac{u_\infty(\xi)}{g(\xi)}$$

For the stream-function, we have

$$\Psi = \frac{u_\infty(\xi)}{g(\xi)}\bar{f}(\bar{\eta})$$

Introducing the new coordinates and the stream-function into the partial differential equation for the stream-function results in

$$\frac{u'_\infty}{vg^2}\left(1 - \bar{f}'^2\right) + \frac{u'_\infty g - g'u_\infty}{vg^3}\bar{f}\bar{f}'' + \bar{f}\bar{f}''' = 0$$
$$u'_\infty = \frac{du_\infty}{d\xi}, \quad g' = \frac{dg}{d\xi}$$

The above given differential equation can only be valid, if all dependence on $\xi$ cancels out. This means that

$$\frac{u'_\infty g - g'u_\infty}{vg^3} = C_1 = \text{const.} = \frac{1}{g}\left(\frac{u}{g}\right)'$$
$$\frac{u'_\infty}{vg^2} = C_2 = \text{const.}$$

Solving this equations results in

$$u_\infty = C_3 x^m; m = \frac{C_2}{2C_1 - C_2}$$
$$g(x) = \sqrt{\frac{C_3}{(2C_1 - C_2)v}x^{m-1}}, \quad \eta = yg(x), \quad \Psi = u_\infty/g\bar{f}$$

Selecting suitable constants in the above equations leads to the same similarity variable and stream-function which has been defined under b).

**Problem 6-6**

(a) Introducing the dimensionless temperature

$$\Theta = \frac{T - T_0}{T_W - T_0}$$

results in

$$\frac{\partial \Theta}{\partial t} = a \frac{\partial}{\partial x} \left[ (1 + b\Theta) \frac{\partial \Theta}{\partial x} \right]$$

$$
\begin{aligned}
t = 0 : & \quad \Theta = 0 \\
x = 0 : & \quad \Theta = 1 \\
x \to \infty : & \quad \Theta = 0
\end{aligned}
$$

(b) Introducing the similarity coordinate $\eta = xg(t)$ into the partial differential equation and into the boundary conditions results in

$$\frac{g'(t)}{g^3(t)} \eta \frac{d\Theta}{d\eta} = a \frac{d}{d\eta} \left[ (1 + b\Theta) \frac{d\Theta}{d\eta} \right]$$

From this equation, we see immediately that

$$\frac{g'(t)}{g^3(t)} = \text{const.}$$

Integration of this ordinary differential equation gives

$$g(t) = \frac{1}{\sqrt{at}}, \quad \eta = \frac{x}{\sqrt{at}}$$

where the free constant has been chosen to be $a$, so that the similarity variable is dimensionless. Introducing the function $g(t)$ into the differential equation for the temperature field results in

$$-\frac{1}{2} \eta \frac{d\Theta}{d\eta} = \frac{d}{d\eta} \left[ (1 + b\Theta) \frac{d\Theta}{d\eta} \right]$$

This ordinary differential equation has to be solved with the following boundary conditions

$$
\begin{aligned}
\eta = 0 : & \quad \Theta = 1 \\
\eta \to \infty : & \quad \Theta = 0
\end{aligned}
$$

**Problem 6-7**

(a) We assume one-dimensional, unsteady heat conduction with no source terms in the area. Thus, we obtain from the general Fourier heat conduction equation

$$\frac{\partial T}{\partial t} = \frac{a}{r^2} \frac{\partial}{\partial r}\left(r \frac{\partial T}{\partial r}\right), \quad a = \frac{k}{\rho c}$$

(b) If we introduce the new temperature $\Theta = (T - T_0)/(T_1 - T_0)$ into the heat conduction equation, one obtains

$$\frac{\partial \Theta}{\partial t} = \frac{a}{r^2} \frac{\partial}{\partial r}\left(r \frac{\partial \Theta}{\partial r}\right)$$

with the boundary conditions

$$r = r_1: \quad \Theta = 1$$
$$r \rightarrow \infty: \quad \Theta = 0$$

(c) Introducing the new coordinates into the heat conduction equation results in the following equation for $\Theta = f(\eta)$

$$\frac{g'}{g^3} \eta \Theta' = \frac{a}{\eta^2}\left(\eta^2 \Theta'\right)'$$

(d) In the above given differential equation all functions should only depend on the similarity variable $\eta$. Thus, one has to assume that

$$\frac{g'}{g^3} = \text{const.} \quad \text{This results in } g = \frac{C}{\sqrt{t}}, \, \eta = \frac{r}{\sqrt{at}}$$

Introducing this result in the ordinary differential equation for $\Theta$ results in

$$-\frac{1}{2}\bar{\eta}^3 \Theta' = \left(\bar{\eta}^2 \Theta'\right)'$$

This ordinary differential equation has the solution

$$\Theta = \int_{\eta_1}^{\eta} \frac{1}{\bar{\eta}^2} \exp\left(-\frac{1}{2}\bar{\eta}^2\right) d\bar{\eta}$$

**Problem 6-8**

(a) The energy equation is given in dimensionless form by

$$\tilde{u}\frac{\partial\Theta}{\partial\tilde{x}} = \frac{1}{Pe_h^2}\frac{\partial^2\Theta}{\partial\tilde{x}^2} + \frac{\partial^2\Theta}{\partial\tilde{y}^2}$$

(b) If the Peclet number is large, the term in the energy equation prescribing the axial heat conduction within the flow can be omitted and one obtains

$$\tilde{u}\frac{\partial\Theta}{\partial\tilde{x}} = \frac{\partial^2\Theta}{\partial\tilde{y}^2}$$

(c) Introducing the new coordinate $\tilde{y}_W$ into the velocity distribution, we obtain by omitting quadratic term

$$u = 4\bar{u}\tilde{y}_W$$

(d) Transforming the $y$-coordinate in the energy equation results in

$$4\tilde{y}_W\frac{\partial\Theta}{\partial\tilde{x}} = \frac{\partial^2\Theta}{\partial\tilde{y}_W^2}$$

(e) Introducing the new coordinates into the differential equation results in the following differential equation for the temperature $\Theta$, if we assume that the temperature is only a function of $\eta$

$$4\eta^2\frac{h'}{h^4}\Theta' = \Theta'', \qquad \Theta' = \frac{\partial\Theta}{\partial\eta}, \qquad \Theta'' = \frac{\partial^2\Theta}{\partial\eta^2}$$

From this equation we can see that the function $h$ has to fulfil the relation

$$\frac{h'}{h^4} = \text{const.} \Rightarrow h = C_1\tilde{x}^{-1/3}, \quad C_1 = 1\,(\text{arbitarily selected})$$

(f) Introducing the result for $h$ into the ordinary differential equation for the temperature results in

$$-\frac{4}{3}\eta^2\Theta' = \Theta''$$

which has the solution

$$\Theta = \frac{\int_0^\eta \exp\left(-\frac{4}{9}\bar{\eta}^3\right)d\bar{\eta}}{\int_0^\infty \exp\left(-\frac{4}{9}\bar{\eta}^3\right)d\bar{\eta}}$$

(g) The Nusselt number can be obtained as

$$Nu = \frac{-\frac{\partial T}{\partial y}\big|_{y=h}\, h}{T_1 - T_0} = \tilde{x}^{-1/3}\frac{\partial \Theta}{\partial \eta}\bigg|_{\eta=0} = \tilde{x}^{-1/3}\int_0^\infty \exp\left(-\frac{4}{9}\bar{\eta}^3\right)d\bar{\eta} = C(\mathrm{Pr})\tilde{x}^{-1/3}$$

This shows nicely that the Nusselt number depends on the axial coordinate proportional to $\tilde{x}^{-1/3}$.

# References

Abbrecht PH, Churchill SW (1960) The thermal entrance region in fully developed turbulent flow. AICHE J 6:268–273

Acrivos A (1980) The extended Graetz problem at low Peclet numbers. Appl Sci Res 36:35–40

Mc Adams WH (1954) Heat transmission. Mc Graw Hill, New York

Agrawal HC (1960) Heat transfer in laminar flow between parallel plates at small Peclet numbers. Appl Sci Res 9:177–189

Akyildiz FT, Bellout H (2004) The extended Graetz problem for dipolar fluids. Int J Heat Mass Transfer 47:2747–2753

Ames WF (1965) Nonlinear partial differential equations in Engineering. Academic Press, New York

Ames WF (1965) Similarity for the nonlinear diffusion equation. Ind Eng Chem Fundam 4:72–76

Andrews LC, Shivamoggi BK (1988) Integral transforms for engineers and applied mathematicians. Macmillian Publishing Company, New York

Antonia RA, Kim J (1991) Reynolds shear stress and heat flux calculations in a fully developed turbulent duct flow. Int J Heat Mass Transfer 34:2013–2018

Awad AS (1965) Heat transfer and eddy diffusivity in NaK in a pipe at uniform wall temperature. PhD thesis, University of Washington, Seattle

Awad M (2010) Heat transfer for laminar thermally developing flow in parallel-plates using the asymptotic method. In: 3rd international conference on thermal issues in emerging technologies theory and applications (THETA), pp 371–387

Azer NZ, Chao BT (1960) A mechanism of turbulent heat transfer in liquid metals. Int J Heat Mass Transfer 1:121–138

Aziz A, Na TY (1984) Perturbation methods in heat transfer. Springer, Berlin

Batchelor GK (1949) Diffusion in a field of homogeneous turbulence. Aust J Sci Res A2:437–450

Bayazitoglu Y, Özisik MN (1980) On the solution of Graetz type problems with axial conduction. Int J Heat Mass Transfer 23:1399–1402

Bhatti MS, Shah RK (1987) Turbulent and transition flow convective heat transfer in ducts. In: Kakaç S, Shah RK, Aung W (eds) Handbook of single-phase convective heat transfer. Wiley, New York

Bilir S (1992) Numerical solution of Graetz problem with axial conduction. Numer Heat Transfer Part A 21:493–500

Birkhoff G (1948) Dimensional analysis of partial differential equations. Electr Eng 67:1185–1188

Bleustein JL, Green AE (1967) Dipolar fluids. Int J Eng Sci 5:323–340

Borisenko AI, Kostinov ON, Chumachenko VI (1973) Experimental study of turbulent flow in a rotating channel. J Eng Phys 24:770–773

Bowman F (1958) Introduction to Bessel functions. Dover Publications, New York

Bradshaw P (1969) The analogy between streamline curvature and buoyancy in turbulent shear flow. J Fluid Mech 36:177–191

Bricteux L, Duponcheel M, Winckelmans G, Tiselj I, Bartosiewicza Y (2012) Direct and large eddy simulation of turbulent heat transfer at very low Prandtl number: application to lead-bismuth flows. Nucl Eng Des 246:91–97

Broman A (1970) Introduction to partial differential equations. Dover Publications, INC, New York

Bronstein IN, Semendjajew KA (1981) Taschenbuch der Mathematik. Verlag Harri Deutsch, Frankfurt

Brown GM (1960) Heat or mass transfer in a fluid in laminar flow in a circular or flat conduit. AICHE J 6:179–183

Burow P, Weigand B (1990) One dimensional heat conduction is a semi-infinite solid with the surface temperature a harmonic function of time: a simple approximate solution for the transient behavior. ASME J Heat Transfer 112:1076–1079

Carslaw HS, Jaeger JC (1992) Conduction of heat in solids. Oxford University Press, London

Cebeci T, Bradshaw P (1984) Physical and computational aspects of convective heat transfer. Springer, New York

Cebeci T, Chang KC (1978) A general method for calculating momentum and heat transfer in laminar and turbulent duct flow. Numer Heat Transfer 1:39–68

Chieng CC, Launder BE (1980) On the calculation of turbulent heat transfer downstream from an abrupt pipe expansion. Numer Heat Transfer 3:189–207

Churchill SW, Usagi R (1972) A general expression for the correlation of rates of transfer and other phenomena. Am Inst Chem Eng J 18:1121–1128

Cochran WG (1934) The flow due to a rotating disk. Proc Cambridge. Philos Soc 30:365–375

Coddington EA, Levinson N (1955) Theory of ordinary differential equations. Mc Graw Hill, New York

Cohen CB, Reshotko E (1956) The compressible laminar boundary layer with heat transfer and arbitrary pressure gradient. NACA report no 1294

Collatz L (1981) Differentialgleichungen. B.G. Teubner, Stuttgart

Courant R, Hilbert D (1991) Methoden der mathematischen Physik. Springer, Berlin

Darcy H (1858) Récherches expérimentales relatives aux mouvements de l'eau dans tuyaux. Mem prés à l'Acedémie des Sciences de l'Institute de France 15:141

Deavours CA (1974) An exact solution for the temperature distribution in parallel plate Poiseuille flow. J Heat Transfer 96:489–495

Deissler RG (1955) Analysis of turbulent heat transfer, mass transfer and friction in smooth tubes at high Prandtl and Schmidt numbers. NACA technical report 1210

Dewey CF, Gross JF (1967) Exact similar solutions of the laminar boundary—layer equations. Adv Heat Transfer 4:317–446

Dhawan S (1953) Direct measurements of skin friction. NACA technical report 1121

Dwyer OE (1965) Heat transfer to liquid metals flowing turbulently between parallel plates. Nucl Sci Eng 21:79–89

Ebadian MA, Zhang HY (1989) An exact solution of extended Graetz problem with axial heat conduction. Int J Heat Mass Transfer 32:1709–1717

Eckert ERG, Drake M (1987) Analysis of heat and mass transfer. Hemisphere Publishing Corporation, New York

Ede AJ (1967) Advances in free convection. Adv Heat Transfer 4:1–64

Eggels JGM, Nieuwstadt FTM (1993) Large eddy simulation of turbulent flow in an axially rotating pipe. In: Proceedings of the 9th symposium on turbulent shear flows, Kyoto, Japan, 16–18 August, pp 1–4

Erdelyi A (1956) Asymptotic expansions. Dover Publications, New York

Faggiani S, Gori F (1980) Influence of streamwise molecular heat conduction on the heat transfer for liquid metals in turbulent flow between parallel plates. J Heat Transfer 102:292–296

Froman N, Froman PO (1965) JWKB approximation, contributions to the theory. North-Holland, Amsterdam

Fuchs H (1973) Wärmeübergang an strömendes Natrium. Thesis, Eidg. Institut für Reaktorforschung, Würenlingen, Switzerland, EIR-Bericht 241

Fuller RE, Samuels MR (1971) Simultaneous development of the velocity and temperature fields in the entry region of an annulus. Chem Eng Prog Symp Ser 113:71–77

Gibson MM, Younis BA (1986) Caculation of swirling jets with a Reynolds-stress closure. Phys Fluids 29:38

Gilliland ER, Musser RJ, Page WR (1951) Heat transfer to Mercury. In: Proceedings of general disc heat transfer, institute of mechanical engineers ASME, London, pp 402–404

Görtler (1975) Dimensionsanalyse: Theorie der physikalischen Dimensionen mit Anwendungen. Springer, Berlin

Gradshteyn IS, Ryzhik IM (1994) Table of integrals, series and products. Academic Press, New York

Graetz L (1883) Über die Wärmeleitfähigkeit von Flüssigkeiten, Teil 1. Ann Phys Chem 18:79–84

Graetz L (1885) Über die Wärmeleitfähigkeit von Flüssigkeiten, Teil 2. Ann Phys Chem 25:337–357

Haji-Sheikh A, Beck JV, Amos DE (2008) Axial heat conduction effects in the entrance region of parallel plate ducts. Int J Heat Mass Transfer 51:5811–5822

Hansen AG (1964) Similarity analyses of boundary value problems in engineering. Prentice-Hall, Englewood Cliffs

Hennecke D (1968) Heat transfer by Hagen-Poiseuille flow in the thermal development region with axial conduction. Wärme- und Stoffübertragung 1:177–184

Hirai S, Takagi T (1987) Prediction of heat transfer deterioration in turbulent swirling pipe flow. In: Proceedings of the 2nd ASME/JSME thermal engineering joint conference, vol 5, pp 181–187

Hirai S, Takagi T, Matsumoto M (1988) Predictions of the laminarization phenomena in an axially rotating pipe flow. J Fluids Eng 110:424–430

Hsu CJ (1965) Heat transfer in a round tube with sinusoidal wall flux distribution. AICHE J 11:690

Hsu CJ (1970) Theoretical solutions for low Peclet number thermal-entry-region heat transfer in laminar flow through concentric annuli. Int J Heat Mass Transfer 13:1907–1924

Hsu CJ (1971a) Laminar flow heat transfer in circular or parallel-plate channels with internal heat generation and the boundary conditions of the third kind. J Chin Inst Chem Eng, pp 85–100

Hsu CJ (1971b) An exact analysis of low Peclet number thermal entry region heat transfer in transversely nonuniform velocity fields. AICHE J 17:732–740

Jaluria Y (1980) Natural convection heat and mass transfer. Pergamon Press, Oxford

Jischa M, Rieke HB (1979) About the prediction of turbulent Prandtl and Schmidt numbers. Int J Heat Mass Transfer 24:1179–1189

Jischa M (1982) Konvektiver Impuls-, Wärme- und Stoffaustausch. Vieweg & Sohn, Braunschweig

Jones AS (1971) Extensions to the solution of the Graetz problem. Int J Heat Mass Transfer 14:619–623

Kader BA (1971) Heat and mass transfer in laminar flow in the entrance section of a circular tube. High Temp (USSR) 9:1115–1120

Kamke E (1983) Differentialgleichungen: Lösungsmethoden und Lösungen, vol 1. B.G Teubner, Stuttgart

Kays WM, Crawford ME (1993) Convective heat and mass transfer. Mc Graw-Hill Inc, New York

Kays WM (1994) Turbulent Prandtl number—where are we? J Heat Transfer 116:285–295

Kays WM, Crawford ME, Weigand B (2004) Convective heat and mass transfer. Mc Graw-Hill Inc, New York

Kevorkian J, Cole JD (1981) Perturbation methods in applied mathematics. Springer, Berlin. (Appl Math Sci, vol 34)

Kikuyama K, Murakami M, Nishibori K, Maeda K (1983) Flow in an axially rotating pipe. Bull JSME 26:506–513

Koosinlin ML, Launder BE, Sharma BI (1975) Prediction of momentum, heat and mass transfer in swirling, turbulent boundary layers. J Heat Transfer 96:204–209

Kumar IJ (1972) Recent mathematical methods in heat transfer. Adv Heat Transfer 8:1–91

Latzko H (1921) Der Wärmeübergang an einem turbulenten Flüssigkeits- oder Gasstrom. ZAMM 1:268–290

Laufer J (1950) Some recent measurements in a two-dimensional turbulent channel. J Aerosp Sci 17:277–280

Lauffer D (2003) Wärmeübertragung im laminar oder turbulent durchströmten Rohr und ebenen Kanal bei kleinen Prandtlzahlen. Diploma-Thesis, Stuttgart University, Germany

Launder BE (1988) On the computation of convective heat transfer in complex turbulent flow. J Heat Transfer 110:1112–1128

Lauwerier HA (1950) The use of confluent hypergeometric functions in mathematical physics and the solution of an eigenvalue problem. Appl Sci Res Sect A 2:184–204

Lawn CJ (1969) Turbulent heat transfer at low Reynolds number. J Heat Transfer 91:532

Lee SL (1982) Forced convection heat transfer in low Prandtl number turbulent flows: influence of axial conduction. Can J Chem Eng 60:482–486

Leveque MA (1928) Les lois de la transmission de chaleur par convection. Ann Mines Mem 13:201–415

Levy F (1929) Strömungserscheinungen in rotierenden Rohren. VDI Forschungsarbeiten auf dem Gebiet des Ingenieurwesens 322:18–45

Levy S (1952) Heat transfer to constant-property laminar boundary-layer flows with power-function free-stream velocity and wall temperature variation. J Aeron Sci 19:341–348

Li TY, Nagamatsu HT (1953) Similar solutions of compressible boundary layer equations. J Aeron Sci 20:653–656

Li TY, Nagamatsu HT (1955) Similar solutions of compressible boundary layer equations. J Aeron Sci 22:607–616

Liouville J (1837) Journal de Math 2:24

Loitsianski LG (1967) Laminare Grenzschichten. Akademie-Verlag, Berlin

Ludwieg H (1956) Bestimmung des Verhältnisses der Austauschkoeffizienten für Wärme- und Impuls bei turbulenten Grenzschichten. Zeitschrift für Flugwissenschaften 4:73–81

Lundberg RE, Mc Cuen PA, Reynolds WC (1963) Heat transfer in annular passages. Hydrodynamically developed laminar flow with arbitrarily prescribed wall temperatures or heat fluxes. Int J Heat Mass Transfer 6:495–529

Mackrodt PA (1971) Stabilität von Hagen-Poiseuille-Strömungen mit überlagerter starrer Rotation. Mitteilungen MPI Strömungsforschung und Aerodynamische Versuchsanstalt Göttingen, vol 55

Malin MR, Younis BA (1997) The prediction of turbulent transport in an axially rotating pipe. Int Commun Heat Mass Transfer 24:89–98

Michelsen ML, Villadsen J (1974) The Greatz problem with axial heat conduction. Int J Heat Mass Transfer 17:1391–1402

Mikhailov MD, Özisik MN (1984) Unified analysis and solutions of heat and mass diffusion. John Wiley, New York

Millsaps K, Pohlhausen K (1952) Heat transfer by laminar flow from a rotating plate. J Aeron Sci 19:120–126

Mizushina T, Ogino F (1970) Eddy viscosity and universal velocity profile in turbulent flow in a straight pipe. J Chem Eng Jpn 3:166–170

Morgan AJA (1952) The reduction by one of the number of independent variables in some systems of partial differential equations. Quart J Math Oxford 3:250–259

Müller EA, Matschat K (1962) Über das Auffinden von Ähnlichkeitslösungen partieller Differentialgleichungssysteme unter Benutzung von Transformationsgruppen, mit Anwendungen auf Probleme der Strömungsphysik. Misz. der angew. Mechanik, Akademie Verlag, Berlin, pp 190–222

Murakami M, Kikuyama K (1980) Turbulent flow in axially rotating pipes. J Fluids Eng 102:97–103

Myers GE (1987) Analytical methods in conduction heat transfer. Genium Pulishing Corporation, Schenectady

Myint- UT, Debnath L (1978) Ordinary differential equations. Elsevier North Holland Inc, New York

Newman J (1969) The Graetz problem. UCRL 18646, Department of Chemical Engineering, University of California at Berkely

Nguyen TV (1992) Laminar heat transfer for thermally developing flow in ducts. Int J Heat Mass Transfer 35:1733–1741

Nikuradse J (1932) Gesetzmäßigkeit der turbulenten Strömung in glatten Rohren. Arb Ing Wesens, Forsch, p 356

Nishibori K, Kikuyama K, Murakami M (1987) Laminarization of turbulent flow in the inlet region of an axially rotating pipe. JSME Int J 30:255–262

Notter RH, Sleicher CA (1971a) The eddy diffusivity in turbulent boundary layer near a wall. Chem Eng Sci 26:161–171

Notter RH, Sleicher CA (1971b) A solution to the turbulent Graetz problem by matched asymptotic expansions—II the case of uniform wall heat flux. Chem Eng Sci 26:559–565

Notter RH, Sleicher CA (1972) A solution to the turbulent Graetz problem—III fully developed and entry region heat transfer rates. Chem Eng Sci 27:2073–2093

Nusselt W (1910) Die Abhängigkeit der Wärmeübergangszahl von der Rohrlänge. VDI Zeitschrift 54:1154–1158

Orlandi P, Fatica M (1997) Direct simulation of a turbulent pipe rotating along its axis. J Fluid Mech 343:43–73

Orlandi P, Ebstein D (2000) Turbulent budgets in rotating pipes by DNS. Int J Fluid Flow 21:499–505

Ostrach S (1953) An analysis of laminar free-convection flow and heat transfer about a flat plate parallel to the direction of the generating body force. NACA report 1111

Ould-Rouiss M, Dries A, Mazouz A (2010) Numerical predictions of turbulent heat transfer for air flow in roating pipes. Int J Heat Fluid Flow 31:507–517

Özisik MN (1968) Boundary value problems of heat conduction. Dover Publications, New York

Özisik MN, Cotta RM, Kim WS (1989) Heat transfer in turbulent forced convection between parallel-plates. Can J Chem Eng 67:771–776

Papoutsakis E, Ramkrishna D, Lim HC (1980a) The extended Graetz problem with Dirichlet wall boundary conditions. Appl Sci Res 36:13–34

Papoutsakis E, Ramkrishna D, Lim HC (1980b) The entended Graetz problem with prescribed wall flux. AICHE J 26:779–787

Papoutsakis E, Ramkrishna D (1981) Heat transfer in a capillary flow emerging from a reservoir. J Heat Transfer 103:429–435

Plaschko P, Brod K (1989) Höhere mathematische Methoden für Ingenieure und Physiker. Springer, Berlin

Prandtl L (1910) Eine Beziehung zwischen Wärmeaustausch und Strömungswiderstand der Flüssigkeit. Z Phys 11:1072–1078

Prandtl L (1925) Über die ausgebildete Turbulenz. ZAMM 5:136–139

Prandtl L (1935) The mechanics of viscous fluids. In: Durand WF (ed) Aerodynamic theory, vol 3, pp 34–208

Rayleigh Lord (1917) On the dynamics of revolving fluids. Proc Roy Soc A 93:148–154

Ramkrishna D, Amundson NR (1979a) Boundary value problems in transport with mixed and oblique derivative boundary conditions—I. Formulation of equivalent integral equations. Chem Eng Sci 34:301–308

Ramkrishna D, Amundson NR (1979b) Boundary value problems in transport with mixed and oblique derivative boundary conditions—II. Reduction to first order systems. Chem Eng Sci 34:309–318

Rannie WD (1956) Heat transfer in turbulent shear flow. J Aeron Sci 23:485

Reed CB (1987) Convective heat transfer in liquid metals. In: Kakac S, Shah RK, Aung W (eds) Handbook of single phase convective heat transfer, chap 8. Wiley, New York

Reich G (1988) Strömung und Wärmeübertragung in einem axial rotierenden Rohr. Dissertation, TH Darmstadt, Germany

Reich G, Beer H (1989) Fluid flow and heat transfer in an axially rotating pipe—I. Effect of rotation on turbulent pipe flow. Int J Heat Mass Transfer 32:551–562

Reich G, Weigand B, Beer H (1989) Fluid flow and heat transfer in an axially rotating pipe—II. Effect of rotation on laminar pipe flow. Int J Heat Mass Transfer 32:563–574

Reichhardt H (1940) Die Wärmeübertragung in turbulenten Reibungsschichten. ZAMM 20:297

Reichhardt H (1951) Vollständige Darstellung der turbulenten Geschwindigkeitsverteilung in glatten Leitungen. ZAMM 31:208–219

Reid WT (1980) Sturmian theory for ordinary differential equations. Springer, Berlin. (Appl Math Sci, vol 31)

Reynolds WC (1974) Recent advances in the computation of turbulent flows. Adv Chem Eng 9:193–246

Reynolds AJ (1975) The prediction of turbulent Prandtl and Schmidt numbers. Int J Heat Mass Transfer 18:1055–1069

Rinck KJ, Beer H (1999) Numerical calculation of the fully developed turbulent flow in an axially rotating pipe with a second-moment closure. J Fluids Eng 120:274–279

Rothe T (1994) Der Einfluß der Rotation auf die Strömung und den Wärmetransport im turbulent durchströmten Ringspalt zwischen zwei rotierenden Wellen. Dissertation, TH Darmstadt, Germany

Rothfus RR, Walker JE, Whan GA (1958) Correlation of local velocities in tubes, annuli and parallel plates. AICHE J 4:240–245

Sadeghipour MS, Özisik MN, Mulligan JC (1984) The effect of external convection on freezing in steady turbulent flow in a tube. Int J Eng Sci 22:135–148

Sagan (1989) Boundary and eigenvalue problems in mathematical physics. Dover Publications, New York

Sakakibara M, Endoh K (1977) Analysis of heat transfer in the entrance region with fully developed turbulent flow between parallel plates. Heat Transfer Jpn Res 6:54–61

Satake S, Kunugi T: Direct numerical simulation of turbulent heat transfer in an axially rotating pipe: Reynolds stress and scalar-flux budgets. Int J Numer Methods Heat Fluid Flow 12:985–1008

Sauer R, Szabó I (1969) Mathematische Hilfsmittel des Ingenieurs, Teil 1–4. Springer, Berlin

Schlichting H (1982) Grenzschicht-Theorie. G. Braun, Karlsruhe

Schmidt E, Bechmann W (1930) Das Temperatur- und Geschwindigkeitsfeld von einer Wärme abgebenden senkrechten Platte bei natürlicher Konvektion. Forsch Ing Wes 1:391

Schneider W (1978) Mathematische Methoden der Strömungsmechanik. Vieweg, Braunschweig

Sellars JR, Tribus M, Klein JS (1956) Heat transfer to laminar flow in a round tube or flat conduit —the Graetz problem extended. Trans ASME 78:441–448

Shah RK (1975) Thermal entry length solutions for the circular tube and parallel plates. In: Proceedings of the 3rd national heat mass transfer conference, Indian institute of technology, vol 1, Bombay, HMT-11-75

Shah RK, London AL (1978) Laminar flow forced convection in ducts. Advance in Heat Transfer. Academic Press, New York

Shchukin VK (1967) Hydraulic resistance of rotating tubes. J Eng Phys 12:418–422

Shibani AA, Özisik MN (1977a) Freezing of liquids in turbulent flow inside tubes. Can J Chem Eng 55:672–677

Shibani AA, Özisik MN (1977b) A solution to heat transfer in turbulent flow between parallel plates. Int J Heat Mass Transfer 20:565–573

Simon V, Weigand B (2006) Laws of similarity in fluid mechanics. In: Liebe R (ed) Flow phenomena in nature: a challenge to engineering design, pp 20–35. ISBN 1-84564-001-2

Simmonds JG, Mann JE (1986) A first look at perturbation theory. R.E. Krieger Publishing Company, Florida

Singh SN (1958) Heat transfer by laminar flow in a cylindrical tube. Appl Sci Res Ser A 7:325–340

Sleicher CA, Tribus M (1957) Heat transfer in a pipe with turbulent flow and arbitrary wall-temperature distribution. Trans ASME 79:789–797

Sleicher CA, Notter RH, Crippen MD (1970) A solution to the turbulent Graetz problem by matched asymptotic expansions—I. the case of uniform wall temperature. Chem Eng Sci 25:845–857

Sleicher CA, Awad AS, Notter RH (1973) Temperature and eddy diffusivity profiles in NaK. Int J Heat Mass Transfer 16:1565–1575

Sleicher CA, Rouse MW (1975) A convenient correlation for heat transfer to constant and variable property fluids in turbulent pipe flow. Int J Heat Mass Transfer 18:677–683

So RMC, Sommer TP (1996) An explicit algebraic heat flux model for the temperature field. Int J Heat Mass Transfer 39:455–465

Sogin HH, Subramanian VS (1961) Local mass transfer from circular cylinders in cross flow. J Heat Transfer 83:483–493

Sommerfeld A (1978) Vorlesungen über Theoretische Physik, Band VI, Partielle Differentialgleichungen der Physik, Verlag Harry Deutsch, Frankfurt

Spalding DB (1961) A single formula for the law of the wall. J Appl Mech 28:455–458

Sparrow EM, Gregg JL (1959) Heat transfer from a rotating disk to fluids of any Prandtl number. J Heat Transfer 81:249–251

Speziale CG, Sarkar S, Gatski TB (1991) Modeling the pressure-strain correlation of turbulence: an invariant dynamical approach. J Fluid Mech 227:245–272

Speziale CG, Younis BA, Berger SA (2000) Analysis and modelling of turbulent flow in an axially rotating pipe. J Fluid Mech 407:1–26

Spurk JH (1987) Strömungslehre. Springer, Berlin

Spurk JH (1992) Dimensionsanalyse in der Strömungslehre. Springer, Berlin

Stein R (1966) Liquid metal heat transfer. Advance in heat transfer, vol 3. Academic Press, New York, pp 101–174

Stephenson (1986) Partial differential equations for scientists and engineers. Longman, London

Sternling CV, Sleicher CA (1962) Asymptotic eigenfunctions for turbulent heat transfer in a pipe. J Aerosp Sci 29:109–111

Taylor GI (1916) Conditions at the surface of a hot body exposed to the wind. British Advisory Commitee for Aeronautics, vol 2, R & M Nr. 272, pp 423–429

Taylor GI (1923) Stability of a viscous liquid contained between two rotating cylinders. Philos Trans Roy Soc London A 223:289–343

Tietjins O (1970) Strömungslehre II. Springer, Berlin

Törnig W (1979) Numerische Mathematik für Ingenieure und Physiker. Band 2: Eigenwertprobleme und numerische Methoden der Analysis. Springer, Berlin

van Driest ER (1951) Turbulent boundary layers in compressible fluids. J Aeron Sci 18:145–160

van Driest ER (1956) On turbulent flow near a wall. J Aeron Sci 23:1007–1011

van Dyke MD (1964) Perturbation methods in fluid mechanics. Academic Press, New York

Vick B, Özisik MN, Bayazitoglu Y (1980) A method of analysis of low Peclet number thermal entry region problems with axial conduction. Lett Heat Mass Transfer 7:235–248

Vick B, Özisik MN (1981) An exaxt analysis of low Peclet number heat transfer in laminar flow with axial conduction. Lett Heat Mass Transfer 8:1–10

von Kármán T (1921) Über laminare und turbulente Reibung. ZAMM 1:233–252

von Kármán T (1939) The analogy between fluid friction and heat transfer. Trans ASME 61:705–710

Weigand B, Beer H (1989a) Wärmeübertragung in einem axial rotierenden, durchströmten Rohr im Bereich des thermischen Einlaufs Teil 1: Einfluß der Rotation auf eine turbulente Strömung. Wärme- und Stoffübertragung 24:191–202

Weigand B, Beer H (1989b) Wärmeübertragung in einem axial rotierenden, durchströmten Rohr im Bereich des thermischen Einlaufs Teil 2: Einfluß der Rotation auf eine laminare Strömung. Wärme- und Stoffübertragung 24:273–278

Weigand B, Beer H (1992a) Fluid flow and heat transfer in an axially rotating pipe: the rotational entrance. In: Kim JH, Yang WJ (eds) Rotating machinery (transport phenomena). Hemisphere Publishing Corporation, London, pp 325–340

Weigand B, Beer H (1992b) Fluid flow and heat transfer in an axially rotating pipe subjected to external convection. Int J Heat Mass Transfer 35:1803–1809

Weigand B, Schmidt J, Beer H (1993) An analytic study of liquid solidification in low Peclet number forced flows inside a parallel plate channel concerning axial heat conduction. In: Proceedings of 4th international symposium on thermal engineering and science for cold regions. Hanover, New Hampshire, USA, pp 39–47

Weigand B, Beer H (1994) On the universality of the velocity profiles of a turbulent flow in an axially rotating pipe. Appl Sci Res 52:115–132

Weigand B (1996) An exact analytical solution for the extended turbulent Graetz problem with Dirichlet wall boundary conditions for pipe and channel flows. Int J Heat Mass Transfer 39:1625–1637

Weigand B, Ferguson JR, Crawford ME (1997a) An extended Kays and Crawford turbulent Prandtl number model. Int J Heat Mass Transfer 40:4191–4196

Weigand B, Wolf M, Beer H (1997b) Heat transfer in laminar and turbulent flows in the thermal entrance region of concentric annuli: axial heat conduction effects in the fluid. Heat Mass Transfer 33:67–80

Weigand B, Kanzamar M, Beer H (2001) The extended Graetz problem with piecewise constant wall heat flux for pipe and channel flows. Int J Heat Mass Transfer 44:3941–3952

Weigand B, Schwartzkopff T, Sommer TP (2002) A numerical investigation of the heat transfer in a parallel plate channel with piecewise constant wall temperature boundary conditions. J Heat Transfer 124:626–634

Weigand B, Wrona F (2003) The extended Graetz problem with piecewise constant wall heat flux for laminar and turbulent flows inside concentric annuli. Heat Mass Transfer 39:313–320

Weigand B, Lauffer D (2004) The extended Graetz problem with piecewise constant wall temperature for pipe and channel flows. Int J Heat Mass Transfer 47:5303–5312

Weigand B, Gassner G (2007) The effect of wall conduction for the extended Graetz problem for laminar and turbulent channel flows. Int J Heat Mass Transfer 50:1097–1105

Weigand B, Eisenschmidt K (2014) The extended Graetz problem with piecewise constant wall temperature for laminar and turbulent flows through a concentric annulus. Int J Therm Sci 54:89–97

Weigand B, Bogenfeld R (2014) A solution to the turbulent Graetz problem by matched asymptotic expansion for an axially rotating pipe subjected to external convection. Int J Heat Mass Transfer 78:901–907

Weigand B, Abdelmoula M (2014) Axial heat conduction effects in the entrance region of laminar duct flows: correlations for the local Nusselt number. Int Commun Heat Mass Transfer 51:45–50

White A (1964) Flow of fluid in an axially rotating pipe. J Mech Eng Sci 6:47–52

Worsoe-Schmidt PM (1967) Heat transfer in the thermal entrance region of circular tubes and annular passages with fully developed laminar flow. Int J Heat Mass Transfer 10:541–551

Younis BA, Speziale CG, Clark TT (2005) A rational model for the turbulent scalar fluxes. Proc Roy Soc 461:575–594

Zagustin A, Zagustin K (1969) Analytical solution for turbulent flow in pipes. La Houille Blanche 2:113–118

Zauderer E (1989) Partial differential equations of applied mathematics. Wiley, New York

Zhang T, Osterkamp TE, Gosink JP (1991) A model for the thermal regime of Permafrost within the depth of annual temperature variations. In: Proceedings of 3rd international symposium on thermal engineering and science for cold regions. Fairbanks, Alaska, USA, pp 341–347

# Index